A Cognitive TV White Space Access Framework

Thesis

A Cognitive TV White Space Access Framework

John H Martin

A thesis submitted in fulfilment of
the requirements for the degree of Doctor of Philosophy

Faculty of Mathematics, Computing and Technology
The Open University
Milton Keynes

September 2016

Abstract

Given the current boom in applications and services for mobile devices, data traffic is rapidly expanding, with the consequence that increasing spectrum capacity is being mandated. Following the switchover from analogue to digital platforms, *Television White Space* (TVWS) affords a fertile opportunity to supplement existing licensed spectrum to ease this scarcity. There are however, a number of obstacles to wide-scale TVWS adoption, including the accurate detection of *primary users* (PU), the hidden node problem and bandwidth availability for unlicensed *secondary users* (SU). Regulatory and industry bodies have sought to address some of these issues using a static database for spectrum access decisions, though this involves manual maintenance and accuracy can be compromised due to a lack of real-time information. While the new IEEE802.11af wireless local area network (WLAN) standard attempts to resolve some SU access issues, there remain many challenges, such as the critical asymmetry between mobile and base station power resources.

This thesis presents a new cognitive TVWS access framework encompassing a real-time sensing paradigm for TVWS deployment that uses a spectrum-efficient scheme to uphold *quality-of-service* (QoS) for both PU and SU. A novel *dynamic spectrum allocation* (DSA) model has been formulated allied with a resilient interference management system which exploits the unique way *digital terrestrial TV* channels are allocated in different geographical areas. A margin strategy has been framed to support efficient TVWS channel reuse, with an exclusion zone established to overcome the hidden node problem, while an innovative routing algorithm using cross-layer information, both extends coverage capacity and maximises QoS provision by ensuring a more balanced resource allocation.

Critical evaluation of the new access framework confirms that significant QoS improvements for SU are achieved compared to existing TVWS techniques. It importantly embodies a generic, practical, resource-efficient solution for TVWS deployment, which is compliant with current PU regulatory requirements.

ACKNOWLEDGEMENTS

This thesis could not have been produced without the love of knowledge that my parents instilled in me at a young age so my gratitude will always be with them for doing so. Also, I'm indebted for the support of my lovely wife who without I doubt I would have got this far.

I would like to give thanks of gratitude to my supervisor Professor Laurence S Dooley for his tireless effort to bring the best out of me. Without his support and guidance, it would not have been possible to complete the research presented in this thesis. I am also indebted to my co-supervisor Dr. Patrick Wong for his constant support and cooperation. They also deserve special thanks for their patience in reading drafts after drafts of all the documents I have written during my candidature. And lastly, I would like to thank my employer, Nokia, for allowing me the time to study for this PhD.

TABLE OF CONTENTS

LIST OF ABBREVIATIONS

3GPP	Third Generation Partnership Project
4G	Fourth Generation
AI	Artificial Intelligence
ANDSF	Access Network Discovery and Selection Function
AODV	Ad hoc On-demand Distance Vector
AR	Autoregressive
ATSC	Advanced Television Systems Committee
BS	Base Station
CLCE	Cross Layer Cognitive Engine
CLP	Cross layer Processing
CMMB	China Multimedia Mobile Broadcasting
CogNeA	Cognitive Networking Alliance
CR	Cognitive Radio
CRN	CR Networks
CSI	Channel State Information
BER	Bit Error Rate
DL	Downlink
DSA	Dynamic Spectrum Access
DSO	Digital Switchover
DSR	Dynamic Source Routing
DTMB	Digital Terrestrial Multimedia Broadcast
DTT	Digital Terrestrial TV
DTV	Digital TV
EDA	Enhanced Detection Algorithm

EB	Exabyte
EIRP	Effective Isotropic Radiated Power
eNB	e-Node B
ePS	Evolved Packet System
FCC	Federal Communications Commission
FER	Frame Error Rate
FFT	Fast Fourier Transform
GBR	Guaranteed Bit Rate
GEDA	Generalised EDA
GPS	Global Positioning System
IMS	IP Multimedia Subsystem
IoT	Internet of Things
IP	Internet Protocol
ITU	International Telecommunication Union
KPI	Key Performance Indicator
LOS	Line-of-Sight
LS	Least Squares
LTE	Long Term Evolution
M2M	Machine-to-Machine
MAC	Medium Access Control
MANET	Mobile Ad hoc Network
MS	Mobile Station
MTM	Multitaper Estimator Method
NC-OFDM	Non-Continuous OFDM
NF	Noise Figure
NTSC	National Television System Committee
OFCOM	Office of Communications

OFDM	Orthogonal Frequency Division Multiplexing
OS	Operating System
OTT	Over the Top
PAL	Phase Alternating Line
PDR	Packet Delivery Ratio
PER	Packet Error Rate
PSD	Power Spectrum Density
PMSE	Program Making and Special Events
PU	Primary User
QAM	Quadrature Amplitude Modulation
QCI	QoS class Identifier
QoS	Quality of Service
RAN	Radio Access Network
RF	Radio Frequency
RSS	Received Signal Strength
SCF	Spectrum Correlation Function
SDR	Software Defined Radio
SF	Scaling Factor
SI	Sterilisation Index
SINR	Signal-to-Interference-plus-Noise Ratio
SIP	Session Initiation Protocol
SNR	Signal-to-Noise Ratio
SSID	Service Set Identifier
SU	Secondary User
SVD	Singular Value Decomposition
TF	Egli Terrain Factor
TTL	Time to Live

TV	Television
TVWS	TV White Space
UHF	Ultra High Frequency
VHF	Very High Frequency
VoIP	Voice over IP
VoLTE	Voice over LTE
VSB	Vestigial sideband
WiMAX	Worldwide Interoperability for Microwave Access
WLAN	Wireless Local Area Network
XG	Next Generation

LIST OF VARIABLES

Att	Attenuator in dB
B	Bandwidth in Hz
D	Distance in metres
$Dist_{PC}$	Protection Contour
DL	DTT Egli Propagation loss in dB
FSL	Free Space Loss
$Freq$	Frequency in Hz
G_R	Receiver Antenna Gain in dB
G_T	Transmitter Antenna Gain in dB
$\mathcal{H}_{Mask}$	DTT spectrum mask transfer function
$\mathcal{H}_{Mask+8MHz}$	DTT adjacent channel interference filter transfer function
h_n	Height of obstruction in m
h_{nr}	Distance from obstruction to receiver in m
h_r	Receiver antenna height in m
h_t	Transmitter antenna height in m
h_{tn}	Distance from transmitter to obstruction in m
$J(v)$	Fresnel Integral
LOS	Line of Sight
N	Thermal noise in dBm
N_{Demod}	Noise into demodulator
NF	Receiver noise figure in dB
N_{Rx}	Noise into receiver input dBm
N_{Total}	Total noise into demodulator including NF
Nx	Interference Noise

P	Transmitter EIRP in dBm
P_d	Detection Probability
P_f	False Detection Probability
P_{Pop}	Subscriber Population
P_{Rx}	Received Packets
P_{Tx}	Transmitted Packets
REN	Receiver Equivalent Noise
RSS	Received Signal Strength in dBm
SI	Sterilisation Index
SL	Sensor Egli Propagation loss in dB
SNR	SNR in dB
SF	Scaling Factor
τ_{Delay}	Signal delay between transmitted signal and received
TF	Egli Terrain Factor in dB
V	Model Volume
X	Sensor Output
X_C	RF Energy for a BER of 2×10^{-6} using the Egli Propagation model terrain factor of 99.9%.
X_0	Sensor output for a BER of 2×10^{-6} using the Egli Propagation model terrain factor of 90%.
X_u	Sensor output for a received signal strength of -120dBm

LIST OF FIGURES

LIST OF TABLES

Chapter 1

1. INTRODUCTION

Mobile communications have become key to every part of our lives from working to our leisure time. Over the last 15 years the mobile phone has become much more than a device to have conversations on. It has developed into a smart device which can interact with the user. Data traffic over mobiles has grown by 400 million times in the last 15 years which is due to the explosion of applications for the smartphones such as music, interactive gaming, video streaming and web browsing to email (Cisco, 2016).

With the emergence of Long Term Evolution (LTE) 4G technology and smart devices, mobile data traffic has exploded to a huge 3.7 exabytes per month in 2015 and is predicted to be upwards of 30 exabytes by 2020 (Cisco, 2016). The major services and applications fuelling this data traffic increase include search sites, social media sites, online medical consultation, emergency service support and video online gaming. In the future however, there will be further traffic explosion with so-called *machine to machine* (M2M) applications, driven by the Internet of Things (IoT) (Nekovee, 2011). A year-by-year breakdown of mobile data traffic forecasts up until 2020 is shown in Figure 1-1 (Cisco, 2016):

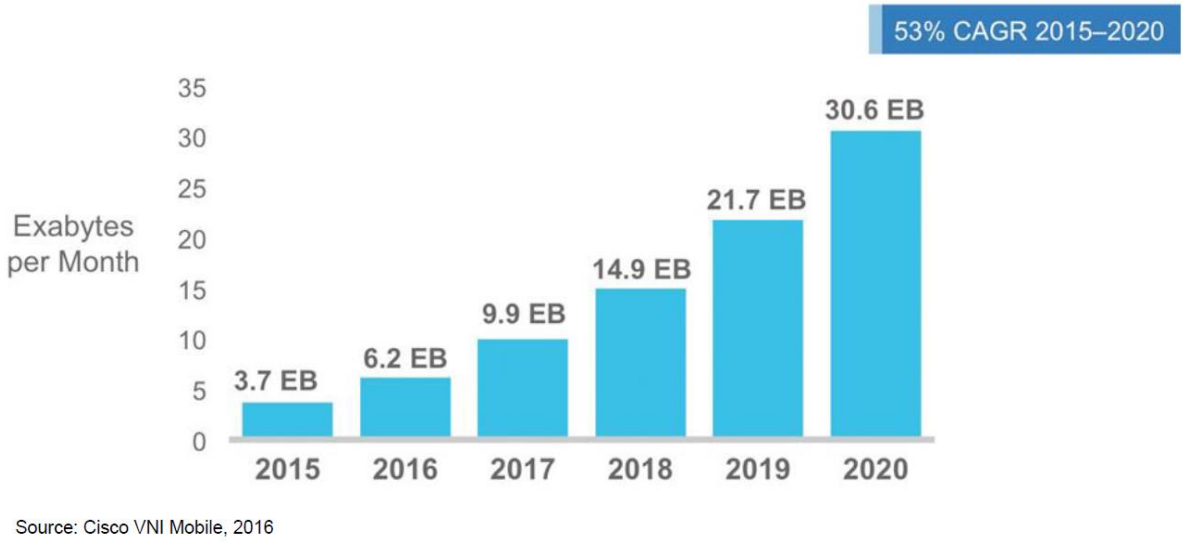

Figure 1-1: Cisco traffic forecast for mobile data traffic up to 2020 (Cisco, 2016)

As evermore applications and services are developed, this dramatic growth in user data traffic has led to the legacy channels becoming congested with the corresponding imperative of requiring more spectrum. This motivated both regulatory bodies and commercial companies to investigate strategies to increase the efficiency of the existing spectrum. Some prominent examples of these are the introduction of LTE which employs *orthogonal frequency-division modulation* (OFDM) technology to improve bandwidth efficiency and heterogeneous networks, which enable data traffic to be offloaded from one technology to another, such as from LTE to Wi-Fi and vice versa.

With 5G mobile technology evolving, there are two viewpoints emerging as to how this will occur: i) a focus on greater coverage (GSMA, 2014) (NGMN, 2015) (EPRS, 2016), ii) increasing throughput and lower latency (GSMA, 2014) (NGMN, 2015) (EPRS, 2016). This thesis provides a framework for how TVWS can effectively address both these criteria to allow 5G services to not only utilise the increased spectrum released by TVWS, but also ensure the long-term benefits of SU access, given that bandwidth scarcity will still be a major issue for 5G.

The techniques discussed so far enable wireless services to occupy existing licensed spectrum in a more efficient way, but in the spatial and temporal domains there is unlicensed spectrum that can potentially be utilised by unlicensed or so-called *secondary users* (SU). With the emergence of cognitive techniques (Akyildiz et al, 2009), (Haykin, 2005), and the transfer of TV channels from analogue to digital platforms, a unique opportunity to exploit unlicensed spectrum by mobile digital service providers emerged, commonly referred to as *TV White Space* (TVWS) (Nekovee, 2011), (Cambridge White Spaces Consortium, 2012), (Nekovee, 2012). The next section will provide some insight into this technology.

1.1 TVWS Overview

TVWS emerged when the terrestrial analogue TV broadcast system was shut down in favour of a more efficient digital platform. The VHF and UHF frequencies that had originally been

allocated for analogue TV broadcasting were separated into two types of spectrum (COGEU, 2009):

- Cleared – the portion of the spectrum released from TV broadcasting and allocated to new applications like LTE technologies.
- Interleaved – this is the spectrum allocated to *digital terrestrial TV* (DTT), which is commonly referred to as TVWS.

DTT receiver antennae are grouped together because a single antenna is unable to cover the whole band (Ægis, 2009), so higher gains can be achieved as only a subset of channels are used at any one location. This means in any geographical area, only a portion of the DTT channels are allocated so the remaining channels are available for potential usage by unlicensed SU.

To illustrate how much bandwidth is potentially available to SU in TVWS, Figure 1-2 shows 18 UK locations, where the red bars indicate the available channels including adjacent *primary users* (PU) channels, while the green bars represent channels excluding adjacent channel PU (COGEU, 2009). When there are adjacent PU channels then without interference management being adopted by the SU then the channel cannot be used. Figure 1-2 reveals that to exploit the available bandwidth, an effective interference management strategy must be implemented to take advantage of the adjacent channel availability. The UK *regulator Office of Communications* (OFCOM) (COGEU, 2009) has indicated that 90% of UK locations have access to at least 100 MHz and 50%, at least 150MHz of bandwidth. This demonstrates that TVWS has the potential to alleviate the issue of scarcity of spectrum for SU access.

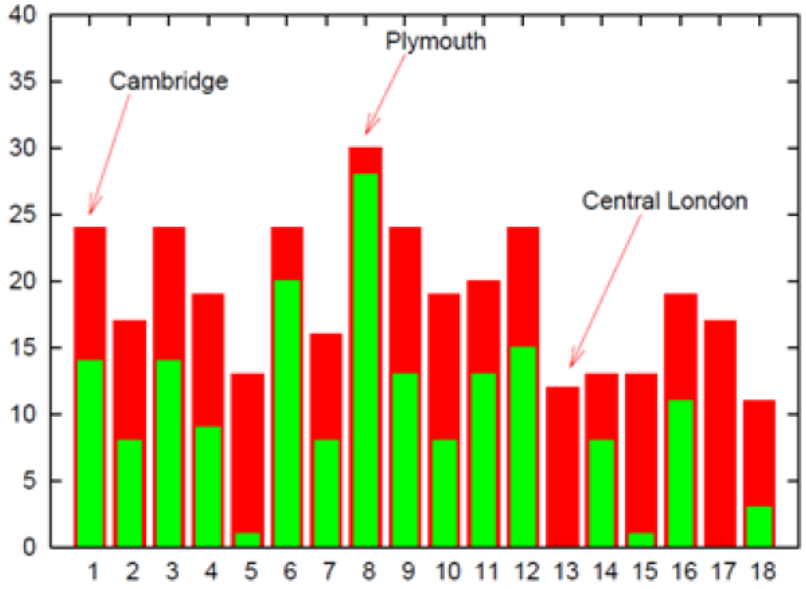

Figure 1-2: Available TVWS channels available in 18 UK locations (COGEU, 2009)

With the availability of TVWS channels and DTT frequencies being in the VHF and UHF bands, both the signal coverage and absorption properties in buildings will be excellent compared to mobile data networks like 4G and Wi-Fi. As a consequence, TVWS represents a fertile opportunity to extend existing licensed spectrum for SU use, particularly given that both the US *Federal Communications Commission* (FCC) and UK OFCOM telecommunication regulators who govern spectrum access in their specific countries, approved rules that would allow broadband mobile devices to operate in TVWS (Nekovee, 2010).

1.2 Research Motivation

From the studies (COGEU, 2009) and (Spectrum Bridge, 2010) which leads to a pragmatic conclusion that although the spectrum plan of licensed TVWS PU users is congested, actual utilisation on a geographical perspective is much lower so offering the potential for opportunist SU access to a significant spectrum capacity, which is currently not utilised.

Having considered the spectrum efficiency benefits of TVWS, the corresponding user benefits will now be considered. In (Nekovee, 2011), emerging applications including

wireless home networks, smart metering, femtocells, mobile broadband and vehicular communications for intelligent transport were identified as lending themselves to potential TVWS spectrum utilisation, particularly as TVWS uses VHF and lower UHF bands, which means good radio coverage and building absorption characteristics. This provides persuasive arguments for investigating how unlicensed access of TVWS can best be exploited considering the aforementioned 5G criteria of increasing coverage, higher throughout and low latency, which allow 5G services to occupy the extra spectrum released by TVWS. This however, brings several major challenges in enabling SU access to PU licensed bands which must be addressed:

1. The main obstacle to TVWS adoption is reliable detection of the PU i.e., TV operators and consumers, allied with the *hidden node* problem **(**Nekovee, 2011) **(**Nekovee, 2012).
2. The avoidance of PU interference which key regulatory bodies like OFCOM and FCC deem mandatory for deploying SU access in TVWS.
3. Once a vacant channel is identified, sufficient resources must be efficiently allocated to a RF channel to enable the required *quality of service* (QoS) provision for SU across all OSI layers.

Wireless access has traditionally been implemented by utilising a licensed framework however with TVWS, consideration to accessing unlicensed spectrum is a key motivation.

To be able to access these TVWS opportunities there are two options. The first is that the regulators encompass this spectrum into a localised PU framework where strict policing will be required to who can or who cannot access a TVWS channel. This would lead to further expensive spectrum auctions on a regional basis which would burden not only the operator from a cost basis but also the regulator would have to put a framework in place to validate legal usage. The final drawback is that once an operator purchases a spectrum allocation then

nobody else can access this so if this operator underutilises the spectrum then it leads to inefficiency of bandwidth which is the very thing this thesis is trying to remedy. The second option however is that the TVWS remains in the SU domain but some smart wireless methods learn about the local RF environment so any operator can access the TVWS channel as long as it does not interfere with the PU and it is free. The second option leads to a more efficient use of spectrum by self-learning which is encompassed by the study of cognitive techniques.

Cognitive techniques develop an understanding of the RF environment around a locality and were first discussed with reference to wireless communications by (Haykin, 2005), with three blocks being introduced which have cognitive functionality:

1. Radio Scene Analysis
2. Channel State Estimation
3. Transmit Power Control and Spectrum Management

The *Radio Scene Analysis* block provides a snapshot of the local RF environment to be used to make spectrum access decisions. The *Channel State Estimation* block also uses this snapshot to estimate the noise level so a channel capacity estimation can be derived. Finally, the *Transmit Power Control and Spectrum Management* block uses the output from the other two blocks to decide whether a channel can be used for secondary access, and if so, to allot the transmit power.

These elements outlined are required to be able to utilise licensed spectrum by a SU which is the reason cognitive techniques are the obvious choice of framework to implement SU access control.

The aim of this thesis is to investigate how best to resolve the above challenges and develop an efficient and robust cognitive TVWS access solution for SU access.

1.3 Research Questions and Objectives

From the discussion in Sections 1.1 and 1.2, the following overarching research question addressed in this thesis was framed:

"How can cognitive techniques provide efficient TV White Space access?"

To facilitate unlicensed user access of unused DTT channels, knowledge of the local PU spectral environment must be dynamically obtained in order to make decisions on potential SU channel allocations. This is a rich area for investigation as it not only mandates novel interference management schemes so RF resources are strategically allocated to always ensure PU interference is avoided, but also new algorithms need to be developed so the available SU resources are maximised to provide the best QoS provision which in this thesis will be defined by the following metrics: coverage, packet error rate and latency. The proposed solutions also must be sufficiently generic and flexible so it can be deployed in different countries and offer consistent accurate performance across a variety of network scenarios. It is against this background that the following three key research objectives were formulated:

1. To design and critically evaluate solutions for accurately detecting DTT PU channels to exploit TVWS opportunities.

   Justification: As highlighted in Section 1.2, one of the major limitations hurdles for SU access of TVWS is its potential interference impact upon a licensed PU. This objective therefore seeks to investigate and develop a pragmatic sensing solution which accurately detects the PU and exploit this information through the way the PU DTT channels are deployed.

2. To develop an integrated interference management model for SU access within a TVWS framework and resolve the hidden node issue which is where the PU transmitter is shielded from the SU sensor by an obstruction.

*Justification: D*evelop possible solutions to the specific spectrum detection *Hidden Node Problem* and effective DTT interference management and power control in the SU transmitter. This objective also allows the SU to occupy adjacent channels to the PU so that it increases the available spectrum to the SU by managing interference.

3. To critically synthesise a SU access mechanism for maximising the QoS provision within the new interference management model.

Justification: This seeks to construct an innovative approach for TVWS channel re-use, using the developed mechanisms to maximise the bandwidth available to a TVWS SU network in a specific locality, without crucially impacting upon the PU. Due to the imbalance of allocated PU and SU RF power by regulators there is a requirement to be able to maximise the coverage area due to the lower SU mobile power. In doing this the SU QoS is increased.

The next section describes the thesis contributions.

1.4 Contributions

i) A new DSA technique has been designed and developed called the *enhanced detection algorithm* (EDA) to specifically address the challenge of PU detection in TVWS by exploiting the unique deployment properties of DTT frequencies in both the UK and America. EDA employs a fuzzy logic inference model which converts a basic energy detector into a feature detector to resolve uncertainty in the DTT signals.

The performance of EDA has been critically analysed and subsequently extended to a *generalised enhanced detection algorithm* (GEDA), which introduces adaptive functionality into the PU sensing process to ensure both OFCOM and FCC regulatory PU detection requirements are consistently upheld.

ii) An innovative solution to the hidden node issue is then proposed. By embedding a *keep-out contour* into GEDA, an interference management strategy for PU protection is framed, with GEDA specifying the permitted transmit RF powers for SU at call set-up, not only ensuring PU do not experience interference, but concomitantly maximising the SU QoS experience from a coverage perspective.

iii) The available SU bandwidth is framed as a QoS metric embodying a *sterilisation index* (SI) which avoids recourse to using physical surveys. Importantly, the SI considers hidden nodes to maximise the available SU bandwidth on a channel and location basis.

iv) Under existing TVWS regulatory requirements (Nekovee, 2012), SU *base stations* (BS) transmit at much higher RF power compared to SU mobile units, so to achieve SU coverage, the uplink signal, from the mobile device to BS, needs to use some innovative routing processes to achieve the additional coverage through a multi-hop networking arrangement. A new cross-layer routing model has been developed and critically evaluated to improve key SU transport QoS metrics of packet error rate and latency. By both minimising packet delay and maximising traffic throughput, this new routing algorithm maximises the QoS provision for SU accessing TVWS.

Figure 1-3 shows the thesis contributions against research objectives.

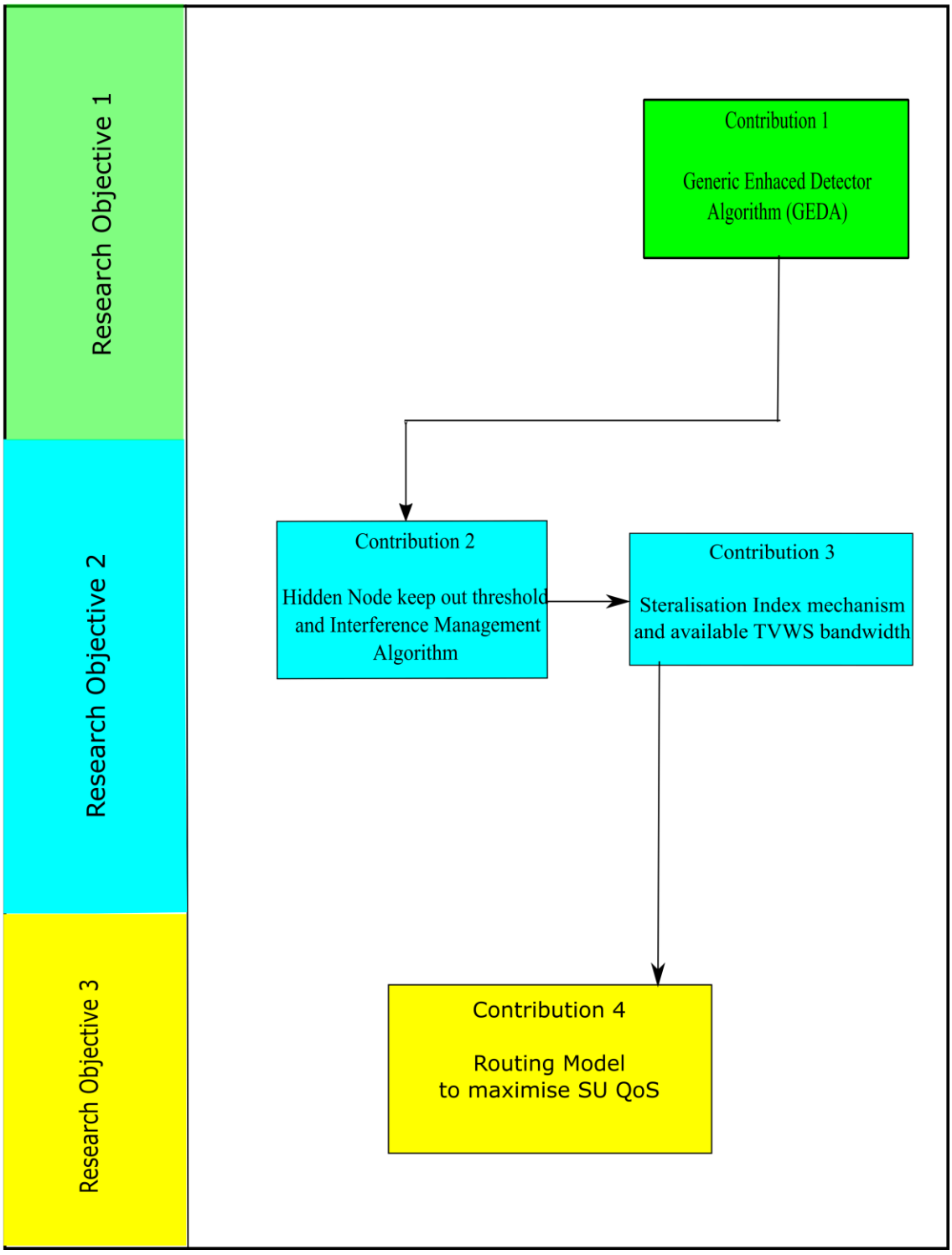

Figure 1-3 Mapping of Research Objectives to Contributions

The following section outlines the thesis structure.

1.5 Thesis Structure

The rest of the thesis is organised as follows:

Chapter 2 presents a rigorous literature review that explores the underlying principles of TVWS, cognitive radio, cross layer processing, wireless routing methodologies. The chapter discusses their roles and the way they be applied to wireless networks.

Chapter 3 details the research methodology adopted, the choice of simulation test platform, the various performance metrics and comparators used for critical evaluation and the software validation processes.

Chapter 4 introduces a new *enhanced detection algorithm* (EDA) which utilises the unique patterns in DTT channel frequency deployment to determine whether a PU is occupying a DTT channel. It importantly turns an energy detector into a feature detector so detection performance can be improved. Work from this chapter has been published in (Martin et al, 2011) and (Martin et al, 2013).

Chapter 5 presents the *generic EDA* (GEDA) model as an extension to the EDA sensing technique developed in Chapter 4. By introducing an adaptive sensing mechanism, the PU detection performance is significantly improved. Work from this chapter has been published in (Martin et al, 2013) and (Martin et al, 2016).

Chapter 6 resolves the important hidden node problem in TVWS by means of a new interference management strategy which applies GEDA to establish a *keep out contour* to protect the DTT PU receiver from interference. This interference management approach not only ensures PU interference protection, but also allocates resources to support unlicensed SU services within TVWS. Work from this chapter has been published in, (Martin et al, 2011), (Martin et al, 2013) and (Martin et al, 2016).

Chapter 7 critically analyses the available resources for SU accessing TVWS which arise directly from instigating the new *keep out contour*. A *sterilisation index* (SI) is introduced as the measure of the extra resources accessible by SU as a corollary of

bandwidth being strategically sterilised for DTT PU usage. Work from this chapter has been published in (Martin et al, 2013) and (Martin et al, 2016).

Chapter 8 critically reviews how MANET routing can address the RF power imbalance in SU base stations and mobiles in the reverse link direction to provide greater coverage and so improve the SU QoS.

Chapter 9 explores some possible future research directions which can be leveraged from the new TVWS access framework, while Chapter 10 draws some overarching conclusions on the main findings and significance of the new framework, set against alternative existing TVWS solutions.

1.6 Summary

This chapter has outlined the research objectives to allow SU users to access TVWS channels and the possible issues such as DSA solutions, hidden node issue and interference management, assessing the resources available to TVWS and a solution to address RF power imbalance in regulatory inputs. The next chapter investigates the work already done in these areas.

Chapter 2

2. LITERATURE REVIEW/BACKGROUND

2.1 Introduction

A key driver for researching *Cognitive Radio Networks* (*CRN*) in a TVWS context is the omnipresent problem of the scarcity of available spectrum (Akyildiz, 2009), (Haykin, 2005) in which *CRN* can offer an efficient means of alleviating this spectrum requirement. *CRN* using sensing offers a totally autonomous system to the PU which can sense the RF environment around it to make spectrum decisions **(**Nekovee, 2011) **(**Nekovee, 2012).

TVWS is a prime candidate for exploiting CRN behaviour because it is static spectrum so channels do not change in a particular location. This relaxes the requirement of efficient primary user (PU) updates since channels change only on a spatial rather than temporally basis (Nekovee, 2011), (Cambridge White Spaces Consortium, 2012). In order to exploit unused TVWS spectrum, spectral holes (Akyildiz et al, 2009), (Haykin,, 2005) must be identified using dynamic spectrum access (DSA) techniques (Akyildiz et al, 2009), (Cambridge White Spaces Consortium, 2012). These can be broadly classified into three categories: beacons, sensing and static databases (Nekovee, 2011), (Nekovee, 2012). DSA techniques are used by CRN to enable it to learn about the RF environment around it and to make spectrum decisions. DSA techniques which are applicable to TVWS are described below:

Beacons are dedicated in-band signals that advertise whether a secondary user (SU) (Nekovee, 2011), can use a PU DTT (Digital Terrestrial TV) channel. However, since the PU has to administer this process, it is not a viable option for DTT broadcasters due to the prohibitive overheads incurred.

Sensing techniques (Nekovee, 2011), in contrast, automatically update a PU static database without human intervention so reducing operational costs while increasing accuracy by dynamically accommodating local variations in propagation. Traditional sensing approaches

include matched filtering, cyclostationary, feature detection and energy detection, with a critique of the gamut of available sensing methods being given in (Akyildiz et al, 2009).

Static databases require manual maintenance, and while system accuracy can be compromised because data is calculated from a theoretical algorithm rather than actually being measured, this option offers greater flexibility in accommodating special scenarios where sensing is not viable. Examples include program making and special events (PMSE) radio microphones **(**Nekovee, 2011), where a temporary licence is given for instance for a venue or auditorium.

To give context for DSA discussion, the principle of CRN, the background and potential of TVWS, and regulatory issues are explained in Section 2.2, 2.3 and 2.4 respectively. A review of the technologies enabling sensing solutions is given in Section 2.5, while existing research on sensing solutions is analysed and reviewed in Section 2.6. Finally, the finding of this literature review and the summary of the Chapter is presented in Section 2.7.

2.2 Cognitive Radio Networks

2.2.1 Introduction

A *cognitive radio* (CR) has to perform tasks which can be classified as either configuration or cognitive in nature. The configuration part is conducted by the *Software Defined Radio* (SDR) while cognitive tasks depend on signal processing and machine learning processes. These tasks are classified in (Haykin, 2005) in Figure 2-1 below:

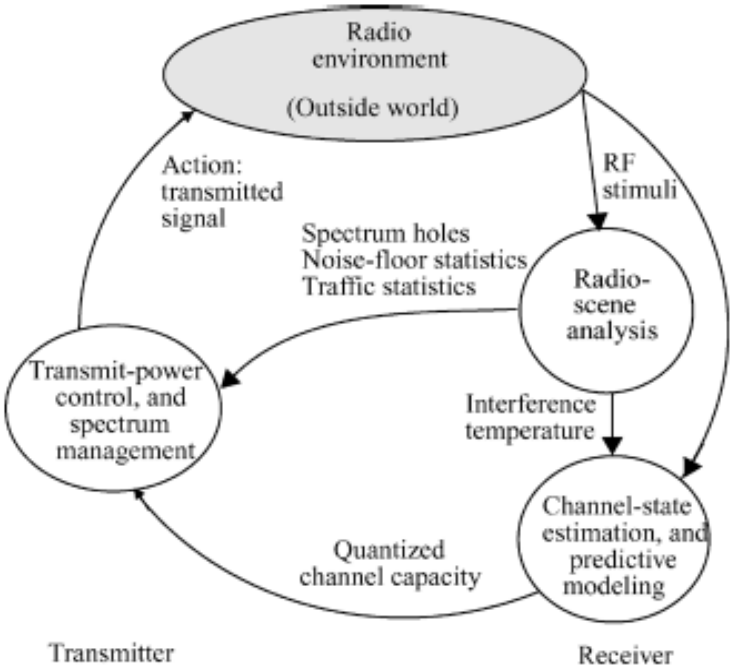

Figure 2-1: CR Tasks (Haykin, 2005)

The tasks classified in Figure 2-1 can be distinguished from legacy radio control functions in that they are receiver rather than transmitter centric which allows a CR node to be autonomous within a network.

The ***radio scene analysis*** is performed at the receiver which forms the DSA function in which it performs spectrum hole detection and an evaluation of the interference temperature. The spectrum hole detection information is passed to the transmitter for power control and spectrum management along with noise floor and traffic statistics so that channel decisions can be made.

The ***Channel-state estimation*** takes the interference temperature from the Radio scene analysis and the RF stimuli and uses predictive modelling of the channel capacity so a certain QoS can be established. The transmission power can then be adjusted accordingly to obtain the required capacity and QoS. In (Haykin, 2005) it is stated that the ***transmit power control and spectrum access*** is implemented in the SU transmitter. However, to overcome the hidden node issue in TVWS it is argued that this needs to be dictated to the SU mobile transmitter by the SU base station due to a lack of PU knowledge by the mobile receiver due to the lower SU receiver antenna height.

This model is found extensively in the literature reviews in which it seems to be have become the de-facto CR model in all major forums (Haykin, 2005) (Akyildiz et al, 2009) (Mitola et al 1999) (Akyildiz et al, 2006). The sensing technique enables the static database to be updated without any human intervention therefore reducing operational cost and increasing database accuracy due to dynamic adjustments accommodating local propagation variations. For this reason, the next section examines the factors determining how to decide whether spectrum holes exist and a review of the sensing technologies employed to enable this.

2.2.2 Sensing Strategies

The radio scene analysis outlined in the CR model primarily involves the detection of spectrum holes (as demonstrated in Figure 2-2) (Haykin, 2005) which are gaps in the licensed spectrum with no PU activity which are candidates for opportunistic CR access. The second activity is to provide a measurement of the interference temperature which is a measure of the overall level of interference (all signals within the environment) of RF signals in the locality and is expressed in degrees Kelvin.

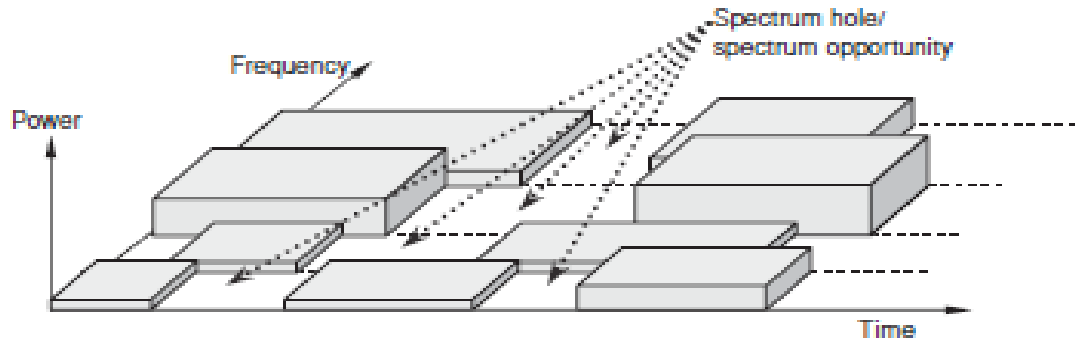

Figure 2-2: Spectrum Holes (Haykin, 2005)

The major activity required for these two goals is to be able to accurately sense the RF environment.

The following section outlines the implications of different sensing strategies. (Haykin, 2005).

The various sensing strategies for spectrum hole detection and the estimation of Interference temperature can be categorised into the following techniques:

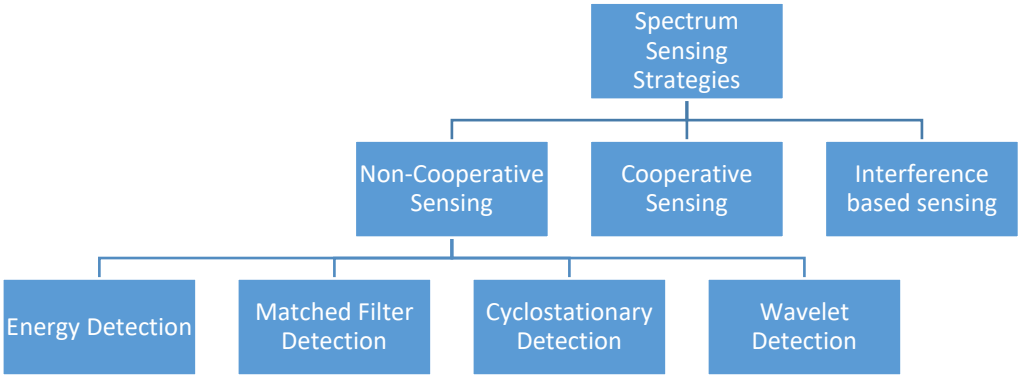

Figure 2-3: Sensing Techniques (Haykin, 2005)

In Figure 2-3, non-cooperative and cooperative sensing techniques are PU transmitter centric, while interference-based sensing is PU receiver centric. For non-cooperative sensing, the different techniques shown in Figure 2-3 are stand-alone solutions, while for cooperative sensing, the same techniques can still be applied with communication links between the sensors sharing information, so a community of sensors make the access decisions instead of only one. For interference-based sensing, the PU receiver local oscillator leakage is sensed instead of the PU transmitter channels.

In a practical network, the most suitable solution to RF sensing for spectrum access and an estimate of interference temperature would be a mixture of non-cooperative, cooperative & Interference based due to the possibility of the hidden node issue.

The two possible solutions would be to use non-cooperative input to form a collective cooperative sensing output based on a community of sensors. The alternative solution would be to use interference based sensing (PU centric) with non-cooperative sensing. Both have benefits to the solution but this will form a part of the research to decide the most appropriate

solution. However, further in this thesis a non-cooperative sensing solution is proposed which is resilient to the hidden node issue alleviating the network complexity the Cooperative sensing would introduce. The sensing solutions are discussed in detail below:

Non-Cooperative Sensing

The table below shows the advantages and drawbacks of each non- cooperative sensing framework.

Table 2.1: Comparison of Detection Strategies

Strategy	Advantages	Drawbacks
Energy Detection	No prior knowledge of PU signal Low Implementation cost	Prior knowledge of noise environment Poor performance at low SNR Cannot distinguish between PU or SU
Matched Filter	Optimal detection performance Low implementation cost	Needs prior knowledge of the PU signal Requires a separate design for each PU type
Cyclostationary	Good performance in low SNR Good tolerance to interfering signals	Requires partial knowledge of PU High implementation cost
Wavelet detection	Effective for wideband sensing	Does not work for Spread Spectrum signals High implementation cost

Energy detection can be seen as optimal since no a priori PU knowledge is assumed, while the receiver assumes only Gaussian noise power. However, it performs poorly in low SNR environments so some knowledge of the local interference noise environment is required to improve detection performance. This is complex to determine due to the unpredictability of interference noise. The Energy Detector is attractive because of its low cost, ease of implementation and that no PU information is required but its performance under low SNR's is a major drawback.

The Matched Filter method maximises the SNR of the received signal in the presence of Gaussian noise to produce an optimal detection method (Haykin, 2005) (Chen and Prasad, 2009). This method requires prior knowledge of the desired signal at both the Physical and MAC layers, so is a form of feature sensing and achieves detection by correlating the unknown signal with a known signal. This method can be used even if only partial knowledge is known of the PU signal. Such partial knowledge could be a pilot signal, preamble or spreading codes which can be used for coherent detection however there needs to be a separate implementation design for each PU given the characteristics change depending on the application.

A cyclostationary detector utilises the periodicity of a signal to detect occupancy (Haykin, 2005) (Chen and Prasad, 2009). First the Spectrum Correlation Function (SCF) is obtained and then the detection is completed by searching for a unique cyclic frequency corresponding to a peak SCF value. Cyclostationary detectors can distinguish noise energy from signal energy but require longer detection periods than energy detectors and partial knowledge of the PU to determine the unique cyclic frequency. Cyclostationary detectors thus have high computational overheads and are complex to implement.

The Wavelet method offers specific advantages to detecting wide band signals in terms of implementation cost and flexibility. In a traditional method multiple, band-pass filters would be used, increasing cost and reducing the flexibility, hence the Wavelet method would be an effective way to detect wide band signals (Chen and Prasad, 2009).

Initial research activities shall be utilising the energy detector because of its ease of implementation and enhanced by CLP algorithms to produce a "feature" detector using a matched filter coupled with an energy detector.

Cooperative Sensing

Cooperative sensing techniques incorporate an array of sensors which share their measurements to decide whether to permit a licensed channel for SU use. This gives geographical diversity to overcome single sensor errors caused by the PU being obstructed. There is a proposed cooperative sensing strategy for CR which is based on the Rao statistical technique in the presence of non-Gaussian noise (Zhu et al, 2013) and this will be examined in further detail later in this chapter.

In the non-cooperative sensing framework, there can be a circumstance when a PU transmitter is hidden from the SU (xG in Figure 2-4) sensing receiver due to range (Figure 2-4a) or large objects which cause shadowing effect (Figure 2-4b). This effect is called the "hidden node problem" (Haykin, 2005), (Chen and Prasad, 2009), (Akyildiz et al, 2006).

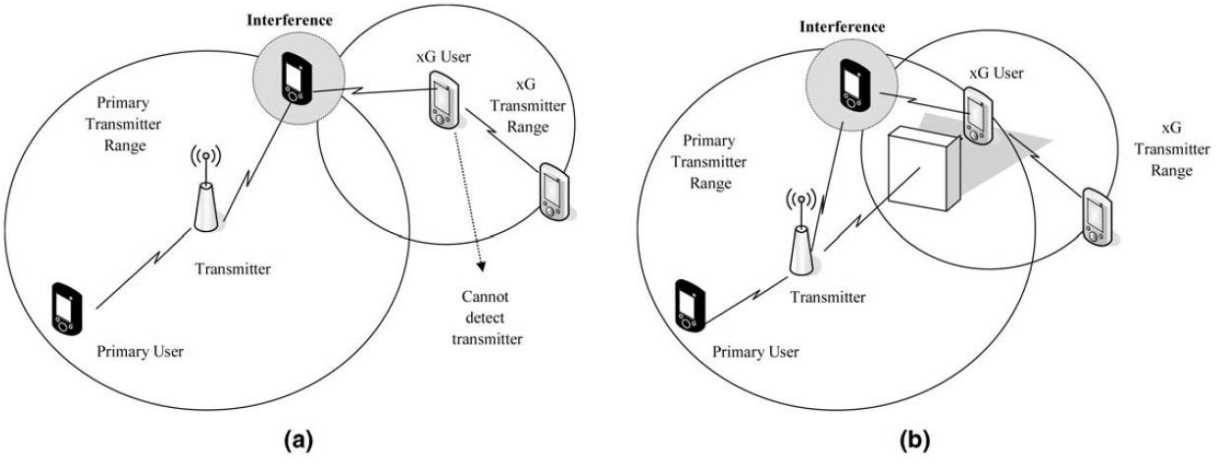

Figure 2-4: Hidden Node Problem (Akyildiz et al, 2006)

To overcome this effect cooperative sensing can be utilised where a community of SU sensors share their sensing results with each other over a shared engineering/control channel. This technique will have to be researched more rigorously for the regulators to authorise the use of CRN (Haykin, 2005), (Chen and Prasad, 2009), (Akyildiz et al, 2006).

The research challenge in this area is how to implement a rigid architecture to be able to share the sensing information but at the same time being flexible enough to have mobile SU join and leave the CR community. To enable a solution which would be considered by the regulators the SU attachments to a SU base station need a controlled . This will be considered as a key part of this research project.

Interference Based Sensing

Interference-based strategies require a PU receiver to share its noise/interference sensing levels with the SU so an acceptable Interference Temperature level for the PU can be established (Chen and Prasad, 2009). In (Ghanekar et al, 2014), a local oscillator leakage solution is proposed which detects low-level transmissions from a local oscillator in a multi-stage receiver, while in (Kuhn, 2013), the low level of this leakage signal cannot be detected beyond 50m from the receiver, which is unlikely to protect the receiver from interference, as will be investigated further in Chapter 6.

2.2.3 Time – Frequency Distribution

Due to the non-stationary behaviour of the PU signal, (Haykin, 2005) concluded that any detection method needs to take account of the time element as well as the frequency in the signal statistics. This means a raw periodogram does not make a good spectrum estimator due to spectral bias and variance issues (Haykin, 2005), (Cristian and Walden, 2002).

For these reasons, a *Multitaper Estimator method* (MTM) is proposed in (Haykin, 2005), (Cristian and Walden, 2002), with the input signal being sub-divided into sufficiently short frames that they can be considered as quasi-stationary but long enough to produce an

accurate spectral estimate. This is a nonparametric method and optimal over wide bands of frequencies. It utilises Slepian sequences called eigenspectra (Fourier Transform) to obtain the maximal energy concentration and hence overcomes the bias and variance issues identified in the periodogram (Haykin, 2005), (Cristian and Walden, 2002).

From the arguments above, MTM would be an option if the PU signal varied temporally but the PU spectrum we shall be considering i.e. TVWS will not. For this reason, a raw energy periodgram will be sufficient to detect spectrum holes for the TVWS scenario.

2.2.4 Interference Temperature

This is a measure of RF power at a receiver antenna caused by other emitters and noise sources per unit bandwidth. It is expressed in °Kelvin. The distribution of the interference temperature varies with time, but a limit will be set by the regulatory bodies to not impact the licensed signal. An example distribution of receiver power with distance from a PU transmitter is shown in Figure 2-5 where the interference temperature limit determines the service:

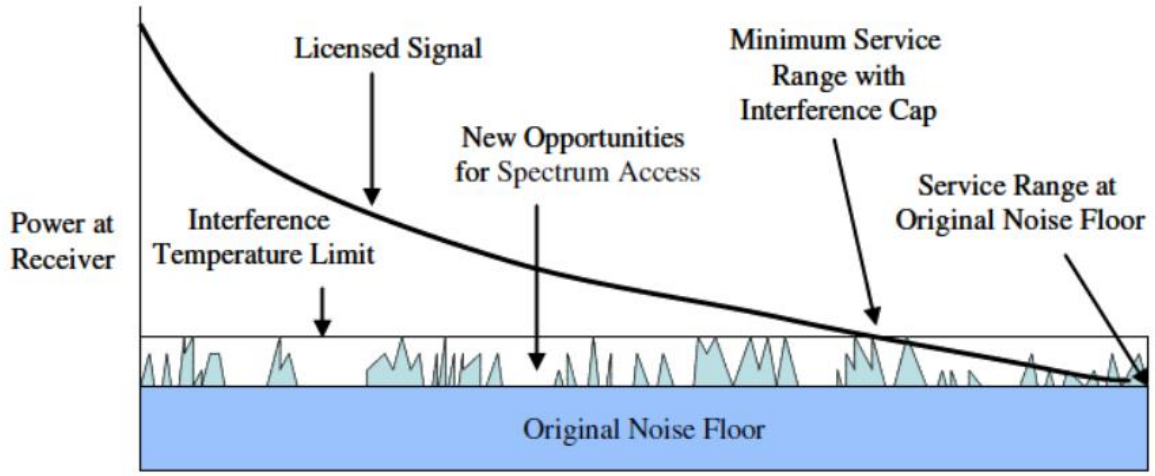

Figure 2-5: Interference Temperature Model (Akyildiz et al, 2006)

Unlike the traditional transmitter-centric approach, the interference temperature model manages interference at the receiver through the interference temperature limit, which is

represented by the amount of new interference that the receiver could tolerate and still maintain a coverage distance which is defined by the minimum service range.

The MTM can be used to measure the interference spectral power so the interference temperature can be calculated (Haykin, 2005), (Cristian and Walden, 2002). This measurement is made up of the unwanted external RF interference noise and internal receiver noise. To eliminate the internal noise component, *singular value decomposition* (SVD) is used with MTM to give the external interference noise spectral power alone and hence the interference temperature.

To overcome geographical variations multiple Sensors (antennae) then cooperative Sensing can be used to increase accuracy.

2.2.5 Determining Channel Capacity

To be able to predict the channel capacity for a CR network, the Channel State Information (CSI) needs firstly to be estimated. Using statistical techniques, one can then predict the CR channel capacity (Haykin, 2005), (Chen and Prasad 2009), (Hossain et al, 2009), (Bhalani et al, 2009), (Hosseini et al, *2009)*.

There are two conventional methods in obtaining the Channel State Estimation:

- Differential Detection – Simple and robust and lends itself to M-ary Modulation but has a degraded Frame Error Rate (FER) vs. SNR performance at the receiver.
- Pilot Transmission – This technique utilises a periodic training sequence known to the receiver which leads to an improved receiver performance. However, this has a cost of being wasteful in channel bandwidth and transmission power.

To overcome these drawbacks and to realise a more efficient of way to estimate the channel state another method was considered called *Semi-Blind Training* (Haykin, 2005), (Bhalani et al, 2009). This is seen to be a more efficient process due to the two operational modes:

- Supervised Training Mode – In this mode, the receiver acquires the channel state by using a limited duration short training sequence (Two to Four symbols known to the Receiver). Once the estimate has been obtained the Supervised Training Mode is switched off and the tracking mode is entered.
- Tracking Mode – Data transmission in which an unsupervised continuous monitoring of the data transmission performance is under taken.

The semi-blind training is a well proven technique seeing it is used in other applications such as channel encryption to synchronise keys. This form of synchronisation is used in the transport layer security (IP) where a handshake phase to establish the secret key is used then it enters a data transmission phase where it monitors the secret key (Forouzan and Fegan, 2003).

2.3 TV White Space

Throughout most countries in the world, the terrestrial TV broadcast networks are changing from an analogue to digital delivery platform. This has already been completed in North America and the UK, as well as Europe (Nekovee, 2010), (Hossain et al, 2009), (Fitch et al, 2011). However, the switchover process has continued apace because during migration, there were maintenance updates to the channel allocations, with the most recent update being in 2016 for the UK (OFCOM, 2016) and in 2015 for the USA (FCC, 2015).

This conversion released valuable spectrum in the UHF band which in turn can be seen in two areas. The first is known as “Digital Dividend” and is the released spectrum that will no longer be used by the terrestrial TV broadcast networks which will go out to auction to mobile operators for such applications as Long-Term Evolution (LTE). The second known as “TV White Space” or “interleaved spectrum” unused within given geographical locations so as to avoid causing interference to co-channel or adjacent channel DTT transmitters**.** Seeing that the “Digital Dividend” spectrum has gone out to auction then the TVWS is the primary spectrum to consider for CR access.

The DTT conversion process reduced the amount of TV frequency channels and hence some channels have gone to auction, while the rest shall be allocated to DTT channels. The DTT channels (8MHz bandwidth) allocated in the UK are shown in Figure 2-6. Purple channels are allocated to DTT, green channels are cleared spectrum for auction and pink channels are for broadcast applications and RF microphones (PMSE- programme making and special events). The DTT channels in a geographical area that are not utilised are termed TVWS or Interleaved spectrum. It is TVWS that is proposed for CR access (Nekovee, 2010), (Hossain et al, 2009), (Fitch et al, 2011) while interestingly, the most recent series of (FCC, 2015) and (OFCOM, 2016) standards corroborate the adoption of TVWS for this purpose. In Figure 2-6 the channel allocation after digital conversion in the UK is shown and the channels which are proposed for TVWS use is the unused Retained/Interleaved spectrum in any location.

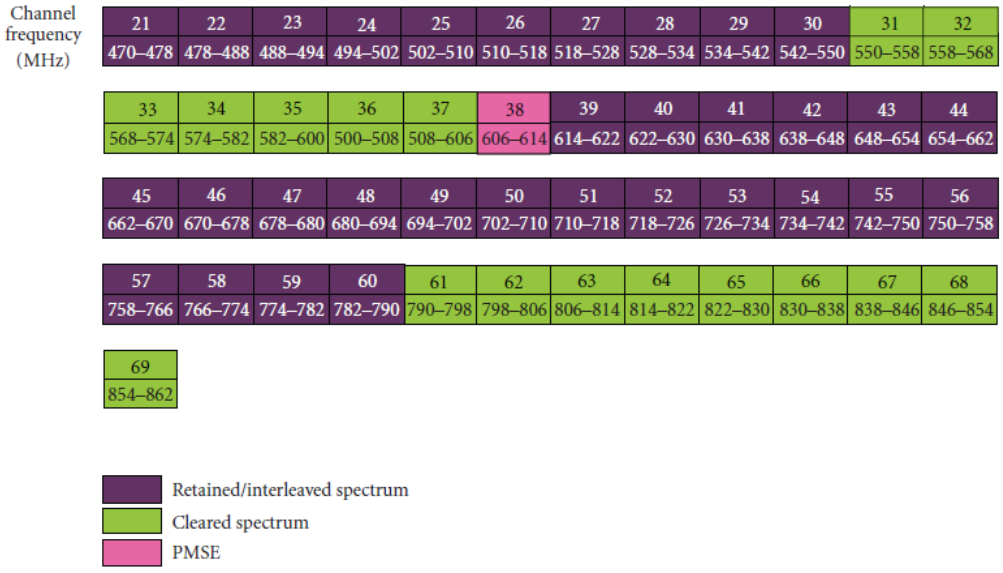

Figure 2-6: Channel allocation after DTT conversion in the UK (OFCOM, 2016)

In (Nekovee, 2010) it has been indicated within the UK that 50% of locations can release 150 MHz of spectrum and from 90% of locations 100 MHz of TVWS. The main issue that is brought out by this point is that any CRN utilising TVWS must be able to allocate non-contiguous channels to its users. Figure 2-7 (each cyan bar represents a free 8MHz channel)

shows the non-contiguous nature of channels allocated to London. It can be seen that the maximum contiguous channel capacity is 16MHz (2 cyan bars together) so to exploit greater capacity, non-contiguous OFDM techniques need to be employed.

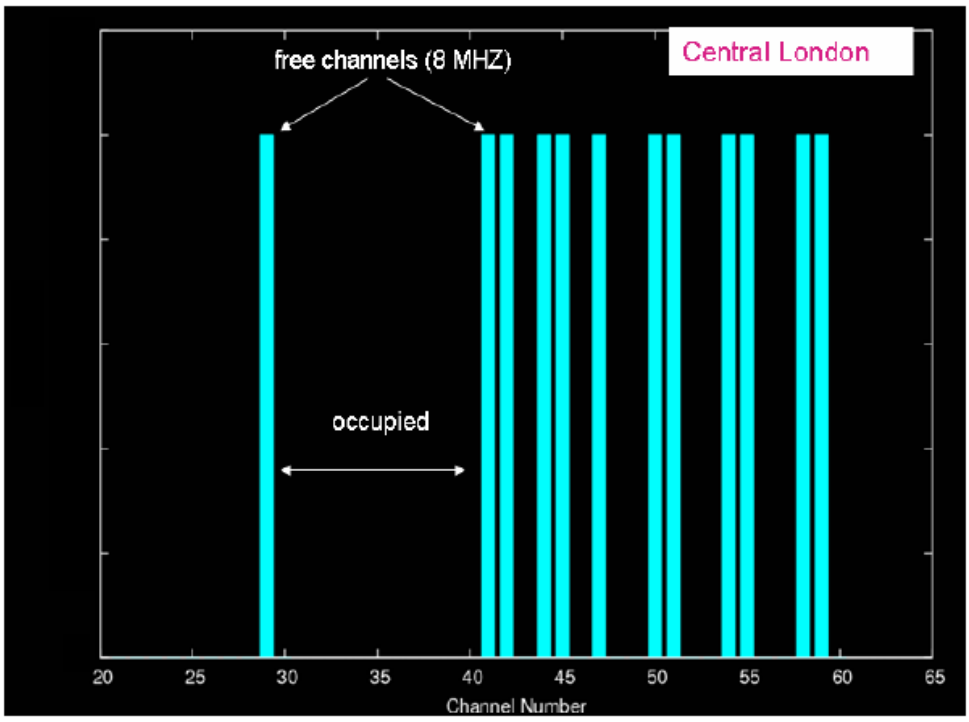

Figure 2-7: Contiguous TVWS Channels in Central London (Nekovee, 2010)

Figure 2-8 gives contiguous capacities for some other locations in the UK.

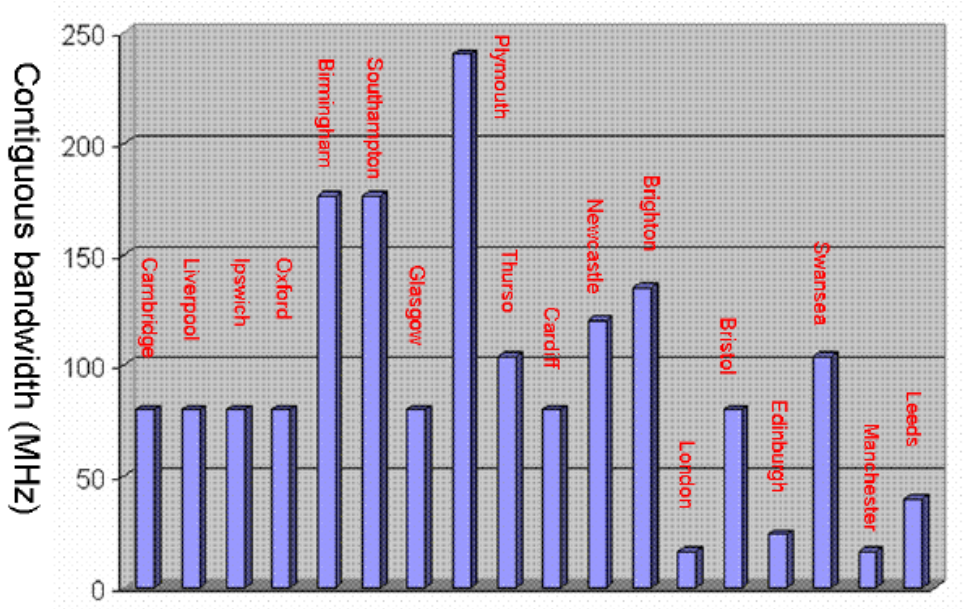

Figure 2-8: Maximum Contiguous capacity values for UK (Nekovee, 2010)

It has been proven (OFCOM 2015), that the minimum number of TVWS channels available in the UK for a SU using a 10m antenna and transmitting at 15dBm, yielded an extra 80MHz of bandwidth for 90% of households and 184MHz for 50% of households, thereby confirming there are significant gains to be leveraged on available SU bandwidth within the TVWS band. The next section will examine the regulatory steps to enable this potential unlicensed bandwidth to be exploited. It is also noteworthy that both OFCOM (OFCOM, 2015) and FCC (Ramjee et al, 2016) have opened a TVWS band for industry proposals.

2.4 Regulatory Issues and Standards

The main consideration for regulatory bodies like OFCOM and FCC is to ensure PU protection within specific country frameworks by establishing the necessary lawful requirements to access licensed spectrum.

In contrast, IEEE and Cognitive Networking Alliance (CogNeA) standards not only address PU protection but also sub-system parameters to maximise the SU QoS such as throughput, from an industrial standardisation point of view. The IEEE 802.22 standard primarily focuses on CR techniques such as sensing for PU detection, power control and DSA to minimise interference to PU and so determines the way a SU can access unlicensed spectrum. The IEEE 802.11af standard considers an implementation of a Wi-Fi WLAN within TVWS frequency band which is focused on the SU. The CogNeA standard is focused on the unification of SU handsets so to maximise interoperability between different manufacturers.

2.4.1 Regulatory Issues

Both FCC and OFCOM consider three methods of access to TVWS so the PU will not be impaired. These three techniques are beacon, geo-location with database (Static database with GPS location knowledge of SU) and sensing described in (Nekovee, 2010), (Hossain, 2009), (Fitch et al, 2011).

In 2008 FCC (US) adopted the second report (Nekovee, 2010) which detailed the rules (FCC, 2012) for CR TVWS access:

The Geo-location and database technique needs to be used for access. However, if a CR node without GPS was connected to a base station which had GPS then this would be acceptable. Any sensing proposals would need to be tested in FCC Labs and to incorporate wireless microphones with a need to detect signals down to -114dBm. This is not practical to achieve since if the technology was available to create this performance it would also produce a problematic effect of false detection where it detects adjacent DTT transmitters which are not operational in the area.

Fixed CR devices could use a transmitter power of 1W Effective Isotropic Radiated Power (EIRP) (FCC, 2012). However mobile CR devices can only use 100mW or 40mW if there are adjacent DTT channels.

In July 2009 OFCOM issued a statement (Nekovee, 2010) detailing that in principle they supported license exempt access to TVWS and this included sensing and Geo-Location and database as the means for access. However, in the short term, geo-location is the most important means of incumbent detection.

During June 2011, a consortium of Telecommunications Operators and equipment vendors came together to test the feasibility of using TV white spaces in locations around Cambridge (Cambridge White Spaces Consortium, 2012).

The Cambridge Trial was designed to assist OFCOM in devising a standards framework proposal for license exempt access to TV White Space spectrum. This objective was achieved by devising measurement tests which measured the impact of using secondary access on the primary users. This helped stipulate protection requirements to maintain the integrity of the primary user, Digital Television (DTT).

The second objective was to stimulate the interest of industry to exploit secondary access technologies to deploy services which would benefit the user. This objective was achieved

by creating a sample set of applications with a number of industry IP/Access vendors and operators. The selected applications were:

- Broadband access in rural areas
- Urban broadband coverage with the option of offloading data from congested mobile broadband networks
- 'Smart City' applications
- Location-based services and local content distribution

Some of the recommendations arising from the technical work carried out during the Cambridge trials are as follows (Cambridge White Spaces Consortium, 2012):

- The trial demonstrated the value of utilising TVWS to deploy the applications listed above in rural and urban environments. Administrations and regulators should recognise the economic and social benefits that TVWS and database enabled access would bring to increase spectrum efficiency.
- The trial successfully tested TVWS concepts to allow co-existence with primary users (DTT and PMSE) namely geo-location database access. It is thought that the database access can cater for flexible and changing nature of the spectrum so to allow new applications to be developed on the TVWS platform but also secure the QoS for the PU.
- Administrations should investigate and where possible, test the benefits of statistically modelling the assumptions and variables used in the geo-location database. Where appropriate, factors should be incorporated into the geo-location database to ensure that interference mitigation is proportionate and not wholly based on a combination of worst case reference geometries, coupling factors and protection ratios.

- Spectrum monitoring could have a role to play in establishing the efficient use of spectrum by increasing the transparency of its use – both authorised and unauthorised. Real-time networks of low-cost monitoring nodes could help white space applications to optimise the selection and use of channels indicated as available by a geo-location database. Administrations should recognise the value of spectrum monitoring and consider promoting its use as part of a progressive approach to managing spectrum more efficiently.

Both the UK OFCOM and the USA FCC regulators have recently adopted standards allowing new CR broadband devices to operate in TVWS (Nekovee, 2011), (Nekovee, 2012), (Lei Qiu Jing et al, 2011), (Chen and Gao, 2011). The key TVWS engagement parameters specified by OFCOM, FCC and the IEEE 802.22 standard (Nekovee, 2012) (FCC, 2012) are defined in Table 2.2. These include: the PU probabilities of detection and false detection; DTT sensing noise floor, SU transmit RF power for a *Base Station* (BS) node in the presence of PU adjacent channels; and SU transmit RF power for a mobile node in the presence of PU adjacent channel.

Table 2.2: Regulatory TVWS engagement parameters (Nekovee, 2012) (FCC, 2012)

Rule	Parameter	OFCOM	FCC	IEEE802.22
1	DTT Sensing Threshold	-120dBm	-114dBm	-114dBm
2	Wireless Microphone Threshold	-126dBm	-114dBm	-114dBm
3	SU Transmit Power Fixed Network Node 1st Adjacent Ch - $P_{BS(N+1)}$	4dBm	16dBm	-
4	SU Transmit Power Fixed Network Node 2nd Adjacent Ch - $P_{BS(N+2)}$	17dBm	30dBm	36dBm
5	SU Transmit Power Mobile Network Node 1st Adjacent Ch - $P_{M(N+1)}$	4dBm	16dBm	-
6	SU Transmit Power Mobile Network Node 2nd Adjacent Ch - $P_{M(N+2)}$	17dBm	20dBm	-
7	Out-of-Band powers	<-46dBm	-55dBc	-
8	DTT Bandwidth	8MHz	6MHz	6MHz
9	Probability of Detection	1	1	0.9
10	Probability of False Detection	-	-	0.1

Both the OFCOM and FCC parameter settings in Table 2.2 are dedicated to protecting PU in their respective countries. In contrast, IEEE802.22 is a SU-focused standard, with the specified parameters being the maximum allowable transmit-power requirements, while corresponding PU protection is the responsibility of the respective country regulators.

While sensing has been discussed by both OFCOM and FCC, currently OFCOM has only submitted a geo-location database solution for industry consultation, while FCC are focusing on the geo-location database solution, with any sensing proposal having to undergo stringent certification with reduced radiating power (Ramjee et al, 2016).

2.4.2 Standards Background

There are three major standardisation projects being conducted in Europe and the US (Nekovee, 2010), (Hossain et al, 2009), (Fitch et al, 2011):

- CogNeA Standard
- IEEE 802.22 Standards

- IEEE 802.11af

The CogNeA Standard aims are to create a CogNeA Brand to indicate compliancy and interoperability and to promote TVWS regulations worldwide. The target devices are commercialised low power Personal/portable CR Platforms which can be utilised worldwide.

The IEEE 802.22 Standards defines the Air Interface (Physical, MAC and CR techniques). This is a point to multipoint wireless interface in which the base station manages all cells within a designated area.

Although these industry standards have not been ratified yet there is a need to keep track of their work because the decisions made in such forums can change the context of the research being carried out and vice versa.

The IEEE802.11af, (IEEE, 2013) also referred to as White-Fi and Super Wi-Fi, is a wireless computer networking standard in the 802.11 family, that allows wireless local area network (WLAN) operation in TV white space spectrum in the VHF and UHF bands between 54 and 790 MHz. The standard was approved in February 2014. Cognitive radio technology is used to transmit on unused TV channels, with the standard taking measures to limit interference for primary users, such as digital TV, and wireless microphone.

2.5 Enabling Technologies for Sensing solutions

Historically the OSI communication stack has been used to communicate information between layers, however for CR applications this is limiting in both the parameters which are available and the time-scales required to acquire them. Once the parameters have been acquired, some analysis is required to interpret an unpredictable RF environment. In the regulatory section (Table 2.2), it was seen the RF transmit power requirement can vary between a fixed SU base station and mobile SU user. Furthermore, the mobile SU will use the minimum RF power so that it minimises the local noise temperature outside the coverage

area of the SU base station which can occur if the mobile SU is at the edge of the BS coverage area. To achieve the coverage area of the fixed SU BS, the uplink from the mobile SU must employ ad-hoc routing. The implications of deploying such a sensing solution will be examined later in the thesis.

2.5.1 Cross Layer Processing

Cross layer processing (CLP) design strategies attempt to optimise key parameters by using information from other OSI layers, allied with information that is not readily available within the OSI communication stack. Unlike normal OSI stack information exchange, CLP is not constrained to information that is of necessity, contained within adjacent layers. This enables faster information retrieval because the information does not have to be transferred through several layers before reaching the layer where it is required. Furthermore, not all information required within a layer to perform its function is passed to other layers, so CLP permits information to be utilised by any OSI layer.

The benefits of utilising CLP are that it reduces the overhead within the protocol stack so lowering the time to acquire information and configure parameters, hence improve the performance of the CR system (Akyildiz et al, 2009). It has been shown that if CR routing in the Network layer also uses information from the spectrum management block then an improved routing performance can be obtained (Akyildiz et al, 2009).

The drawbacks in using CLP are that firstly proprietary information models need to be implemented across the cross-layer block which will vary from one implementation to the next. Standards could be formulated between all stakeholders to ensure a standard information model is deployed so ensuring interoperability. This is the end goal but it takes a considerable amount of time to establish standards. The other pitfall is that a greater computational resource is required to implement a cross layer processing block with the associated increase in overall power resources.

In past CR research, this has not been such an issue because the topics have been predominantly physical layer. However now the emphasis is to optimise the resources to

improve the QoS for the user hence the CR system needs to influence parameters in most of the OSI layers at the same time, examples of this are from optimising the RF power for routing to spectrum access decisions which are tailored to the layer 5 requirements.

Some of the challenges that present themselves in implementing the CLCE (Baldo and Zorzi, 2008), (Chen and Prasad, 2009), (Hossain et al, 2009) include:

- **Modularity** – The OSI layers have been designed with inherent modularity so they are independent from each other so when the cross layer block is designed this modularity needs to be maintained. However, there needs to be abstraction of the technology specific information in the OSI layers when the information is exported into the Cross Layer block. This prevents the need to design a different Cross Layer block for each technology deployed. There may have to be compromises in this area due to the cross layer block being designed by different vendors hence the model of abstraction could be different. This can be avoided by standard bodies being involved at an early stage of development.
- **Information Interpretability** – It is important to choose a knowledge representation base that can accommodate the different implementations of the layer modules. An example of this would be if we used SNR as useful Link layer information. If this was passed to other layers it would be misinterpreted because for SNR to infer any knowledge of a wireless link quality, then the modulation type and forward error correction/automatic repeat request strategies need to be known.
- **Dealing with Imprecision & Uncertainty –** Seeing the different layers are designed independently then the parameters to be exported may have measurement inaccuracies from layer to layer imposed on them. Any Cross-Layer block needs to be able to work with this inherent inaccuracy. Again, SNR is a good example since for most IEEE 802.11 devices there is only a few dB between excellent and bad

wireless performance hence large feasibility of misinterpretation of the SNR parameter.

- **Complexity and Scalability -** Seeing that CR can work using different wireless configurations to optimise the wireless link to what the user requires then the Cross-Layer Block required to do the optimisation will get very complex. Also, to be able to optimise the configuration, many parameters will be exported to the Cross-Layer Block adding to its computational overheads.

There have been several proposals how to implement the Cross-Layer Block and the most prominent one's are listed below with the advantages and drawbacks (Ghosh and Agrawal, 2007), (Baldo and Zorzi, 2008), (Mitola and Maguire, 1999):

- **Radio Knowledge Representation Language** (Mitola and Maguire, 1999), **(**Kokar and Lechowicz, 2009) - This language is proposed as a knowledge representation base across the Cross-Layer Block and is made up of a collection of micro-worlds. Each micro-world represents a specific wireless technology. This implies that the Cognitive Engine needs explicit knowledge of each technology which does not meet the Modularity and Scalability challenges.
- **Artificial Intelligence** (Hossain et al, 2009), (Mitola and Maguire, 1999), (He et al, 2010) - AI solutions such as Genetic Algorithms are well suited to handling large sets of variables but they require long learning times which is not practical for most wireless applications.
- **Fuzzy Logic Controllers** (Baldo and Zorzi, 2008), (Hossain et al, 2009), (Mitola and Maguire, 1999) – Modular by definition. Technology specific information is kept in the layers with a more generic information representation base used in the Cross-Layer Block. Improved information interpretability by using linguistic attributes for each membership function defining it. Precision and accuracy issues have been avoided by using what is an imprecise knowledge representation base. Complexity of the Cross-Layer Block is less than that of the other proposals. Fuzzy Logic

Controllers require low computational power and dedicated Fuzzy Logic Controllers can be used for critical scenarios.

From the above appraisal, the rest of this thesis will investigate which implementation to use for achieving Cross-layer block optimisation.

2.5.2 Ad Hoc Routing

At the start of Section 2.5, it was stressed that due to regulatory requirements, the RF transmit power of both fixed and mobile SU nodes could vary up to the maximum values shown in Table 2.2 and due to a fixed node antenna height being higher than the mobile node, greater coverage would be achieved. To compensate for this asymmetrical coverage in the down and uplink directions, ad hoc routing can be innovatively applied in the uplink direction (mobile to fixed node) to achieve the same coverage in both directions. This is the basis of a novel routing solution for the TVWS framework which is presented in Chapter 8.

To enable the re-use of frequencies and hence increase spectral efficiency then low RF power needs to be used. However, if low power is used then ad-hoc networks need to be employed in which for a CR message to reach its destination then other CR nodes need to relay the message. To minimise the effect of delay on sensitive applications then consideration needs to be paid to how the message is routed through the CR network to its destination (Chen and Prasad, 2009), (Hossain et al, 2009).

Routing protocols for Mobile Ad-Hoc Networks (MANET) (Chen and Prasad, 2009), (Hossain et al, 2009), (Sheng et al, 2010), (Yuanzhou and Weihua, 2010) are well established but CR brings with it some new challenges which need to be addressed. These include:

i. Link Availability- From Figure 2-9 we can see that there is a limited available spectral hole window for the CR to exploit. Unlike MANET networks the window of opportunity for CR is measured in milliseconds rather than seconds, hours or days except for the TVWS example:

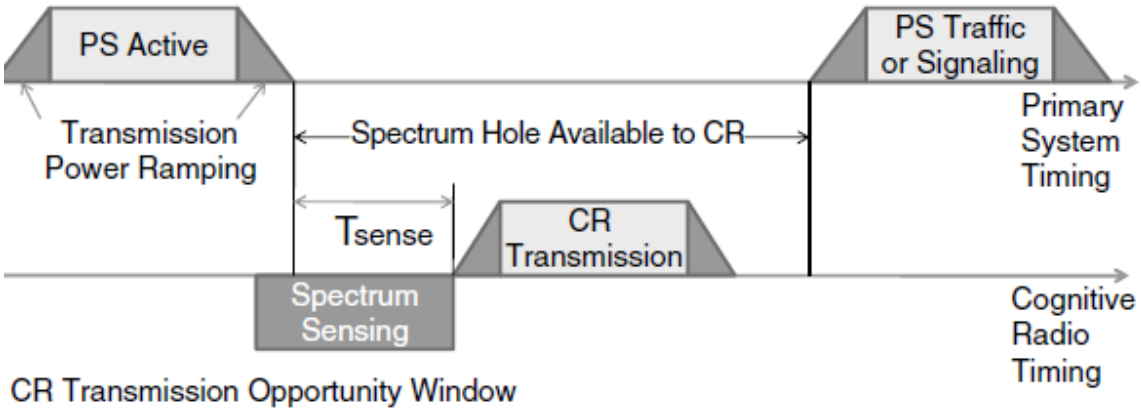

Figure 2-9: CRN Transmission Opportunity Window (Chen and Prasad, 2009)

ii. Unidirectional links – Typical wireless networks have bi-directional links though this is unlikely for CRN due to i) above but also in the TVWS scenario due to the regulatory SU unidirectional power allocation, so realistically there is only the opportunity for uni-directional links. This poses specific constraints on the Network Layer design.

iii. Heterogeneous wireless networks – Normal wireless networks are made up in a structured way, while CRN's have a more ad -hoc, heterogeneous node structure. This means that CRN's require inter-system handover but with just very short duration links routing relies on cooperative relaying. Such heterogeneous networks also pose a security issue in that the link duration is small so there is not enough time to obtain a security certificate.

Reactive protocols devised for typical wireless networks can be adopted for CRN to overcome some of the issues above. The two most common routing protocols are Dynamic Source Routing (DSR) (Sheng et al, 2010) and *Ad-Hoc On Demand Distance Vector* (AODV) (Yuanzhou and Weihua, 2010).

The DSR protocol is based on source routing whereby all the routing information is maintained by the mobile nodes. It is a simple and efficient routing protocol designed specifically for use in multi-hop links for mobile nodes. DSR allows the network to be completely self-organizing, without the need for any existing network administration. The protocol is composed of two main phases namely "Route Discovery" and "Route

Maintenance", which work together to allow nodes to discover and maintain routes to destinations in the ad hoc network. All aspects of the protocol operate entirely on demand, allowing the routing packet overhead of DSR to scale automatically to only what is needed. However, the important factor is that only when a route to the destination has been found will packet transmission take place.

The AODV routing protocol in contrast is intended solely for use by mobile nodes in ad hoc networks. It offers quick adaptation to dynamic link conditions, low processing and memory overheads, low network utilization, and determines unicast routes to destinations within the network. AODV route table entries are dynamically setup at each intermediate node as the packet is transmitted towards the destination so reducing the traffic overhead.

Chapter 8 will undertake an analysis of both DSR and AODV routing protocols in terms of their QoS provision, i.e., throughput and packet delay.

2.6 Existing Research in Sensing Techniques

The regularity framework in Table 2.2 has formed the basis for a variety of spectrum sensing proposals such as non-cooperative feature sensing (Lei Qiu Jing et al, 2011), (Chen and Gao, 2011) and cooperative sensing using a non-Gaussian noise covariance Rao test (Zhu et al, 2013). This section shall critically analyse these three sensing solutions with regards to the regularity criteria.

2.6.1 Non-cooperative feature sensing

In (Lei Qiu Jing et al, 2011) and (Chen and Gao, 2011), an autocorrelation algorithm for spectrum sensing was developed based upon the correlation of the frame headers and synchronisation blocks which are a form of matched filter feature detection.

Paper (Lei Qiu Jing et al, 2011) was written for IEEE Globecom in 2011. The paper explores spectrum sensing in the context of the three main TV standards deployed in China, Digital Terrestrial Multimedia Broadcast (DTMB), China Multimedia Mobile Broadcasting

(CMMB) and Phase Alternating Line –D/K (PAL-D/K**).** For the purposes of comparing results the DTMB shall only be reviewed since it is the standard that most resembles the UK standard DVB-T i.e. frame structure and transmission bandwidth.

For a DTMB signal, the frame header appears periodically at the beginning of each frame and can be utilised for sensing and detection. Figure 2-10 shows the data flow for frame header detection:

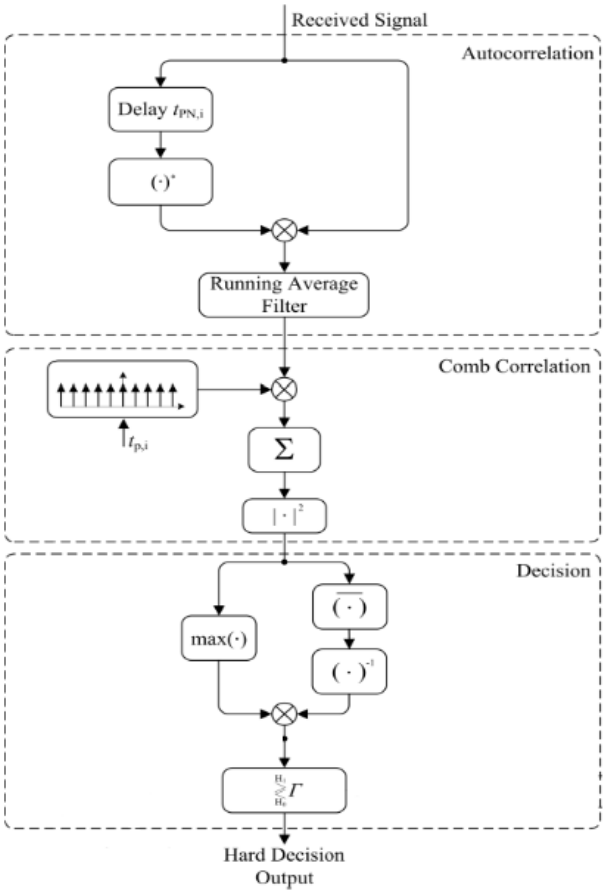

Figure 2-10: Data Flow of DTMB autocorrelation algorithm (Lei Qiu Jing et al, 2011)

The proposed autocorrelation detector for DTMB can be divided up into three parts, namely, autocorrelation, comb correlation, and decision. In the first stage, a running autocorrelation value is calculated for the period of the frame header. In the second stage, a comb correlator collects the energy of all frames within the sensing period. In the decision block, the decision on the presence of the signal is implemented by comparing the maximum comb correlator output to the mean value output. The decision block is designed so a soft decision (i.e. the

detection data) and a hard decision are delivered by comparing to a threshold, which depends on the sensing time and false-alarm tolerance probability.

From this design, a simulation platform was constructed along with a laboratory prototype model and the results are shown Figure 2-11:

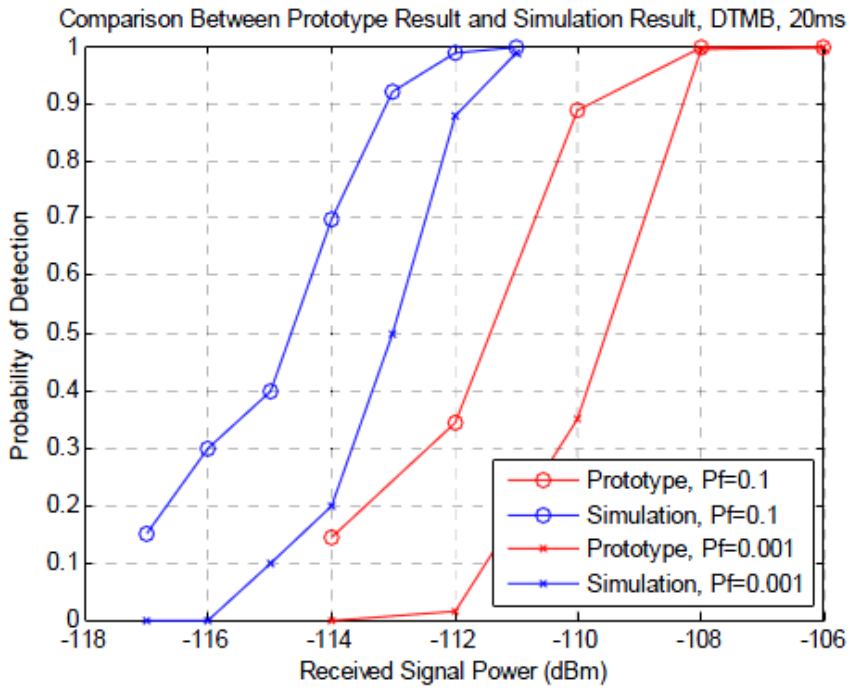

Figure 2-11: Simulation and laboratory results for DTMB detection (Lei Qiu Jing et al, 2011)

Figure 2-11 shows both simulation and laboratory prototypes at a false detection of 0.1 and 0.01. The results for the prototype can be seen to be degraded by 3 to 4 dB compared to the simulation results. This can be explained by the simulation not considering analogue RF stage impairments such as frequency offsets and amplifier nonlinearity. However, by comparing the detection and false detection probabilities for the IEEE 802.22 P_d = 0.9, P_f= 0.1 at -114dBm (Table 2.2), and from Figure 2-11 the simulation results for P_f= 0.1 then only P_d =0.7 is achieved at -114dBm signal strength. From this it can be concluded that this solution does not comply to the IEEE 802.22, OFCOM or FCC requirements (Table 2.2).

This paper concluded from the results that a digital TV signal can be detected in a relatively low SNR environment. This work validates the feasibility of the sensing-based TVWS devices from the implementation aspect.

Paper (Chen and Gao, 2011) examines the development of spectrum sensing algorithms for ATSC (DTT), NTSC (Analogue) and radio microphones in North America. The spectrum sensing algorithm for ATSC and NTSC is a unified signature based spectrum sensing algorithm (For the ATSC this is the autocorrelation of the SYNC segment of the ATSC frame). ATSC DTV signals consist of consecutive data segments. A complete data segment has 832 symbols: 4 symbols for data segment SYNC, and 828 data symbols. Pilot tone is widely used to perform spectrum sensing in variety of algorithms however, algorithms utilizing this pilot carrier severely suffer from adjacent channel interference. Thus, instead of utilizing the pilot tone, the data segment SYNC is used to perform spectrum sensing.

Again, this thesis will only review the ATSC (DTT) which is the US DTT standard. The ATSC results are shown in Figure 2-12, which give the probability of detection against the probability of false detection for differing SNR values.

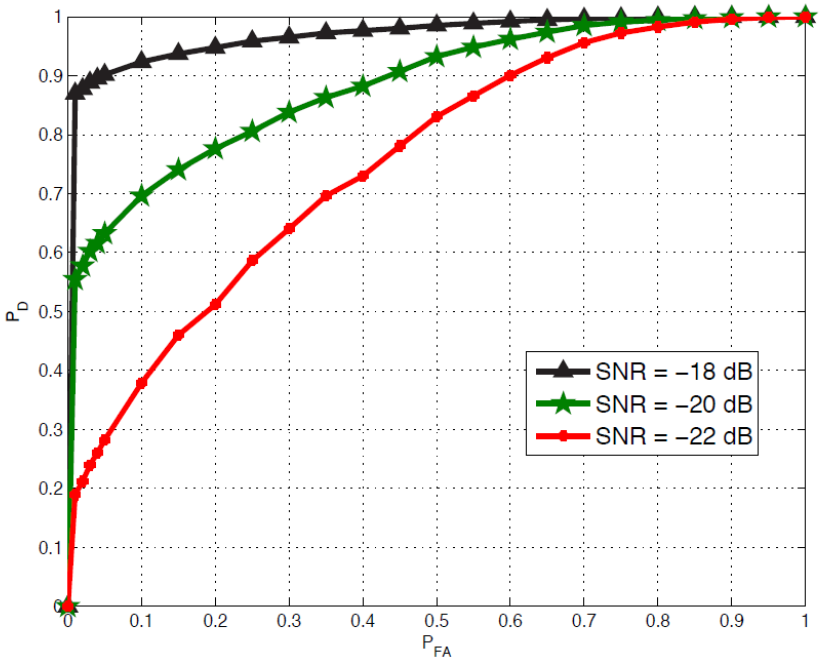

Figure 2-12: Family of ROC curves for ATSC DTT Signals at different levels of SNR (Chen and Gao, 2011)

Assuming a noise floor of -100dBm within a bandwidth of 6MHz, which is the TVWS bandwidth in USA, then a SNR of -18dB is represented by a signal of -118dBm which lies

below the sensing threshold of -114dBm for both IEEE 802.22 and FCC (Table 2.2). From Figure 2-12 for a SNR of -18dB a P_d of 0.9 is achieved for a P_f = 0.05, then this is the only SNR which complies to IEEE 802.22 however it does not comply to the FCC probability of detection (Table 2.2). Results for both SNR = -20dB and -22dB do not comply to either the IEEE 802.22 or FCC requirements.

The paper concludes that the spectrum sensing algorithms can be used to detect DTT primary signals so that channel availability can be detected to deploy TVWS applications.

2.6.2 Cooperative sensing using a non-Gaussian noise covariance test Rao

Spectrum sensing for CR networks in the presence of non-Gaussian noise is challenging due the CR having to have knowledge of both the PU and SU. To overcome this limitation, the generalized likelihood ratio test (GLRT) is used which combines unknown parameter estimation with a traditional likelihood ratio test. GLRT is an optimal detector, but it needs to perform the maximum likelihood estimation (MLE) of the received signal power for a wanted signal and noise variance as well as unwanted signal and as such, incurs a large computational burden. The Rao test is an approximate form of the GLRT which only estimates system model parameters for unwanted signal conditions. This simplifies the Rao structure and (Zhu et al, 2013) examined it use in the cooperative mode, which is a commonly used technique in spectrum sensing since it overcomes the harmful effects of fading and shadowing by taking advantage of spatial diversity. It thus offers a solution to PU sensing for non-Gaussian noise conditions. In this paper, cooperative spectrum sensing is considered for a CR sub-network comprising of one SU base station and multiple SU mobiles, which together seek to detect the presence/absence of a PU within a given frequency band. Each SU employs a Rao detector to independently sense the PU signal in the presence of non-Gaussian noise characterized by a generalised Gaussian distribution (GGD). The local decisions of the SU are then forwarded to the BS which makes a global decision. GGD reduces to a Gaussian distribution when β = 2 and to the Laplacian

distribution when $\beta = 1$. By varying β, different tail behaviours can be obtained: for $\beta > 2$, the tail decays faster than for the normal, while for $0 < \beta < 2$, it decays more slowly. The GGD with $0 < \beta < 2$ is therefore well suited to fit the "heavier" than normal tail behaviour found in practical CR systems.

The co-operative spectrum sensing system in (Zhu et al, 2013), is an IEEE 802.22-based solution that uses the Rao test to measure the non-Gaussian noise level to improve the energy detection performance and includes a multi-user extension. The following results are for four SU sensors at differing β representing noise profiles ranging from Gaussian (β=2) to Laplacian (β=1). Also in the results, four strategies for cooperative sensing were evaluated. The first is the traditional cooperative sensing technologies (OR, AND) where the proposed solution uses the cooperative technologies coupled with the Rao test measure.

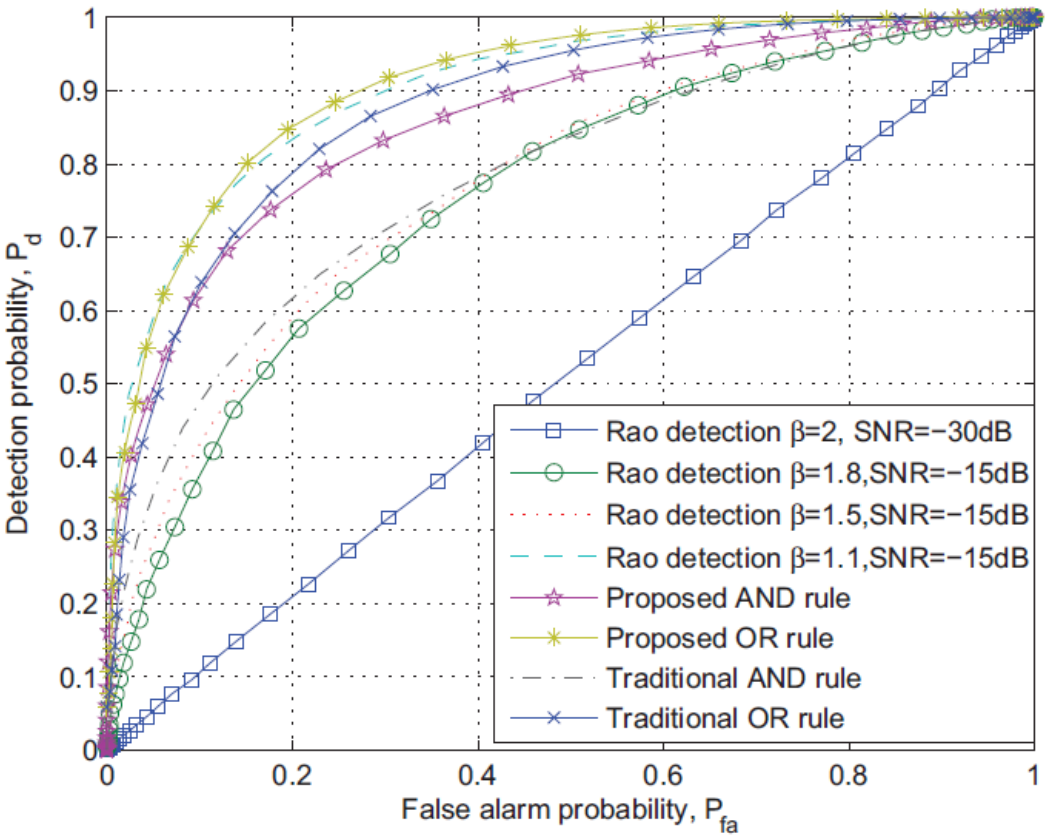

Figure 2-13: Family of ROC curves of cooperative for different values of β (Zhu et al, 2013)

Using the IEEE 802.22 P_f = 0.1 requirement the proposed OR rule provides the best performing strategy giving a Pd = 0.7, though this result does not uphold any of the stringent IEEE 802.22, OFCOM and FCC requirements. These findings therefore provide significant impetus to investigate further new alternative sensing algorithms for CR applications.

2.7 Summary

This chapter presented CRN technologies as a way to address the scarcity of spectrum for the increasing demand for wireless applications. The key benefits were outlined and also the challenges which are presented to CR being adopted. It was also highlighted that TVWS presented a lower risk option to implement CR due to the static temporal characteristics of the PU spectrum. The effects of interference on the PU was also reviewed and it is concluded that interference management will be required to protect the PU.

An overview of the TVWS regulatory and standards scene was presented where the PU centric country related regulatory requirements were outlined and also the SU centric standards were also discussed. One of major outcomes of this review was that any proposed sensing solution would need to demonstrate its resilience against the hidden node problem.

The chapter reviewed the supporting technologies which can assist the introduction of CR namely CLP and Ad-Hoc routing. With the challenges of implementing SU TVWS CR and CLP were identified as being a strong technology choice in overcoming the issues of ensuring the correct information is delivered to the required OSI layers in a timely fashion. Also Ad Hoc routing was highlighted as a way to ensure unidirectional transmission caused by SU RF power differences and so will not affect user QoS.

The chapter then concluded with a review of existing DSA sensing techniques which concluded that the relevant results fell short of meeting the regularity requirements out lined

in Table 2.2 so further research is required to enable sensing to be adopted by the regularity bodies.

This thesis addresses the challenge of PU detection by introducing a new DSA technique called the *generalised enhanced detection algorithm* (GEDA) that utilises sensing coupled with the static database. This allows the efficiency and accuracy of the sensing mechanism but the flexibility of the static database to provide a solution for PMSE radio microphones. The next chapter will present simulation and evaluation methodology together with the key performance metrics to evaluate the performance of new models and algorithms proposed in this thesis.

Chapter 3

3. METHODOLOGY AND MODEL VALIDATION

3.1 Introduction

Wireless systems are complex by nature due to the environment they work in, from the transmitter power used to the modulation techniques and propagation factors in the deployed terrain. To analyse such complex test scenarios via traditional non-simulation techniques (Tranter et al, 2003) infers a large amount of hardware, with many different parameter combinations, which to prototype would be an impractical design option.

With advanced low cost personal computer performance, simulation models have become a popular methodology in analysing RF systems (Kasch et al, 2009) (ITU-R, 2009). These provide valuable insights with reference to cause-and-effect within a RF system, without requiring the development of expensive prototyping hardware and laboratory test equipment. This provided the motivation to use a simulation methodology in the design and development of the new TVWS access framework which this chapter will describe, including tools used to analyse TVWS cognitive SU access and the associated QoS performance metrics.

3.2 High-Level Modelling Scenarios

The following section outlines the high-level modelling scenarios for this thesis. Figure 3-1 displays four basic modelling scenarios with each now being described.

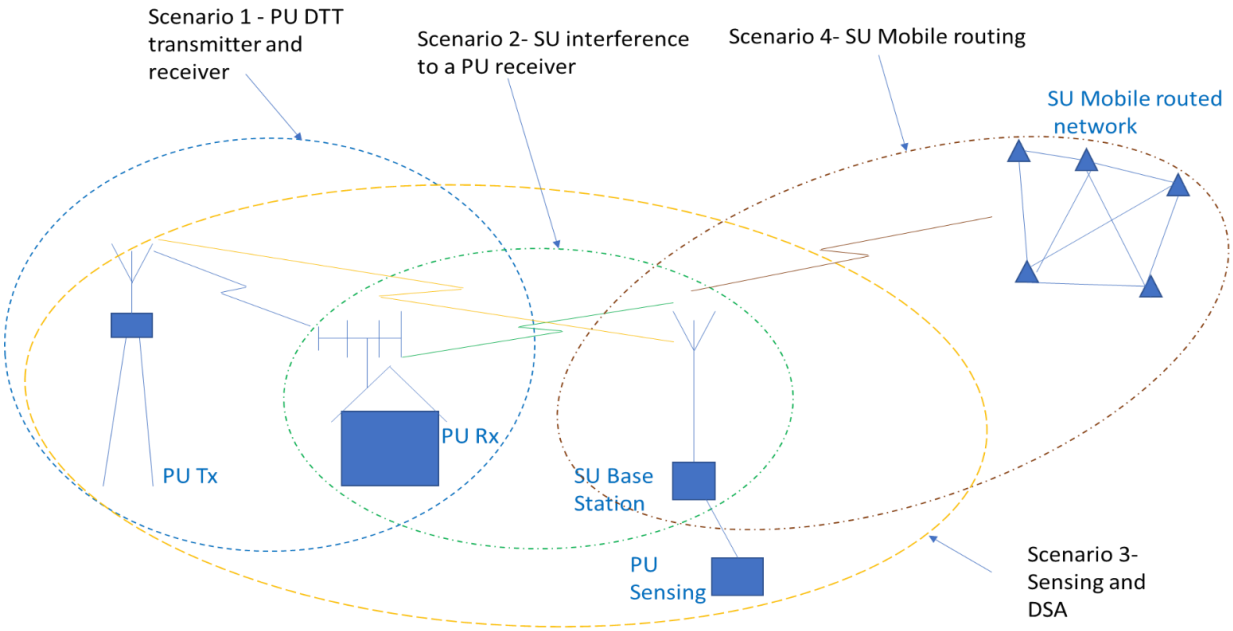

Figure 3-1: High-Level Modelling Scenarios

Scenario 1- This is where PU DTT network behaviour is defined so any SU intervention can be assessed from a PU perspective.

Scenario 2- This scenario models the impact of a SU network on a PU receiver.

Scenario 3- This model's the PU sensing and DSA logic so that the PU transmitter can be accurately detected.

Scenario 4- This model's a SU mobile network using ad-hoc routing to improve the reverse link performance.

3.3 General Evaluation Methodology

There are two general simulation methodologies (Zhang et al, 2011), namely link-level and system-level. The former is where a single transceiver along with Gaussian noise and propagation/channel are incorporated into the simulation, whereas the system-level involves a multi-transceiver network being simulated, which due to the many interactive effects such as causing interference with each other, makes the resulting model of much greater complexity. TVWS is a prime candidate for exploiting CR behaviour because it is static spectrum so channels do not change in a location. This relaxes the requirement of efficient

PU updates since channels change only on a spatial rather than temporally basis. To exploit unused TVWS spectrum, spectral holes must be identified using dynamic spectrum access (DSA) techniques. Three models are considered, namely a basic RF model which encompasses the PU and SU transceivers, a fuzzy logic DSA model that uses a Fast Fourier Transform (FFT) energy detector and a routing model which analyses the requirement of utilising routing on the uplink due to potential disparity of RF power in the fixed SU and mobile SU. All models encompass the regulatory requirements for the three TVWS standards, with Table 2.2 giving the corresponding TVWS engagement parameters. The models used in this thesis will be the system-level type as these are able to analyse the co-existence of DTT services alongside the SU access network within the same spectrum. The various simulation components used are shown in Figure 3-2.

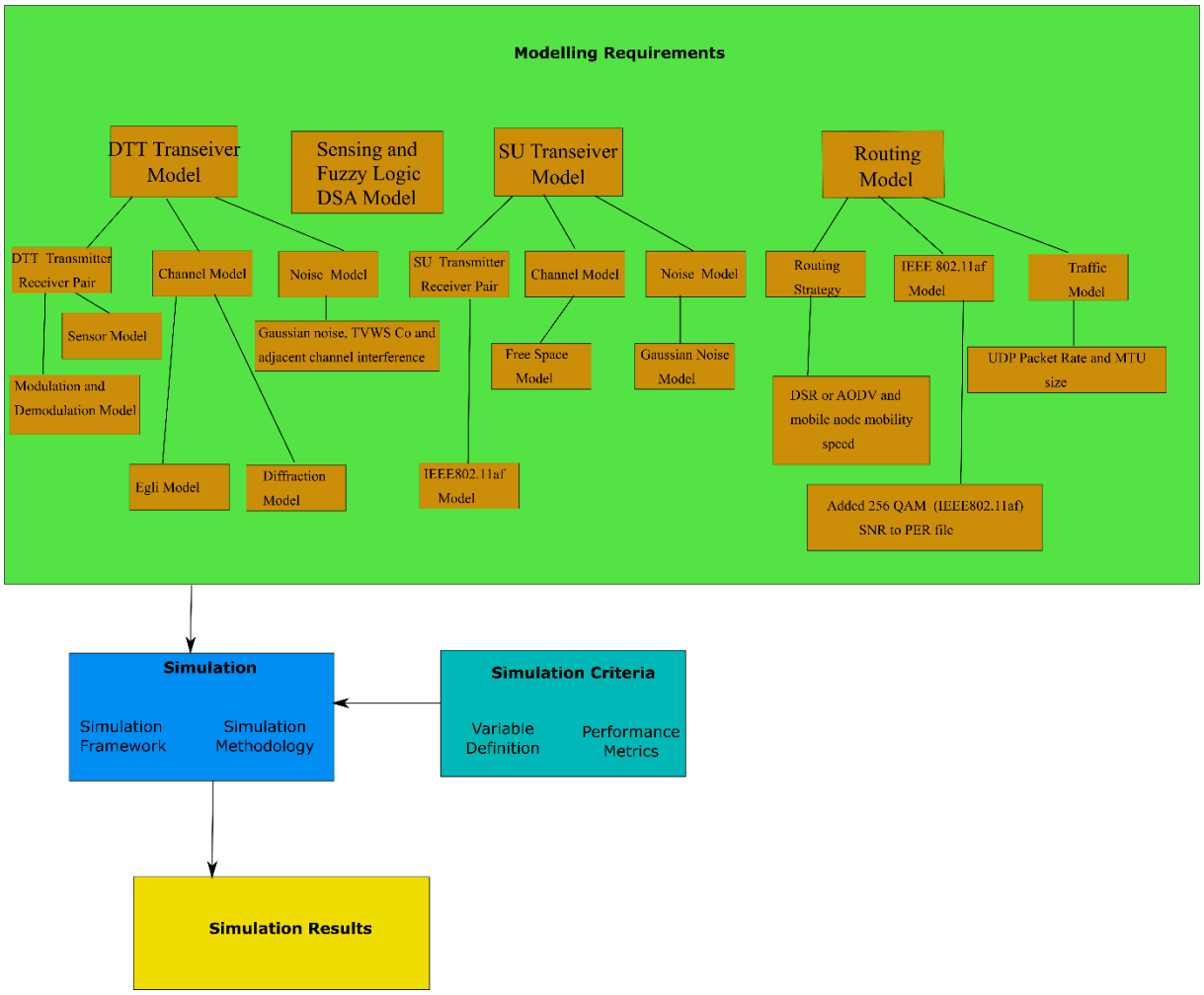

Figure 3-2: Simulation Components

The DTT transceiver model is comprised of two models, namely a basic RF model and a sensor model that uses a FFT energy detector and covariance detector.

The basic RF model comprises three constituent blocks: i) the DTT TVWS transmitter-receiver pair; ii) the channel model, which comprises an Egli propagation model which is specifically designed for TV distribution systems and includes a diffraction loss algorithm for obstructions including beyond Line of Sight (LOS); and iii) A noise block which includes Gaussian, adjacent and co-channel noise generators which all mimic IEEE 802.11af interferers.

The Fuzzy Logic DSA model takes the output from the sensing platform and a fuzzy logic block which exploits *a priori* information concerning DTT frequency allocations and shares information between the MAC and physical layers in making DSA decisions. This is fully elaborated on in chapter 4.

The SU transceiver model incorporates the same RF blocks as the DTT transceiver though it uses the IEEE802.11af physical parameters (256 QAM) to evaluate the keep out distances from the co and adjacent channel interference thresholds from the DTT transceiver model. This model is used to evaluate the coverage distance for a SU transmitter.

The routing model assumes a multi-nodal architecture which is transitory thereby reflecting a real-life situation. The model, assesses the SU IEEE802.11af user QoS using packet error and delay for the DSR or AODV routing protocols with a UDP transport layer.

The model also allows for different data traffic parameters such as packet rate and *maximum transmission unit* (MTU) size.

3.4 Simulation Model Requirements

To be able to analyse the effect of introducing a cognitive SU network on the PU DTT system, many simulation models are required. The DTT model is included to simulate the PU requirements including interference, while the SU and the routing model defines the QoS

issues in the context of the SU. Each component block within Figure 3-2 will now be discussed.

3.4.1 DTT Transceiver Model

The DTT transceiver model is developed on a Matlab/Simulink platform (Matlab, 2010) and has a generic specification consisting of a DTT transceiver pair with configurable modulation schemes of 16, 64, 256 *quadrature amplitude modulation* (QAM) or 8 *vestigial sideband* (VSB), depending on the country scenario. It also includes a Gaussian noise block.

The model includes the sensor receiver and a RF power detector with a sensing time of *T*, co and adjacent channel IEEE802.11af interference generators (IEEE, 2013) and noise measurement. A covariance detector was modelled to compare with the RF power detector.

There are three specific DTT models which incorporate the above generic specification, namely distance, signal strength and SNR which are driven by different criteria where these are used as comparators for the new TVWS framework. The transceiver design is shown at Figure 3-3.

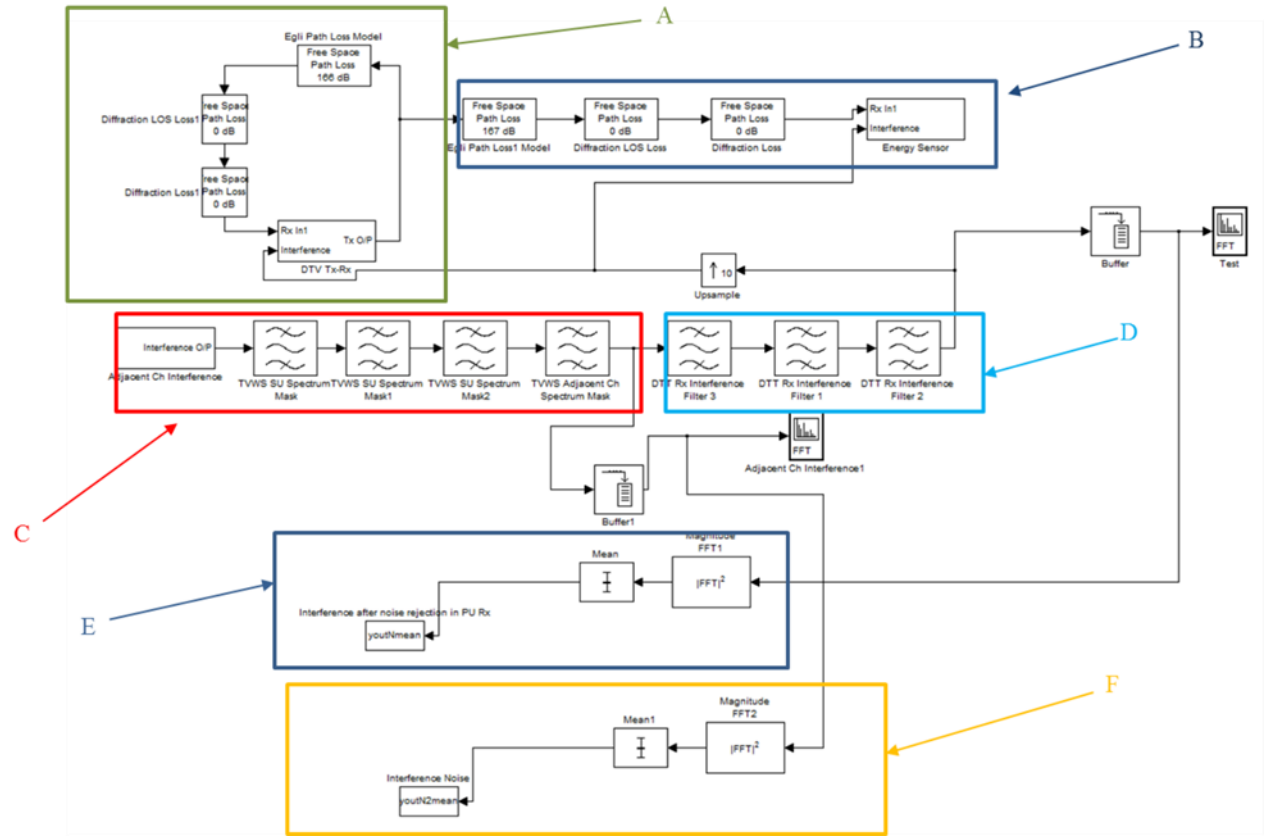

Figure 3-3: DTT Transceiver and Sensor Model

The distance model will be used evaluate the protection contour and keep out (see Chapter 6) where signal strength and SNR models are used to critically evaluate the new TVWS models against existing Chinese and American comparators (Lei Qiu Jing et al, 2011) and (Chen and Gao, 2011). Figure 3-3 illustrates the distance model, where Block A in Figure 3-4 is the DTT transceiver pair including a traffic generator and sink, a propagation model and a diffraction module which is specifically defined by a Matlab script named <Test_Script2> which will be examined later in this section. Within the Block A transceiver, the equaliser in the receiver chain utilises synchronisation patterns to enable it to overcome group delay.

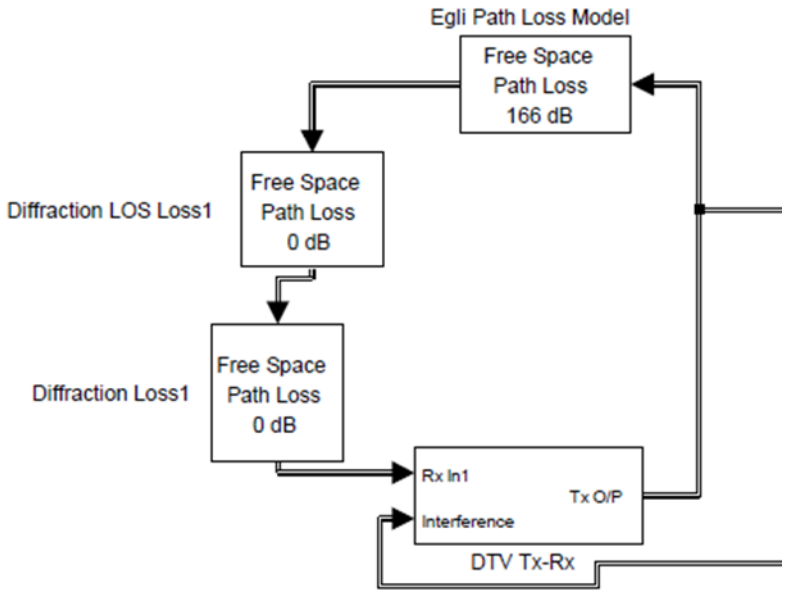

Figure 3-4: Block A

Block B in Figures 3-3 and 3-5 provides the propagation module plus diffraction, RF mixer and Receiver front end for the sensor receiver where the sensor location is at the same point as the DTT receiver but antenna height and gain can differ.

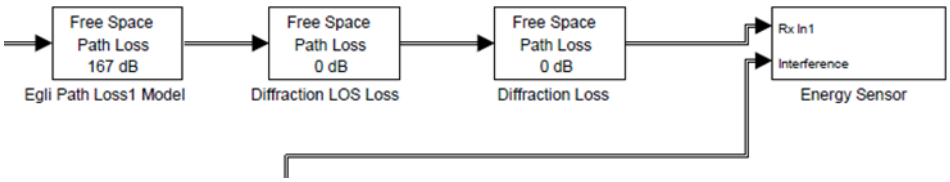

Figure 3-5: Block B

Block C of Figures 3-3 and 3-6 depicts an IEEE 802.11af interferer which conforms to the DTT relevant spectrum masks (ETSI, 2004) and (ATSC, 2008). The interference can be either co-channel (where the mask filters' centre is set to the DTT channel frequency) or adjacent channel (where the mask filters centre is offset by the DTT bandwidth x1 or x2 for the first or second adjacent channels respectively).

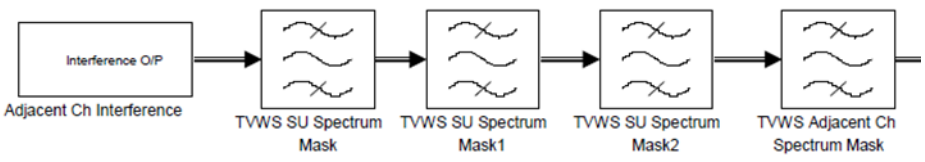

Figure 3-6: Block C

In Block D of Figures 3-3 and 3-7, adjacent channel noise rejection filters have been designed which mimic the break-points of the common DTT receiver noise rejection filters outlined in (DVB, 2011) and (FCC, 2007).

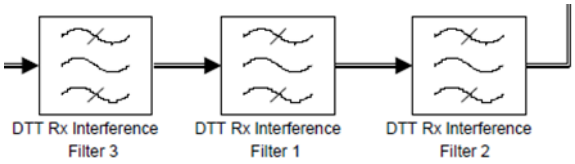

Figure 3-7: Block D

Blocks E and F of Figures 3-3 and 3-8 monitor the interference noise after the noise rejection filters and before at the receiver terminals respectively, to enable the SNR to be calculated.

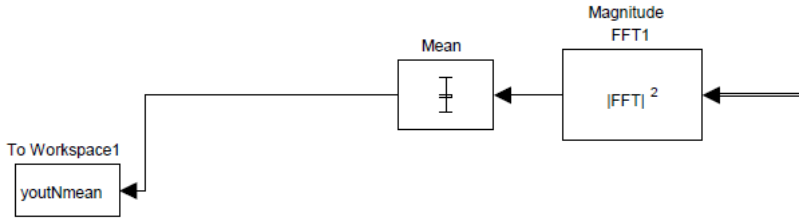

(a)

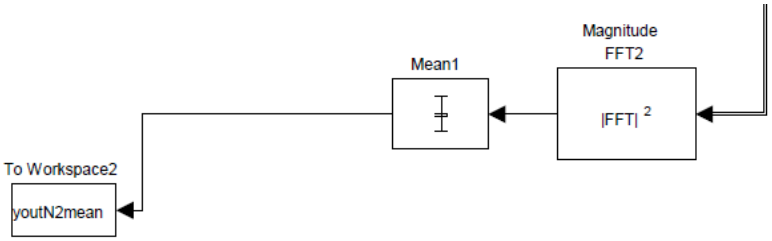

(b)

Figure 3-8: Block E (a) and Block F (b)

Most of the parameters within the DTT transceiver model are configured by the user in two associated Matlab (Matlab, 2010) algorithms namely <Test_Script1> and <Test_Script2> which will be examined later in this chapter including both the propagation and diffraction models. The remainder of the parameters are all fully compliant with the standards and are formally defined in Table 3.1.

Table 3.1: DTT transceiver model parameter settings

Parameter	Value	Comments
DTT Receiver Noise Figure	7.5dB	(TTP, 2005)
Sensor Receiver Noise Figure	10dB	(FCC, 2007)
Sensor detector	FFT^2/ Covariance	(Matlab, 2010)
IEEE 802.11af interferer with DTT Spectrum Mask Filter Parameters	Set by IEEE 802.11af standard and relevant regulatory spectral masks	Table 19 in (ETSI, 2004) for UK and Figure 5.1 in (ATSC, 2008) for the US
Noise Rejection Filters	Set by the relevant regulatory bodies	Figure 17 in (DVB, 2016) for UK and Figure 4-4 in (FCC, 2007) for the US

The difference between this distance model, the signal strength and SNR models is that the propagation and diffraction blocks are replaced by a single attenuator which sets the relevant signal strength or SNR to the required values.

3.4.2 SU Transceiver Model

The SU transceiver model follows the same framework as the DTT model and since the majority of parameters including the modulation technique and EIRP are set via Matlab scripts, namely <Test_Script1> and <Test_Script2> which determine whether it is either a DTT or IEEE 802.11af SU network.

The SU transceiver model follows the *free space loss* (FSL) framework (Seybold, 2005) and because of the short distances involved, diffraction loss is not considered. Also, the *effective*

isotropic radiated power (EIRP) is low so the coverage is low, hence only free space losses must be considered, with the parameters set by the IEEE 802.11af standard (IEEE, 2013). Using FSL the following process is used to calculate the distance to the edge of SU cell and the RSS at distance *D* (km) from the SU transmitter.

The FSL in dB used for the SU is defined as (Seybold, 2005):

$$FSL = 20Log(D) + 20Log(Freq) + 20Log\left(\frac{4\pi}{c}\right) \quad (3\text{-}1)$$

where:

D= Distance between SU transmitter and receiver (m)

Freq= Frequency (Hz)

c= Speed of light 3x 10^8 m/s

Having determined the propagation loss, the noise at the demodulator block has to be calculated. This is given by the *receiver actual noise* (RAN) which is composed of the Gaussian noise and the receiver *noise figure* (NF) in dB in equation (3-2) (Seybold, 2005) from which the received signal in the demodulator can be derived.

$$RAN = 10Log(k \cdot T_o \cdot B) - NF \quad (3\text{-}2)$$

k= 1.38 x 10^{-23} (Boltzmann constant)

T_0= 290 ^oK (Ambient temperature 17^oC)

B= DTT bandwidth (8MHz in the UK and 6MHz in America)

NF= Receiver Noise Figure 7.5dB

With the EIRP (in dBm) the following equation (3-3) is resolved for *D* contained in the *FSL* equation 3-1 to find the distance to cell edge and RSS can be resolved from equation 3-4 to give signal strength at distance *D*:

$$SNR = EIRP - FSL + G_R - RAN \quad (3\text{-}3)$$

$$RSS = EIRP - FSL + G_R \quad (3\text{-}4)$$

Where:

SNR = Signal-to-noise ratio for a PER of 10^{-6} for a 256 QAM signal is 35dB

G_R=Receiver Antenna Gain is 2dB

RSS = Received Signal Strength in dBm

3.4.3 Routing Model

The routing model is based on the INET software package & defines the Ad-Hoc routing protocols to be analysed. The INET Framework (INET, 2012) builds upon OMNeT++ platform (OMNeT++, 2011), which uses modules that communicate by message passing. Hosts, routers, switches and other network devices are represented by OMNeT++ compound modules. These compound modules are assembled from simple modules that represent protocols, applications, and other functional units. A network is again an OMNeT++ compound module that contains host, router and other modules. The external interfaces of modules are described in NED files. NED files describe the parameters and gates (i.e. ports or connectors) of modules, and also the submodules and connections (i.e. netlist) of compound modules.

The routing model is based upon the OMNet++ v4.3 (OMNeT++, 2011) platforms in which there is a INET framework (INET, 2012) which models the IEEE 802.11 standard which is the wireless LAN standard which SU users are based upon i.e. IEEE 802.11af. This LAN standard outlines how a single channel using MANET routing protocols such as AODV can support multi-user environment with using lower power but achieve the same coverage area as the down link from the base station. But of course there are drawbacks to this such as packet delay and throughput considerations which are examined in chapter 8. The opening screen for a network contains 2 types of host, fixed and mobile which is embedded in the model file called Net80211_aodv.ned.

All the hosts are contained within a defined area in a random pattern and can be static or moving at a randomly defined speed. A traffic channel is set up between the fixed host and a defined mobile host where the rest of the mobile hosts are able to relay packets between the two using the selected routing protocol. At the end of the simulation the results are stored and then analysed to generate performance metrics of the given network.

3.5 Simulation Framework and Parameter settings

For the first two models described in Section 3.3, there are parameter settings which drive the simulation model. For the PU DTT and SU models, the configuration files are <Test_Script1> and <Test_Script2> and are produced on by Matlab script platform. These scripts set such parameters as operation frequency, modulation, traffic bitrate, propagation model, distance between transmitter and receiver and diffraction model. The main reason for this model is to mimic real-life DTT and SU networks hence within the propagation model, the terrain specific parameters will be validated against real world data from UK and US networks.

For the routing model the file omnetpp.ini sets the parameters required to drive the routing simulation phase on the OMNet++ and INET platform. This file sets up such parameters as routing protocol, area definition, frequency, host traffic model and host mobility.

3.4.1 <Test_Script1>

<Test_Script1> sets the basic parameters of the PU and SU transceivers which are not specific to the actual simulation in testing and are shown in table 3.2 below:

Table 3.2: <Test_Script1> Parameters

Parameter	Value	Comments
Frequency	*Freq*	Hz
PU or SU Transmitter Antenna Height	h_t	Metres
DTT or SU Receiver Height	h_r	Metres
Sensor Height	h_r'	Metres
Height of obstacle at horizon	0.1	Metres (Horizon diffraction loss)
Height of obstruction	h_n	Metres
Distance of obstruction from PU or SU Transmitter	h_{tn}	Metres (if 0 then no obstruction)
PU or SU Transmitter Antenna Gain	0	(0dB if transmitter power is given has EIRP)
PU or SU Receiver Antenna Gain	2	dBi
Sensor Receiver Antenna Gain	1	dBi
Modulation Level of PU or SU	64 QAM	Range: 16 to 256 QAM & 8-VSB
Modulation Level of co-channel or adjacent channel interferer	16 QAM	Range: 16 to 256 QAM
PU or SU data rate	64 Mbs	Raw data rate including overheads
Interferer data rate	32 Mbs	Raw data rate including overheads
PU or SU Transmitter power	80 dBm	EIRP
Gaussian Noise Floor	Equation (3-1)	dBm
Reception Percentage of locations	97%	Chosen to enable Egli terrain factor

The DTT receiver antenna gain was assumed to be that of a half-wave dipole which is 2dBi. This was chosen so that omnidirectional (360^o) performance can be used for interference analysis. The DTT receiver performance of this antenna is corrected by choosing the

appropriate Egli terrain factor which is correlated against real life performance statistics as discussed below. The sensor antenna has to be omnidirectional so a theoretical antenna with a gain of 1dBi is chosen to reflect that the sensor will be small to fit the available footprint and also allow for poor earthing systems in challenging environments.

The Egli Terrain factor is the terrain loss to enable DTT reception to a certain percentage of locations at a certain frequency which is compiled from real life DTT data (Seybold, 2005). Figure 3-3 shows the relationship between terrain factor, frequency and reception percentage.

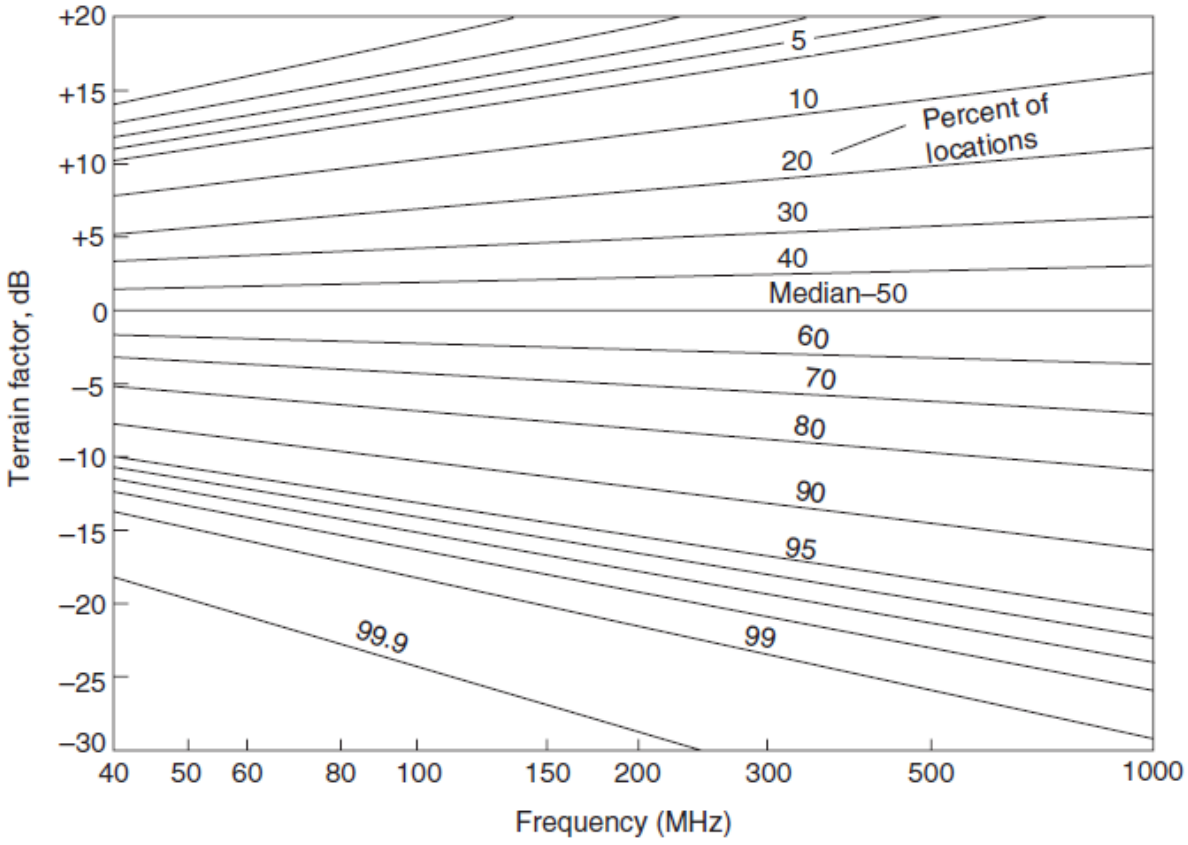

Figure 3-9: Egli Terrain Factor Data (Seybold, 2005)

This terrain factor is added to the Egli propagation loss model (<Test_Script2>) to give the overall loss to achieve the specific reception. The terrain factor data is contained in <Test_Script1> as a set of basic straight-line equations and a look up table and is used to calculate the terrain factor from the entered reception percentage of locations.

The Gaussian noise floor parameter is included into Test_Script1 which can be calculated using the normal thermal calculations shown by equation (3-5) below:

$$N = kT_0B \qquad (3\text{-}5)$$

From the above equation, the following results were found:

N= -105 dBm AWGN Noise Floor for UK DTT network and -106.2dBm for the US

To complete the flexible noise model, both co-channel and adjacent channel noise mechanisms are developed within Matlab/Simulink. The modulation type and data rate for these interferers are set within <Test_Script1> but the level is set in <Test_Script2>.

3.5.2 <Test_Script2>

As described in 3.4.1 <Test_Script1> describes the basic model parameters whereas <Test_Script2> outlines the dynamic simulation parameters such as specific distances from the transmitter, signal strength at receiver and signal to noise ratio at the receiver. The following table shows the parameters set in <Test_Script2>:

Table 3.3: Test_Script2 Parameters

Parameter	Value	Notes
Distance from the Transmitter	*D*	In Km
Set Receiver input for required Signal Strength	*DI* (DTT) *SI* (Sensor)	dB (If Distance from transmitter is not used)
Set Receiver input for required SNR	*DI* (DTT) *SI* (Sensor)	dB (If Distance from transmitter is not used)
Co-Channel or Adjacent Channel Interference	*Nx*	dBm

Egli propagation Model Path Loss Equation (3-2)	*DL* (DTT) and *SL* (Sensor)	dB (If Distance from Transmitter is used)
Line of Sight Horizon Diffraction Loss	*DF* (DTT) and *F*(Sensor)	dB (If Distance from Transmitter is used)
Obstacle Diffraction Loss	*DDF* (DTT) and *FF* (Sensor)	dB (If Distance from Transmitter is used)
DTT Receiver AGC Attenuator	*Attenuator*	dB (From look up table)

The Egli propagation model was developed specifically for VHF and UHF television transmission and is obtained from real world data so agrees with the empirical data of actual networks (Seybold, 2005). The Total Egli path loss is made up of the median path loss plus the terrain factor explained in the <Test_Script2> section and gives a path loss which is validated by real life data (Seybold, 2005). The Egli propagation path loss equation is thus:

$$Path\ Loss(DL) = 10Log_{10}\left(\left(10^{\frac{(G_T+G_R)}{10}}\right)\cdot\left[\frac{h_t\cdot h_r}{D^2}\right]^2\cdot\beta\right)+TF \qquad (3\text{-}6)$$

The equation (3-6) variables are defined in Table 3.4:

Table 3.4: Equation (3-6) Variables

Variable	Description	Note
G_T	Transmitter Antenna gain	dB (From <Test_Script1>)
G_R	Receiver Antenna gain	dB (From <Test_Script1>)
h_t	Transmitter Antenna height	Metres (From <Test_Script1>)

h_r	Receiver Antenna height	Metres (From <Test_Script1>)
β	$\left(\frac{40}{f}\right)^2$	f=Frequency in MHz (From <Test_Script1>)
TF	Egli Terrain Factor	dB (From <Test_Script1>)

From this the overall path loss can be obtained however, this does not include diffraction loss due to an obstacle which is an important factor in examining the hidden node problem. Hence, a diffraction model was developed based on the knife edge diffraction equations below (Seybold, 2005) (ITU-R, 1997):

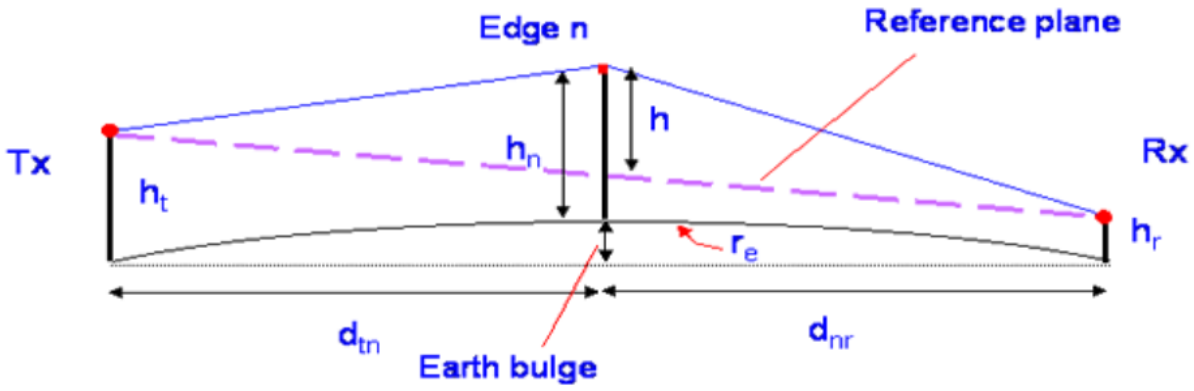

Figure 3-10: Knife Edge Diffraction Geometry (Seybold, 2005)

Using the geometry in Figure 3-4, the knife edge diffraction loss can be determined for the system diagram blocks A and B in Figure 3-2 for an obstacle of height h_n, where:

$$r_e = Earth's\ Radius$$

$$r_e = 6.35 \times 10^6 \quad m$$

$$h \approx h_n + \frac{d_{tn}d_{nr}}{2r_e} - \frac{h_t d_{nr} + h_r d_{tn}}{d_{tn} + d_{nr}} \qquad (3\text{-}7)$$

where h is the approximate height above the reference plane to the top of the obstruction and $r_e = 6.35 \times 10^6\,(m)$ is the earth's radius. Hence the Fresnel-Kirchhoff diffraction parameter v can now be evaluated from:

$$v = h\sqrt{\left(\frac{2(d_{tn} + d_{nr})}{\lambda d_{tn} d_{nr}}\right)} \quad (3\text{-}8)$$

Where $\lambda(Wavelength) = \frac{3\times10^8}{Frequency\ (Hz)}$

From this the approximate diffraction loss in dB's is given by *J(v)* in equation (3-9) which is an approximation of the Fresnel integral:

$$J(v) = 6.9 + \left(20\log_{10}\sqrt{(v-0.1)^2} + v - 0.1\right) \quad (3\text{-}9)$$

$J(v)$ is the diffraction loss *DDF* and *FF* in the model.

From block A in Figure 3-2, it can be seen there are two diffraction losses; LOS diffraction where the receiver exceeds the LOS distance and the curvature of the earth causes diffraction loss, and the obstacle diffraction loss where a large object, such as a building, obstructing the signal. For the LOS diffraction, the distance d_{tn} in (3-7) and (3-8) is the LOS distance given by:

$$LOS = \sqrt{(2\times r_e)} + \sqrt{(h_t)} + \sqrt{(h_r)} \quad (3\text{-}10)$$

The height h_n in Figure 3-3 is 0.1m, which is a slight undulation in the ground contour and thus closer to real life conditions than a perfectly flat surface.

For the obstacle diffraction block both d_{tn} and h_n are defined in <Test_Script1> and are based on the location and size of the obstacle. All the diffraction calculations are repeated for the sensor block B so that different sensor heights can be set compared to the DTT receiver height.

If the signal strength or SNR are chosen has the test criteria, then both the Egli Propagation and the diffraction blocks are omitted and a generic attenuator is inserted into the transmission path to set the correct signal strength or SNR values. The equations which set the attenuator in these cases are shown below.

Table 3.5: RSS and SNR Parameters

Parameter	Value	Notes
Required signal strength	*DI*	dBm
Required SNR	*SNR*	dB
Transmitter Power	*P*	dBm EIRP
Attenuator	*Att*	dB
Total Interference Noise	N_X	Co-Channel or Adjacent Channel dBm
Receiver Antenna Gain	G_R	dB

For Signal Strength:

$$Att = DI + P + G_R \qquad (3\text{-}11)$$

For SNR:

$$Att = SNR + N_X + P + G_R \qquad (3\text{-}12)$$

All of the above is repeated for the DTT and sensor networks due to the sensor antenna receiver height and gain may be different from the DTT receiver antenna.

The noise regime that is used consists of three types, Gaussian, adjacent channel and co-channel noise plus a receiver *NF* which is caused by electronic devices i.e., thermal noise. For the Gaussian noise, this is always present as a noise floor and is defined in equation (3-5) which is input into the model via the AWGN module in blocks A and B in Figure 3-2. For the adjacent and co-channel interference, this is generated by an IEEE 802.11af interferer block C in Figure 3-2, with the transmission spectrum shape defined by the DTT spectrum mask transfer function ($\mathcal{H}_{Mask}$). This transfer function is defined in (ETSI, 2004) and

(ATSC, 2008) and is implemented by spectrum mask filters in block C which defines the noise at the receiver input. A further filter chain is included at the front end of the receiver to define the adjacent channel rejection within the receiver and is defined by transfer function ($\mathcal{H}_{Int}$) in (DVB, 2011) and (FCC, 2007) and implemented in block C by a set of interference filters.

The equation for the co-channel interference at the receiver input in dBm, where filter $|\mathcal{H}_{Mask}|$ is assumed to be centred on the channel frequency is:

$$N_{Rx} = 10Log(10^{\frac{N_X}{10}} \cdot |\mathcal{H}_{Mask}|) \quad (3\text{-}13)$$

To quantify the amount of noise input into the mixer and demodulator after the adjacent interference filter the following equation is applied:

$$N_{Demod} = 10Log(10^{\frac{N_{Rx}}{10}} \cdot |\mathcal{H}_{Int}|) \quad (3\text{-}14)$$

The value of N_{Demod} is the injected noise into both blocks A and B (Figure A-1) as interference.

For the adjacent channel scenario, (3-13) is modified so the transfer function $|\mathcal{H}_{Mask}|$ centre frequency is offset by the DTT channel spacing used in the country of interest. For example, the UK first adjacent channel equation would be:

$$N_{Rx} = 10Log(10^{\frac{N_X}{10}} \cdot |\mathcal{H}_{Mask+8MHz}|) \quad (3\text{-}15)$$

The equation (3-14) is used as above to determine N_{Demod}.

The final noise component in the model is the receiver *NF* (Seybold, 2005) (TTP, 2013) which is introduced by electronics devices so this can vary between receivers. A median value for the DTT receiver *NF=7.5dB* was therefore chosen (TTP, 2013), so the total noise (dBm) input to the demodulator becomes:

$$N_{Total} = N_{Demod} + NF \quad (3\text{-}16)$$

3.5.3 OMNet++ and INET platform parameters

The OMNet++ and INET platform IEEE 802.11 routing model is utilised to evaluate the packet performance metrics like packet delay and throughput in a TVWS SU access MANET routing network. The physical parameters are based upon 802.11af (IEEE, 2013) using 256 QAM and a data throughput of 36Mbps. The setup parameters for such a routing simulation are shown in Table 3.6.

Table 3.6: MANET routing Parameters

Parameter	Value	Notes
Routing Area – "Playground"	constraintArea Min X, Y and Max X, Y Co-Ordinates	This is set to the BS RF Power coverage area so that the routing effect can be evaluated for the upstream link where routing is required
Number of Hosts	numHosts	Number of Mobiles
Host Mobility	RandomWPMobility	Random Waypoint Mobility
Number of Fixed Hosts	1	Following a single BS and multiple mobile network infrastructure
Fix Host mobility	Stationary Position X, Y co-ordinates	
Packet Time to Live in IPv4 or Hop Limit in IPv6	TTL	Number of routing hops until packet is discarded

IP Processing Delay	98µs	UDP Process Delay from (Carlsson et al, 2011)
SU Transmit Power	radio. transmitterPower	mW
SU Receiver Sensitivity	receiver. sensitivity	dBm (IEEE, 2013)
SU Receiver Packet Error Rate	radio. berTableFile	BER v SNR File which defines demodulation performance. Modelled IEEE802.11af
Host mobility speed	Minimum and Maximum speed with uniform distribution	metres per second
SU Transmit Frequency	Carrier Frequency	Hz
Propagation Model	Free Space	dB
Simulation Time	1000s	

The major change to the generic tool is the BER file which enables the simulation to mimic an 802.11af SU using Manet routing. The BER file records the packet size, PER and SNR for mode 36 (IEEE, 2013) in the BER file and is taken from the 256 QAM data in (Rohde and Schwarz, 2015) and (ACP, 2014), so:

$$PER = 1 - (1 - BER)^N \quad (3\text{-}17)$$

Where N is the number of bits in a packet

This allows the physical layer of the OMNet++ platform to behave as IEEE 802.11af unlicensed SU.

3.6 System Level Evaluation Methodology

The DTT transceiver will be used to assess the PU sensing solutions where the SU transceiver and OMNet++ routing platform will assess the SU efficiency to work in the PU constraints.

3.6.1 PU Sensing Evaluation

To evaluate the sensing strategies, the simulation model calculates the received signal FFT^2 sensor output for a distance from transmitter or alternatively for a particular signal strength or SNR as in (3-5 to 3-9) using the PU transmitter EIRP power. These sensor measurements are taken for the highest DTT frequency used in an arbitrary country location, which is the worst-case noise regime, so establishing a baseline for the PU detection probability (P_D) as detailed in chapters 4 and 5.

3.6.2 SU Routing Evaluation

The INET framework on the OMNet++ routing platform models a fixed node (BS) with a number of mobile nodes within a pre-defined area termed the *playground* (OMNeT, 2011). By considering various test scenarios, parameters such as TTL, RF power, routing protocol and number of mobile hosts can be adjusted so the network behaviour changes. These changes can be measured using metrics such as packet delivery ratio (PDR) and packet delay.

3.7 Performance Metrics

To critically assess the performance of a system it is important to choose appropriate performance metrics. For the PU, the key receiver parameters to be measured include *received signal strength* (RSS), SNR, BER and sensor outputs which describe the receivers' behaviour under varying channel conditions and noise environments. For the routing model, the main aim is to assess the quality of packet delivery with regards to the end user applications which include in particular, packet delivery ratio (PDR) and packet delay

(Carlsson et al, 2004) (Yagci, 2011). A short review of these assorted metrics will now be presented.

3.7.1 Received Signal Strength

This is the RF power measurement at the receiver input. The assumption is of an antenna input impedance of 50Ω as this is standard for most receiver inputs. RSS is then given by:

$$RSS = 10Log\left(\frac{\overline{(|\mathcal{F}(v(t))|^2)}}{50\times1\times10^{-3}}\right) \qquad (3\text{-}18)$$

RSS is normally referenced to 1mW so the signal strength is expressed in dBm. *v(t)* is the DTT receiver signal which usually will incur both propagation and diffraction losses. Since the receiver performance is baselined against the RSS this is a key parameter to monitor.

3.7.2 Receiver SNR

This is the received signal divided by the total noise and can also be expressed in dB as (Chen and Gao, 2011):

$$SNR = RSS + N_{Total} \qquad dB \qquad (3\text{-}19)$$

3.7.3 Bit Error Rate (BER)

This parameter evaluates the measure of the trueness of the received data content to the transmitted data. As this will be impacted by the propagation channel delay, this needs to be measured to ascertain the BER. In Simulink, this is calculated in block A (Figure 3-3), by the *system performance* module shown in Figure 3-11.

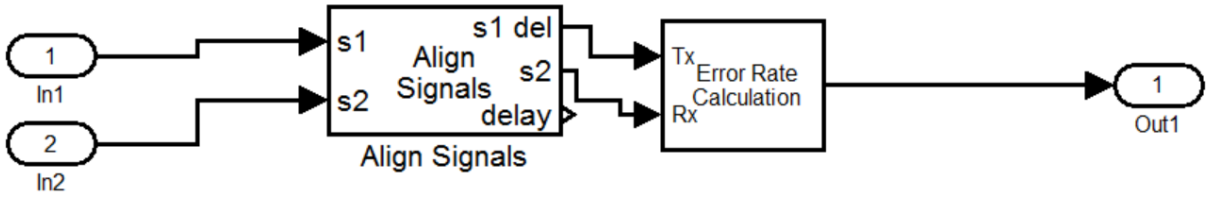

Figure 3-11: DTT PU BER Measurement System

In the *align signals* block there are two input signals, *s1* is the transmitted data and *s2* is the received data signal from the demodulator. Using a cross correlation function, this module then calculates the delay with the best alignment for *s1* and *s2*:

$$\tau_{Delay} = \arg\max_{t}((s1 \times s2)(t)) \quad (3\text{-}20)$$

The BER is then calculated by comparing the two aligned signals on a bit-wise basis.

3.7.4 Sensor Outputs

The new DSA framework employs sensing for making critical access decisions. There are two sensing methods used, the first is a FFT^2 energy detector which is the basic detector and the second is a covariance detector, which is more complex in design and is used as a comparator.

The FFT^2 classical energy detector uses a Fast Fourier Transform block and amplifier of gain *K* which is set to 1000, so for a sensing period *T*, the output *X* is:

$$\max_{0-T} X = |\mathcal{F}(v(t))|^2 \times K \quad (3\text{-}21)$$

To examine the trade-off between cost and performance, this thesis will provide comparative results on using a covariance-based detector in critically evaluating the new EDA and GEDA solutions. This comparison is made by investigating the application of a covariance-based detector to negate the effect of the desired signal being below the Gaussian noise floor. This method fits an autoregressive model to the input signal by minimising the forward prediction error in a LS (least squares) sense. The covariance detector output is given by:

$$\max_{0-T} X = cov|\mathcal{F}(v(t))|^2 \times K \quad (3\text{-}22)$$

3.7.5 Packet Delivery Ratio (PDR)

To evaluate the routing model, the metric used is the PDR (Carlsson et al, 2004) (Yagci, 2011) which reflects how effectively transmitted packets are delivered to an end user. The PDR is formally defined as:

$$PDR = \frac{\sum P_{Rx}}{\sum P_{Tx}} \quad (3\text{-}23)$$

Where:

P_{Rx} – Received Packets

P_{Tx} – Transmitted Packets

3.7.6 Packet End to End Delay

The end-to-end packet delay is a measure of the time elapsed from when the packet is transmitted to when it is received at the destination (Carlsson et al, 2004) (Yagci, 2011). The way that the OMNe++/INET platform does this is that the transmitted packet has a source time-stamp inserted and when the packet is received at the destination this time-stamp is subtracted from the simulation time to give the end-to-end delay in seconds, that is:

$$d_{end-end} = t_{ST} - t_{TS} \quad (3\text{-}24)$$

t_{ST} - simulation time

t_{TS} - source time-stamp

3.8 Calibration and Performance Validation

Throughout the development of the various PU and SU physical and SU routing models in the new TVWS access framework, software validation techniques were applied. Using the internal validation mechanisms within both Matlab and OMNeT++, early in the development coding errors were quickly resolved which aided rapid iterative model development.

To validate the PU physical model, the performance of the baseline model was established by setting various simulation parameters and using verifiable test scenarios. The

performance evaluation methodology was to verify the baseline performance against the real performance data available in (UK Free TV, 2013) and (FCC, 2015).

Figure 3-6 shows the coverage of the Mendip DTT area, which was used in the analysis as the UK case study, for which real measurement data is available (UK Free TV, 2013):

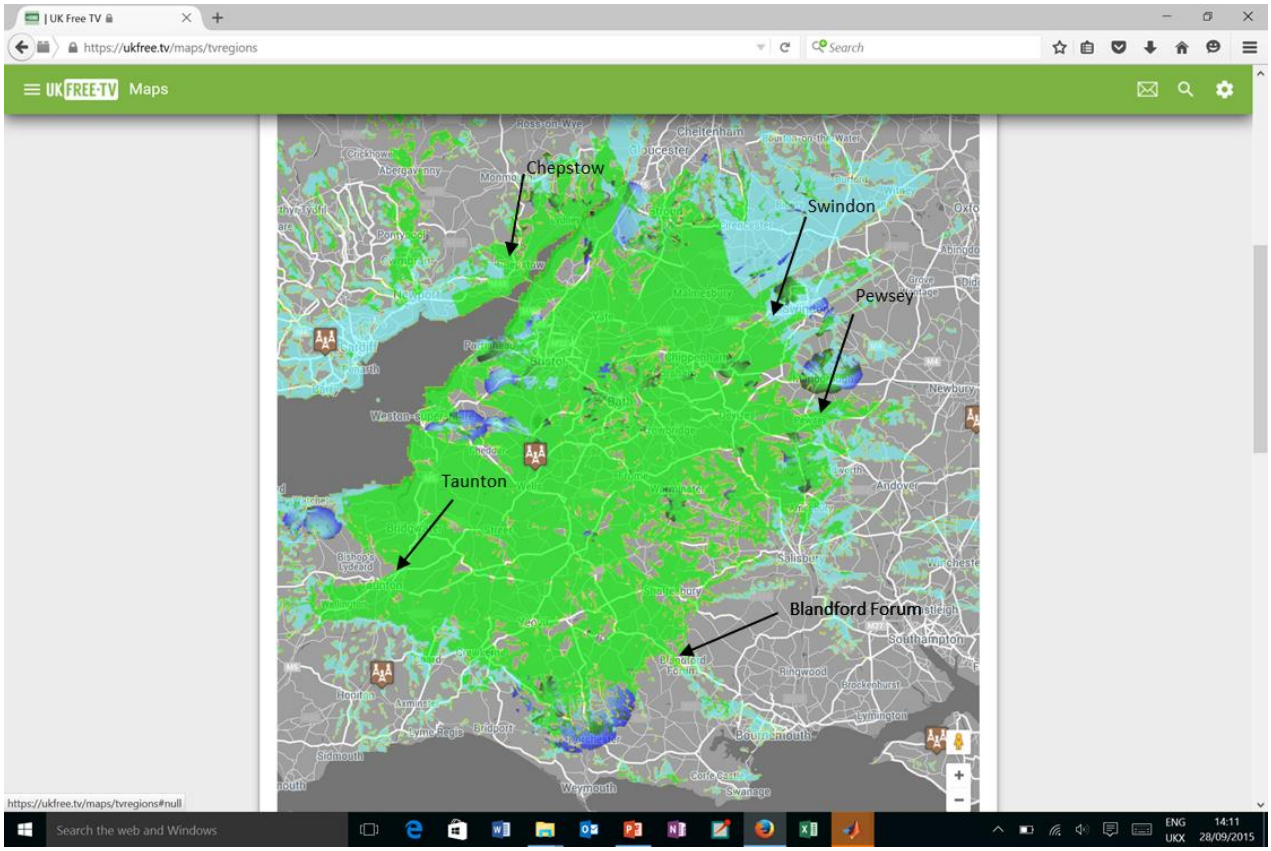

Figure 3-12: Mendip Transmitter coverage green area (UK Free TV, 2013)

To validate the new DTT model, five points at the edge of the coverage area and also the average coverage radius were calculated. These five points and their respective distances were:

Table 3.7: Defining the edge of Reception for Mendip Transmitter

Location at Edge of Reception	Distance from Mendip Transmitter Km
Taunton	44.00
Swindon	68.80
Blandford Forum	49.11

Chepstow	45.00
Pewsey	61.21

The average coverage radius for the Mendip transmitter was thus found to be 53.62 Km. Now with the DTT model, the Egli terrain factor parameter (Seybold, 2005) was adjusted until the nearest coverage radius to the average coverage radius from the real measurement data was obtained, and this occurred at a distance of 54 Km using a terrain factor of 97%, thus validating the DTT model. The same validation process was performed for the US DTT case study, using real measurement data from the Washington region transmitter WFDC shown in Figure 3-7, where the circle shows the coverage for DTT services in this scenario was found to be 80 Km.

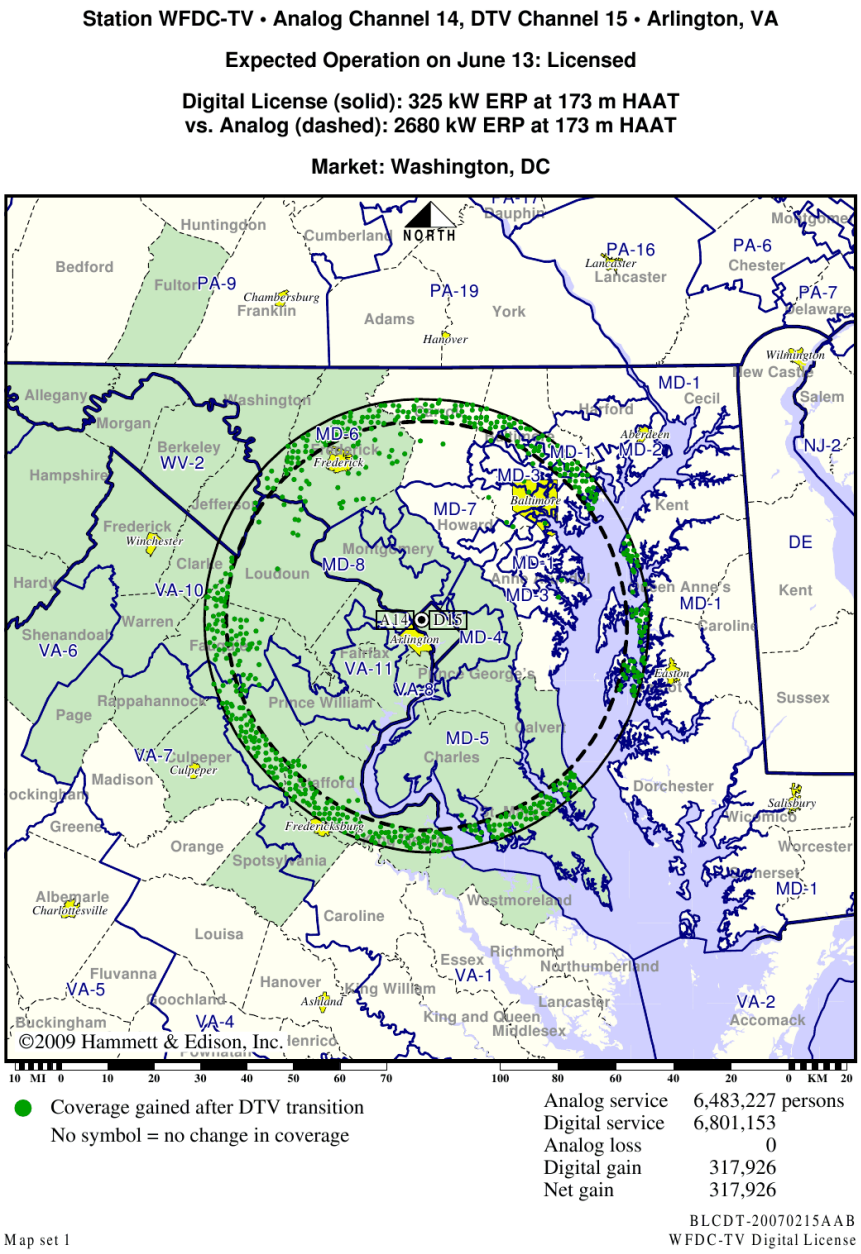

Figure 3-13: WFDC coverage real life data (FCC, 2015)

The solid circle shows the real-life coverage for DTT services which is found to be 80 Km from the scale at the bottom of Figure 3-6. It is then found using the DTT model with a terrain factor of 95% gives a coverage of 80 Km hence validating the DTT model in the US.

For the Matlab SU physical model and the OMNeT++ routing model this is verified against the IEEE802.11af specification (IEEE, 2013) and (INET, 2012) and the INET routing model is verified against IEEE 802.11 by (Yagci, 2011). Now by calculating the coverage radius

using equation 3-3 and comparing this to the modified wireless infrastructure in the modified INET model can be validated. The INET model is set up for a SU mobile EIRP and the time to live is set to 1 (No multi hops) and gives a maximum coverage of 80m. This is now compared to equation 3-3 which gives a coverage of 83m so validating the wireless infrastructure of the INET routing model.

3.9 Simulation Platforms

Two simulation platforms were used to evaluate the new TVWS access framework; namely Matlab/Simulink and OMNE++/INET. The platform requirements are detailed in the following sections. Matlab/Simulink is well positioned for wireless network modelling as there are many pre-developed wireless blocks which meet all the requirements for DTT modelling.

OMNE++/INET was developed to examine routing networks because the established IEEE802.11 blocks were a good fit for the MANET routing model. The one constraint was that the IEEE802.11 wireless block did not support IEEE802.11af, hence a customised TVWS block had to be designed, developed and tested.

3.9.1 Matlab/ Simulink Simulation Platform

Table 3.8 shows the Matlab/Simulink platform specification used:

Table 3.8: Matlab/Simulink Platform specification

Matlab Version	**PC Specification**	
MATLAB R2010a	Processor	Intel® Core™ i5 4300U CPU @ 1.9GHz – 2.5GHz
	RAM	8GB
	Hard Drive	237 GB
	OS	Windows 10 Professional

The MATLAB models were developed using the command language which is popular for mathematical modelling environments. The alternative to the MATLAB command language is Simulink, which is a MATLAB graphic editor which is intuitive to use with click and drop actions and a considerable model library to choose from. Both PU and SU physical models were built using Simulink with MATLAB command language used to control the simulation and parameters through <Test_Script1> and <Test_Script2> (see Section 3.4).

3.9.2 OMNeT++/INET Simulation Platform

Table 3.9 shows the OMNeT++/INET platform specification used:

Table 3.9: OMNeT++/INET Platform specification

OMNeT++/INET Version	**PC Specification**	
OMNeT++ version 4.3 and INET version 2.4.0	Processor	Intel® Core™ i5 4300U CPU @ 1.9GHz – 2.5GHz
	RAM	8GB
	Hard Drive	237 GB
	OS	Windows 10 Professional

The OMNeT++ is the platform (OMNeT++, 2011) which simulates IEEE802af with Manetrouting. OMNeT++ is an object-orientated modular discrete event network simulation framework which has a generic architecture which can be adapted to many problem domains including wireless communication networks and routing protocols. The INET platform is built upon the OMNeT++ platform and forms a library of communication models including IEEE 802.11 and Manetrouting networks which will be adapted within this thesis to validate network conditions.

3.10 Summary

This chapter has detailed the system model methodology, the simulation framework and supporting tools together with the performance metrics to be applied for a critical evaluation

of the various TVWS access framework contributions presented in subsequent chapters. MATLAB and OMNeT++ are the main simulation tools used with the Egli propagation approach used for the PU simulation and FSL for the SU routing model. Finally, a discussion on how the assorted software models were validated has been presented. The next chapter introduces the first contribution in the TVWS access framework, namely the *enhanced detection algorithm*.

4. ENHANCED DETECTION ALGORITHM (EDA)

4.1 Introduction

The unused television (TV) bands which have arisen from the transfer from analogue to digital TV (DTT) are commonly called *TV White Space* (TVWS) (Nekovee, 2010), (Cambridge White Spaces Consortium, 2012), (Nekovee, 2012). These have been created by the localised allocation of DTT frequencies, so frequencies not allocated in a particular geographical area are available for usage by, for example, *cognitive radio networks* (CRN), services and applications. Regulators including the Office of Communications (OFCOM) in the UK and the US Federal Communications Commission (FCC) have recently adopted proposals to allow new broadband devices to operate within TVWS (Nekovee, 2011).

To allow CRN to access TVWS, both OFCOM and FCC have imposed a number of constraints relating specifically to the access methods and spectral definition (Nekovee, 2011). Concomitantly, the IEEE 802.22 community (Nekovee, 2011) (Nekovee, 2012) have developed a framework standard for TVWS. All these constraints to some degree influence the secondary access channel performance of the sensing solutions presented in this chapter. The OFCOM, FCC and IEEE 802.22 constraint rules are summarised in Table 4.1:

Table 4.1: Regulatory TVWS Sensing Rules

Rule	Parameter	Ofcom	FCC	IEEE802.22
1	DTT Sensing Threshold	-120dBm	-114dBm	-114dBm
2	Wireless Microphone Threshold	-126dBm	-114dBm	-114dBm
3	Probability of Detection	1	1	0.9
4	Probability of False Detection	-	-	0.1

One of the major requirements of any system wanting to access TVWS is reliable detection of *primary users* (PU) to avoid interference to local users of the DTT system. Both OFCOM and FCC have favoured the geo-location database approach (Nekovee, 2011), (Nekovee, 2012) (Cambridge White Spaces Consortium, 2012), however this strategy entails considerable expense and effort to implement and keep the database infrastructure updated. Furthermore, the geo-location database utilises theoretical algorithms for calculating the safety margins to protect the PU which are not based upon real life measurements hence an overly conservative algorithm would exclude the use of too many channels to make this spectrum worthwhile where a relaxed algorithm would result in interference to DTT users (Nekovee, 2011), (Nekovee, 2012). However, if real time measurements are used to make these decisions, greater accuracy can be levered due to the fact that it is adapting to the propagation and interference conditions at the time. Due to these points, sensing mechanisms are considered in this chapter.

The benefits of using an energy sensing detection strategy as opposed to the more sophisticated cyclostationary or Wavelet detection techniques (Haykin, 2005) is the lower cost of implementation which is crucial when cognisance is made that this will be implemented in all distributed broadband wireless access points. To examine the vital trade-off between cost and performance, this chapter will provide quantitative results on the performance and complexity of applying a covariance-based detector as the comparator to

the proposed FFT ^{2} solution. The covariance detection method fits an autoregressive (AR) model to minimise the errors generated by the desired signal being under the noise floor.

This chapter also investigates a cross layer mechanism called the *cross layer cognitive engine* (CLCE) which shares information between the medium access control (MAC) and physical layers, so sensing measurements can influence spectrum access decisions (Baldo and Zorzi, 2008), (Chen and Prasad, 2009), (Hossain et al, 2009), (Martin et al, 2011) and (Martin et al, 2013). The CLCE forms the basis of a new *enhanced detection algorithm* (EDA) (Martin et al, 2011) (Martin et al, 2013) (Martin et al, 2016) which defines the way a TVWS channel is accessed. The EDA utilises the patterns in which the DTT frequencies are deployed to determine whether a PU is occupying a channel, and importantly utilises an energy detector which behaves as a feature detector when a fuzzy logic algorithm is applied which exploits local real-time measurements in the decision making.

4.2 EDA Design

Conventionally the OSI model passes information serially between layers, which inherently introduces latency into the decision making process decisions (Baldo and Zorzi, 2008), (Chen and Prasad, 2009), (Hossain et al, 2009), (Martin et al, 2011) and (Martin et al, 2013). This has not been a major issue so far because CRN research has predominantly focused to date on the physical layer. As the emphasis shifts however, towards optimising the available resources to improve the QoS for the end-user, CRN systems need to concomitantly influence parameters in different OSI layers. The CLCE offers a mechanism to achieve this as opposed to the sequential operation of the OSI model and so reducing delays in getting parameter changes and indeed some changes could not be implemented because the parameter transference mechanism is not in the OSI model (Baldo and Zorzi, 2008), (Chen and Prasad, 2009), (Hossain et al, 2009), (Martin et al, 2011) and (Martin et al, 2013).

Examples of this are optimising RF power for routing through to dynamic spectrum access decisions both in layer 1 and 2 which are tailored to the requirements of layers 3, 4 and 5.

The EDA fits into the cross-layer architecture (Akyildiz et al, 2009) with the EDA performing the following functions as defined:

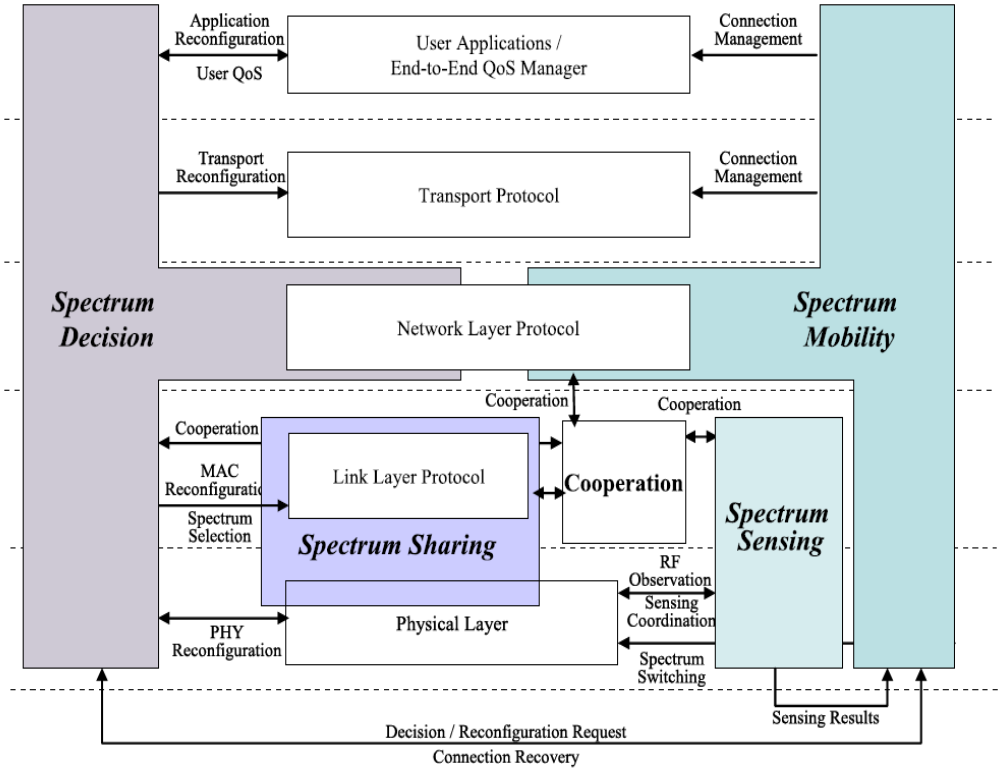

Figure 4-1: Block diagram of a generic Cross-Layer Cognitive Engine (CLCE) architecture (Akyildiz et al, 2009)

Figure 4-1 reflects the mapping to the OSI model where User Application/ End to End QoS manager represents OSI layers 5, 6 and 7 where the lower layers are as per the OSI model.

i) ***Spectrum sensing***: this block transmits the energy sensing measurements from the physical layer to both the *spectrum decision* and *spectrum mobility* blocks.

ii) ***Spectrum decision***: this block makes the decision as to whether a particular channel is vacant.

iii) ***Spectrum mobility***: this block manages channel handoffs in the event of a PU becoming active during a SU session. In the TVWS scenario this is when the regional DTT

frequency allocation is adjusted which is very rare but if it does the EDA application would automatically adjust to the new allocation.

Sensing results are available for both the spectrum decision and mobility blocks so channel data can be assessed to determine whether it can be utilised by a TVWS SU. It also enables a PU database to be constructed so SU channel availability is logged. Once a SU channel choice is made by the BS, it is communicated to all OSI layers of the SU transceiver pair along with other data including RF power to use, available data rate and MTU size. This information is communicated to each OSI layer instantaneously to ensure fast system configuration. If this information was serially transmitted to the SU pair through the OSI communication blocks, the channel acquisition time for a SU would be greater and the user QoS impacted due to longer latency.

The initial goal of the EDA is to achieve better channel allocation decisions, so the blocks which have been implemented in the CLCE architecture are those directly related to spectrum mobility, spectrum decision and spectrum sensing. The main challenges to using a sensing solution is to be able to detect a PU down at the sensing thresholds (Table 2.2) which for the UK is -120dBm and for US -114dBm, both of which are below the noise floor. EDA presents a novel solution for these low sensing thresholds, however in PMSE scenarios, the noise floor is set in the UK at -126dBm (Nekovee, 2012) due to the fact they can be used in auditoriums, so making it very difficult to sense. This functionality should be implemented by the SU base station because of the hidden node issue impacting mobile SU because of the low antenna height and then the decision is communicated to mobile SU devices by an engineering channel. This engineering channel could be for instance for an integrated TVWS access into a heterogeneous LTE network where the LTE session attachment signalling channels act as the engineering channel for the TVWS BS SU to the mobile SU. This then achieves accurate PU detection which in this case is licensed DTT transmitter in the UK and

overcomes the issue of hidden node problem at low antenna heights for mobile SU. PMSE systems such as radio microphones are not included in the EDA design and should be entered manually into the PU database as per the geo-location database due to the sensing threshold being beyond the range of EDA.

The EDA PU detection mechanism is achieved by exploiting *a priori* information about the DTT system and sharing this between the MAC and physical layers together with the cognitive cycle (Akyildiz et al, 2009) in making a spectrum access decision. The net outcome from this mechanism is to transform an energy/covariance sensor into a feature sensor, which as will be evidenced (Martin et al 2011) (Martin et al 2013) in this section, consistently provides superior performance for the TVWS scenario compared to other solutions (Lei Qiu Jing et al, 2011), (Chen and Gao, 2011).

Several approaches for implementing CLCE blocks have been previously proposed (Ghosh and Agrawal, 2007), (Baldo and Zorzi, 2008), (Hossain et al, 2009)**, (**Kokar and Lechowicz, 2009), (He et al, 2010) with their respective advantages and drawbacks being outlined as follows:

Radio Knowledge Representation Language - Each micro-world represents a specific wireless technology which implies the CLCE needs explicit knowledge about these technologies. This is contrary to the aforementioned modularity and scalability features.

Artificial Intelligence (AI) - established solutions like genetic algorithms and neural networks are well suited to handling large sets of variables, but they generally require long supervised learning times which is not practical for wireless applications.

Fuzzy Logic Controllers – technology- specific information is kept in the OSI layers with a more generic information representation base used in the CLCE such as energy

sensing values in a channel. Improved information interpretability is achieved by exploiting linguistic attributes for membership functions using fuzzy logic controllers. Precision and accuracy issues are avoided by using what is an imprecise knowledge representation base. Fuzzy Logic Controllers require low computational power and dedicated Fuzzy Logic Controllers can be used for critical scenarios in a distributed architecture.

The fuzzy logic inference model comprises the following blocks: a fuzzifier, a set of fuzzy rules and a de-fuzzifier (Baldo and Zorzi, 2008). The role of the fuzzifier is to translate the input into a fuzzy set which is allocated a membership function. The fuzzy rules govern the complete behaviour of the fuzzy logic model and encompass the knowledge base of the system it is representing. The de-fuzzifier is where a crisp output is produced using the *centre of area method* (Baldo and Zorzi, 2008). This model has the capability to predict the output with uncertain and inaccurate inputs due to the linguistic rules used (Baldo and Zorzi, 2008).

A fuzzy logic controller can be embedded into either the OSI layer or a cross layer block to represent the knowledge base of the CLCE (Baldo and Zorzi, 2008). The fuzzy rules are then capable of representing the unpredictable nature of the propagation of the DTT signal.

Since fuzzy logic fulfils many of the essential requirements of a CR-based CLCE for TVWS applications, allied with relatively being straightforward to implement and incurring low computational overheads. For the reasons outlined the EDA will utilise the fuzzy logic option for achieving improved channel allocation within the CLCE design which turns an energy detector into a feature detector by implementing knowledge of the DTT channel deployment into the knowledge base**.**

EDA shares information between the *medium access control* (MAC) and physical layers, so energy sensing measurements dynamically influence DSA decisions (Akyildiz et al, 2009), (Martin et al, 2013). EDA innovatively exploits inherent patterns in the DTT frequency deployment to determine whether a PU occupies a particular DTT channel. By scanning adjacent frequencies on either side of the channel under investigation, this effectively turns the energy detector into a feature detector, with the *scan range* parameter *B* determining the number of channels to be sequentially scanned. Hence, if *Ch_A* is the DTT channel under review, EDA symmetrically scans *Ch_A*±1, *Ch_A*±2… up to *Ch_A*±B. Symmetrical scanning is used because the probability of a neighbouring DTT channel being below Ch A or above is equal.

This affords a unique sensing option for DTT transmitters because regional DTT frequencies are deployed in clusters of 6 channels in the UK and due to DTT domestic receiver antennae groupings (Ægis Systems and i2 Media, 2009) and (Australian Government Digital Switch Over Taskforce, 2009), these 6 channels can only lie within a possible bandwidth of 16 DTT channels. The corollary is that by scanning *B* channels either side of the channel of interest, the majority of occupied DTT channels in a region are detected, with crucially, low false detection probabilities being achieved by maintaining a low *B* value. EDA (Martin et al 2011) uses the sensed energy values in the scanned channels to resolve whether the DTT channel is occupied. This approach allied together with a geo-location database means EDA generates an accurate map of PU channel usage. The advantage of EDA, when coupled with a geo-location database, is that an accurate mapping of PU channel usage is obtained. PMSE devices can also be included in the database so reducing PU interference and increasing the available bandwidth for SU.

Figure 4-2 shows the block diagram of the EDA (Martin et al, 2011) (Martin et al, 2013) (Martin et al, 2016):

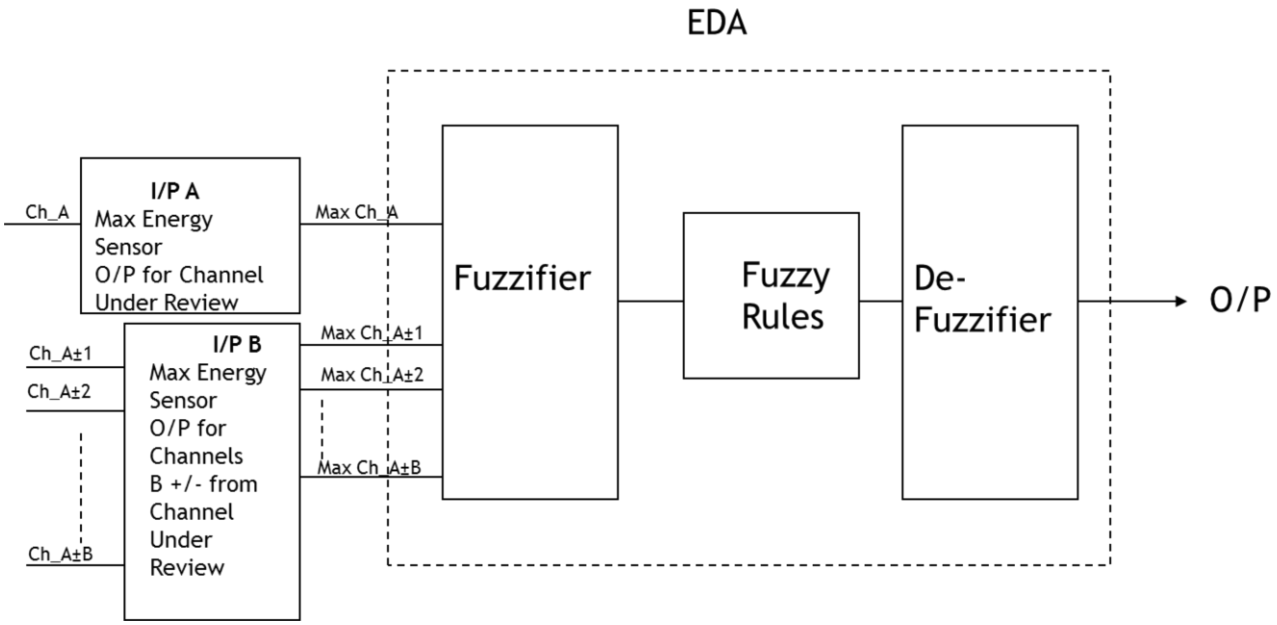

Figure 4-2: EDA Block Diagram

Figure 4.2 shows the fuzzy logic inference model for the EDA, in which it adopts the classic fuzzy logic framework (Baldo and Zorzi, 2008), so the I/P A is from the sensor output for the channel under investigation and the I/P B is the maximum sensor output for either 1 to *B* channels up or down from the channel under investigation. The parameter *B* and the choice of value will be discussed later in this chapter.

The role of the fuzzifier is to translate the input into a fuzzy set which is allocated a membership function. This follows a normal (Gaussian) probability function used for RF detection. The Fuzzy Rule block defines how the EDA behaves under practical conditions. The final block is the de-fuzzifier where a crisp output is produced using the *centre of area* method (Baldo and Zorzi, 2008).

4.2.1 Fuzzy Logic Membership Functions

The following sections outline how the fuzzy logic membership functions are specified for both the FFT^2 and covariance sensor technologies to enable a comparison to be achieved later in the chapter.

4.2.1.1 FFT [2] Design

The transition points for the three membership functions *Lo*, *Med* and *Hi* follow the following strategy where the horizontal axis depicts the RF energy and vertical axis is the probability of the specific membership function. The resulting membership function shown is for a FFT[2] detector:

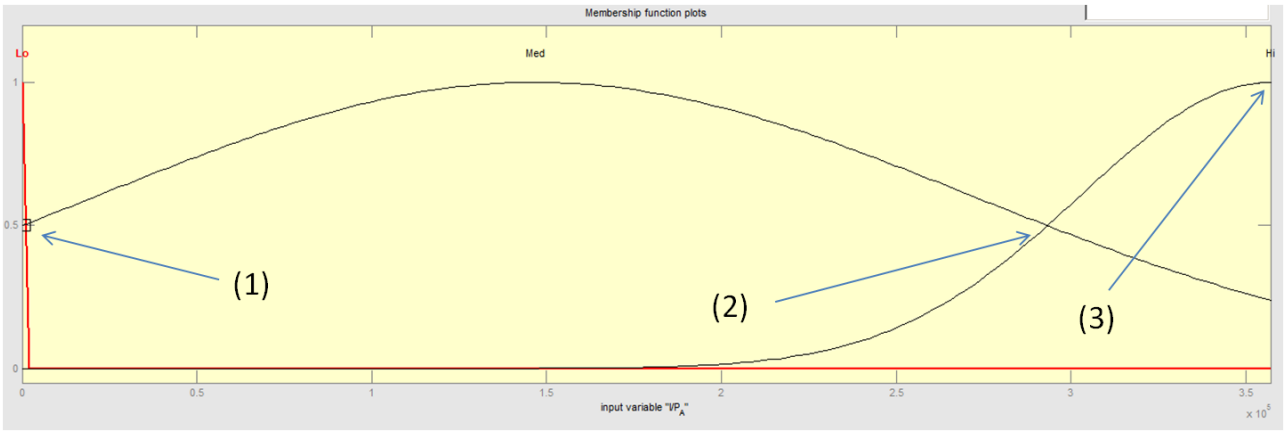

Figure 4-3: Membership Function Thresholds for FFT [2]

The y axis is the probability and x axis is the sensor output from 0 to the sensor output to achieve a BER of 2 x 10^6 using a Egli terrain factor of 99.9%.

Membership function ***Lo*** is where the detector deems the PU to be not present. The transition point **(1)** is defined by regulatory bodies as the sensing floor signal strength (OFCOM = -120dBm) and is the transition point between ***Lo*** and ***Med***.

Membership function ***Med*** is where an energy measurement falls into the category of uncertain and the PU may be present or not so this condition is resolved by the fuzzy rules implemented.

Transition point **(2)** defines the overlap between ***Med*** and ***Hi*** and is where the signal strength will achieve a BER of less than 2 x 10^6 for 90% service availability to PU users from the Egli model.

Transition point **(3)** is where the ***Hi*** Gaussian curve reaches maximum i.e. achieving a BER of less than 2 x 10^6 for 99.9% service availability to PU from Egli model.

Table 4.2: Transition reference RF Model Parameters for FFT[2]

Reference Region Parameter	Value
DTT EIRP	100KW
Modulation Scheme	256 QAM
Frequency	786 MHz
Gaussian Noise	-105 dBm
Adjacent Noise	-400 dBm
Propagation Model	Egli TF 90% and 99.9%
DTT Rx Noise Figure	7.5 dB
Sensor Rx Noise Figure	10 dB
Sensor Technology	FFT [2]

The following thresholds were calculated using the highest DTT frequency used in the UK which is 786MHz and the highest order modulation scheme used which is 256 QAM. These parameters allow evaluation of the model under worst case conditions seeing higher the frequency lower the received signal power to demodulate a signal without errors while higher modulation schemes increases the received signal power required to demodulate the signal without errors.

The DTT transmitter is at 100KW EIRP which is representive of a the EIRP of a major UK DTT transmitter and the noise regime for these energy calculations is a white noise floor of -105dBm. This is calculated from the equation below:

$$N = kT_0B \qquad (4\text{-}1)$$

Where:

k= 1.38 x 10^{-23} – Boltzmann constant

T_0= 290 ^oK – Ambient temperature 17^oC

B= 8MHz for the UK

This is the worst-case RF energy results for the threshold values, so it ensures that all possible scenarios are covered.

The transition point (1) in Figure 4-3 is X_U the RF energy for a RSS (Received Signal Strength) which will be the sensing floor determined by the regulatory body of the country in question at the receiver antenna and defines the *Lo* to *Med* membership function transition.

$$\max_{0-T} X_U = \left|\mathcal{F}(RSS_y)\right|^2 \qquad (4\text{-}2)$$

Where:

X_U = RF Energy for a received signal strength of -120dBm at receiver antenna

RSS_y = -120dBm (For the UK)

T = Sensing period (50mS)

X_U = 7.9832546e+001

The transition point (2) in Figure 4-3 is X_0 the RF energy at a distance to achieve a BER of 2x10^{-6} using the Egli propagation model terrain factor of 90% and defines the *Med* to *Hi* membership function transition.

$$\max_{0-T} X_0 = |\mathcal{F}(RSS_x)|^2 \qquad (4\text{-}3)$$

Where:

X_0 = RF Energy for a BER of 2 x 10^{-6} using the Egli Propagation model terrain factor of 90%.

T = Sensing period (50mS)

RSS_x = Received Signal strength using Egli Propagation Model of fade probability of 90%.to give BER of 2 x 10^{-6}

X_O = 2.9293831e+05

The transition point (3) in Figure 4-3 is X_C the RF energy for a BER of 2 x 10^{-6} using the Egli propagation model terrain factor of 99.9% that defines the value of RF energy where adjacent channels are not required to resolve channel occupancy.

$$\max_{0-T} X_C = |\mathcal{F}(RSS_x)|^2 \qquad (4\text{-}4)$$

Where:

X_C = RF Energy for a BER of 2 x 10^{-6} using the Egli Propagation model terrain factor of 99.9%.

T = Sensing period (50mS)

RSS_x = Received Signal strength using Egli Propagation Model of fade probability of 99.9%.to give BER of 2 x 10^{-6}

$$X_C = 3.5672237e+05$$

The fuzzy membership function response is defined in the equations below for an energy range 0 to X_C for the fuzzy logic tool within Matlab and for the FFT^2 sensor is shown in Figure 4-3:

$$fuzzy\ set\ Lo\ is\ \backslash\ shaped\ (gaussmf) = 0, \sqrt{(-(X_U - 0)^2/2 \cdot Ln(0.5))} \quad (4\text{-}5)$$

$$fuzzy\ set\ Med\ is\ /\backslash\ shaped\ (gaussmf) = \frac{(X_O - X_U) - X_U}{2}, \sqrt{(-(X_O - X_U)^2/2 \cdot Ln(0.5))} \quad (4\text{-}6)$$

$$fuzzy\ set\ Hi\ is\ /\ shaped\ (gaussmf) = X_C, \sqrt{(-(X_O - X_C)^2/2 \cdot Ln(0.5))} \quad (4\text{-}7)$$

4.2.1.2 Covariance Design

A further comparison was made by investigating the use of a covariance detection method which can be used to negate the effect of the lower threshold being under the Gaussian noise floor (-105dBm). This method fits an autoregressive model to the signal by minimising the forward prediction error in a LS (least squares) (Matlab, 2010) sense to minimise the errors generated by the desired signal being below the noise floor.

The transition points for the three membership functions *Lo*, *Med* and *Hi* follow the following strategy where the horizontal axis depicts the RF energy and the vertical axis is

the probability of the specific membership function. The resulting membership function shown is for a covariance detector:

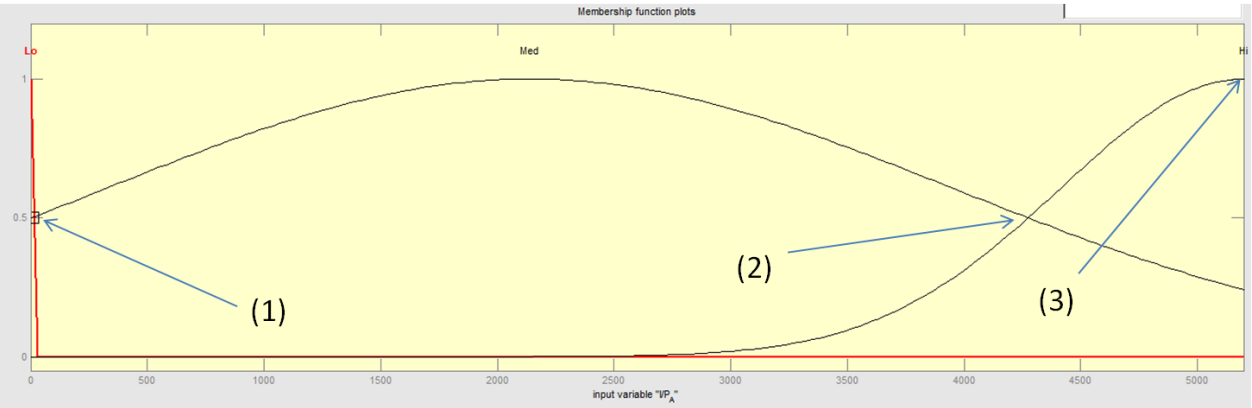

Figure 4-4: Membership Function transition points for covariance

Table 4.3: Transition reference RF Model for Covariance

Reference Region Parameter	Value
DTT Effective Radiated Power (EIRP)	100KW
Modulation Scheme	256 QAM
Frequency	786 MHz
Gaussian Noise	-105 dBm
Adjacent Noise	-400 dBm
Propagation Model	Egli TF 90% and 99.9%
DTT Rx Noise Figure	7.5 dB
Sensor Rx Noise Figure	10 dB
Sensor Technology	Covariance

Using the RF parameters in Table 4.3, the worst-case RF energy results for the thresholds were calculated which ensures that the thresholds represent the worst case and hence all situations.

The transition point (1) from Figure 4-4 is X_U the RF energy for a RSS (Received Signal Strength) which will be the sensing floor determined by the regulatory body of the country in question at the receiver antenna and defines the Lo to Med membership function transition.

$$\max_{0-T} X_U = cov\left|RSS_y\right| \qquad (4\text{-}8)$$

Where:

X_u = RF Energy for a received signal strength of -120dBm at receiver antenna

RSS_y = -120dBm (For the UK)

T = Sensing period (50mS)

$$X_U = 1.6239516$$

The transition point (2) from Figure 4-4 is X_0 the RF energy at a distance to achieve a BER of 2×10^{-6} using the Egli propagation model terrain factor of 90% and defines the Med to Hi membership function transition.

$$\max_{0-T} X_O = cov|RSS_x| \qquad (4\text{-}9)$$

Where:

X_0 = RF Energy for a BER of 2×10^{-6} using the Egli Propagation model terrain factor of 90%.

T = Sensing period (50mS)

RSS_x = Received Signal strength using Egli Propagation Model of fade probability of 90%.to give BER of 2×10^{-6}

X_O = 4.2744575e+003

The transition point (3) from Figure 4-4 is X_C the RF energy for a BER of 2 x 10^{-6} using the Egli propagation model terrain factor of 99.9% that defines the value of RF energy where adjacent channels are not required to resolve channel occupancy.

$$\max_{0-T} X_C = cov\left|RSS_y\right| \qquad (4\text{-}10)$$

Where:

X_C = RF Energy for a BER of 2 x 10^{-6} using the Egli Propagation model terrain factor of 99.9%.

T = Sensing period (50mS)

RSS_y = Received Signal strength using Egli Propagation Model of fade probability of 99.9%.to give BER of 2 x 10^{-6}

X_C = 5.1980315e+003

Equations 4-5, 4-6 and 4-7 define the membership functions *Lo*, *Med* and *Hi* within the Matlab fuzzy logic tool and for the covariance sensor shown in Figure 4-4.

4.2.2 Fuzzy Logic Rules

The fuzzy rules block then dictates the behaviour of the EDA with the membership functions defined above and the de-fuzzifier produces a crisp output of either occupied or un-occupied. The weighting factor is applied to compensate for the membership functions overlapping and outputs were evaluated by experimental methods. The rules adopted are shown below and are common to all sensor technologies:

1. IF (I/P A *Max Ch_A*) = *Lo* THEN (O/P) = *unoccupied* – Weight=0.97

2. IF (I/P A *Max Ch_A*) = *Med* AND (I/P B *Max Ch_A±2* to *Max Ch_A±B*) = *Lo* THEN (O/P) = *unoccupied* - Weight=0.97
3. IF (I/P A *Max Ch_A*) = *Med* AND (Inclusive OR [I/P B *Max Ch_A±2* to *Max Ch_A±B*]) = *Hi* AND (I/P B Max Ch_A±1) = *Hi* THEN (O/P) = *unoccupied* – Weight=1
4. IF (I/P A *Max Ch_A*) = *Med* AND (Inclusive OR [I/P B *Max Ch_A±2* to *Max Ch_A±B*]) = *Med* AND (I/P B *Max Ch_A±1*) = *Hi* THEN (O/P) = *occupied* – Weight = 0.97
5. IF (I/P A *Max Ch_A*) = *Med* AND (Inclusive OR [I/P B *Max Ch_A±2* to *Max Ch_A±B*]) = NOT *Lo* AND (I/P B *Max Ch_A±1*) = NOT *Hi* THEN (O/P) = *occupied* – Weight=0.97
6. IF (I/P A *Max Ch_A*) = *Hi* THEN (O/P) = *occupied* – Weight=1
7. IF (I/P A *Max Ch_A*) = *Med* AND (I/P B *Max Ch_A±1*) = NOT *Lo* THEN (O/P) = *occupied* – Weight=0.97

Rule 1 defines the behaviour when I/P A energy level is less than that for RSS for the sensing floor therefore returns an O/P of *unoccupied*. Rule 2, 3,4,5 and 7 define the situations where I/P A falls into the uncertain range and will require adjacent channels to identify to determine the O/P. Rule 3 and 4 defines the EDA O/P in the presence of high adjacent channel interference. Rule 6 applies to a situation where I/P A is high and because of this the output can only be occupied.

The de-fuzzifier output (O/P) follows a linear function, so 0 to 0.49 represents an *unoccupied* channel, while 0.5 to 1 reflects that it is *occupied*.

4.2.3 *B* Parameter Selection

The EDA scans channels up and down from the channel under investigation to *B*, where *B* is an integer which dictates to the EDA which channels to scan. For a particular channel which lies within the *Med* range and any other channel which is either within *B* up or down

and also lies within either the *Med* or *Hi* detection ranges, then the outcome is weighted according to a set of fuzzy rules which is defined above and a crisp occupied or unoccupied result is returned. This reflects the phenomena that DTT channels in a local area are generally deployed in a cluster configuration due to DTT antenna groupings (Ægis Systems and i2 Media, 2009) in which another DTT channel either *B* channels up or down can be located. The EDA detection/false detection response against *B* for signal strength of -120dBm and averaged over 22 Major DTT transmitter sites in the UK, is shown in Figure 4.5:

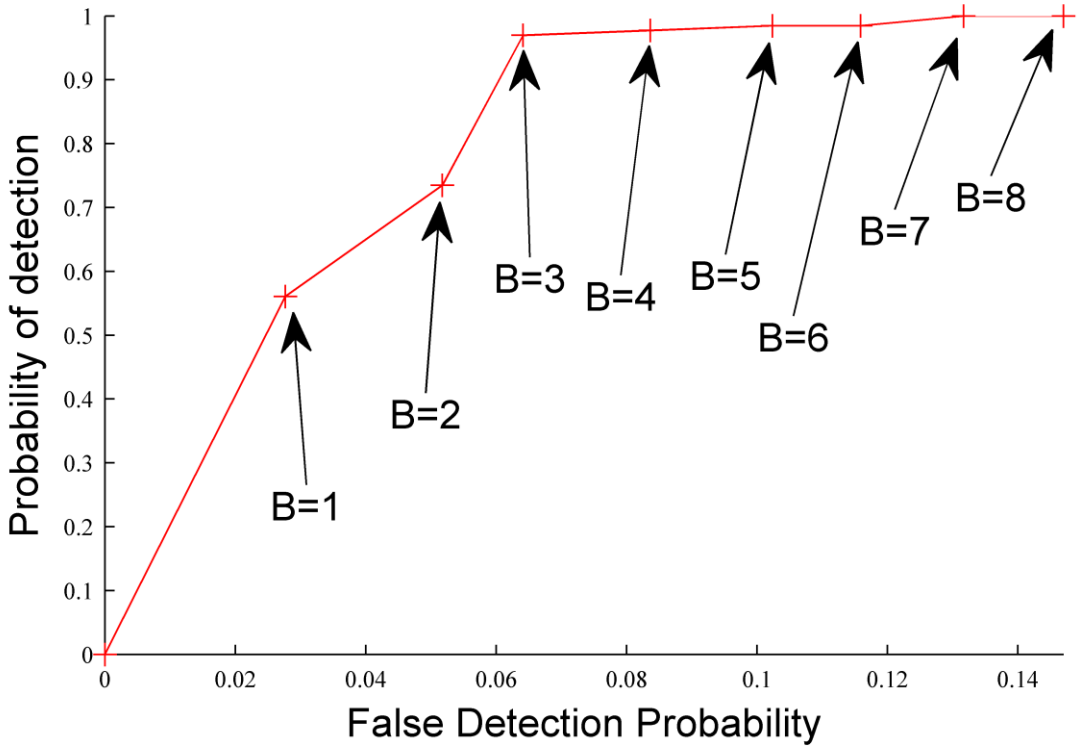

Figure 4-5: *B* Response for the UK

The parameter *B* in Figure 4-5 is calculated from two bespoke Matlab programs called detection probability (Appendix A) and false detection probability (Appendix B). These were designed as a tool to aid this thesis to determine the value of *B* to yield a certain detection probability and false detection probability from a channel deployment matrix using the EDA mechanism. This is to check that separation between channels governed by *B* will give the required P_d while P_f in specific DTT transmitter sites in the country channel deployment plan which comes from the regulators (UK Free TV, 2013), (FCC, 2015). The

process is to establish a B which yields the highest P_d while P_f remaining $\leq 10\%$. From this B is identified which will be bespoke to the country of the channel deployment matrix used.

The IEEE 802.22 standard (Nekovee, 2011) has been used for comparison with a detection probability threshold of $\geq 90\%$ and a false detection rate of $\leq 10\%$, hence the parameter used is B=4 from Figure 4-5 where the detection probability is 97.73% and the false detection probability is 6.9%. This value of B maximises the detection probability but at the same time minimises the false detection probability within the IEEE 802.22 standard window.

4.3 Results

The results are based on the EDA deployed in the UK and compared to results generated by a sensing algorithm in China (Lei Qiu Jing et al, 2011) which was chosen because the DTT bandwidth and modulation schemes are the same as the UK. Also, as the detection probability using the EDA is using a FFT^2 and a covariance sensor so in this section also produces a complexity analysis so that they can be compared from the results.

4.3.1 Probability of Detection

The performance of the EDA was compared with the results given in paper (Lei Qiu Jing et al, 2011) which is a set of results calculated from a feature sensor deployed in China which is described in Chapter 2. The reason that a China example is used was because the lack of UK examples and China using the same modulation schemes and bandwidth requirements for PUs (64/256 QAM and 8MHz bandwidth).

The strategy for evaluation of the EDA is to first produce physical results for a reference region which is the worst RF case of 256 QAM modulation and the highest DTT frequency in the UK which is 786MHz with both white Gaussian and adjacent channel noise and varying signal strength at the receiver. Once this has been produced with detection

probabilities using the Matlab fuzzy logic model for the EDA assuming a DTT PU is within *B* range which produces the probability value P_X which is the averaged detection probability across all values of interference noise for every value of signal strength. Then to evaluate the detection probability across the UK and for every channel the probability of a channel being within the *B* range for all DTT channels and across 22 major DTT transmitter regions in the UK is calculated by using the algorithm in Appendix A to produce P_{CH}. The *B* parameter is chosen as a trade-off between the detection and false detection probabilities (Table 2.2) which the solution needs to satisfy. From this an overall probability of detection (P_D) can be calculated by $P_D = P_x \cdot P_{CH}$ to give a probability of detection which is true for all sites in UK and all channels for each signal strength value.

Table 4.4: Detection Results reference RF Model

Reference Region Parameter	Value
DTT EIRP	100KW
Modulation Scheme	256 QAM
Frequency	786 MHz
Gaussian Noise	-105 dBm
Adjacent Noise	-400 to -28 dBm
Signal Strength at DTT and Sensor Rx	-125 to -75 dBm
DTT Rx Noise Figure	7.5 dB
Sensor Rx Noise Figure	10 dB
Sensor technology	FFT [2]/ Covariance

The series of physical results collate the probability of detection against the incoming signal strength, -125dBm to -75dBm for reference region which formed transceiver bench testing test where a DTT signal is applied to both the DTT transceiver and sensor. The noise regime for all tests is a Gaussian noise floor of -105dBm and on adjacent channels interferer's of -

400dBm to -28dBm was used with a noise figure 7.5dB for the DTT receiver and 10dB for the sensor receiver. The reference RF results for FFT^2 and covariance probability of detection P_X raw results are shown in Appendix C and the result P_D is shown in Table 4.7.

The next step is to generate the detection probability for the whole country and for this 22 major transmitter sites were chosen. The channel deployment design for the 22 sites is shown in Table 4.5.

Table 4.5: Channel distribution for 22 Major UK transmitter sites

Tx Site	Channel Matrix					
	Ch 1	Ch 2	Ch 3	Ch 4	Ch 5	Ch 6
Central Sutton Coldfield	43	46	40	42	45	39
Wales Wenvoe	41	44	47	42	45	39
Anglia Sandy Heath	27	24	21	51	52	48
Borders Caldbeck	25	28	30	23	26	29
Channel Islands Freemont point	44	41	47			
Granada Winter Hill	50	59	54	58	49	55
London Crystal Palace	23	26	30	25	22	28
Northern Ireland Divis	27	21	24	23	26	29
Meridian Rowbridge	24	27	21	25	22	28
STV Central Black Hill	46	43	40	41	44	47
Tyne Tees Bilsdale	26	29	23	43	46	40
West Country Caradon Hill	28	25	22	21	24	27
Yorkshire Belmont	22	25	28	30	53	60
STV North Durris	28	25	22	23	26	29
Mendip (West)	49	54	58	48	56	52
Cenral-Oxford	53	60	57	50	59	55
Central - Ridge Hill	28	25	22	21	24	27
Cenral-The Wrekin	26	23	30	41	44	47
Central-Waltham	49	54	58	29	56	57
Anglia-Sudbury	44	41	47	58	60	56
Anglia-Tacolneston	55	59	50	42	45	39
Border- Selkirk	50	59	55	57	53	60

The probability detection matrix for the 22 regions was calculated by a Matlab program which correlated the detection probability for the chosen *B* value against the channel deployment patterns for the 22 DTT UK regions using the detection probability and false detection probability algorithm. The matrix shown below in Table 4.6 is for a *B*=4 which is

the highest *B* value which still produces a false detection value of 0.1 which is the IEEE 802.22 standard threshold (Table 2.2).

Table 4.6: EDA Detection Probability Matrix for *B*=4 for 22 major UK transmitter sites

Tx Site	Channel Matrix					
	Ch 1	Ch 2	Ch 3	Ch 4	Ch 5	Ch 6
Central Sutton Coldfield	1	1	1	1	1	1
Wales Wenvoe	1	1	1	1	1	1
Anglia Sandy Heath	1	1	1	1	1	1
Borders Caldbeck	1	1	1	1	1	1
Channel Islands Freemont point	1	1	1	0	0	0
Granada Winter Hill	1	1	1	1	1	1
London Crystal Palace	1	1	1	1	1	1
Northern Ireland Divis	1	1	1	1	1	1
Meridian Rowbridge	1	1	1	1	1	1
STV Central Black Hill	1	1	1	1	1	1
Tyne Tees Bilsdale	1	1	1	1	1	1
West Country Caradon Hill	1	1	1	1	1	1
Yorkshire Belmont	1	1	1	1	0	0
STV North Durris	1	1	1	1	1	1
Mendip (West)	1	1	1	1	1	1
Cenral-Oxford	1	1	1	1	1	1
Central - Ridge Hill	1	1	1	1	1	1
Cenral-The Wrekin	1	1	1	1	1	1
Central-Waltham	0	1	1	1	1	1
Anglia-Sudbury	1	1	1	1	1	1
Anglia-Tacolneston	1	1	1	1	1	1
Border- Selkirk	1	1	1	1	1	1

The key to the Table 4.6 is 1 is detected and 0 is undetected. From Table 4.6 it can be seen that Belmont and Waltham (Highlighted Red) cannot be resolved by using *B*=4 but Freemont point does not contribute to the probability degradation because there are only 3 channels deployed in that location. It also can be seen that for all major UK transmitter sites there are 6 channels allocated for each site except for Freemont point (Highlighted Green) which is 3 channels so a single aggregated probability of P_{CH} which is calculated over all channels used in all sites shown in Table 4.7 by using algorithm in Appendix A. From P_{CH} and P_X the

overall detection probability P_d is calculated using P_X and P_{CH} which are non-exclusive events so $P_d = P_x \cdot P_{CH}$ which the results are shown below in Table 4.7:

Table 4.7: Detection Probability P_d

Signal Strength	EDA P_X assuming neighboring DTT Ch within B	Probability of a DTT Ch being within B P_{Ch} -For a UK DTT deployment B=4	$P_D = P_X \cdot P_{Ch}$
-125 dBm	0.00	0.98	0.00
-122dBm	0.00	0.98	0.00
-120dBm	1.00	0.98	0.98
-117dBm	1.00	0.98	0.98
-115dBm	1.00	0.98	0.98
-112dBm	1.00	0.98	0.98
-110dBm	1.00	0.98	0.98
-95dBm	1.00	0.98	0.98
-90dBm	1.00	0.98	0.98
-85dBm	1.00	0.98	0.98
-80dBm	1.00	1	1.00
-75dBm	1.00	1	1.00

The aggregated detection probability from Table 4.7 is calculated to be 0.98 due to the unresolved sites outlined. The overall probability results are shown in Figure 4-6 where the detection probability follows that of the P_{CH} which is 0.98 up to a signal strength of -85dBm but above this level the sensor returns a probability of 1. This is due to the RF level being

equal to or higher than the X_C threshold which means that the EDA does not look at adjacent channels to resolve occupancy and detection probability of 1.0 is returned.

The EDA false alarm probability was first derived so that the curve of the China algorithm paper (Lei Qiu Jing et al, 2011) could be chosen for comparison. From the China TVWS Detection paper the curves with false detection of 0.1 best matches the EDA false detection of 0.069 which is obtained by a false detection probability algorithm which was created in Matlab for the 22 sites using a *B=4*.

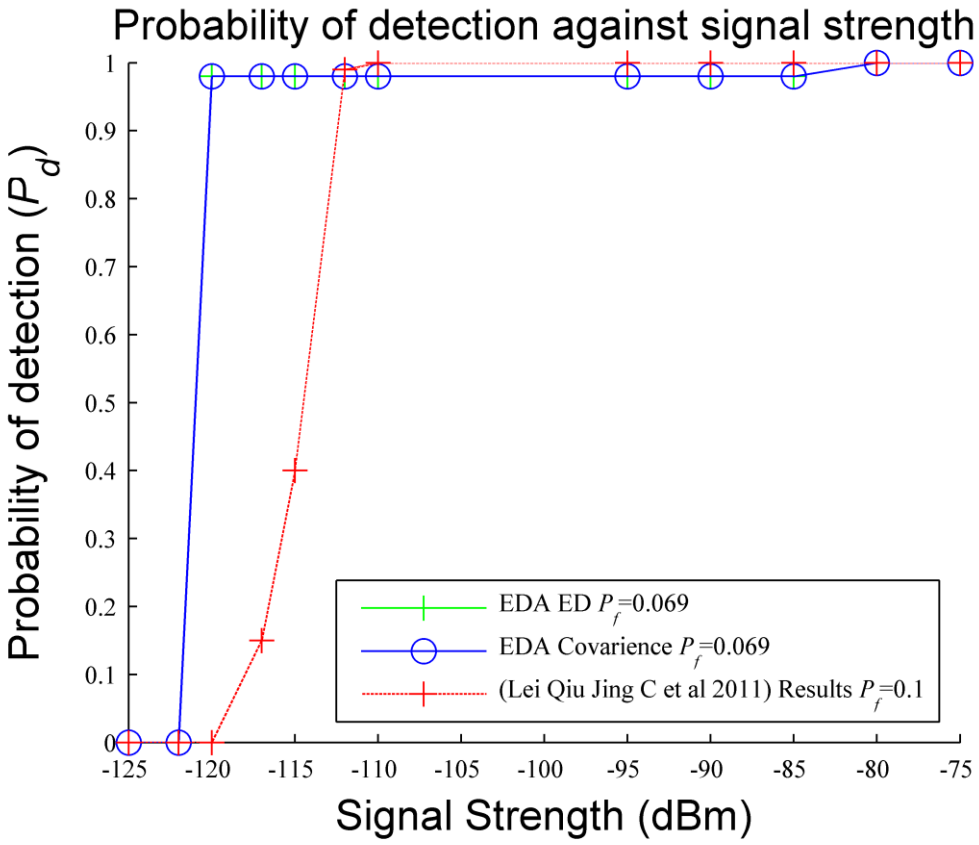

Figure 4-6: Detection Probabilities versus Signal Strength

The paper (Lei Qiu Jing et al, 2011) simulation results in Figure 4-6 achieved a P_d of 1 at a signal strength -111dBm where the EDA using energy detector simulation achieved this at -80dBm. From this paper (Lei Qiu Jing et al, 2011) outperform the EDA at a detection probability of 1.0 however both algorithms conform to the IEEE 802.22 WRAN (Nekovee, 2011) standard, where the P_d and false P_f targets are 0.9 and 0.1 respectively in an 8MHz DTT channel. Also looking at the EDA P_d of 0.98 which is achieved at -120dBm where paper (Lei Qiu Jing et al, 2011) does not achieve this till -111dBm which means the EDA

has a 9dB improvement. Comparing the false detection of both algorithms shows that the EDA outperforms paper (Lei Qiu Jing et al, 2011) by 0.069 to 0.1.

The EDA conforms to the IEEE 802.22 but as far as paper (Nekovee, 2011) conformance to OFCOM's requirement of detection probability of 1.0 at -120dBm it does not achieve the requirement. This requirement shall be reviewed again in chapter 5.

4.3.2 Complexity comparison between FFT^2 energy detector and the covariance detector

Based on the Halstead metric of a Simulink Model (Loeffler and Wegener, 2012), an assessment of the complexity of the FFT^2 energy detector against the covariance energy detector can be gained. The complexity can be determined from the following formula:

$$V = N \cdot \log_2 n \qquad (4\text{-}11)$$

Where V = Model Volume (Complexity), N = Total number of operators and operands, n = number of distinct operators and operands.

The greater the V parameter is the more memory, CPU usage, cost and power consumed can be assumed.

We apply the Halstead metrics to the Simulink models by calculating the number of operations taken in the model. The definition of an operator and operand are as follows.

- Operator of the model - Any block in the model which has one or more incoming lines and has one or more outgoing lines is an Operator.
- Operand of the model - Any incoming line to an operator is an Operand.

Figure 4-7 shows the FFT2 energy detector versus covariance detector analysis.

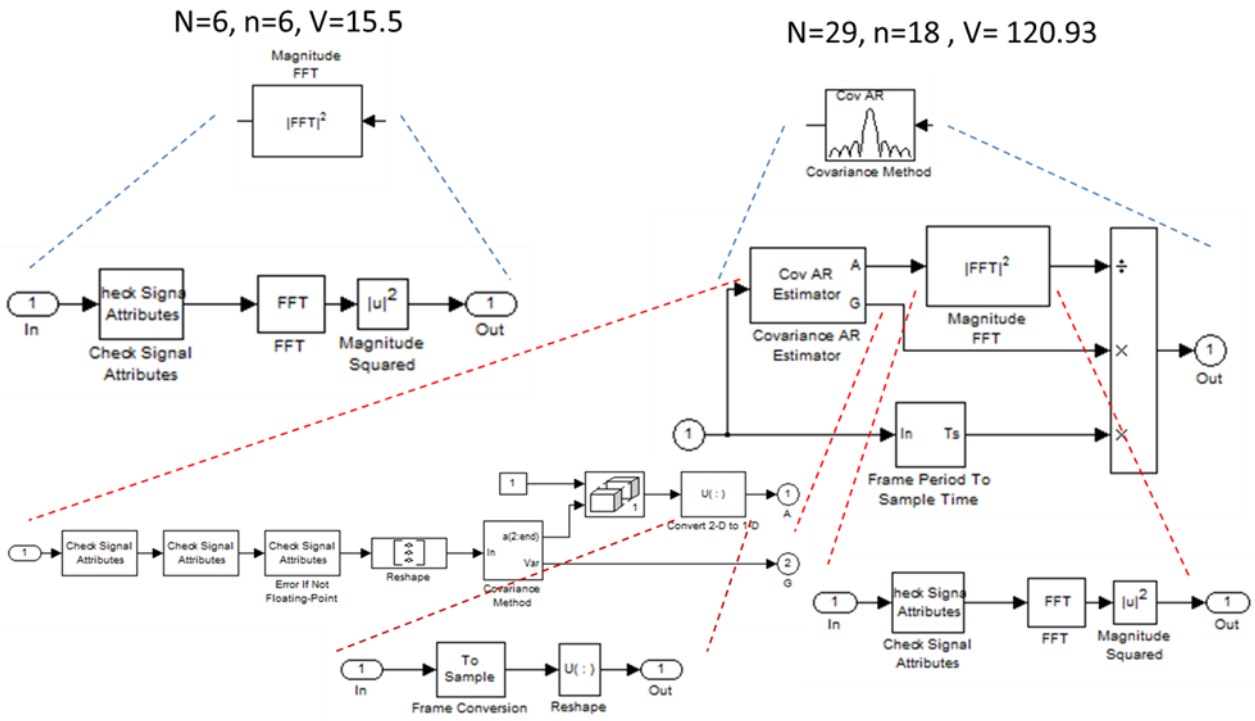

Figure 4-7: FFT^2 energy detector versus covariance detector analysis

In Figure 4-7, a distinct operator is a block which is not duplicated in the model, while a distinct operand is either an input or output which does not branch to or from another operator. So, for example for the FFT^2 model n=6 and N=6 which using equation 4-11 gives V= 15.5, while for the covariance model, n= 18 and N= 29 so V= 120.93.

From Figure 4-7 the covariance V parameter is more than six times greater in terms of complexity than the FFT^2 energy detector. This has a proportional increase in computational complexity and hence power consumption.

4.4 Summary

This chapter has shown that EDA consistently out performs existing PU detection algorithms by 9 dB when applying the IEEE 802.22 WRAN standard thresholds of 90% for detection and 10% false detection. However, in comparing both EDA and paper (Lei Qiu Jing et al,

2011) against the OFCOM requirement of *Pd* of 1.0 at a RSS of -120dBm both algorithms fell short of the mark but the (Lei Qiu Jing et al, 2011) algorithm outperforms EDA by 26dB. In comparing the covariance detector with the energy detector there was negligible improvement gained for the added complexity incurred, so the overall conclusion is for an energy detector to be used with the EDA.

This chapter also has demonstrated that a sensing strategy is feasible for TVWS applications and with the further study able to achieve detection probabilities of 100% will start to persuade the regulatory bodies to re-think their geo-location database decisions. Further work is presented in the next chapter to enable the EDA to be adaptive and achieve the detection probability of 100% in all circumstances.

5. GENERALISED EDA (GEDA)

5.1 Introduction

EDA in (Chapter 4), (Martin et al, 2011), (Martin et al, 2013) was designed for PU detection to access TVWS channels by utilising energy sensing allied with a fuzzy logic decision block, which uses information from both the MAC and physical layers to make the spectrum access decisions. The fuzzy block input was the sensor output for a reference channel and the maximum sensor output for either *B* channels up or down from the reference channel. For a specific DTT channel lying within the *uncertainty* range, and any other channel within *B* and also lying within the *uncertain* or *occupied* detection ranges, then the decision is weighted according to a set of fuzzy rules (Chapter 4), (Martin et al, 2013).

As highlighted in Chapter 4, while EDA upholds the P_f =0.1 requirement of IEEE 802.22 (Chen and Gao, 2011), it fails to achieve P_d =1.0 for the DTT sensing threshold (Nekovee, 2011), (Nekovee, 2012). This provided the motivation for the development of the GEDA paradigm, which uses certain EDA components, but importantly integrates a new refinement mechanism for selecting the *B* parameter to secure significant performance improvements.

This chapter will also demonstrate that the GEDA solution can be adapted to different TVWS strategies i.e. in different countries and still achieve the P_d and P_f results to comply to P_d =100% and $P_f \leq$10%. The North American DTT model was used to demonstrate the adaptability of the GEDA and the results of this analysis are shown in this chapter to prove this assertion.

5.2 GEDA Design

Figure 5-1 shows a block diagram of the GEDA model. In comparison with EDA (Chapter 4), (Martin et al, 2011), (Martin et al, 2013), GEDA (Martin et al, 2016) introduces three new system parameters, namely B_{Pri}, B_{Sec} and a *scaling factor* (*SF*). B_{Pri} is the initial scan range value of *B* used to evaluate channel occupancy in accordance with the IEEE 802.22 standard i.e., $P_d = 0.9$ and $P_f = 0.1$, while B_{Sec} is a higher *B* value, if required, which ensures an overall $P_d = 1$ once the first frequency scan using B_{Pri} has been completed. It is important to stress that B_{Sec} cannot be directly used at the outset of sensing by GEDA because its higher value increases the likelihood of false detection which will compromise detection performance. It is thus, only used on occupied DTT channels that B_{Pri} cannot detect. Both B_{Pri} and B_{Sec} are country-specific and are determined from EDA using the corresponding *B* value that yields the respective P_d and P_f values.

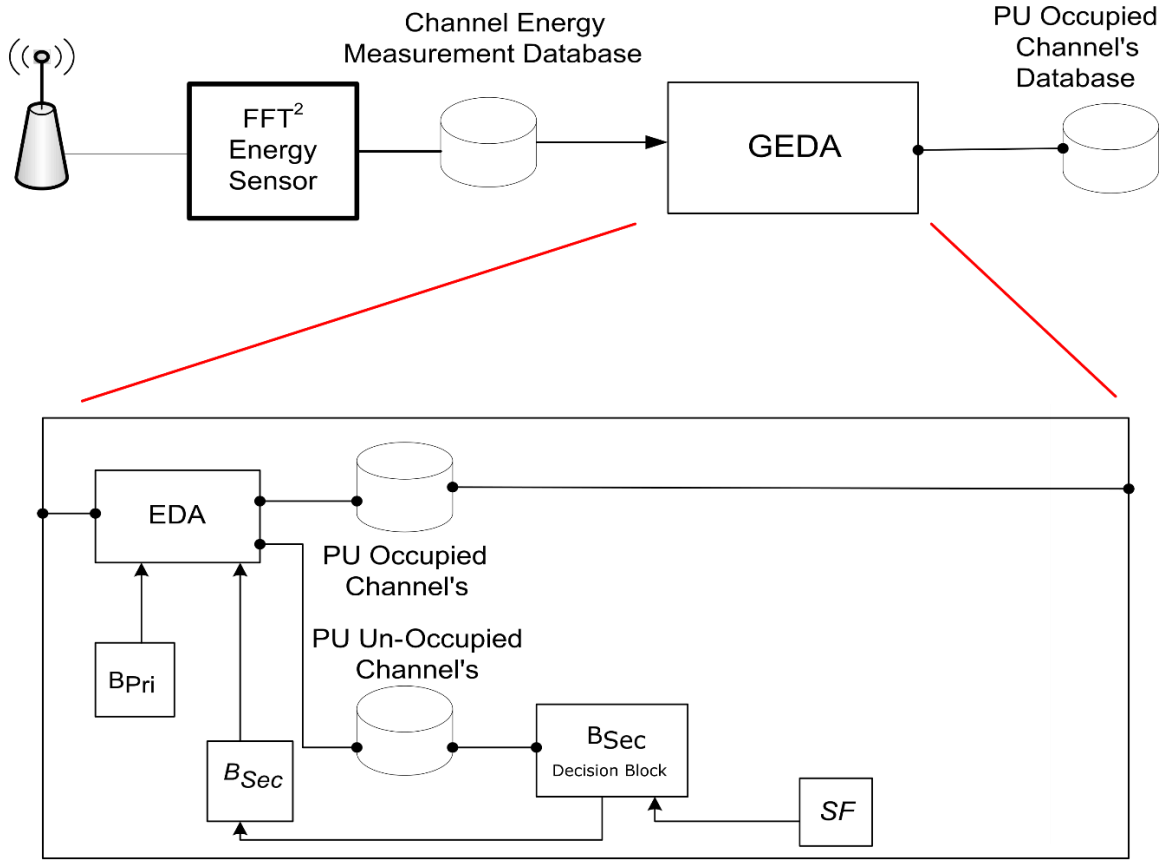

Figure 5-1: GEDA Block Diagram

Figure 5-1 shows the overall block diagram of the GEDA block in which three new input parameters are introduced, B_{Pri}, B_{Sec} and Scaling Factor (*SF*). B_{Pri} and B_{Sec} are two values of *B* used by the GEDA algorithm to achieve a detection probability of 1.0 and a false detection within the IEEE 802.22 specification while the *SF* parameter is the trigger to switch between B_{Pri} and B_{Sec}.

GEDA detection can thus use either B_{Pri} or B_{Sec} for its DTT scanning range. The former is the initial scan range *B* value and in many cases, this is the only value required. In a few cases however, B_{Sec} has to be used to achieve P_d =1. Whether B_{Sec} is used is governed by the *SF*, which is the ratio of the highest to the lowest DTT frequency energy values, both of which are stipulated by the relevant regulatory authority (Nekovee, 2012).

Both B_{Pri} and B_{Sec} are calculated from two bespoke Matlab programs called the detection probability (Appendix A) and the false detection probability (Appendix B) algorithms. These were designed as a tool to aid this thesis to determine the value of B_{Pri} and B_{Sec} to yield a certain detection probability and false detection probability from a channel deployment matrix using the GEDA mechanism. This checks the separation between channels governed by B_{Pri} and B_{Sec} and will calculate the resulting P_d and P_f in specific DTT transmitter sites in the country channel deployment plan which comes from the regulators (UK Free TV, 2013), (FCC, 2015). The process is to establish a B_{Pri} which yields the highest P_d while P_f remaining ≤ 10%. For B_{Sec} the value is increased until P_d=1 and the overall P_f is ≤ 10%. From this B_{Pri} and B_{Sec} are identified to achieve a P_d =1 while minimising P_f to ≤ 10% which will be bespoke to the country of the channel deployment matrix used.

5.2.1 Scaling Factor

Using this highest frequency (lowest RF energy) to the lowest frequency (highest RF energy) ratio enables a window of energy measurements to be defined within which it is feasible that a PU DTT channel may trigger using B_{Sec}, provided the channel is in the unoccupied channel

database. Thus, by scaling the lowest frequency energy measurement in the DTT channel occupied database obtained using B_{Pri}, a threshold for using B_{Sec} on an unoccupied DTT channel is established. *SF* is formally expressed as:

$$SF = \frac{\left|\mathcal{F}\left(RSS_{Hi\_DTTFreq}\right)\right|^2}{\left|\mathcal{F}\left(RSS_{Lo\_DTTFreq}\right)\right|^2} \tag{5-1}$$

where $RSS_{Hi\_DTTFreq}$ and $RSS_{Lo\_DTTFreq}$ are the respective *received signal strength* (RSS) measurements for the highest and lowest DTT frequencies for a preset distance between the DTT transmitter and receiver.

5.2.2 GEDA Algorithm

The flowchart of the complete GEDA process is shown in Fig. 5-2.

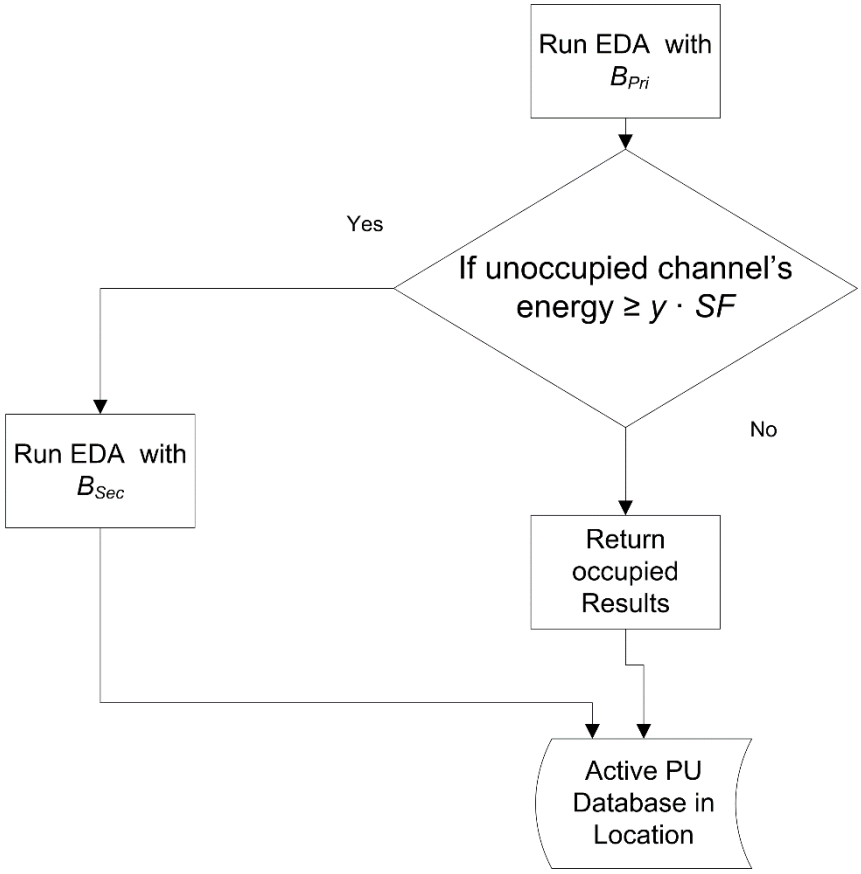

Figure 5-2: Flowchart for the GEDA model with *y* being the energy measurement of the lowest occupied DTT channel

Using B_{Pri}, the initial PU sensing results are determined using EDA, from which a PU unoccupied list is compiled. If the criteria in (5-2) is upheld, EDA is reapplied but this time the DTT channel scanning is performed using B_{Sec} to assemble the final PU DTT channel occupied list (see Figure 5-2).

$$IF\ unoccupied\ DTT\ channel\ energy\ \geq y \cdot SF \quad THEN\ B = B_{Sec} \tag{5-2}$$

5.3 Numerical Evaluation of the GEDA mechanism

To demonstrate how the GEDA resolves undetected PU channels due to this being outside the B_{Pri} capture range we shall examine the Yorkshire Belmont UK scenario using the B_{Pri} value at the minimum value which is compliant to the IEEE 802.22 P_d using the UK channel deployment matrix (UK Free TV, 2013), (OFCOM, 2016). To also demonstrate how the GEDA can be easily transferred to other countries, the Washington DC FCC (FCC, 2015) scenario shall also be examined using the B_{Pri} which adheres to the IEEE 802.22 P_d for the US channel deployment matrix. To replicate this for any other country, firstly the corresponding DTT frequency plan is required to generate B_{Pri} and B_{Sec} so GEDA can produce results which conform to the regulatory requirements in (OFCOM, 2016) and (FCC, 2015). Most countries do publish their DTT frequency plans so this will be available to third parties who need to know what infrastructure for the DTT network must be built. This is for example, demonstrated in (COGEU, 2009), where the DTT frequency details for EU countries are managed in a standardised way.

5.3.1 Yorkshire Belmont - UK Channel Deployment GEDA numerical analysis

The first part of the analysis is where the B_{Pri} value is calculated for the UK DTT channel deployment plan, which is done using the Matlab algorithm presented in chapter 3. This algorithm calculates the minimum B value which complies to the IEEE 802.22 standard which is the definition of B_{Pri}. For the UK using the channel deployment shown in Table 5.1

B_{Pri} is found to be 4 which gives a P_d of 0.98 and P_f of 0.0692. Table 5.1 (OFCOM, 2016) shows the channel number allocation for the 6 or 3 channels per location.

Table 5.1: UK Channel DTT Deployment matrix

Tx Site	Channel Matrix					
	Ch 1	Ch 2	Ch 3	Ch 4	Ch 5	Ch 6
Central Sutton Coldfield	43	46	40	42	45	39
Wales Wenvoe	41	44	47	42	45	39
Anglia Sandy Heath	27	24	21	51	52	48
Borders Caldbeck	25	28	30	23	26	29
Channel Islands Freemont point	44	41	47			
Granada Winter Hill	50	59	54	58	49	55
London Crystal Palace	23	26	30	25	22	28
Northern Ireland Divis	27	21	24	23	26	29
Meridian Rowbridge	24	27	21	25	22	28
STV Central Black Hill	46	43	40	41	44	47
Tyne Tees Bilsdale	26	29	23	43	46	40
West Country Caradon Hill	28	25	22	21	24	27
Yorkshire Belmont	22	25	28	30	53	60
STV North Durris	28	25	22	23	26	29
Mendip (West)	49	54	58	48	56	52
Cenral-Oxford	53	60	57	50	59	55
Central - Ridge Hill	28	25	22	21	24	27
Cenral-The Wrekin	26	23	30	41	44	47
Central-Waltham	49	54	58	29	56	57
Anglia-Sudbury	44	41	47	58	60	56
Anglia-Tacolneston	55	59	50	42	45	39
Border- Selkirk	50	59	55	57	53	60

Table 5.2 shows the detection matrix for the UK using B_{Pri} = 4

Table 5.2: GEDA Detection Probability Matrix for B_{Pri}=4 for 22 major UK transmitter sites 0= No detection and 1= Detection

Tx Site	Channel Detection Matrix					
	Ch1	Ch2	Ch3	Ch4	Ch5	Ch6
Central Sutton Coldfield	1	1	1	1	1	1
Wales Wenvoe	1	1	1	1	1	1
Anglia Sandy Heath	1	1	1	1	1	1
Borders Caldbeck	1	1	1	1	1	1
Channel Islands Freemont point	1	1	1	0	0	0
Granada Winter Hill	1	1	1	1	1	1
London Crystal Palace	1	1	1	1	1	1
Northern Ireland Divis	1	1	1	1	1	1

Meridian Rowbridge	1	1	1	1	1	1
STV Central Black Hill	1	1	1	1	1	1
Tyne Tees Bilsdale	1	1	1	1	1	1
West Country Caradon Hill	1	1	1	1	1	1
Yorkshire Belmont	1	1	1	1	0	0
STV North Durris	1	1	1	1	1	1
Mendip (West)	1	1	1	1	1	1
Cenral-Oxford	1	1	1	1	1	1
Central - Ridge Hill	1	1	1	1	1	1
Cenral-The Wrekin	1	1	1	1	1	1
Central-Waltham	0	1	1	1	1	1
Anglia-Sudbury	1	1	1	1	1	1
Anglia-Tacolneston	1	1	1	1	1	1
Border- Selkirk	1	1	1	1	1	1

From Table 5.2 above we can see that the B_{Sec} parameter will be invoked for two transmitter sites, Yorkshire Belmont and Central-Waltham. This analysis will investigate the Yorkshire Belmont transmitter site in Table 5.2 where two channels have failed to be detected using B_{Pri} so B_{Sec} is invoked, however to achieve a positive outcome, adjacent transmitters will then need to be analysed. For the Central-Waltham case, only one channel is not detected by B_{Pri} however by using B_{Sec} in the same transmitter region, this easily resolves this channel. Yorkshire Belmont is chosen as the most challenging case study due to two PU channels being not detected while Scunthorpe is the location for the SU base station, since it is at the edge of the DTT transmission area. The Channel Islands entry interestingly shows detection for only 3 channels, however there are only 3 actual channels allocated to this major DTT region instead of 6, though GEDA is still able to accommodate this spectral anomaly.

The channels which will not be resolved to be occupied are DTT channels 53 and 60 from Table 5.1 and 5.2. The Yorkshire Belmont DTT transmitter model is built from the transmitter parameters in (OFCOM, 2016) then we can start to see how DTT channel 53 and 60 can be resolved by the GEDA.

First the *SF* for the UK has to be calculated from equation (5-1). The lowest DTT frequency in the UK is 474 MHz and the highest is 786 MHz and the energy references were 60Km away from a 100KW DTT transmitter. The DTT distance model in chapter 3 is used to obtain the two energy values below from the sensor with the stated parameters:

$$SF = \quad 3.4482118e+004 / 1.4930635e+005$$

$$SF = \quad 0.23$$

The next step is to map the Yorkshire-Belmont scenario which can be seen in Figure 5-3:

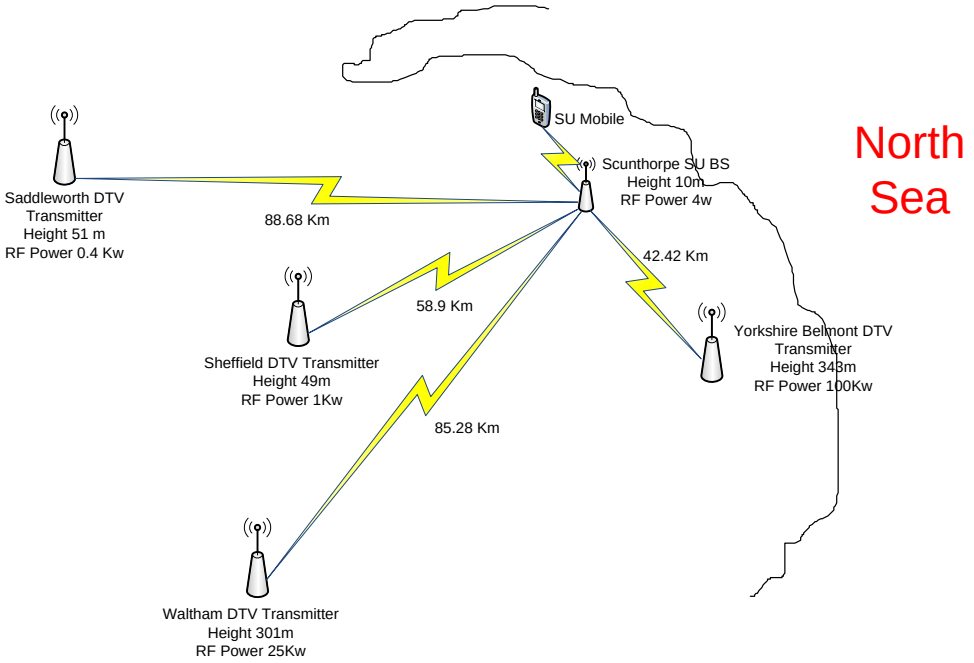

Figure 5-3: Yorkshire Belmont Analysis

The network diagram above forms the basis of the analysis where Yorkshire Belmont is the primary DTT transmitter and Saddleworth, Sheffield and Waltham are adjacent region transmitters to it. The energy responses for each DTT transmitter is calculated to a SU BS in Scunthorpe by the DTT distance model using the SU BS antenna height (10m) and the sensor results are shown below in Table 5.3:

Table 5.3: Energy responses for Yorkshire Belmont transmitter area to a Scunthorpe SU BS

Transmitter Site and Channel	Sensor Measurement at SU BS in Scunthorpe
Saddleworth Ch 39	6.0904529e+01
Sheffield Ch 21	6.2628017e+01
Waltham Ch 29	6.3129225e+01
Yorkshire Belmont Ch 53	2.5336327e+05
Yorkshire Belmont Ch 60	2.0449943e+05
Yorkshire Belmont Ch 22 lowest Channel detected by GEDA using B_{Pri}	8.4410224e+05

The next part of the process is to calculate the trigger for expediting a scan for a channel using B_{Sec}. This is calculated from taking the lowest frequency channel sensor measurement which is detected by the GEDA using B_{Pri} which in this case is channel 22 and multiplying it by *SF* (0.23) giving the trigger point. From Table 5.3 this can be seen to be 8.4410224e+05 x 0.23 = 1.94143e+05. Now from the GEDA algorithm shown in Figure 5.2 the unoccupied channel scan using B_{Sec} is conducted and if the channel sensor measurement is equal to or greater than 1.94143e+05 which means from Table 5.3 Yorkshire Belmont channels 53 and 60 the B_{Sec} parameter is triggered. This means when applying B_{Sec} = 7 that these channels are detected which is shown by Table 5.4 below:

Table 5.4: GEDA Detection Probability Matrix for B_{Pri}= 4 and B_{Sec} = 7 for 22 major UK transmitter sites

Tx Site	Channel Matrix					
	Ch 1	Ch 2	Ch 3	Ch 4	Ch 5	Ch 6
Central Sutton Coldfield	1	1	1	1	1	1
Wales Wenvoe	1	1	1	1	1	1
Anglia Sandy Heath	1	1	1	1	1	1
Borders Caldbeck	1	1	1	1	1	1
Channel Islands Freemont point	1	1	1	0	0	0
Granada Winter Hill	1	1	1	1	1	1
London Crystal Palace	1	1	1	1	1	1
Northern Ireland Divis	1	1	1	1	1	1
Meridian Rowbridge	1	1	1	1	1	1
STV Central Black Hill	1	1	1	1	1	1
Tyne Tees Bilsdale	1	1	1	1	1	1
West Country Caradon Hill	1	1	1	1	1	1
Yorkshire Belmont	1	1	1	1	1	1
STV North Durris	1	1	1	1	1	1
Mendip (West)	1	1	1	1	1	1
Cenral-Oxford	1	1	1	1	1	1
Central - Ridge Hill	1	1	1	1	1	1
Cenral-The Wrekin	1	1	1	1	1	1
Central-Waltham	1	1	1	1	1	1
Anglia-Sudbury	1	1	1	1	1	1
Anglia-Tacolneston	1	1	1	1	1	1
Border- Selkirk	1	1	1	1	1	1

From this we have validated that the GEDA mechanism works in the UK scenario however not all countries follow the same channel deployment rules so to demonstrate the agility of the GEDA algorithm the North American scenario is used to demonstrate this key feature of the GEDA. The next section will now demonstrate how the GEDA B_{Sec} trigger works in North America.

5.3.2 Washington DC - North American Channel Deployment GEDA numerical analysis

The North American scenario is quite different from the UK one. The major difference between the North American and UK approach are summarised below:

1. The DTT channel bandwidth utilised in North America is 6MHz as opposed to 8MHz in the UK.
2. The modulation scheme utilised in North America is 8 *Vestigial Sideband* (VSB) modulation where in the UK 64 and 256 *Quadrature Amplitude Modulation* (QAM) are used.
3. Lastly the final difference is the way the DTT channels are distributed which is mainly driven through geography. In the UK central DTT transmitter sites are used with a group of 6 channels (In Freemont point it is 3) to be enable economic use of real estate. Where in the North American situation distributed transmitter, sites are used to service a region due to the fact that real estate is not a driving factor and the number of channels can vary from 3 to 21 channels due to the varying terrain and size of region.

In Table 5.5, the channel allocation for the 22 major UK transmitter sites chosen is shown (FCC, 2015). To undertake this analysis, data is required upon channel and RF parameters for the DTT deployment which is generally available from the relevant regulator. However, this information is not standardised so considerable research is required in some countries to obtain this information and even lobbying of the government bodies. The red channel numbers are channels from an adjacent region which are used by the GEDA to detect certain channels within the region.

Table 5.5: 22 North American DTT transmitter channel deployment (FCC, 2015)

Site	Ch 1	Ch 2	Ch 3	Ch 4	Ch 5	Ch 6	Ch 7	Ch 8	Ch 9	Ch 10	Ch 11	Ch 12	Ch 13	Ch 14	Ch 15	Ch 16	Ch 17	Ch 18	Ch 19	Ch 20	Ch 21
New York	33	28	38	24	31	30	44	36	40	51	29	18	27	21	48	0	0	0	0	0	0
Chicargo	44	51	45	19	29	47	43	38	36	50	21	31	27	17	0	0	0	0	0	0	0
Dallas	46	43	45	42	32	36	48	35	14	41	29	40	39	19	23	30	0	0	0	0	0
Washington DC	15	48	34	36	50	35	33	27	24	30	0	0	0	0	0	0	0	0	0	0	0
Orlando	23	17	22	46	41	40	51	43	27	26	39	48	33	49	30	0	0	0	0	0	19
Los Angeles	24	33	31	48	35	32	36	49	51	47	39	29	43	18	34	41	28	38	42	26	23
Des Moines	16	19	23	34	39	0	0	0	0	0	0	0	0	0	0	0	0	0	0	0	0
Omaha	17	22	20	45	33	43	38	35	0	0	0	0	0	0	0	0	0	0	0	0	0
Indianapolis	25	20	45	29	21	42	48	44	32	27	14	23	0	0	0	0	0	0	0	0	0
Atlanta	39	27	19	20	43	44	48	25	21	41	51	0	0	0	0	0	0	0	0	0	0
Charlotte	27	34	23	50	22	47	44	39	15	17	0	0	0	0	0	0	0	0	0	0	0
Philadelphia	26	17	34	42	29	35	32	27	31	44	22	25	43	46	49	39	36	0	0	0	0
South Bend-Elkhart	46	42	22	28	35	0	0	0	0	0	0	0	0	0	0	0	0	0	0	0	0
Cincinnati	35	22	28	29	33	34	24	0	0	0	0	0	0	0	0	0	0	0	0	0	0
Baltimore	38	40	46	41	42	29	0	0	0	0	0	0	0	0	0	0	0	0	0	0	0
Tampa	19	21	32	29	25	34	47	44	42	24	0	0	0	0	0	0	0	0	0	0	0
San Diego	18	19	30	40	0	0	0	0	0	0	0	0	0	0	0	0	0	0	0	33	39
Terre Haute	36	39	19	0	0	0	0	0	0	0	0	0	0	0	0	0	0	0	0	0	18
Chattanooga	42	29	40	16	33	0	0	0	0	0	0	0	0	0	0	0	0	0	0	0	20
Greensboro-High Point-Weston Salem	31	32	19	29	51	33	35	43	0	0	0	0	0	0	0	0	0	0	0	0	23
Minneapolis	22	32	29	35	45	34	23	40	27	0	0	0	0	0	0	0	0	0	0	0	0
Albuquerque	27	24	29	26	42	22	35	45	17	0	0	0	0	0	0	0	0	0	0	0	0

Using the channel deployment shown in Table 5.5 the P_d was calculated using $B_{Pri} = 4$ which was used because it produced a $P_d = 90.16$ % and $P_f = 5.03$%. conforming to the IEEE 802.22 P_d and P_f criteria. In Table 5.6 the channel deployment matrix is converted into a detection matrix by using the detection probability algorithm.

From Table 5.6 it can be seen that the channel 1 of the Washington DC is not detected having a resultant 0 from the detection probability algorithm using $B_{Pri} = 4$. This relates to the real DTT channel 15 from Table 5.5 we can now start to create the Washington DC scenario model to prove the GEDA mechanism. Figure 5-4 shows the Washington DC DTT transmitter model along with a SU BS in the centre of Washington in which this forms the basis of my analysis:

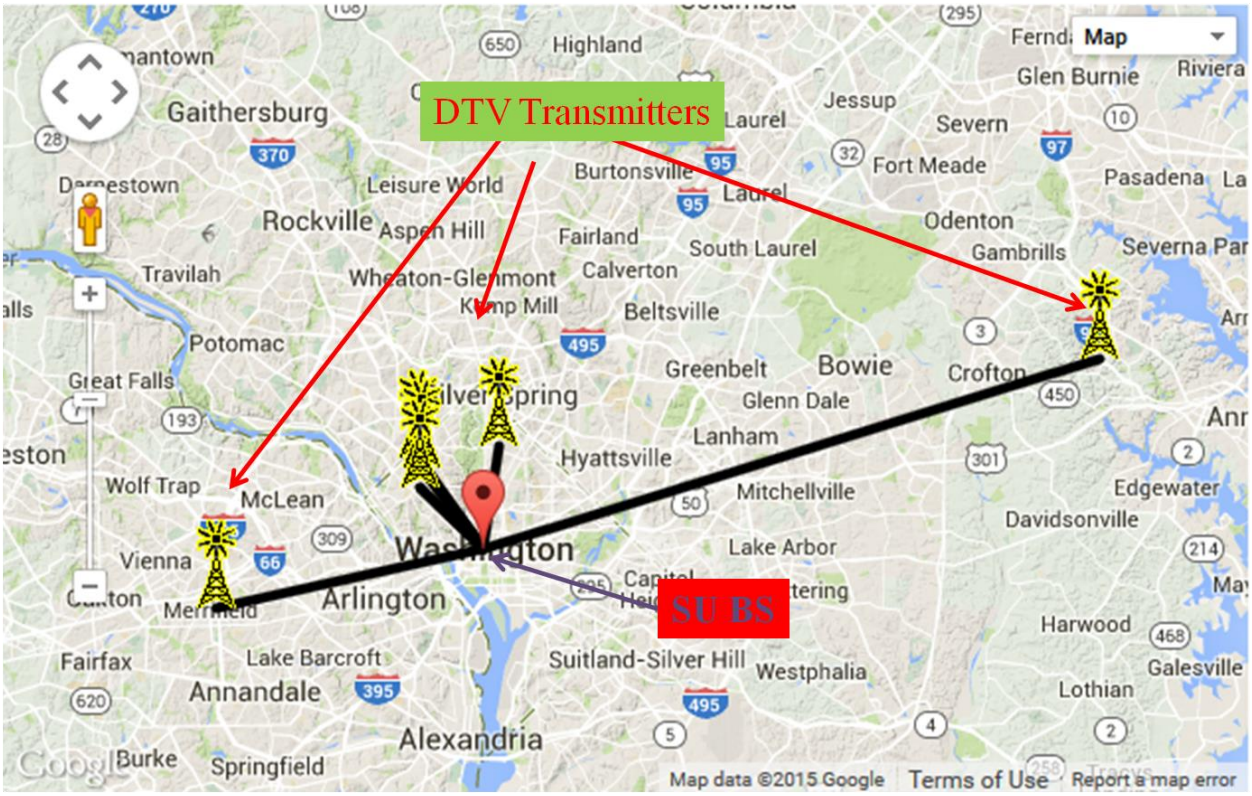

Figure 5-4: Washington DC DTT Model (FCC, 2015)

Table 5.6: GEDA North American Detection Matrix B_{Pri} = 4 - 0= No detection and 1= Detection

Site	Ch 1	Ch 2	Ch 3	Ch 4	Ch 5	Ch 6	Ch 7	Ch 8	Ch 9	Ch 10	Ch 11	Ch 12	Ch 13	Ch 14	Ch 15	Ch 16	Ch 17	Ch 18	Ch 19	Ch 20	Ch 21
New York	1	1	1	1	1	1	1	1	1	1	1	1	1	1	1	0	0	0	0	0	0
Chicargo	1	1	1	1	1	1	1	1	1	1	1	1	1	1	0	0	0	0	0	0	0
Dallas	1	1	1	1	1	1	1	1	0	1	1	1	1	1	1	1	0	0	0	0	0
Washington DC	0	1	1	1	1	1	1	1	1	1	0	0	0	0	0	0	0	0	0	0	0
Orlando	1	1	1	1	1	1	1	1	1	1	1	1	1	1	1	0	0	0	0	0	1
Los Angeles	1	1	1	1	1	1	1	1	1	1	1	1	1	0	1	1	1	1	1	1	1
Des Moines	1	1	1	0	0	0	0	0	0	0	0	0	0	0	0	0	0	0	0	0	0
Omaha	1	1	1	1	1	1	1	1	0	0	0	0	0	0	0	0	0	0	0	0	0
Indianapolis	1	1	1	1	1	1	1	1	1	1	0	1	0	0	0	0	0	0	0	0	0
Atlanta	1	1	1	1	1	1	1	1	1	1	1	0	0	0	0	0	0	0	0	0	0
Charlotte	1	0	1	1	1	1	1	0	1	1	0	0	0	0	0	0	0	0	0	0	0
Philadelphia	1	0	1	1	1	1	1	1	1	1	1	1	1	1	1	1	1	0	0	0	0
South Bend-Elkhart	1	1	0	0	0	0	0	0	0	0	0	0	0	0	0	0	0	0	0	0	0
Cincinnati	1	1	1	1	1	1	1	0	0	0	0	0	0	0	0	0	0	0	0	0	0
Baltimore	1	1	1	1	1	0	0	0	0	0	0	0	0	0	0	0	0	0	0	0	0
Tampa	1	1	1	1	1	1	1	1	1	1	0	0	0	0	0	0	0	0	0	0	0
San Diego	1	1	1	1	0	0	0	0	0	0	0	0	0	0	0	0	0	0	0	1	1
Terre Haute	1	1	1	0	0	0	0	0	0	0	0	0	0	0	0	0	0	0	0	0	1
Chattanooga	1	1	1	1	1	0	0	0	0	0	0	0	0	0	0	0	0	0	0	0	1
Greensboro-High Point-Weston Salem	1	1	1	1	1	1	1	1	1	0	0	0	0	0	0	0	0	0	0	1	1
Minneapolis	1	1	1	1	1	0	1	1	0	1	0	0	0	0	0	0	0	0	0	0	0
Albuquerque	1	1	1	1	1	1	1	0	1	0	0	0	0	0	0	0	0	0	0	0	0

From Figure 5-4 the Washington DC DTT Transmission model it can be seen and that the 10 DTT channels allocated to the Washington DC region are supported by 6 transmitter sites. Each transmitter is identified by a four-letter call signs and the ones we shall be focussing on are WFDC which is the transmitter whose channel cannot be detected, WNVC which is the transmitter whose channel is the lowest frequency which is detected using B_{Pri} and WMPB which is in the adjacent region to Washington DC.

Tables 5.5 and 5.6 show that channel 15 cannot be detected using B_{Pri} and the lowest frequency which can be detected using B_{Pri} is channel 24. Figure 5-5 shows the model for these two transmitters WNVC (Channel 24) and WFDC (Channel 15). Also, WMPB (Channel 29) which is a channel used to service Baltimore which is an adjacent region to Washington DC. This is included to demonstrate that false triggering of B_{Sec} will not be caused by any adjacent regions as this would have the effect of increasing the P_f probability i.e. triggering B_{Sec} when not required.

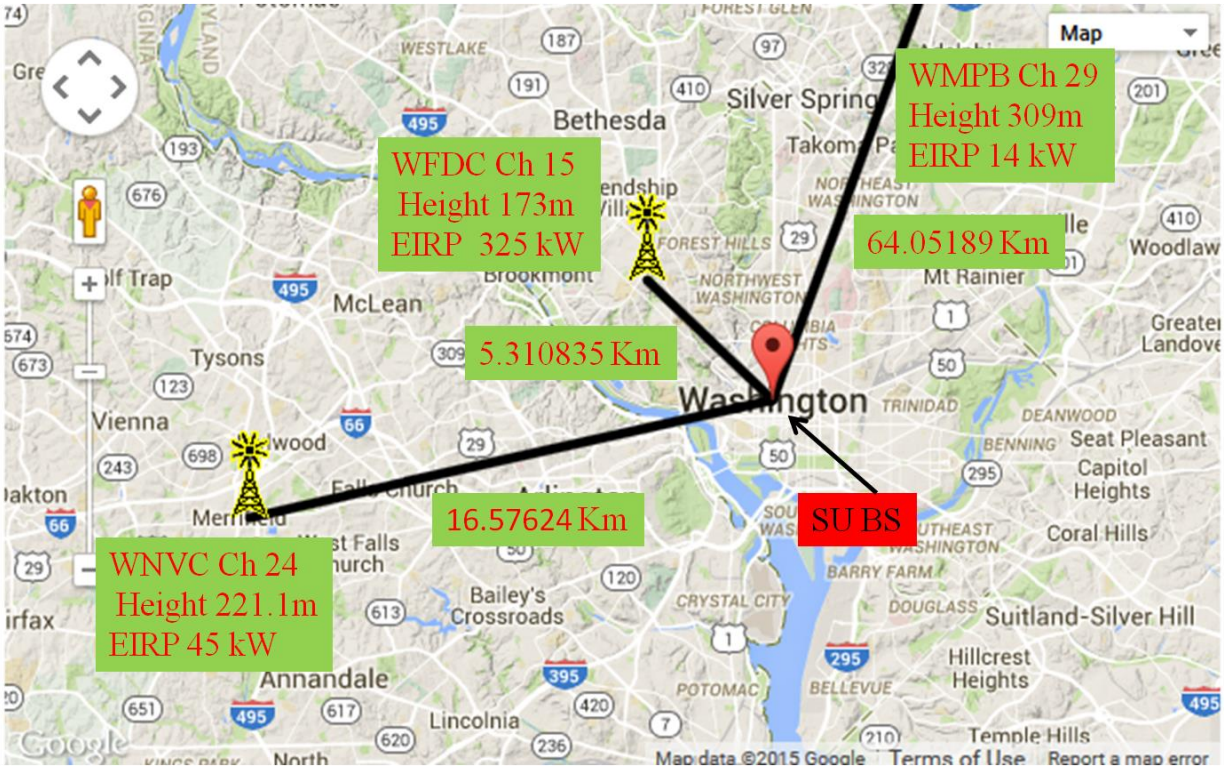

Figure 5-5: Washington DC - WNVC, WFDC and WMPB DTT Model (FCC, 2015)

The model above shows the transmitter call sign WFDC which is the channel 15 is not detected using B_{Pri} and WNVC is the lowest frequency detected in the Washington DC region which defines the value at which the B_{Sec} parameter is used in conjunction with *SF*.

SF is calculated from equation (5-1) using the lowest and the highest DTT frequency in the US which is 473 MHz and 887 MHz respectively.

$$SF = \quad 1360281 / 7907096.5 = 0.172033$$

The next step of the process is to calculate the sensor outputs for the three transmitters shown in Figure 5-5 to the SU BS shown in Table 5.7.

Table 5.7: Washington Model sensor measurements

Transmitter Site and Channel	**Sensor Measurement at SU BS in Washington**
WFDC Ch 15	1.1846454e+010
WMPB Ch 29 Adjacent Region	4.9109495e+04
WNVC Ch 24 lowest Channel detected by GEDA using B_{Pri}	2.0910753e+07

The next part of the process is to calculate the trigger for expediting a scan for a channel using B_{Sec}. This is calculated by taking the lowest frequency channel sensor measurement which is detected by the GEDA using B_{Pri} , which in this case is channel 24 and multiplying it by *SF* (0.172033) gives the trigger point. From Table 5.7 this can be seen to be 2.0910753e+07 x 0.172033 = 3.597339e+06. Now from the GEDA algorithm shown in Figure 5-2, the unoccupied channel scan using B_{Sec} is conducted and if the channel sensor measurement is equal to or greater than 3.597339e+06 which means from Table 5.5 WFDC

channel 15 the B_{Sec} is triggered. This means when applying B_{Sec} = 9 from the detection and false detection algorithms then this channel is detected which as shown in Table 5.8.

Table 5.8: GEDA North American Detection Matrix B_{Pri} = 4 and B_{Sec} =9

Site	Ch 1	Ch 2	Ch 3	Ch 4	Ch 5	Ch 6	Ch 7	Ch 8	Ch 9	Ch 10	Ch 11	Ch 12	Ch 13	Ch 14	Ch 15	Ch 16	Ch 17	Ch 18	Ch 19	Ch 20	Ch 21
New York	1	1	1	1	1	1	1	1	1	1	1	1	1	1	1	1	0	0	0	0	0
Chicargo	1	1	1	1	1	1	1	1	1	1	1	1	1	1	1	0	0	0	0	0	0
Dallas	1	1	1	1	1	1	1	1	1	1	1	1	1	1	1	1	0	0	0	0	0
Washington DC	1	1	1	1	1	1	1	1	1	1	0	0	0	0	0	0	0	0	0	0	0
Orlando	1	1	1	1	1	1	1	1	1	1	1	1	1	1	1	0	0	0	0	0	1
Los Angeles	1	1	1	1	1	1	1	1	1	1	1	1	1	1	1	1	1	1	1	1	1
Des Moines	1	1	1	1	1	1	0	0	0	0	0	0	0	0	0	0	0	0	0	0	0
Omaha	1	1	1	1	1	1	1	1	1	0	0	0	0	0	0	0	0	0	0	0	0
Indianapolis	1	1	1	1	1	1	1	1	1	1	1	1	0	0	0	0	0	0	0	0	0
Atlanta	1	1	1	1	1	1	1	1	1	1	1	0	0	0	0	0	0	0	0	0	0
Charlotte	1	1	1	1	1	1	1	1	1	1	0	0	0	0	0	0	0	0	0	0	0
Philadelphia	1	1	1	1	1	1	1	1	1	1	1	1	1	1	1	1	1	1	0	0	0
South Bend-Elkhart	1	1	1	1	1	1	0	0	0	0	0	0	0	0	0	0	0	0	0	0	0
Cincinnati	1	1	1	1	1	1	1	1	0	0	0	0	0	0	0	0	0	0	0	0	0
Baltimore	1	1	1	1	1	1	1	0	0	0	0	0	0	0	0	0	0	0	0	0	0
Tampa	1	1	1	1	1	1	1	1	1	1	0	0	0	0	0	0	0	0	0	0	0
San Diego	1	1	1	1	1	0	0	0	0	0	0	0	0	0	0	0	0	0	0	1	1
Terre Haute	1	1	1	1	0	0	0	0	0	0	0	0	0	0	0	0	0	0	0	0	1
Chattanooga	1	1	1	1	1	1	0	0	0	0	0	0	0	0	0	0	0	0	0	0	1
Greensboro-High Point-Weston Salem	1	1	1	1	1	1	1	1	1	0	0	0	0	0	0	0	0	0	0	1	1
Minneapolis	1	1	1	1	1	1	1	1	1	1	0	0	0	0	0	0	0	0	0	0	0
Albuquerque	1	1	1	1	1	1	1	1	1	1	0	0	0	0	0	0	0	0	0	0	0

5.4 GEDA Results

The GEDA was compared to two set of results. One outlining data from Chinese study (Lei Qiu Jing et al, 2011) and the other a North American study (Chen and Gao, 2011). Both set of results were generated from a DTT deployment matrix of 22 sites. Due to the fact that the Chinese scenario follows the UK with DTT bandwidth and modulation schemes this study was compared to the GEDA in a UK scenario using the site and channel allocation in Table 5.2. For the North American study, it is compared to the GEDA in the North American scenario which follows Table 5.5.

5.4.1 UK GEDA results compared to the Chinese Study

For the Chinese study (Lei Qiu Jing et al, 2011) the UK scenario was used to compare the GEDA due to the fact that it utilises the same channel bandwidth and modulation schemes. DTMB is the DTT standard used in China where the DTT bandwidth is 8 MHz and 5 modulation constellations are used which are 4-QAM NR, 4-QAM, 16-QAM, 32-QAM and 64-QAM. In the UK DVB-T is the DTT standard where the bandwidth is 8 MHz and the modulation constellations are 64-QAM and 256-QAM. It can be seen that in paper (Lei Qiu Jing et al, 2011) the DTT bandwidth is 8 MHz which is the same as for the UK GEDA scenario hence the justification for comparing these two sets of results. However, the Chinese paper modulation schemes are 4 QAM to 64 QAM and for the UK GEDA it utilises 64 and 256 QAM and to ensure that the worst case for the UK is obtained, 256 QAM is used for the GEDA results. This ensures that when comparing these two solutions the UK GEDA is always using results which the theory would say that the paper (Lei Qiu Jing et al, 2011) should outperform GEDA due to the fact that the same bandwidth and same carrier signal strength is seen at the antenna, and that 64 QAM will display a greater energy level than the 256 QAM i.e. a greater E_b/N_o is required to decode a 256 QAM signal than a 64 QAM signal to produce the same throughput as per Shannon's Law.

The B_{Pri} and B_{Sec} are calculated using the detection and false detection probability algorithms for a compliance to P_d of 1. For the UK B_{Pri} was found to be 4 and B_{Sec} 7. The GEDA results are shown below which also show the simulation results from paper (Lei Qiu Jing et al, 2011) at a P_f of 0.1:

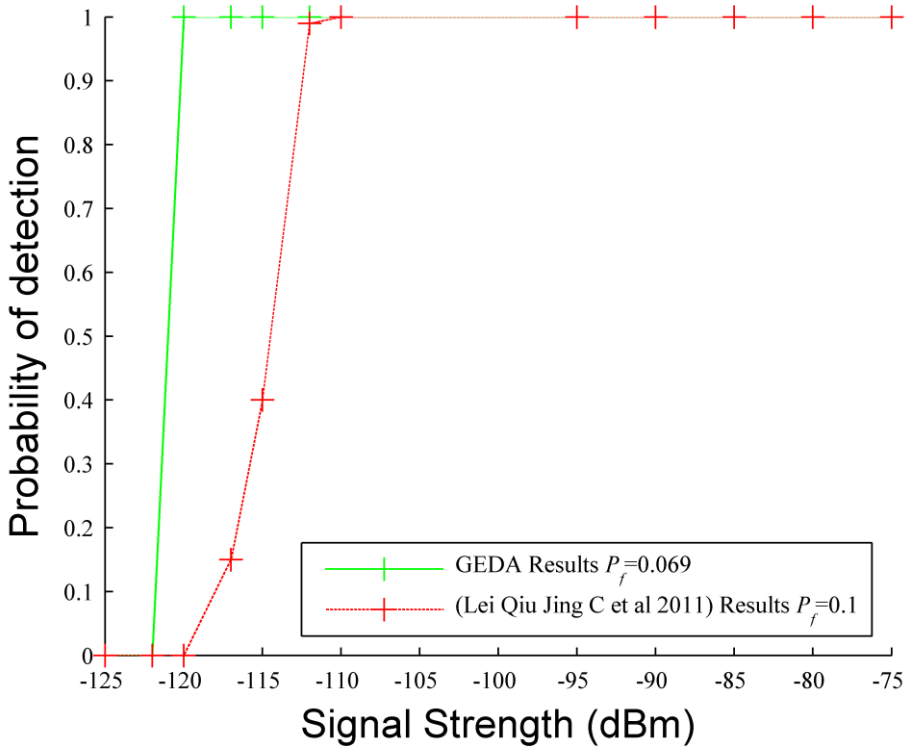

Figure 5-6: GEDA Results

From the results in Figure 5-6 it can be seen that GEDA ED sensor out performs the paper (Lei Qiu Jing et al, 2011) by achieving a detection probability of 1.0 at a signal strength of -120dBm. This shows an improvement of 9dB for probability of detection on paper (Lei Qiu Jing et al, 2011). It can also be seen to achieve these results the GEDA false detection is 0.069 whereas paper (Lei Qiu Jing et al, 2011) is 0.1 which the GEDA also shows an improvement over paper (Lei Qiu Jing et al, 2011).

5.4.2 North American GEDA results compared to the North American Study

As outlined earlier in North America, the major differences between the UK and North America are DTT bandwidth, Modulation scheme and distributed transmitter sites for a region. This means that no comparison can be made to the UK results hence a test model needed to be constructed for the North American scenario. For this purpose a 8 VSB, 6MHz bandwidth and a 22 US site model was constructed using a channel deployment plan shown in Table 5.5.

The following set of results show how the GEDA performs in the North American scenario using paper (Chen and Gao, 2011) for comparison. For the North American channel deployment B_{Pri} =4 and B_{Sec} = 9 is calculated from the detection and false detection probability algorithms but to achieve a thorough comparison the B_{Pri} and B_{Sec} value were varied between 1 and 9 so that the range of false detection probabilities could be achieved. This is demonstrated by the results below in Table 5.9 which are the results for a SNR of -22dB.

The same results were collected for SNR -20 dB and -18 dB and are shown in the graph at Figure 5-7 using paper (Chen and Gao, 2011) as a comparison.

Table 5.9: SNR -22dB results showing the B_{Pri} and B_{Sec} distribution

BPri	*BSec*		P_f GEDA	P_d GEDA	American IEEE Journal Paper P_d	P_f American Paper
1	1		0.0132	0.3809	0.22	0.0368
2	2		0.0132	0.6419	0.28	0.0552
3	3		0.0132	0.8005	0.3	0.0641
4	4		0.0503	0.9017	0.35	0.0837
4	5		0.0508	0.9518	0.39	0.1024
4	6		0.0514	0.9788	0.4	0.1159
4	7		0.0519	0.9879	0.42	0.1317
4	8		0.0525	0.9879	0.46	0.147
4	9		0.0531	1	0.48	0.1605
4	10		0.0536	1	0.49	0.1743
4	11		0.0542	1	0.5	0.1893
4	12		0.0547	1	0.51	0.2054
4	13		0.0552	1	0.53	0.2222
4	14		0.0562	1	0.56	0.2388
4	15		0.0572	1	0.59	0.2567
4	16		0.0581	1	0.61	0.2751
4	17		0.0586	1	0.62	0.2925
4	18		0.0594	1	0.64	0.3114
4	19		0.0604	1	0.66	0.3296
nth			1	1	0.7	0.3455

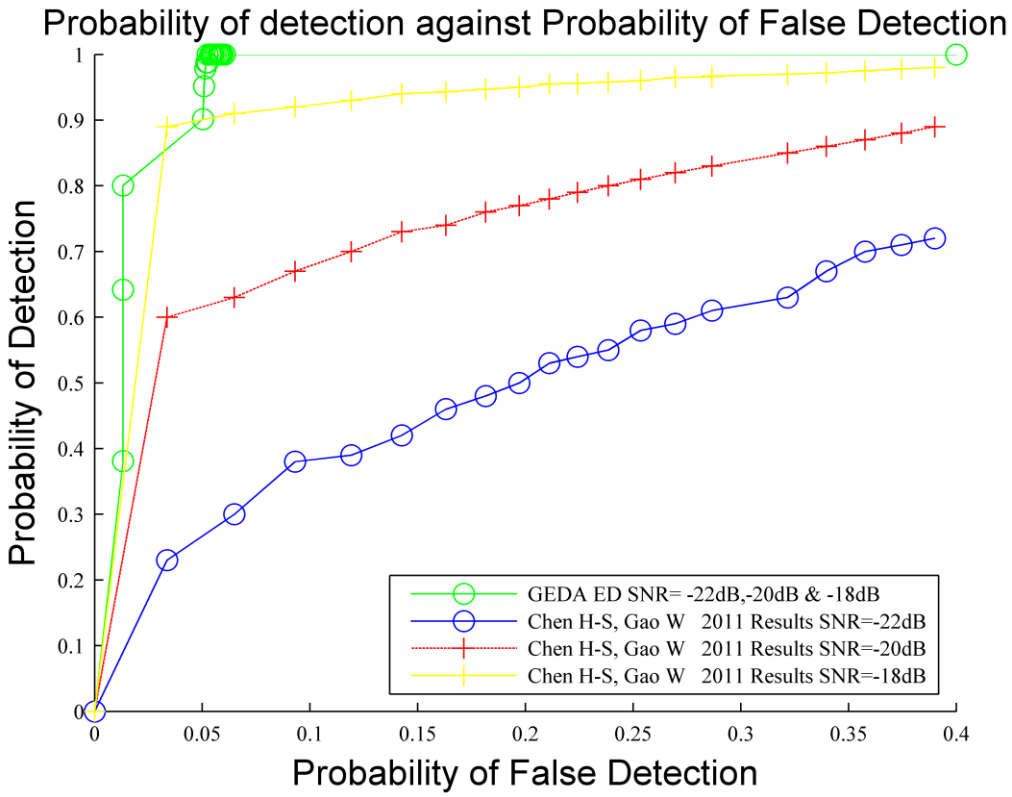

Figure 5-7: FCC SNR Results

The results demonstrate that GEDA out performs paper (Chen and Gao, 2011) for SNR values of -22, -20 and -18dB by obtaining a detection probability of 1.0 at a false detection of 0.0531. Also from these results it can be seen that the GEDA is not sensitive to noise seeing its performance is consistent over the whole SNR range which is not the case for paper (Chen and Gao, 2011).

5.5 Comparison of GEDA results for UK and US

In Figures 5-6 and 5-7, GEDA has been compared to other sensing solutions deployed in the UK and US, however GEDA has not been compared using the same criteria. So, this section compares the GEDA results for both countries using the SNR, and detection and false detection metrics. Figure 5-8 compares how the two countries performance differs when using the same criteria.

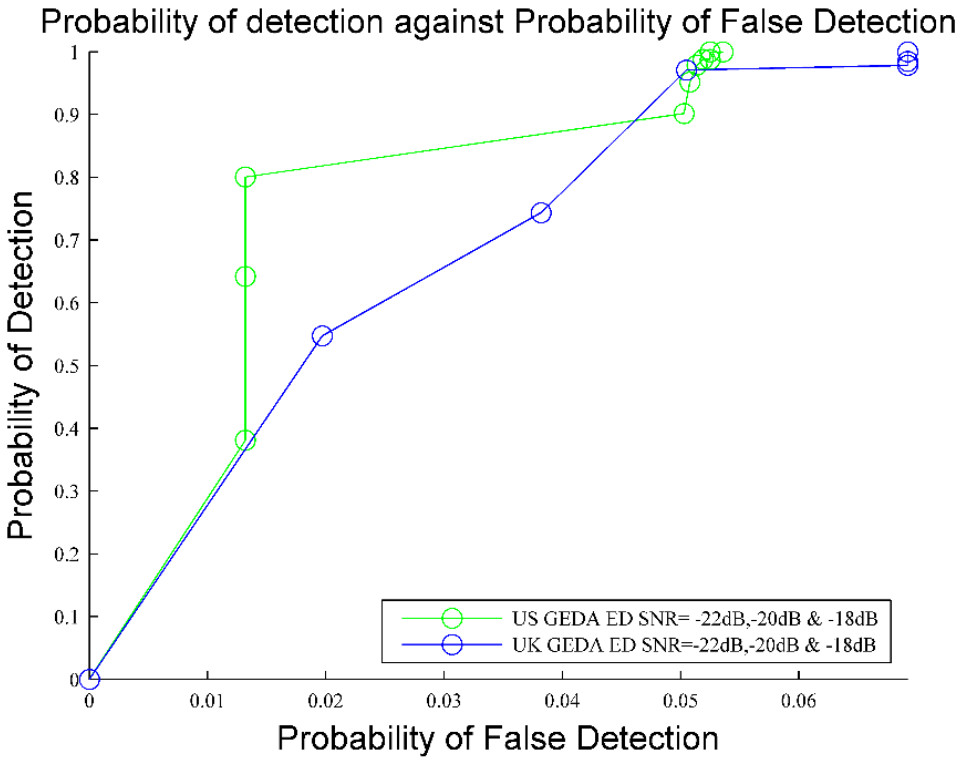

Figure 5-8: Comparison between GEDA UK and US results

The results reveal that the main difference is that the US results attain a detection probability of 1 before the UK, though both sets of results obtain a detection probability of 1 and a false detection probability of 0.1, which are within the regulatory and IEEE 802.22 requirements. The difference is directly attributable to the diverse DTT channel deployment patterns between the UK and US (demonstrated by different the B parameters used), while the RF detection parameters are exactly the same (sensing threshold = -120dBm).

5.6 Summary

This chapter has demonstrated that an energy sensing mechanism and knowledge of how the DTT channels are deployed can allow a sensing algorithm to be designed which can detect the active PU channels with a 100% probability of accuracy while also a false detection probability which lies within that prescribed by IEEE 802.22. This design is that which is outlined for the GEDA algorithm in which three parameters are introduced: B_{Pri}, B_{Sec} and SF. These parameters are the only variations which are required from one country to the next and can be calculated using the channel deployment matrix for the county and the software tools designed in this piece of work.

The two scenario's that are analysed using the GEDA are Yorkshire Belmont in the UK and Washington DC in the US which not only demonstrates that the GEDA algorithm works but also with minimum alteration it can meet different country requirements and still work in a predictable fashion.

This chapter has described the GEDA design and demonstrated the B_{Sec} triggering mechanism in the UK and the US.

The chapter has presented a GEDA which produces significant improvements in detection probability of a DTT PU over existing techniques. This is shown by using signal strength results in the UK and signal to noise ratio in the North American arena.

Chapter 6

6. NEW GEDA AND HIDDEN NODE PROBLEM

6.1 Introduction

From the bandwidth usage analysis in (Cisco, 2016) which is reviewed in chapter 1, the bandwidth requirement of mobile wireless devices is projected to grow tenfold by 2020. To be able to accommodate this increase in demand then unlicensed bandwidth such as TVWS needs to be utilised alongside the existing licensed bandwidth. To be able to facilitate this increase this chapter critically evaluates the potential of TVWS to make available extra bandwidth for SU cognitive devices using the GEDA detection solution with an interference management algorithm which negates the impact on the primary user.

The main factors influencing this goal are the signal strength at the edge of reception of a DTT area so the corresponding maximum interference signal level can be determined which will not interfere with the DTT signal. From this a minimum keep out distance can be established so both the PU and SU can co-exist on co and adjacent channels without interference. This increases the spectral efficiency by allowing TVWS SU to utilise channels which are otherwise forbidden to them presently.

Importantly, the solution investigates the hidden node issue **(**Nekovee, 2011) **(**Nekovee, 2012) and how it can provide a generic way of solving this problem by incorporating the keep out contour.

Using the Mendip DTT area (UK Free TV, 2013) for the UK and Washington DC (FCC, 2015) for the US as case studies, it will be shown how the solution can innovatively

determine a keep out contour which will protect the PU in the presence of the hidden node issue but increase the bandwidth that is available to TVWS cognitive devices in different countries where diverse DTT channel deployment strategies are utilised as well as different modulation techniques.

To encompass the above there are three main areas which need to be studied which are:

1. Protection Contour and Interference Management.
2. Hidden Node Issue.
3. Keep Out Contour.

These will now be looked at in detail.

6.2 Protection Contour and Interference management

The protection contour proposed by (Kang et al, 2012) depends upon the DTT receivable signal at the edge of a DTT area which defines the coverage area with no interference then co and adjacent channel interference is introduced to determine how a DTT receiver would perform at the edge of a reception area. The next few sections will examine two scenarios based on the UK and US DTT deployment cases which were chosen because they embodied both European and North American DTT standards which between them form the models used throughout the world (Newnes, 2003).

6.2.1 UK Protection Contour Analysis

The geometry which defines the UK contour is illustrated in Figure 6-1 and is based on the Mendip DTT Transmitter case study for the mid-band channel 54 (738MHz) using the lower modulation scheme of 64 QAM at a data rate of 64 Mbs. This provides an indicative range seing it uses the mid band channel and the lowest modulation scheme available and thus represents the worst case scenario for any channel re-use in order to characterise the protection contour. The DTT receiver antenna gains were chosen from the average omni-

directional gain of a Yagi antenna with corner reflector which was found to be 2dBi. A Yagi with corner reflector is a typical outdoor antenna for DTT reception. The Mendip coverage area is shown below:

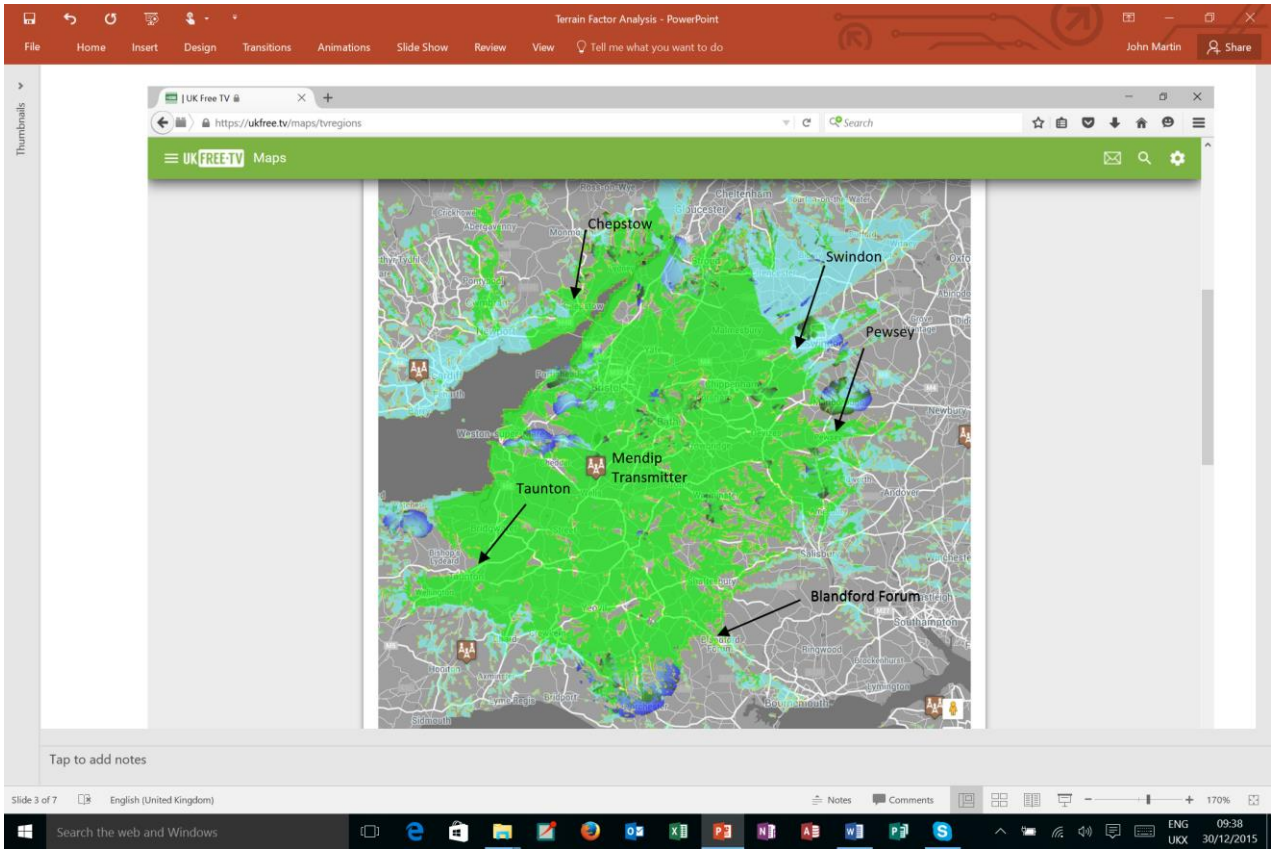

Figure 6-1: Mendip Transmitter Coverage Area (UK Free TV, 2013)

From Figure 6-1 (UK Free TV, 2013) the following analysis was performed to determine the Egli propagation terrain factor (TF):

1. Take multiple points on the edge of coverage area which are spaced 360^0 around the area as shown in Figure 6-1 and measure the distance to the Mendip transmitter:
    a. Taunton - 44 Km
    b. Swindon - 68.8 Km
    c. Blandford Forum - 49.11 Km
    d. Chepstow - 45 Km
    e. Pewsey - 61.21 Km
2. Once we have distances of the various locations to the Mendip transmitter we calculate the average distance. From this the average coverage radius = 53.62 Km

3. Using the distance DTT model introduced in chapter 3 the Egli TF parameter was adjusted to obtain a BER value that is transitioning to > $2x10^{-6}$ at a distance closest to the average coverage radius. Egli TF for the UK terrain was found to be 97%.

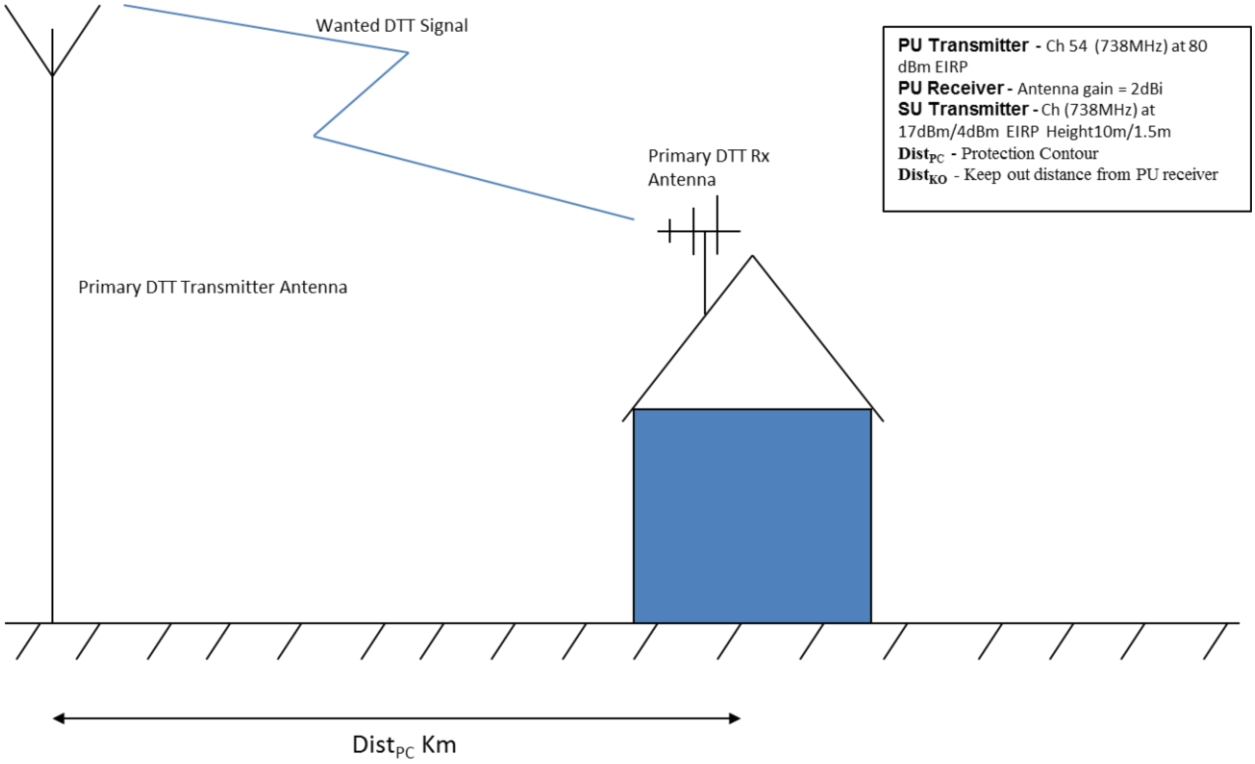

Figure 6-2: Protection Contour Geometry for a Primary DTT Transmitter

The protection contour distance is found by developing a model and Test Scripts 1 and 2 which are described in chapter 3, and from equations (6-1) and (6-2) the four unknowns, $Dist_{PC}$, RSS_{PC}, *TF* and *DF* are resolved for a DTT traffic threshold of BER=$2x10^{-6}$. The protection contour distance is derived from resolving the following equations.

Using the Egli path loss equation (6-1) and (6-2) with the following parameter definition:

Table 6.1: Protection Contour Equation Parameter Definition

Parameter	Description	Value
h_m	Mobile station antenna height (DTT PU Receiver) in metres	10 m
h_b	Base station antenna height (DTT PU Transmitter) in metres	281.6 m
β	$\left(\frac{40}{f}\right)^2$ where f = frequency in MHz	f = 738 MHz
G_b	base station antenna gain (PU Tx)	1 (0 dBi)
G_m	mobile station antenna gain (DTT Rx)	1.5849 (2 dBi)
DF	LOS diffraction loss (Chapter 3)	dB
P_p	PU transmitter power output (EIRP)	80 dBm
M	Modulation Technique	64 QAM
TF	Egli Terrain Factor (Chapter 3)	dB
RSS_{PC}	Received Signal Strength at protection contour	dBm

From the Egli path loss and over the horizon diffraction loss equations:

$$Total\ Path\ Loss = 10Log\left[G_b G_m \beta \left(\frac{h_b h_m}{{Dist_{PC}}^2}\right)^2\right] + TF + DF \qquad (6\text{-}1)$$

Where *Total Path Loss*:

$$Total\ Path\ Loss = RSS_{PC} - P_P \qquad (6\text{-}2)$$

From equation (6-1):

$$Total\ Path\ Loss = 10Log\left[0.0046\left(\frac{2816}{{Dist_{PC}}^2}\right)^2\right] + (-22.5599)$$

From equation (6-2):

$$Total\ Path\ Loss = -86.2429 - 80\ \ dB$$

$$Total\ Path\ Loss = -166.2429\ \ dB$$

By equating the above:

$$-166.2429 = 10Log\left[0.0046\left(\frac{2816}{{Dist_{PC}}^2}\right)^2\right] + (-22.5599)$$

$$Dist_{PC} = 54023\ m$$

The protection contour for the Mendip area $Dist_{PC}$ is resolved from (6-1) and (6-2) when BER= $2x10^{-6}$ is satisfied and is found to be 54.023 Km at a RSS_{PC} = -86.2429 dBm. However, the protection contour does not take interferers into account, of which there are two types namely: co-channel interference (interferer on the same channel) and adjacent channel (interferer using channels adjacent to the PU). The impact of interference on the minimum keep out distance will be analysed in the next section.

6.2.2 UK Interference Management

The interference behaviour of a system depends on the interference power and spectral position in comparison to the wanted signal. The relevant standard OFCOM power output specifications for SU TVWS devices are used in the following model and can be found in chapter 2.

The geometric model which the interference tests were based upon is shown in Figure 6-3:

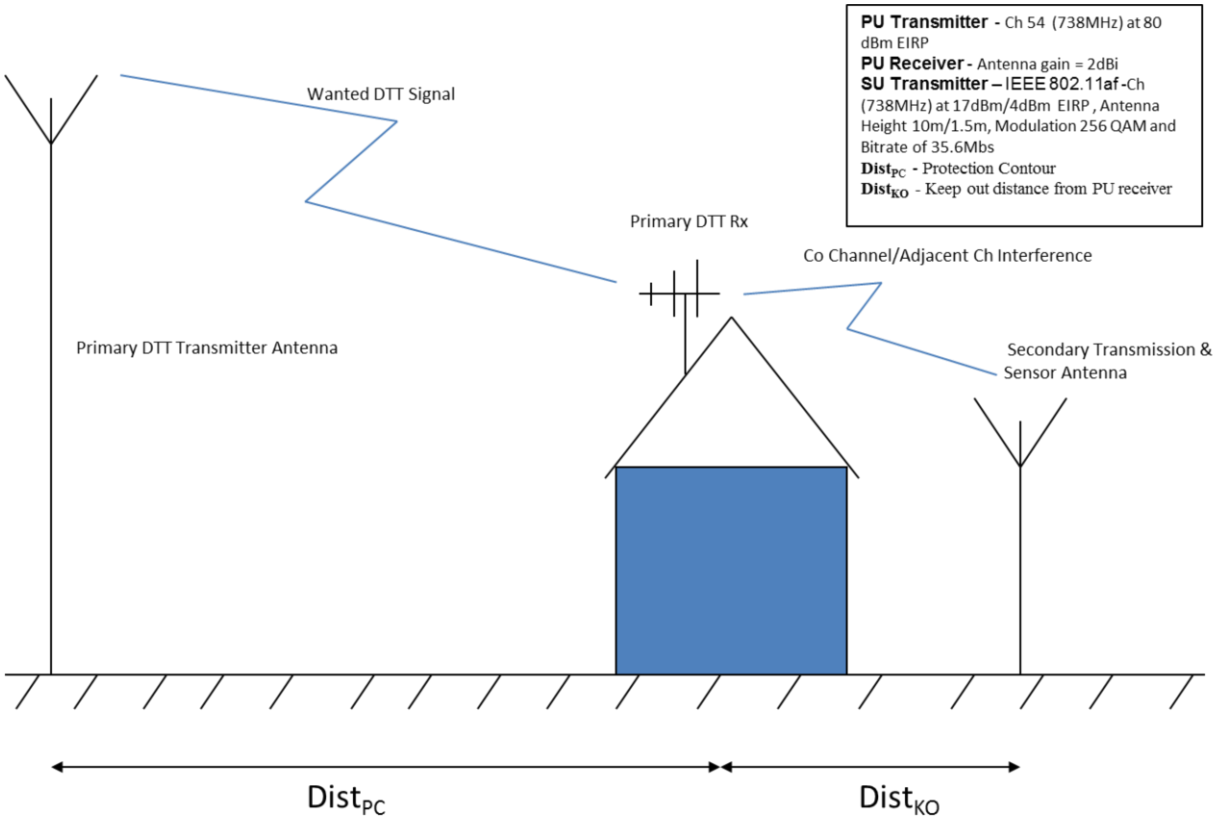

Figure 6-3: UK Interference Test Model

For the co-channel scenario, the DTT receiver is located on the protection contour which was defined in section 6.21. Now a IEEE 802.11af interference signal is introduced in which it is increased until the TV service threshold is exceeded which is at a BER> $2x10^{-6}$. The corresponding interference signal value of -131.9 dBm is used to calculate the minimum keep out distances ($Dist_{KO}$) by using a IEEE 802.11af distance model in which the results are shown in Table 6.2.

Table 6.2: Minimum Keep Out Distances for Co-Channel Interference

SU Transmit Power (OFCOM standards)	$Dist_{KO}$
17 dBm (Fixed)	3.75 Km
4 dBm (Fixed)	1.77 Km
4 dBm (Mobile)	0.69 Km

These calculations crucially assume no margin for the hidden node issue. Later in the chapter we shall compare these $Dist_{KO}$ values against those for a new hidden node solution to ensure all interference scenarios are addressed.

For adjacent channel interference, the adjacent channel interference on channel (*N+1*) was increased on the DTT receiver at the protection contour until the BER exceeded the $2x10^{-6}$ limit, which occurred when *RSS=-47.77dBm*. This is the maximum allowable SU signal strength in this adjacent channel. Repeating the analysis for the *(N+2)* adjacent channel gave a maximum *RSS=196.4dBm* for a SU. The overriding outcome of this analysis is that the N+1 channel interference is the most dominant by a factor of $1x10^{12}$ which means that the N+1 channel interference is the significant interference.

To critically evaluate whether the OFCOM SU maximum transmit EIRP of 4dBm for *(N+1)* and 17dBm for the *(N+2)* adjacent channel interference provides sufficient DTT PU defence against interference, the SU BS and mobile scenarios where the interfering RSS is calculated for both 4dBm and 17dBm SU transmit EIRP on *(N+1)*, 14m away from a DTT receiver which is assumed to be the minimum separation of a SU BS from a PU receive antenna. The respective *(N+1)* BS results were -47.78dBm and -34.78dBm, which endorses the OFCOM decision to limit the *(N+1)* transmit EIRP to only 4dBm, as this is lower than -47.77dBm so it will not generate interference from 14m, unlike the 17dBm SU BS. The SU mobile

scenario for (N+1) using 4dBm SU transmit EIRP gives protection to the PU receiver up to 5.4m away from the PU receiver. In contrast, for the *(N+2)* channel case, the -13dBm RSS caused by a 17dBm SU BS at 4m from the PU receiver is much lower than 196.4dBm, so no interference is generated. In the 17dBm SU mobile case, a RSS of -5.4dBm is generated when 1m away from the PU receiver which again is much lower than 196.4dBm, so no interference is produced to any PU.

While these co-channel results demonstrate the minimum distance away from the protection contour that a SU can reliably transmit on the same channel, the hidden node issue (Martin et al, 2013), (Randhawa et al, 2008) has not been considered in this solution. From the above adjacent channel interference discussion, the results confirm that no interference is generated provided the OFCOM regulatory settings (Chapter 2) on the (*N+1)* and (*N+2)* SU power restrictions and SU BS are at least 14m for BS and 5.4m for mobile away from residential DTT antennas. For this analysis the mobile devices are at 1.5m, BS are at 10m above ground level and the PU receiver is at height of 10m are upheld.

With these findings the Hidden Node Issue was not considered which will be analysed later in this chapter. The next section repeats the protection contour and interference analysis for the North American scenario.

6.2.3 US Protection Contour Analysis

The protection contour geometry for the US adopts the same arrangement as the UK case study in Figure 6-1. However due to DTT deployment differences, instead of one transmitter supporting 6 channels as in the UK, US transmitters supports only 1 channel in the majority of cases (FCC, 2015). The other main differences between the UK & US transmitters is the modulation technique used. UK transmitters use either 64 or 256 QAM with a spectral bandwidth of 8 MHz where as in the US 8 VSB with lower spectral bandwidth of 6 MHz

and a corresponding lower bit-rate which is reflected in the models used below. The Washington transmitter WFDC was used for the evaluation of the US protection contour as it is the capital and hence the bandwidth requirement for secondary access would be large. From (FCC, 2015) the WFDC transmitter has a radius coverage of 80 Km which equates to a Egli TF of 95%. From this the protection contour distance is calculated using equations (6-1) and (6-2), and the parameter table below:

Table 6.3: Protection Contour parameters for Transmitter WFDC Equations

Parameter	Description	Value
h_m	Mobile station antenna height (DTT PU Receiver) in metres	10m
h_b	Base station antenna height (DTT PU Transmitter) in metres	173m
β	$(40\ (f^{-1})\ )^2$ where f = frequency in MHz	f = 479 MHz
G_b	base station antenna gain (PU Tx)	0 dBi
G_m	mobile station antenna gain (DTT Rx)	2 dBi
P_p	PU Transmitter power output (EIRP) in dBm	89.6 dBm
TF	Egli terrain factor loss which best matches the practical data (US TF=95%). In dB	
DF	Over the horizon Diffraction Loss in dB	
M	Modulation Technique	8-VSB

From these parameters, the protection contour equations were resolved for the protection distance which was found to be 78.39 Km for the WFDC transmitter with a RSS_{PC}=-90.15

dBm. The main contributorily factors for the protection contour distance to be greater than the UK case is that the transmitter EIRP is greater than the UK case (From Tables 6.1 and 6.3) and the frequency is lower (From Tables 6.1 and 6.3). Again this does not take into account of any margin which needs to be added for hidden node issue which will be discussed later in this chapter and again like the UK case study the next section will define the impact on the minimum keep out distance for the US scenario.

6.2.4 US Interference Analysis

This section will examine the effect of interference on US DTT users in the presence of co-channel and adjacent channel interference. This will differ from the UK scenario due to differing allowable SU transmit powers as shown in Table 6.4 below which the SU modulation techniques follow the IEEE 802.11af specification (IEEE, 2013) using 6 MHz bandwidth and 256 QAM modulation while the PU uses 8 VSB PU modulation (Newnes, 2003):

Figure 6-4 below shows the model used to measure the effect of interference on the PU receiver in the US using the FCC SU power specifications in chapter 2.

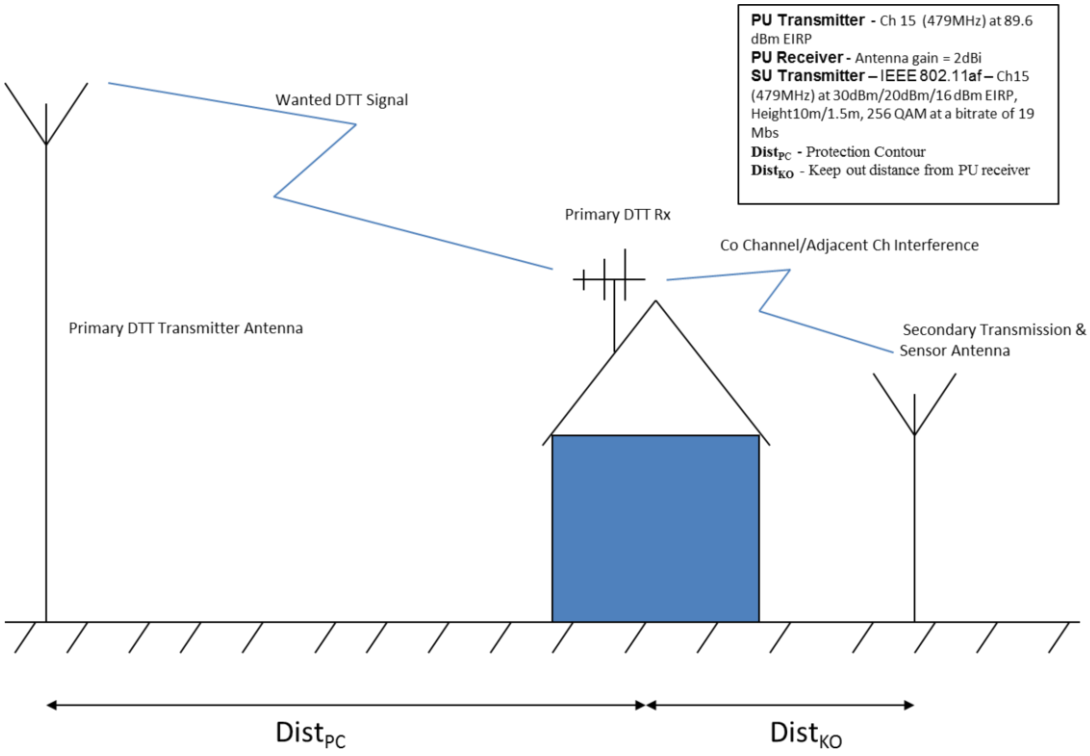

Figure 6-4: US Interference Test Model

The co-channel scenario is considered first where the WFDC DTT transmitter is taken with the receiver on the protection contour. The secondary TVWS interferer is introduced transmitting on the same frequency as the PU and uses the same properties has the UK model except the bandwidth is 6 MHz instead of 8 MHz and the modulation technique is 8 VSB instead of 64 QAM. To determine the minimum $Dist_{KO}$ the interfering signal is increased until the BER reaches 2 x 10^6 which is the maximum interfering signal allowed. For the US, this is found to be -133.13 dBm which when a IEEE 802.11af distance model the following minimum $Dist_{KO}$ are obtained for the different SU allowable transmit powers from FCC SU specifications in chapter 2 and are shown in Table 6-4:

Table 6.4: Minimum Keep Out Distance for Co-Channel Interference

SU Transmit Power	Dist$_{KO}$
30 dBm (Fixed)	13.66 Km
20 dBm (Mobile)	2.98 Km

16 dBm (Fixed)	6.1 Km
16 dBm (Mobile)	2.36 Km
17 dBm (Fixed)	6.46 Km

In (FCC 2012) where SU transmit antenna height against exclusion zone with reference to co-channel fixed nodes is specified where a 10m SU transmit antenna 11.1 Km is stipulated. However, from Table 6.4 for a 30 dBm fixed node a 13.66 Km exclusion zone is needed so the FCC requirement is not stringent enough. Using the alternative fixed node SU of 17 dBm then 6.46 Km is within the 11.1 Km specified by the FCC.

In (FCC, 2012) there is also another SU transmit power category which is for a sensing solution only which is specified as 17 dBm maximum for fixed nodes. Using this criterion then the exclusion zone is 6.46 Km which is still within the 11.1 Km criteria from FCC. From these results, it can be reasonably concluded that with 16dBm and 17dBm fixed node for co-channel interference, then there is a corresponding 5 and 4.64 Km margin respectively which means that the FCC specifications for exclusion zones are very conservative in protecting the PU. This judgement has been supported in (FCC, 2012) where a company Spectrum Bridge Inc proposed increasing the allowable fixed SU transmitter power by 6dB but this was rejected by FCC on the grounds that a SU could use the maximum power setting using a much lower bandwidth (FCC, 2012). In doing so the scenario of multiple SUs being able to use the same channel and hence increase the aggregate power spectrum density (PSD) over the permissible limit of 12.6dBm/100kHz could be a problem. In the proposed SU access process, this would not happen because there is a command and control hierarchy where the BS tells the SU what power and bandwidth to use so this situation shall not occur. For adjacent channel interference, the adjacent channel interference signal ($N+1$) was increased on the DTT receiver at the protection contour until the BER exceeded the $2x10^{-6}$ limit, which occurred when $RSS=-53.55dBm$. Using a 16dBm fixed SU BS stipulated by

FCC for a (*N+1*) interferer then a minimum $Dist_{KO}$ of 70m is required and 24.22m for a 16dBm SU mobile. But with an exclusion zone of 1.2 Km for (*N+1*) (FCC, 2012) and a IEEE 802.11af signal range of 155m means for the fixed BS SU there is a margin of 1.2-0.07=1.13 Km and for a mobile SU 1.2-0155-0.024=1.021 Km. The margin of over a 1 Km in each case again implies as in the co-channel case that there is scope to either increase the SU transmitter power or relax the HAAT (Height above average terrain) restriction and thus the exclusion zone.

In contrast, for the *(N+2)* channel case, the adjacent channel gave a maximum *RSS=195.58dBm* for a SU before causing interference. A -5.79dBm RSS caused by a 16dBm SU BS fixed node at 4m from the PU receiver is much lower than 195.58dBm, so no interference is generated. In the 16dBm SU mobile case a RSS of 1.81dBm is generated when 1m away from the PU receiver which again is much lower than 195.58dBm, so no interference caused. From these results, it can be said that no impact to the PU receiver is caused by a (*N+2*) interfere which is exactly the same finding as the UK case study.

In this section, we have looked at the protection contour for both the UK and US case studies and from this, the maximum DTT service distance from the DTT transmitter. From this the impact of the two types of interference was found on the DTT receiver on the protection contour where the most significant were found to be co-channel and adjacent channel (*N+1*). From the interference study the minimum keep out distances for both the UK and US case studies were found.

The interference analysis so far in this chapter does not consider the hidden node issue (Angrueria et al, 2015) which is why it is termed the minimum keep out distance. The hidden node issue is a major hurdle to implementing a CR network in the TVWS spectrum as far as interference management and the next section shall look in some detail at the interference rules for UK and US in light of hidden node analysis.

6.3 A Review of the Hidden Node Issue

This section introduces a novel margin strategy utilising a *keep out contour* where the hidden node issue is resolved and a viable secondary user sensing solution formulated for both the UK and US case studies. The analysis shall start by referencing the obstruction height which will form the starting point for this solution.

The height of an obstruction can be classified into 4 categories, according to the building heights and topologies in the Royal Borough of London (Martin et al, 2013) (The Royal Borough of Kensington and Chelsea Council, 2010). This approach was taken due to any city in the world being unique from an architectural point of view but by taking a large city such as London as a reference, a robust approach to incorporating building heights can be considered in the model. The following building categories will be considered in the following analysis:

i) Typical Height – 15m such as urban residential areas and rural building structures.

ii) Local Landmark – up to 22.5m such as the parish church steeple, meeting hall, local library or town hall.

iii) District Landmark – up to 60m such as Natural History Museum, Brompton Oratory and the Earl's Court Exhibition Centre.

iv) Metropolitan Landmark – up to 90m such as Tower 42 and the Gherkin in the City of London and Canary Wharf in the Docklands.

The aim of the following analysis is to investigate the behaviour of the hidden node problem by first investigating the effect close to obstructions and looking at further away distances.

By doing this, a new power control and access algorithm can be designed to complement the GEDA algorithm from chapter 5 to overcome the effects of the hidden node issue and maintain the interference management so the PU performance at the protection contour is not compromised. The model shall take the maximum height for the above categories as basis to examine the hidden node issue.

6.3.1 Effect of the hidden node issue at distances close to an obstruction

Figure 6-5 shows the detection probability results for the GEDA against sensor height for each of the four obstacle categories identified above using the DTT RF model and combined with the GEDA Fuzzy Logic model from chapter 4 and chapter 5. The results were averaged over the sensor height range between 10m and 20m from the obstacle, as this encompasses the shadowing effect which is the phenomenon that creates the hidden node issue i.e. can't detect the PU reliably (Martin et al, 2013).

It can be observed that typical and local landmark obstruction heights could be serviced from a sensor at a height of 6m which means, that this can for instance be achieved by deploying lamppost TVWS cognitive devices. In contrast, for large towns and cities, minimum sensor heights of 30m and 42m are needed.

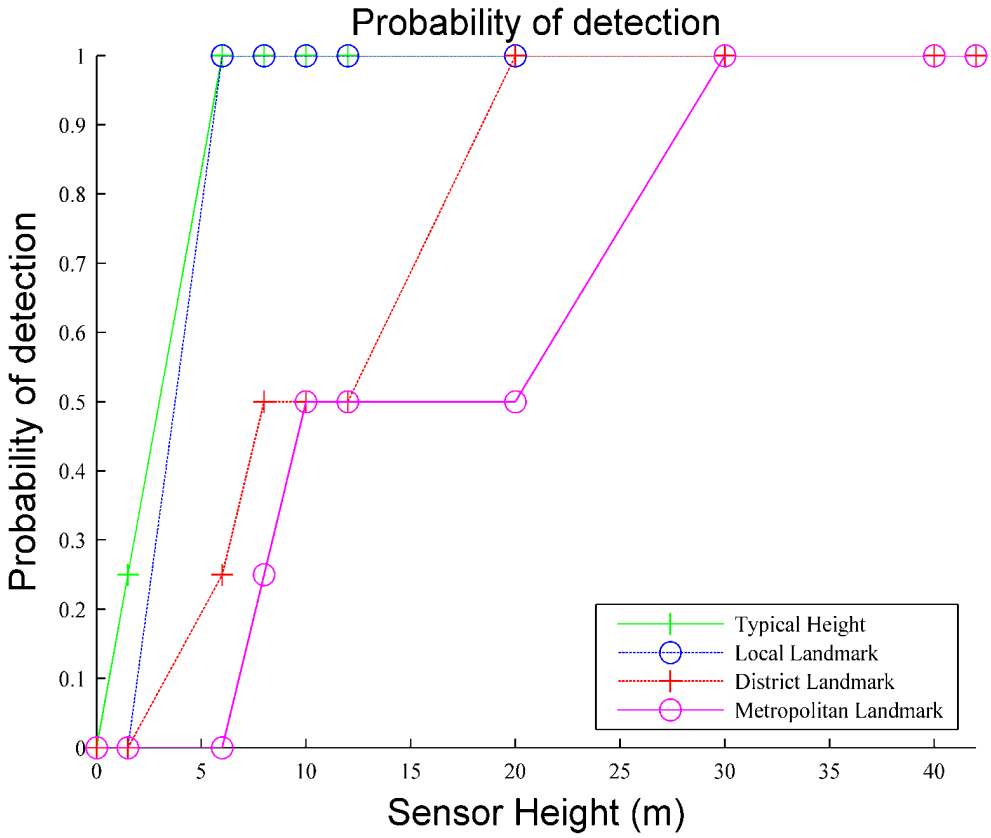

Figure 6-5: Hidden Node Results

Figure 6-5 shows that the lowest sensor antenna height to obtain a detection probability of 1 is 6m which implies a BS architecture is required i.e., sensor antenna height must be greater than 1.5m. As the building height increases so does the required sensor antenna height so mobile sensors are unable to operate in any category and distributed sensors at differing heights are required to ensure PU information can be distributed to all users, to avoid the requirement of some form of co-operative sensing (Akyildiz et al, 2009) to be employed which is not desirable due to the fact that extra infrastructure would have to be deployed to support this, as investigated in chapter 2.

6.3.2 Hidden node effects at longer distances from obstruction

So far, the effect of the hidden node has been only considered to sense a PU close to an obstacle i.e. 10 and 20m. The graph in Figure 6-6 shows the sensor output at various distances up to 38 Km away from the obstacle.

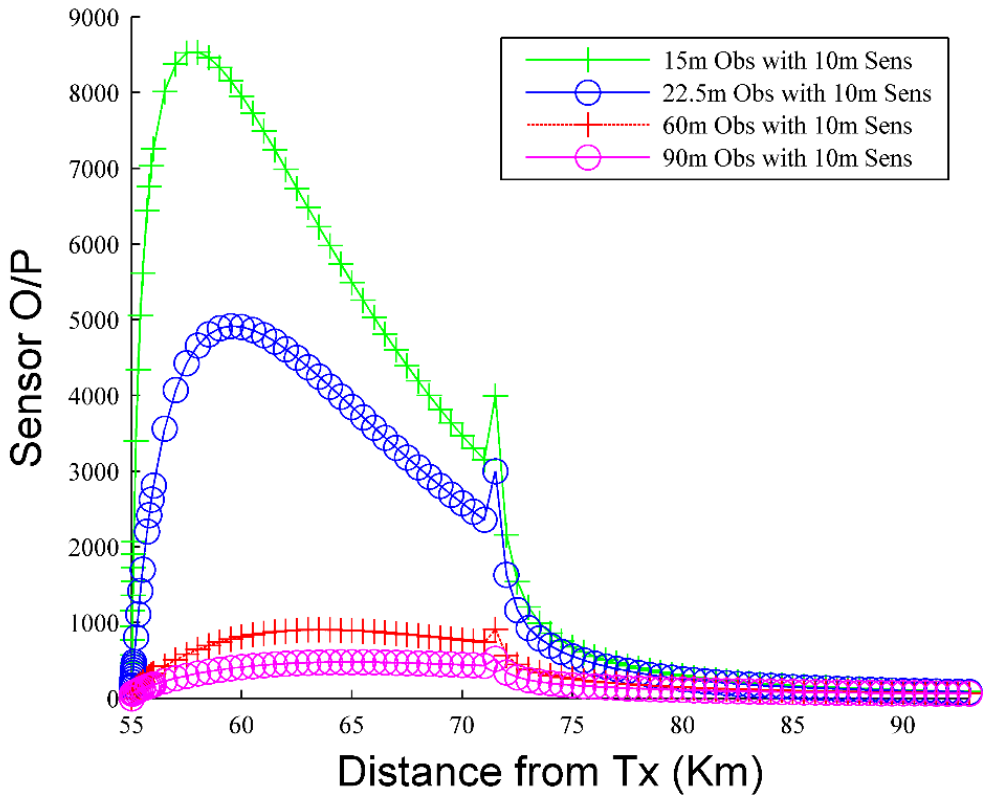

Figure 6-6: Sensor O/P up to 38Km away from Obstacle

These results confirm that any solution adding a margin figure to the protection contour to compensate for hidden nodes will be a compromise between reducing the detection threshold for the 90m obstacle close to the obstacle and increasing the distance at which the PU is detected at the 15m obstacle far distance point which effectively increases the channel keep out distance. The spikes observed in Figure 6-6 at 72 Km are caused by the RF horizon diffraction loss in which the horizon obstruction cuts more even than odd Fresnel zones having an accumulative effect of increasing the RSS (Seybold, 2005) (ITU-R, 1997).

The implications of the diffraction loss by an obstruction is to create the situation where a hidden node occurs where the obstruction is between a PU transmitter and a SU sensor. From Figure 6-6 it can be seen that the energy response is specific to the obstruction height so any solution will need to accommodate differing obstruction heights. Other hidden node issue solutions (Angueira et al, 2016) opt for a diffraction margin on top of the protection contour RSS which are only applicable to certain situations, whereas the proposed keep out contour

in the next section encompass the different height categories defined and will adapt itself to all situations and so will give a universal solution.

6.4 Keep out contour

This is an exclusion zone around the DTT transmitter which offers protection to the PU receiver at the protection contour even when there is a hidden node present. It also provides sufficient bandwidth to TVWS devices to ensure their users receive the best QoS. The keep out contour is an extension of the protection contour where an energy threshold is introduced which defines the detection distance from an obstruction at the near distance and at the far distance for obstruction heights within the defined categories. The near distance threshold defines how far from the obstruction the sensor will start detecting a PU, using the highest obstruction. This threshold should be as close to the obstruction as possible. The far distance threshold defines the keep out contour which is the final exclusion zone since it stipulates the furthest point from the lowest obstruction that a PU can be detected. Using this exclusion zone, the hidden node issue is shown to resolved and the best QoS to SU is produced without any interference to the PU. The interference was analysed is section 6.22 and 6.24 where a minimum $Dist_{KO}$ was determined for the different scenarios and the measure of the keep out contour will be to exceed this distance to ensure no interference.

Figure 6-7 shows the model configuration for determining the effectiveness of a hidden node issue solution with the PU receiver on the protection contour and the SU transmitter on the keep out contour which is the worst case for the PU receiver.

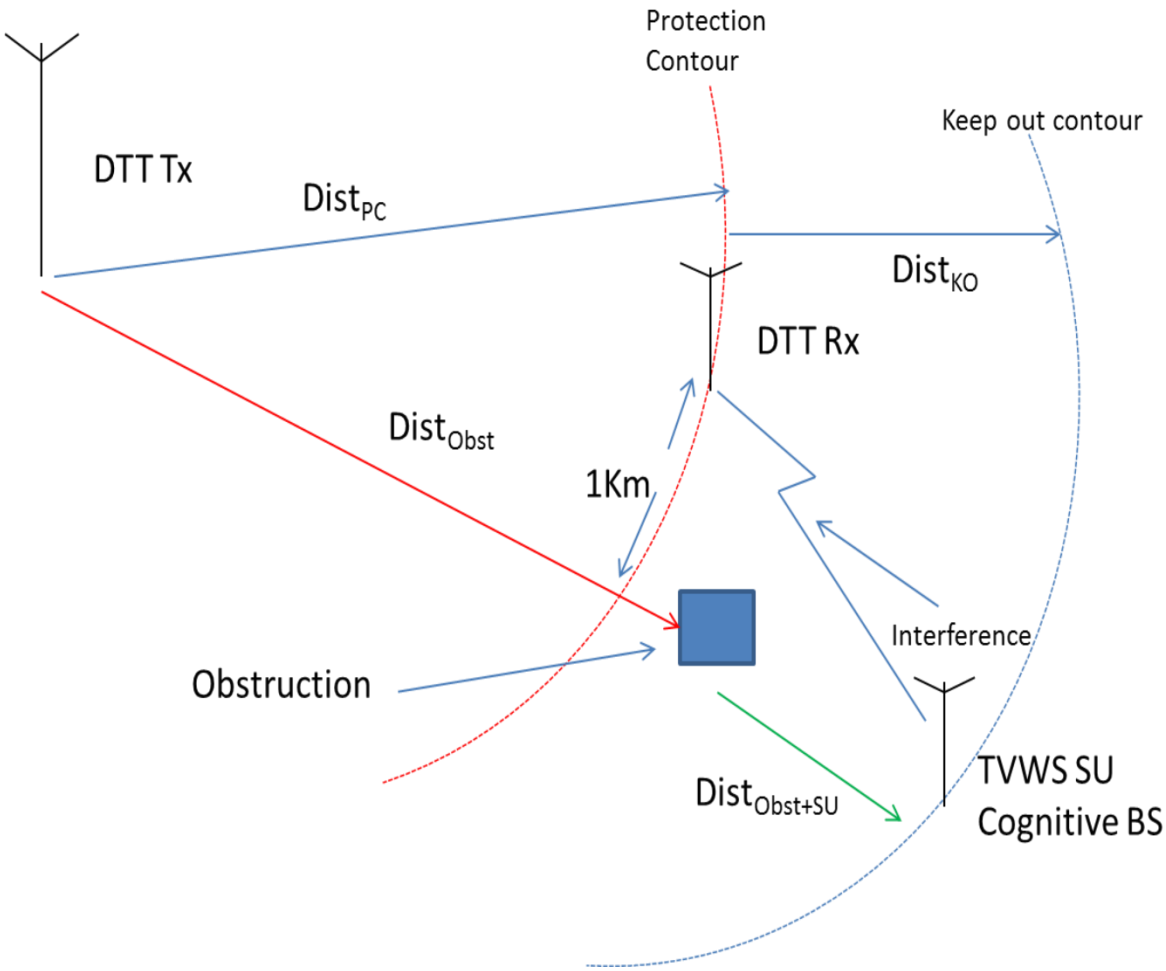

Figure 6-7: Keep out contour geometry

In the *keep out contour* geometry of Figure 6-7 the main parameters are:

Dist$_{PC}$ = *protection contour* for the lowest modulation scheme in the DTT deployment (see Sections 6.21 and 6.23).

Dist$_{KO}$ = Distance from the *protection contour* to *keep out contour*

Dist$_{Obst}$ = Distance between an obstruction and DTT transmitter.

Dist$_{Obst+SU}$ = Distance from an obstruction to the SU Sensor.

The protection contour distance (*Dist$_{PC}$*) is determined by PU signal whose RSS is such that the resultant *BER* equal or better than 2 x 10^{-6} which describes the PU edge of service. The interfering co-channel RSS is determined by the distance model described in section 3.4.1 for a SU co-channel interferer that is introduced into the PU model at the protection contour to obtain the maximum interference RSS to still maintain a *BER* of 2 x 10^{-6}. The distance

$Dist_{PC}$ + $Dist_{KO}$ is an exclusion zone around the DTT transmitter which offers protection to the PU receiver at the protection contour even when there is a hidden node present by maintaining the *BER* criteria of 2 x 10^{-6} for a co-channel SU interferer. It also provides sufficient bandwidth to TVWS devices to ensure their users receive the best *QoS*. The key difference between the protection and keep out contours is that the latter includes a margin loss alongside the protection contour to permit prescribed interference RSS in the presence of hidden nodes as illustrated in Figure 6-7.

To define the keep out contour, the energy threshold which the SU sensor will be monitoring needs to be obtained. This threshold is derived from the average diffraction loss variation of the 90m obstacle at a distance up to 1Km away from an obstacle, where the minimum variation can be considered 5% lower than the maximum variation. From this, the distance to the average diffraction loss variation can be found and from this X_{KO} in which the detailed analysis for UK and the US is shown in the following sections.

The keep out contour solution proposed assumes that if the SU is close to the obstruction then the only way for the PU channel to be detected is to use higher sensor heights as in Figure 6-5 or co-operative sensing. This solution will assume that sensing is only viable at 1Km and beyond from the obstruction which would be a practical distance up to where visual surveys can manage the correct sensor height.

Once X_{KO} has been found it can be used to extend the GEDA to enable power and interference control through a new algorithm which is introduced in the next section.

6.4.1 New GEDA using the Keep Out Contour to determine channel access

The new GEDA model employs the *keep out contour* to determine active PU channels and to govern whether these channels can be used by a SU and what RF power to utilise to avoid interference to the PU. The adjacent and co-channel interference management process is

formally presented in pseudo-code form in Algorithm 6.1, with Table 6.5 defining the key parameters:

Table 6.5: Power control parameters

X_{KO}	Keep Out Contour energy (Sections 6.312 and 6.313)
$P_{BS(N+1)}$	Regulatory definition for base station EIRP for adjacent channel (Tables 6.2 and 6.5)
$P_{BS(N+2)}$	Regulatory definition for base station EIRP (Chapter 2)
$P_{M(N+1)}$	Regulatory definition for mobile EIRP for adjacent channel (Chapter 2)
$P_{M(N+2)}$	Regulatory definition for mobile EIRP (Tables 6.2 and 6.5)
DB_{PU}	GEDA identified PU Channel database (Chapter 5)
DB_{DTT}	DTT Channel database containing channel numbers and energy measurements
$DB_{DTT}^{(Ch)}$	DTT Channel database channel number
$DB_{PU}^{(Ch)}$	GEDA identified PU Channel database channel number
$DB_{DTT}^{(E)}$	DTT Channel database energy measurement

Algorithm 6.1: Pseudo code for co-channel access and adjacent channel interference management using the *keep-out contour*

```
1:  Inputs: X_KO, P_BS(N+1), P_BS(N+2), P_M(N+1), P_M(N+2), DB_PU, DB_DTT.  Outputs: P_BS, P_M
2:  Initialise: DB_DTT^(Ch) ∈ DB_DTT, DB_PU^(Ch) ∈ DB_PU, DB_DTT^(E) ∈ DB_DTT
3:  FOR each channel DB_DTT^(Ch) DO
4:      FOR each channel DB_PU^(Ch) DO
5:          IF DB_DTT^(Ch) = DB_PU^(Ch) THEN
6:              IF DB_DTT^(E) > X_KO THEN
7:                  P_BS = 0
8:                  P_M = 0
9:              ELSE
10:                 P_BS = P_BS(N+2)
11:                 P_M = P_M(N+2)
12:             END IF
13:         ELSE
14:             IF DB_DTT^(Ch) = DB_PU^(Ch)+1 AND DB_DTT^(E) > X_KO THEN
15:                 P_BS = P_BS(N+1)
16:                 P_M = P_M(N+1)
17:             ELSE
18:                 P_BS = P_BS(N+2)
19:                 P_M = P_M(N+2)
20:             END IF
21:         END IF
22:     END FOR
23: END FOR
```

Step 1 declares all the variables while step 2 loads the GEDA PU database and the relevant sensor energy readings.

Step 3 sets up a for loop for testing every DTT channel.

Step 4 sets a for loop if DTT channel sensor reading is greater than X_{KO}.

Steps 5 to 13 allocate SU transmit RF powers when it is a co-channel interferer to a PU channel, while Steps 14 to 20 determine if the SU is an adjacent channel interferer *(N+1)* or *(N+2)* to a PU channel. If either $\boldsymbol{P_{BS}=0}$ or $\boldsymbol{P_M=0}$, then a SU is not allowed to transmit on the given channel.

The major input to this algorithm is X_{KO} where the analysis for the UK and US are detailed in the next two sections.

6.4.2 UK keep out contour

The approach adopted is to first define the diffraction response at the protection contour. This is found for a 90m obstruction (Highest obstruction in reference model) at 55Km ($Dist_{Obst}$) from the Mendip transmitter which is less than 1Km from the protection contour (54.023Km) $Dist_{PC}$. The diffraction response for these conditions at Mendip DTT frequency 738MHz is plotted in Figure 6-8:

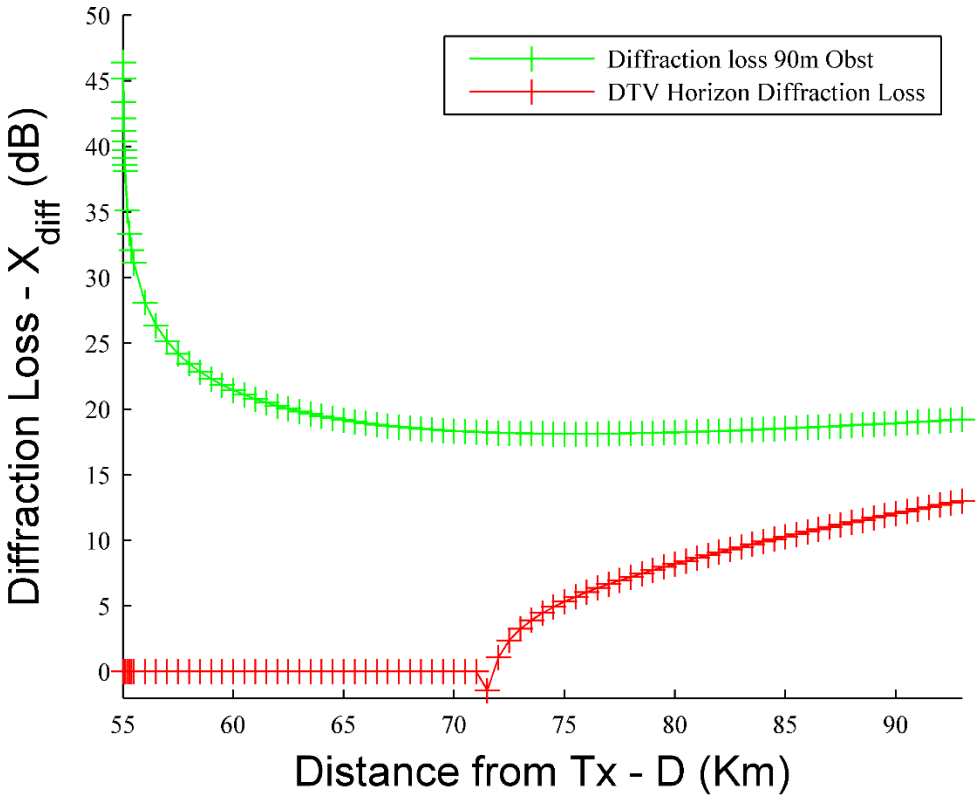

Figure 6-8: Mendip diffraction response with a 90m obstacle

The majority of diffraction loss occurs 1Km from the obstacle. Again the decrease in losses at 72Km is caused by the horizon diffraction where more even than odd Fresnel zones are being cut by the obstruction.

The next step is to evaluate $\frac{dX_{Diff}}{dD}$ against distance D so that the X_{Diff} variation can be mapped against distance from obstruction hence an appropriate keep out threshold can be formulated. Figure 6-9 shows the X_{Diff} variation with distance from obstruction:

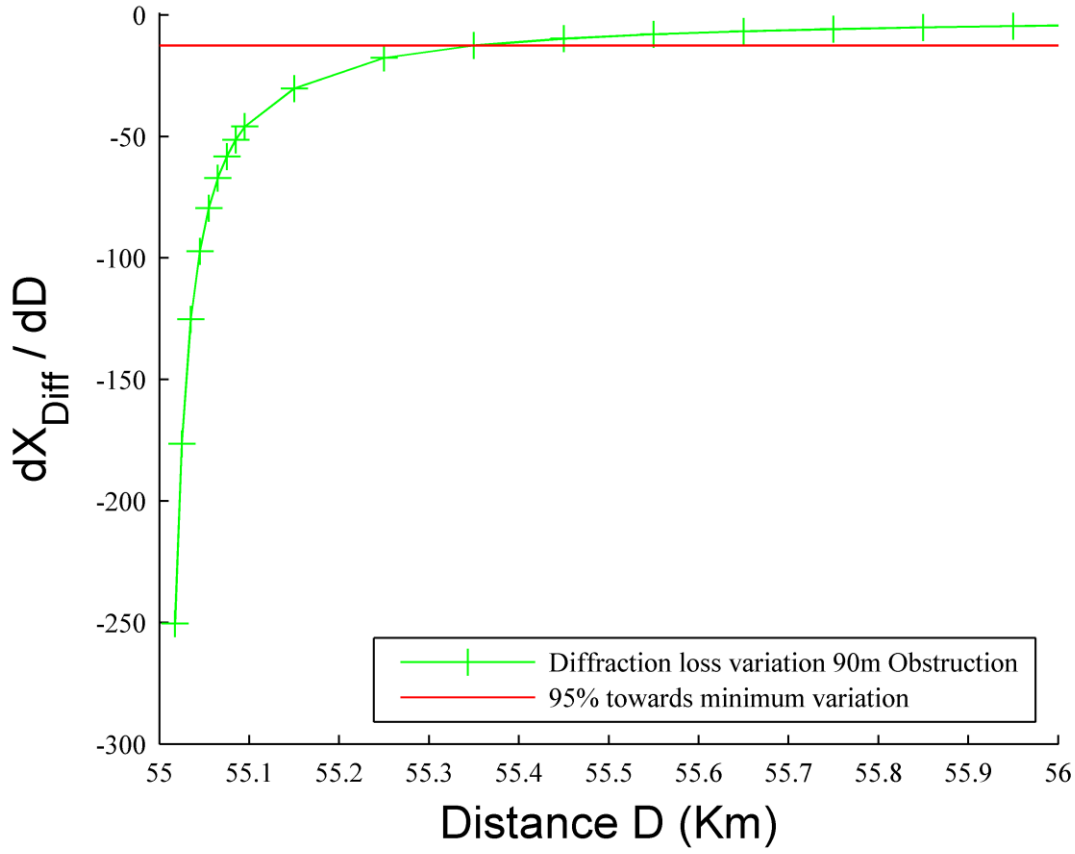

Figure 6-9: UK X_{Diff} variation with distance D

To provide a single margin parameter to enable a solution to the hidden node issue then diffraction variations need to be small. The margin parameter X_{KO} needs to lie in the region where X_{Diff} variation is a minimum i.e. 95% ≤ of minimum variation as seen in Figure 6-9.

An extract of the data generated in Figure 6-9 is shown in Table 6.6 and focuses on the criteria we have discussed being up to 1Km from obstacle and having percentage of minimum variation ≥ 95% for data that is within the sensing window for the country.

Table 6.6: Diffraction variation analysis at 738MHz

Distance from DTT Transmitter D Km ($Dist_{PC} + Dist_{Obst+SU}$)	**Diffraction variation $\frac{dX_{Diff}}{dD}$**	**% of minimum variation**	**Diffraction Loss due to 90m Obstacle dB**
55.35	-12.54	95.0	32.40
55.45	-9.72	96.1	31.30
55.55	-7.93	96.8	30.43
55.65	-6.70	97.3	29.71
55.75	-5.79	97.7	29.08
55.85	-5.10	98.0	28.54
55.95	-4.56	98.2	28.06

From Table 6.6 the diffraction variation column is summed and then divided by the number of data objects to give an average $\frac{dX_{Diff}}{dD}$**.** From this average value, a corresponding distance *D* is obtained from Figure 6-9. D for the UK is 55.58 Km.

To complete the keep out equation this distance D and using the Mendip DTT frequency 738MHz then X_{KO} is found from equations 6-4 and 6-3.

$$RSS_{KO} = -ObstacleDiff - RSS_{(D)} \qquad (6\text{-}3)$$

Where:

RSS_{KO} - Signal Strength at Keep Out Contour

ObstacleDiff - Diffraction Loss of a 90m Obstacle at 55Km and sensor at D using equations from chapter 3

$RSS_{(D)}$ - Signal Strength at D Km from DTT Transmitter at 738MHz with no Obstruction using model introduced in chapter 3

The output of the energy sensor at the keep out contour is X_{KO} given by:

$$\max_{0-T} X_{KO} = |\mathcal{F}(RSS_{KO})|^2 \qquad (6\text{-}4)$$

where X_{KO} is the RF energy at keep out contour where RSS is the received signal strength RSS_{KO} which using the sensor described in Chapter 3 gives the output of X_{KO} =138.73 which defines the keep out contour.

6.4.3 US keep out contour

As with the UK case study we start the analysis by firstly considering the diffraction loss response of a 90m obstacle just beyond the protection contour at 79Km for the Washington transmitter WFDC using parameters given in Table 6.3.

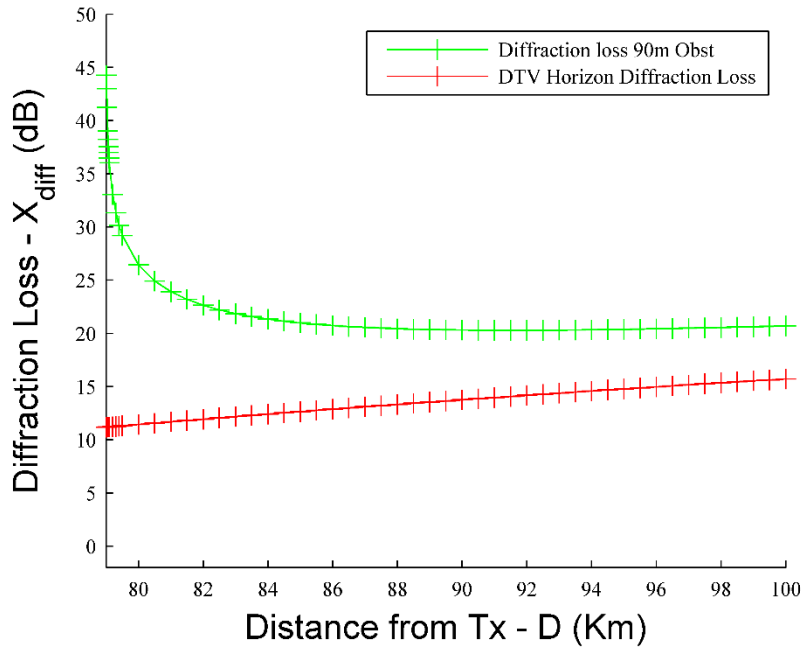

Figure 6-10: Diffraction Response of WFDC Transmitter area with 90m Obstacle at 79Km

The one crucial difference with the UK example is that the protection contour distance is much greater due to the use of 8-VSB modulation being used so a BER of less that $2x10^{-6}$ can be maintained at a lower S/N. This is why there is no spike due to the horizon point since the protection contour is well past this point. To define the margin due to the hidden node issue we now map $\frac{dX_{Diff}}{dD}$ against D to establish the point where the diffraction variation

tends towards zero but within 1 Km of the obstacle. The variation is show in Figure 6-11 below:

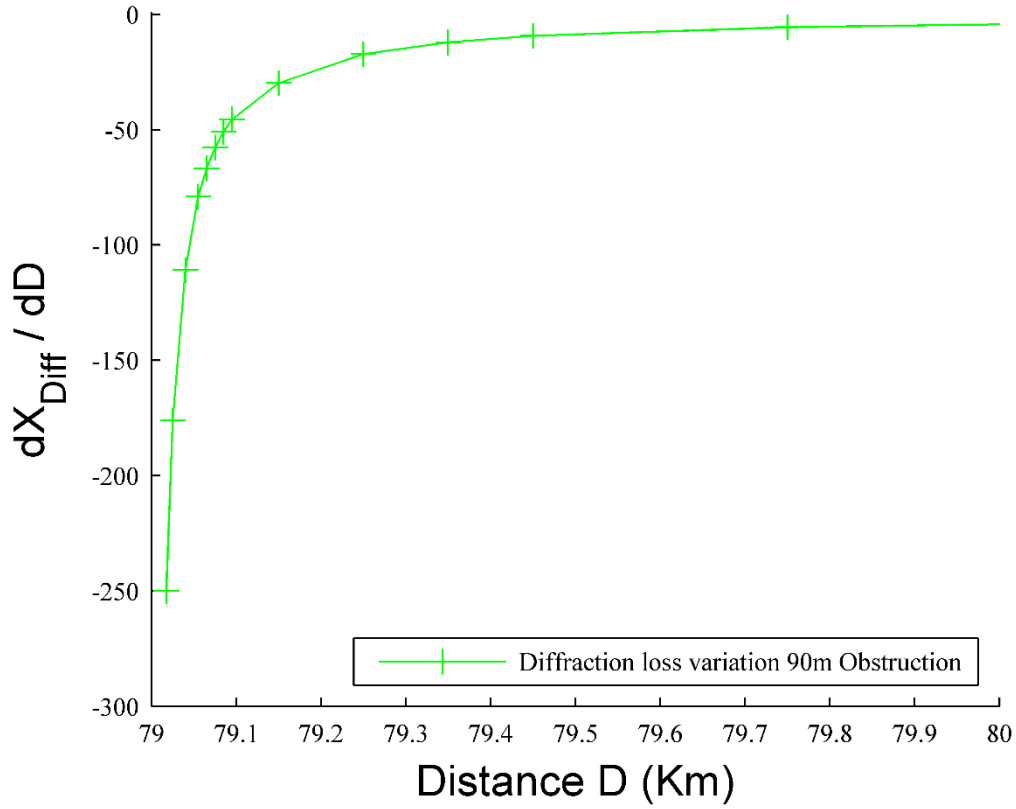

Figure 6-11: US X_{Diff} variation with distance D

Again, for the margin criteria we have taken 1Km from the obstacle has a bench mark for practical deployment being easily assessed by line of sight and is therefore taken has the maximum point from the obstacle where the sensing solution will take over. Below Table 6.7 below shows how the diffraction variation tappers off towards 1Km from an obstacle while obeying the same three criteria as for UK, ≥ 90% of minimum variation, within 1Km of an obstacle and within the sensing range used for the country. In the US FCC have set the sensing range to -114dBm **(**Nekovee, 2012) where this does not occur until 4 Km from the 90m obstacle. It is proposed that the GEDA solution will use -120 dBm sensing range so that the hidden node issue can be addressed. Table 6.7 assumes that the GEDA uses -120 dBm sensing range.

Table 6.7: US Diffraction variation analysis

Distance from DTT Transmitter D Km ($Dist_{PC} + Dist_{Obst+SU}$)	**Diffraction variation $\frac{dX_{Diff}}{dD}$**	**% of minimum variation**	**Diffraction Loss due to 90m Obstacle dB**
79.45	-9.23	96.3	29.64
79.75	-5.54	97.8	27.56
80.00	-3.03	98.8	25.59

Using the same procedure as the UK case study the average diffraction loss variation $\frac{dX_{Diff}}{dD}$ is found and from this the distance at which this average value occurred. This is distance in conjunction with equations (6-3) and (6.4) the energy sensor output at the keep out contour (X_{KO}) is found to be 120.9.

6.4.4 Keep out contour results analysis

First the UK keep out contour results shall be critically discussed with the interference management as the criteria. The X_{KO} is first overlaid on to the sensor output response graph for all the obstacle heights as seen in Figure 6-12 then we obtain the minimum (2) and maximum (3) keep out distances for an SU transmitter.

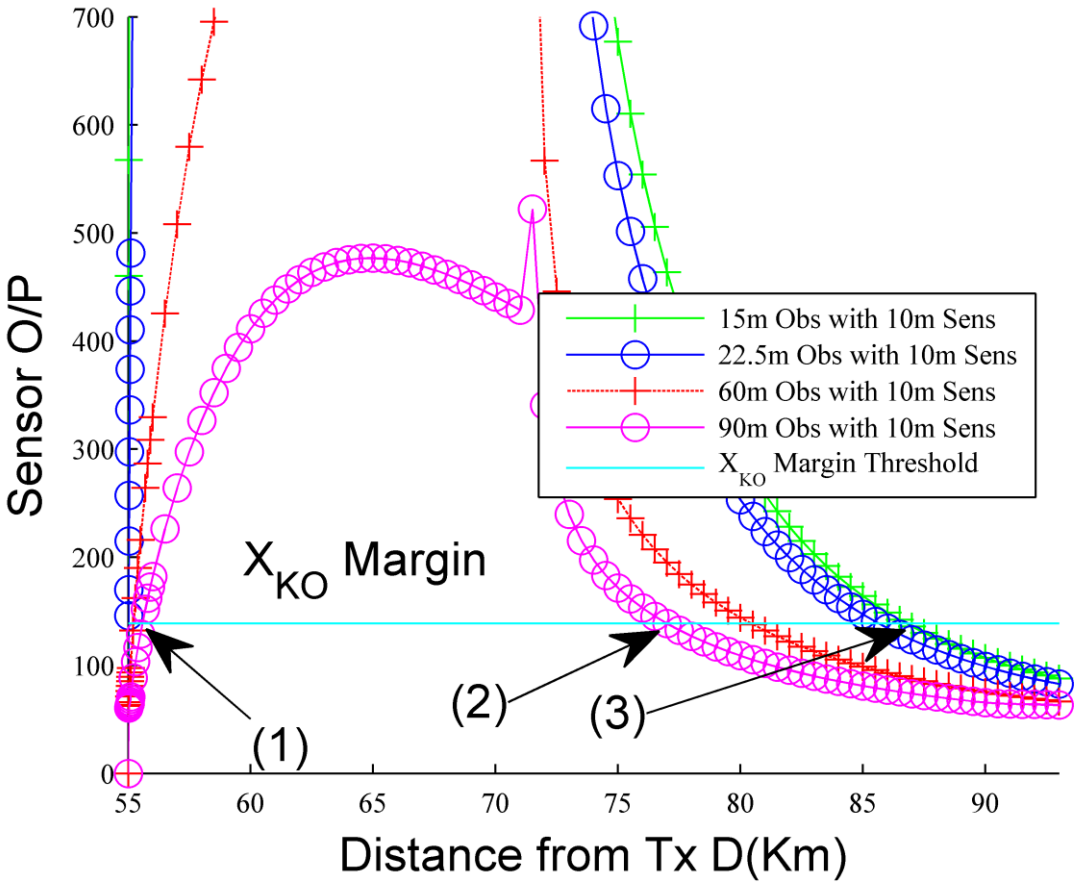

Figure 6-12: Mendip Keep Out Contour at 738MHz

Figure 6-12 reveals that while the distance to the *keep out contour* distance varies between points (2) (minimum) and (3) (maximum), depending on the obstacle height, X_{KO} remains constant. At (2) the minimum distance at 76.89 Km is 22.87 Km from the nearest DTT receiver ($Dist_{KO}$) on the protection contour. This means from Table 6.4 where for a 17dBm, the maximum allowed transmit power from OFCOM, a minimum distance of 3.75 Km is required to avoid co-channel interference. It can then be assumed by using the keep out margin X_{KO}, that no interference is caused by a SU transmitter with an obstacle height of 90m. For a typical residential scenario and a 15m obstruction, it can be assumed the maximum *keep out contour* distance is 86.69 Km (3), which is the value used in channel re-use calculations. Note, the distance from the obstruction to point (1) is just 0.58 Km which represents a special case where PU detection is only achievable using either a co-operative

sensing strategy or special sensor heights discussed in section 6.31 (Martin et al, 2013) and needs to be within 1Km of the obstruction in which it is.

Now we shall examine the US results using the same criteria. The X_{KO} energy threshold is again superimposed on to the sensor responses of the various obstacle heights which will define the keep out contour for the WFDC US DTT transmitter.

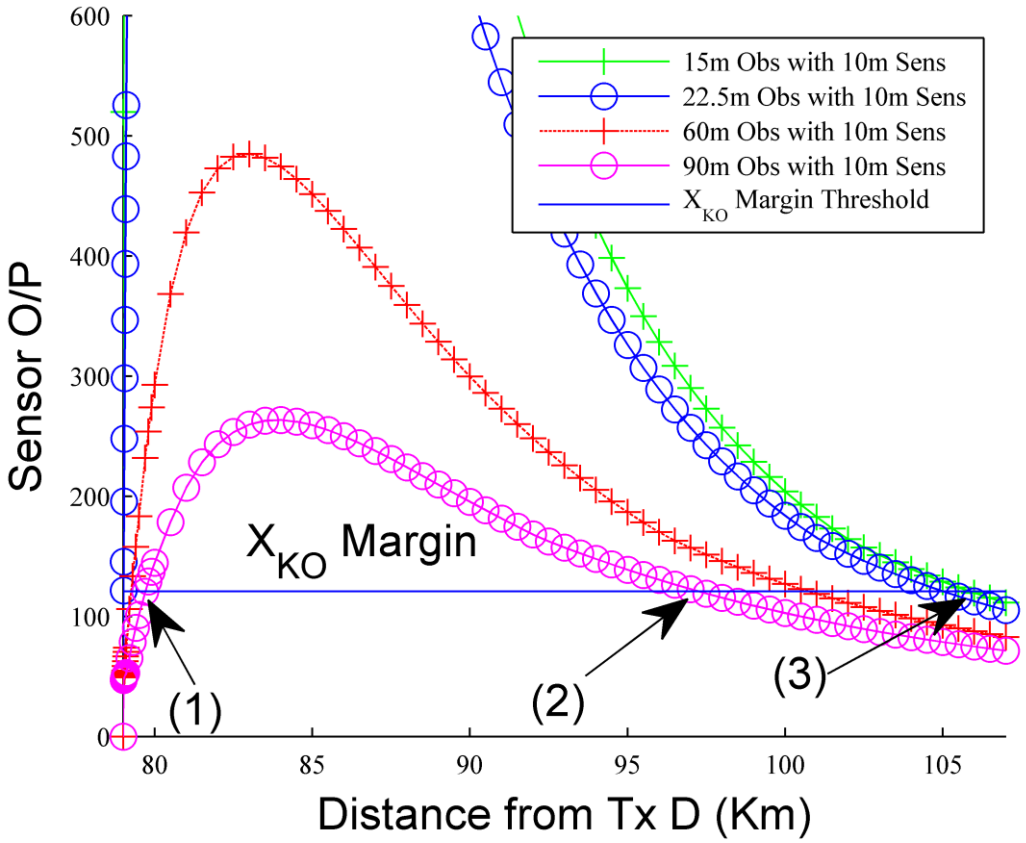

Figure 6-13: US Keep Out Contour

From Figure 6-13 (2) is the minimum distance, 97.19 Km which means that it is 18.8 Km from the nearest DTT receiver on the protection contour. This means for a 30dBm SU transmitter (Table 6.4), the maximum allowed transmit power from (FCC, 2012) and (Nekovee, 2012), a minimum distance of 13.66 Km is required for co-channel interference. From this it can be assumed by using the keep out margin X_{KO} then no interference will be caused by a SU transmitter with an obstacle height of 90m. For the most typical residential scenario and a 15m obstruction, it can be assumed the maximum *keep out contour* distance

is 105.79 Km (3), which is the value used in channel re-use calculations. Note, the distance from the obstruction to point (1) is just 0.70 Km which represents a special case where PU detection is only achievable using either a co-operative sensing strategy or special sensor heights discussed in section 6.31 and (Martin et al, 2013) and again it is still within 1Km of the obstruction.

6.5 Summary

This chapter has defined the protection contour for both the UK and the US in which forms the basis for a keep out contour to protect the PU receiver but also minimise the keep out distance for SU channels. Co-Channel and Adjacent Channel interference was also analysed in both scenarios to set the criteria for any hidden node solution to conform to. Finally, the keep out contour parameter X_{KO} is defined so a new GEDA algorithm can be presented which incorporates the solution to the hidden node issue and PU interference management.

In the next chapter the available TVWS bandwidth to a SU is calculated using the GEDA algorithm using the *keep out contour* and introducing the *sterilisation index* (SI).

7. RESOURCES FOR TVWS SECONDARY USERS

7.1 Introduction

In (Cambridge White Spaces Consortium, 2012) and (COGEU, 2009) the assessment of TVWS bandwidth available in any location was determined by physical RF surveys. This method incurs a considerable amount of resources, so an alternative strategy was developed as a part of this research called the *sterilisation index* (*SI*) which determines the amount of TVWS bandwidth available. By using the "*Keep out Contour*" threshold the *SI* gives a measure of TVWS channel sterilisation within a transmitter area and so the available bandwidth from simulation techniques.

The *SI* is a simulation based method which calculates the amount of area a neighbouring transmission is encroaching into the main transmitter area and so produces an index of how much the neighbouring channel cannot be utilised in the main area by a TVWS SU. To validate the process two case studies are used, one is the Mendip area in the UK and the other is the Washington DC area in the US. These were chosen because the Mendip area includes some interesting geographical features such as the Bristol Channel, Mendip hills and large cities such as Bristol, while Washington DC is the US capital so would have a dense population and so demonstrates this method can work in different geographical area and DTT deployments.

7.2 Sterilisation Index (*SI*)

The *keep out contour* area of the secondary DTT transmitters transmitting within a primary DTT area where the intersecting area is F Km^2 per DTT channel per transmitter (F_1, F_2 and F_3).

If Y Km^2 is the area covered by the furthermost keep out contour of a major transmitter serving a UK DTT region, then for a distributed deployment such as that employed in the USA, this represents the area covered by the radius of the furthest away transmitter keep out contour, added to the distance from this transmitter to the centre of the region under analysis. *SI* is thus formally defined as:

$$SI = \frac{F}{Y} \qquad (7\text{-}1)$$

Using (7-1), the SI is calculated on a per channel, per transmitter basis as shown in Figure 7-1.

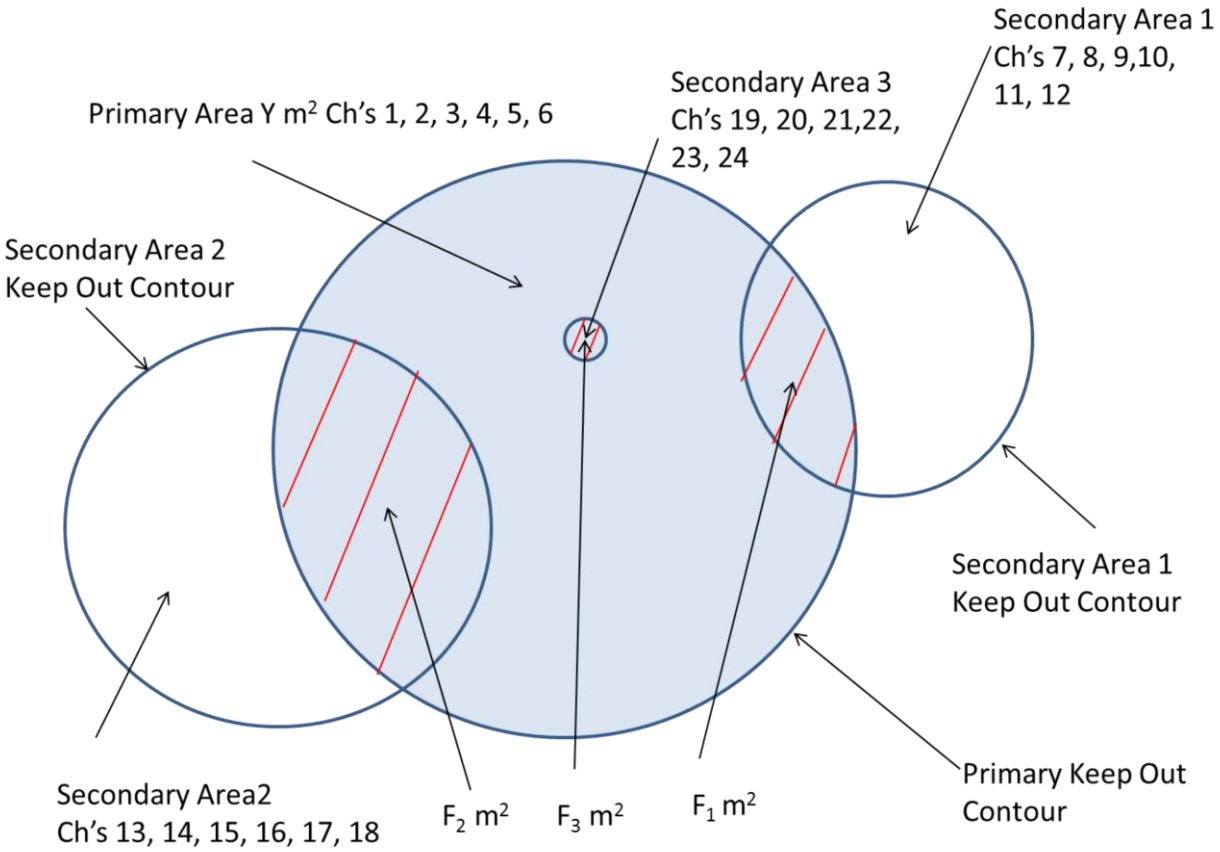

Figure 7-1: SI breakdown for a primary area

The example shown in Figure 7-1 is generic and does not depict any specific location but shows the SI mechanism used to evaluate the available channels for TVWS. Specific examples will be presented in sections 7.3 and 7.4 for the UK and US locations. In Figure 7-1 a primary area *Y* is shown with channels 1 to 6 with a minor secondary area 3 transmitter within the primary *Y* area which serves has a rebroadcast station for the primary transmitter where are local propagation issues. These rebroadcast stations are very low power and may be spread around the primary area so to evaluate the *SI* for these the average RF power across all such transmitters were taken to determine the average keep out area for each transmitter per a channel. This *SI* is then multiplied by the number of the rebroadcast stations in a primary area per channel. Also, there are two further secondary area's 1 and 2 which are adjacent primary area's and overlap the primary area *Y* which is under investigation. The intersection areas which fall into the primary area Y are respectively labelled F1, F2 and F3 and when used in (7-1) give a SI value for each of the channel in the secondary area.

The intersecting area and *SI* for Secondary Area 1 and 2 are calculated by Algorithm 7.1 and the principal is shown in Figure 7-1. This calculates (Wolfram, 2015) the intersection area between two circles which will be equal to the secondary DTT coverage area within the primary DTT area, i.e., F_1 and F_2. For a minor secondary DTT transmitter nested within a primary area, e.g. Secondary Area 3 in Figure 7-1, then a straight forward area of a circle is used where the radius is the keep out contour of the minor transmitter, e.g. F_3. From this the individual *si* value for the primary area imposed by the secondary channel is found and will be used to form a complete *SI* matrix for the primary area.

Algorithm 7.1: Primary and Secondary DTT intersection area and *SI*

1:	***r* = Keep Out contour of primary DTT area**
2:	***R* = Keep Out contour of secondary area**
3:	***d* = Distance between primary and secondary DTT transmitters**
4:	**IF $R < r$ THEN**
5:	$RR = r$
6:	$rr = R$
7:	**ELSE**
8:	$rr = r$
9:	$RR = R$
10:	**END IF**
11:	$a = \cos^{-1}((d^2 + rr^2 - RR^2)/(2 \times d \times rr))$
12:	$b = \cos^{-1}((d^2 + RR^2 - rr^2)/(2 \times d \times RR)$
13:	$B = rr^2 \times a$
14:	$C = RR^2 \times b$
15:	$D = \frac{1}{2} \times (\sqrt{(-d + rr + RR) \times (d + rr - RR) \times (d - rr + RR) \times (d + rr + RR)}$
16:	$A = B + C - D$
17:	$E = \frac{A}{\pi \times r^2}$
18:	***A* = Primary DTT Area sterilised by secondary DTT Area**
19:	***E* = *si***
22:	**END**

The individual *si* values are used to construct the primary area *SI'* matrix shown in (7-2).

$$SI' = \begin{pmatrix} si_{11} & \cdots & si_{1n} \\ \vdots & \ddots & \vdots \\ si_{m1} & \cdots & si_{mn} \end{pmatrix} \qquad (7\text{-}2)$$

where *n* is the number of DTT Channels i.e. 32 in the UK, and *m* is the number of transmitters radiating in area *Y*. If the same channel is used in two different transmitters where one keep out contour area is nested within the other, then the smaller si_{mn} value is set to zero.

The final step is to sum all columns and resulting rows in (7-2) to form a final *SI* value in (7-3).

$$SI = \sum_{i=1}^{n} \sum_{j=1}^{m} si_{ij} \qquad (7\text{-}3)$$

The *SI* determines the available bandwidth in the DTT area under investigation for an SU to exploit. This is given by:

$$Total\ TVWS\ Bandwidth = (n - SI) \cdot BW \qquad (7\text{-}4)$$

where *n* is the number of DTT channels and *BW* MHz is the DTT channel bandwidth for the country of interest, which in the UK for example, is 32 Channels and 8MHz, 43 Channels and 6MHz in the USA.

The UK DTT network consists of major regions, with each having minor transmitters operating within their boundaries to overcome local propagation issues so ensuring populated areas have service coverage. In contrast to this DTT deployment, America has distributed major transmitter sites covering a region, though the *SI* technique is still applicable.

The next two section investigates how the *SI* can be applied to determine the number of TVWS channels available in the specific case study area of the Mendip region in the UK and the Washington area in the US.

7.3 SI analysis of the Mendip DTT area

All the major, adjacent and minor transmitters of either 50W or more (OFCOM, 2016) in the Mendip DTT transmitter area, together with their corresponding channels numbers against the relevant allocation number (# number) are shown in Table 7.1.

Table 7.1: Mendip area adjacent, major and minor DTT transmitter ≥ 50W channel distribution

DTT Transmitter	Channel #1	Channel #2	Channel #3	Channel #4	Channel #5	Channel #6
Mendip	49	54	58	48	56	52
Wenvoe	41	44	47	42	45	39
Pontypool	23	26	29	25	22	28
Bristol Kings	43	40	46	53	57	60
Stocklands Hill	26	23	29	25	22	28
Salisbury	57	60	53	50	59	55
Bristol IC	41	44	47	42	45	39
Cirencester	23	29	26	-	-	-
Stroud	40	43	46	-	-	-
Bath	25	28	22	-	-	-
Hannington	42	45	39	41	44	47
Cerne Abbas	29	26	23	-	-	-

Using Table 7.1 the individual *si* values can be determined from Algorithm 7.1 and matrix SI' formed as in (7-5). In the cases of the Pontypool and Bristol IC (highlighted in red) which are minor transmitters, their corresponding si_{mn} values are set to zero because they are nested within the Wenvoe and Stocklands Hill areas respectively (From the channel numbers highlighted in yellow).

$$SI' = \begin{pmatrix} 1 & 1 & 1 & 1 & 1 & 1 \\ 0.6231 & 0.6231 & 0.6231 & 0.5908 & 0.5908 & 0.5908 \\ 0 & 0 & 0 & 0 & 0 & 0 \\ 0.1338 & 0.1338 & 0.1338 & 0.1338 & 0.1338 & 0.1338 \\ 0.5663 & 0.5663 & 0.5663 & 0.5358 & 0.5358 & 0.5358 \\ 0.1613 & 0.1613 & 0.1613 & 0.1613 & 0.1613 & 0.1613 \\ 0 & 0 & 0 & 0 & 0 & 0 \\ 0.1052 & 0.1052 & 0.1052 & 0 & 0 & 0 \\ 0.0630 & 0.0630 & 0.0630 & 0 & 0 & 0 \\ 0.0893 & 0.0893 & 0.0893 & 0 & 0 & 0 \\ 0.1957 & 0.1957 & 0.1957 & 0.1880 & 0.1880 & 0.1880 \\ 0.1131 & 0.1131 & 0.1131 & 0 & 0 & 0 \end{pmatrix} \quad (7\text{-}5)$$

Using the equation (7-3) and (7-4) the overall *SI =16.98*, which equates to an available bandwidth of:

$$SU\ BW = 120.15MHz$$

This means there is approximately 120MHz available for TVWS SU devices when consideration is made of all transmitters of either 50W or greater. However, there are also 55 minor DTT transmitters operating below 50W that must also be taken into account. To do this efficiently, the average antennae heights and EIRP values are used in calculating the *SI*, which for each minor transmitter is found to be 0.01148. Since 3 channels are allocated to each minor transmitter this equates to a *SI=2*, which when combined with the *SI* for the major transmitters gives a total *SI=19*, which slightly lowers the average available bandwidth for TVWS over the entire Mendip area to 104MHz.

7.3.1 UK Results

While the available TVWS bandwidth of 104MHz represents the average available bandwidth for the Mendip DTT region, it recognises this will vary according to locality. In more heavily populated areas, it will reduce while in rural areas it will increase. This corroborates the findings in (Nekovee, 2012), which is based on measured availability and geo-location database access, showed in the largest city (Bristol) in the Mendip DTT region,

12 x 8MHz = 104MHz of bandwidth was available for TVWS devices as demonstrated in Figure 7-2:

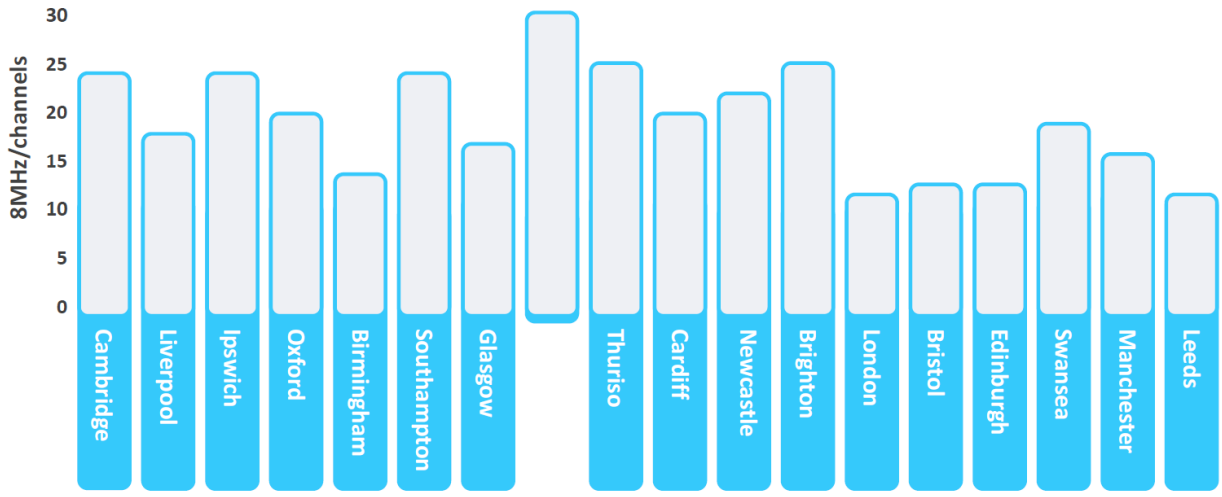

Figure 7-2: TVWS allocation in the UK

Other OFCOM studies (COGEU, 2010) suggest that over 90% of the population can access at least 100MHz, aggregated across the interleaved spectrum. They also estimated that ≈50% of the population could have access to 150MHz or greater and some rural communities could enjoy more over 200MHz of this spare capacity (Randhawa et al, 2009). These findings highlight the key role the *keep out contour* and *SI* play in releasing valuable resources for SU TVWS exploitation, while concomitantly ensuring the *QoS* provision for PU DTT users. Figure 7-3 below shows the bandwidth allocation for the UK per operator (Analysys Mason, 2013):

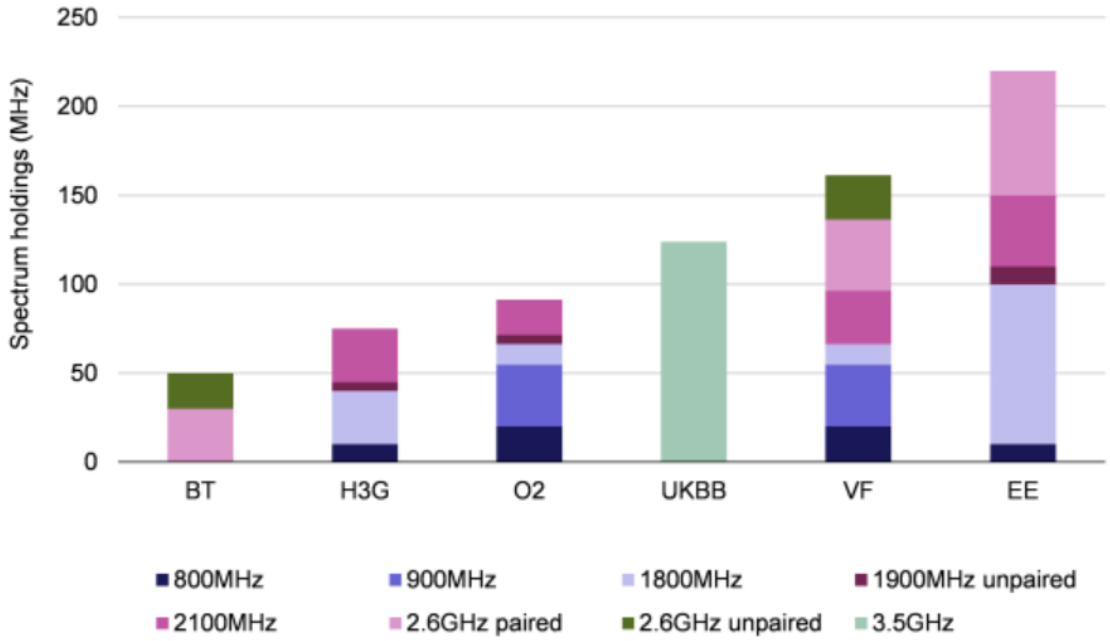

Key: BT = Niche Spectrum Ventures (a subsidiary of BT); H3G = Hutchison 3G UK (trading as '3'); O2 = Telefónica UK (trading as O2); UKBB = UK Broadband; VF = Vodafone; EE = Everything Everywhere.

Figure 7-3: LTE spectrum allocation in the UK

In Figure 7-3 it can be seen that the extra 104MHz gain in any locality is a significant increase for any of the operators shown. As an illustration, the SU gains secured for the Mendip region using the *keep out contour* and *SI* is equivalent to approximately 5 x 20MHz LTE RF bearers per location. This translates to an increase in the number of active data users in a LTE cell location from 800 to 4000, if a TVWS access node is used in conjunction with an LTE eNodeB, i.e., an improvement factor of 5.

The US scenario where the Washington area shall be analysed using the *SI* method in the next section.

7.4 SI Analysis for the US Washington DTT area

For the US case study, the DTT transmitters are defined by a three or four letter call sign where the Washington DTT transmitter is WFDC and has the primary area and the secondary

area transmitters are selected whose *keep out contour* intersect this primary area (FCC, 2015). The primary and secondary channels are shown in Table 7.2

Table 7.2: Washington area adjacent, major and minor DTT transmitter channel distribution

Washington DTT Transmitter	DTT Channel
WFDC	15
WRC	48
WPXW	34
WTTG	36
WDCW	50
WJLA	7
WUSA	9
WDCA	35
WHUT	33
WETA	27
WNVC	24
WMPT	42
WNVT	30
WBAL	11
WNUV	40
WMAR	38
WJZ	13
WBFF	46
WUTB	41
WMPB	29
WFPT	28

WGAL	8
WVPY	21
WHAG	26
WWPB	44
WWPX	12
WJAL	39

Table 7.2 reveals that in contrast to the UK DTT channel distribution, only one channel is allocated per transmitter area in the US, whereas in the UK six channels are allocated, though importantly transmitters can be co-located (FCC, 2015) (Spectrum Bridge, 2010). As in Section 7.3, the individual *si* values are calculated from Algorithm 7.1 and matrix *SI'* formed as:

$$SI' = \begin{pmatrix} 1 \\ 0.94 \\ 0.77 \\ 1 \\ 0.95 \\ 1 \\ 1 \\ 0.90 \\ 0.79 \\ 0.76 \\ 0.78 \\ 0.68 \\ 0.51 \\ 0.79 \\ 0.73 \\ 0.71 \\ 0.75 \\ 0.71 \\ 0.49 \\ 0.53 \\ 0.31 \\ 0.57 \\ 0.42 \\ 0.47 \\ 0.38 \\ 0.57 \\ 0.29 \end{pmatrix} \quad (7\text{-}6)$$

This gives an overall *SI*=19. As the US, has 43 DTT channels each with a bandwidth of 6MHz, using (7-4), this equates to an available TVWS SU bandwidth of 144MHz within the WFDC area.

7.4.1 US Results

In Section 7.4 the TVWS bandwidth results for the Washington WFDC DTT area are 144MHz which is the average bandwidth available within the WFDC protection contour. In examining the keep out contours of the transmitters that were adjacent to WFDC it is found that point (2) of the diffraction sensor results (Figure 6-9) does not give the 13.66 Km (Table 6.4) clearance to avoid PU interference. Consequently, a special rule is imposed with the maximum SU transmitter power being 17dBm. Assuming this, then the TVWS bandwidth is compared to the average bandwidth available using the portable/mobile figures which use 16dBm transmitter power (Blue bars in Figure 7-4) (Spectrum Bridge, 2010). Figure 7-4 shows the aggregated TVWS bandwidth per State (Spectrum Bridge, 2010).

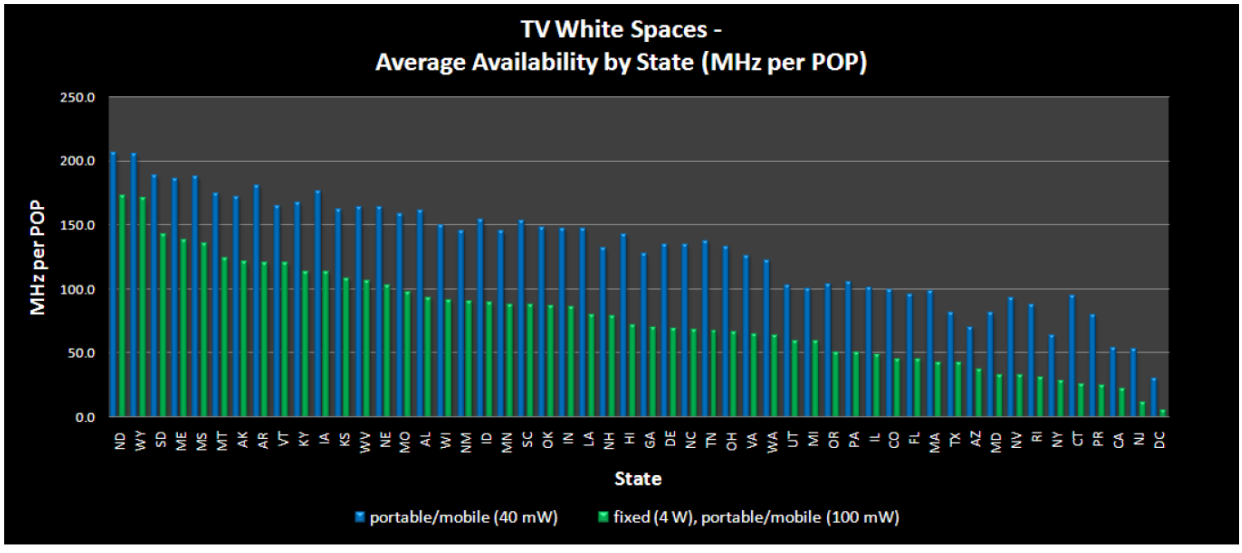

Figure 7-4; Average TVWS bandwidth per State (Spectrum Bridge, 2010)

From Figure 7-4 the available TVWS bandwidth available in the State of Virginia (The State Washington is bordering on) is 125MHz (Blue bar for State VA in Figure 7-4) while the *keep out contour* calculation for the WFDC area gives 144MHz. This discrepancy can be explained by the relatively smaller area of the WFDC coverage area (35,159.20 Km^2) compared to the much larger Virginia State area (102,558 Km^2) and because of this greater amount of DTT transmitters are required to service Virginia state area. With this increase in DTT transmitters more DTT channels are required so fewer available for TVWS as an aggregated total within Virginia state.

The LTE Bandwidth Allocation (Uplink and Downlink) for the Major Operators in the US are given below (GSA, 2016) which gives similar information presented in Figure 7-3 for the UK scenario:

Table 7.3: US LTE Operators bandwidth allocations

Operator	Bandwidth
AT&T	114MHz
Sprint	324MHz
T-Mobile	246MHz
Verizon	230MHz

From Table 7.3 it can been deduced that the 144MHz released from TVWS using the keep out contour is a significant increase to operator capability in any specific location compared to the bandwidth allocation above.

7.5 Summary

This chapter has presented a novel technique to measure the bandwidth available within a locality using the *SI*. Using the *SI* technique, the TVWS bandwidth for two case studies in UK and US were carried out with results being produced for both scenarios. Using the protection contour within the US case study, an SU transmitter power restriction was

identified to avoid interference to the PU which means the maximum transmitter power in US is 17dBm.

From these case studies, it is shown that significant amount of bandwidth can be freed to warrant TVWS implemented with the proposed protection contour that has been presented without incurring interference to the PU.

The next chapter focuses on wireless routing which can maximise the performance using this freed bandwidth within a SU network and how this can improve QoS to an SU user.

8. MULTI-LAYER ROUTING STRATEGIES FOR TVWS SECONDARY USERS

8.1 Introduction

The thesis has examined the issues of detecting a DTT PU, the interference impact of deploying a TVWS SU network and the bandwidth gains available when using the proposed GEDA and interference management algorithms. The way a SU can exploit the available bandwidth to maximise performance will now be investigated. As stated in Chapter 6, sensing solutions cannot solve the hidden node issue when the sensor height is below 10m which then shifts the sensing functionality to the BS for practical reasons, because it is a fixed node with a higher antenna height than the mobile station. With the BS making the sensing decisions means any solution must rely on the BS-to-mobile topology with the sensor physically located at the BS, so all control information emanates from the BS. With the BS and mobile connection vital for control and user traffic and the disparity of coverage between BS and mobiles due to RF power and antenna height differences, to support the BS coverage in both the forward and reverse link directions, an ad-hoc routing solution is required in the reverse link direction. One such topology is shown in Figure 8-1.

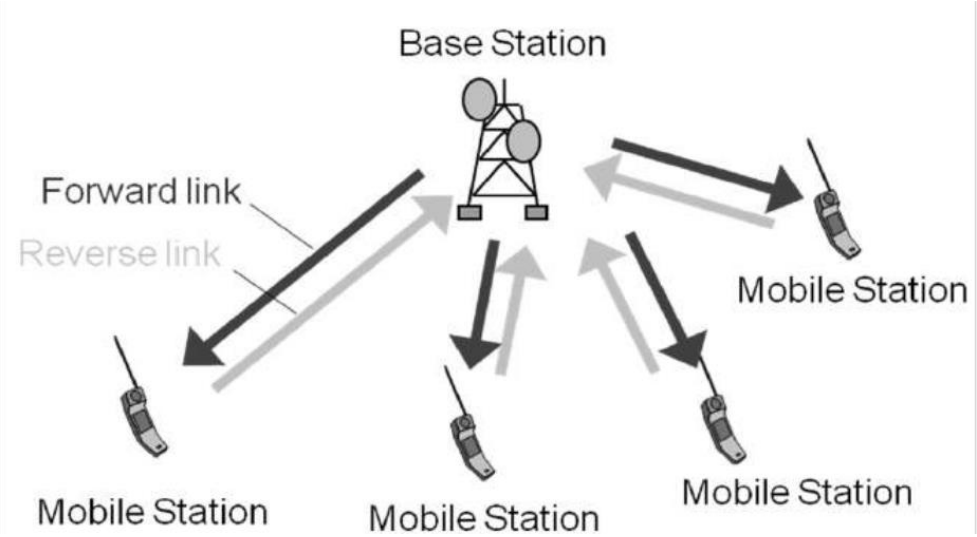

Figure 8-1: Base Station – Mobile Topology

This topology is based on IEEE802.11af WLAN (IEEE, 2013) using the OFDM standard. IEEE802.11af is designed for TVWS access with up to four channels bonded in either one or two contiguous blocks. The bandwidth resource is shared on a time basis with an opportunistic access policy. The maximum achievable data rate per spatial stream is 106.7 Mbit/s for 6 and 7 MHz DTT channels and 142.2 Mbit/s for 8 MHz channels when utilising IEEE802.11af (IEEE, 2013) recommendations using 256QAM. With four spatial streams and four bonded channels, the maximum data rate is 426.7 Mbit/s in 6 MHz channels and 568.9 Mbit/s for 8 MHz channels (IEEE, 2013). The bonding of these channels helps to achieve greater throughput for the bandwidth values detailed in Chapter 7, however this chapter will only consider single-channel streams which for the UK and US means that 8MHz and 6MHz channels are respectively able to support multiple mobile SU on a single BS access point.

In most cases however, the BS and mobile transmitter power specifications of OFCOM (UK) and FCC (US) (Nekovee, 2012) are greater than the mobile transmitter powers. This coupled with the mobile antenna heights being lower than the BS, means the BS service area will always be greater than that of the mobile. This leads to the requirement of some form of routing to enable the TVWS SU mobile to occupy the same service area as the BS. Consequently, the proposed network structure has a forward link directly connected to the

SU mobile nodes and the reverse link comprising multiple routes to the BS. The proposed strategy is to use several cross-layer parameters to maximise the coverage radii using parameters of distance (in layer 1), *time to live* (TTL in layer 3) and QCI (in layer 4) to maximise the coverage and the SU QoS.

The mobile network changes continually with the movement of the nodes and the RF propagation conditions which means that the route an IP packet will take is changing also. To ensure the route information updates occur rapidly to the ever-changing conditions so packets are not lost, MANET routing protocols were developed. The following sections are going to examine two types of MANET routing protocols, DSR and AODV which are widely adopted, and can be applied to an IEEE804.11af model to achieve a symmetrical service area for the forward and reverse link. The next section is going to define the BS and mobile models and determine the BS service area.

8.2 BS Service Area Analysis

To understand the behaviour of MANET routing protocols operating in an IEEE802.11af model, the BS service area which forms the boundary of the routing area needs to be defined. This is determined from three system parameters:

1. Maximum EIRP used for a BS SU. This is governed by the relevant regulatory body (Nekovee, 2012) i.e., 17dBm in both the UK and US (see Chapter 7).
2. The *packet error rate* (PER) to support the service to be provided to a customer.
3. The IEEE802.11af modulation type used to give WLAN throughput and corresponding SNR required to achieve the desired PER.

To define a BS service boundary, the PER needs to be determined for the worst-case scenario and to achieve this, the 3GPP QoS class identifier (QCI) has been used. Since QCI reflects the packet forwarding behaviour in LTE networks, it was chosen as the most pragmatic solution for defining TVWS SU QoS classification so it can be easily integrated into the LTE core network, so this can be re-used for the TVWS access. The various QCI parameter

settings are shown in Table 8.1, for data services with both *guaranteed bit rate* (GBR) and non-GBR data resource types.

Table 8.1: 3GPP QCI Category Specifications

QCI	Resource Type	Priority	Packet Delay Budget (ms)	Packet Error Rate (PER)	Example Services
1	GBR	2	100	10^{-2}	Conversational Voice
2		4	150	10^{-3}	Conversational Video (Live Streaming)
3		3	50	10^{-3}	Real Time Gaming
4		5	300	10^{-6}	Non-Conversational Video (Buffered Streaming)
5	Non-GBR	1	100	10^{-6}	*IP Multimedia Subsystem* (*IMS*) Signalling
6		6	300	10^{-6}	Video (Buffered streaming) TCP-based applications (www, e-mail, chat, ftp, p2p file sharing, progressive video)
7		7	100	10^{-3}	Voice, Video (Live Streaming) Interactive Gaming
8		8	300	10^{-6}	Video (Buffered streaming) TCP-based applications (www, e-mail, chat, ftp, p2p file sharing, progressive video)
9		9			

Evidently the lowest PER=10^{-6}, will now be used to determine the service boundary by converting this to a corresponding BER as follows (ACP, 2014):

$$P_p = 1 - (1 - P_e)^N \qquad (8\text{-}1)$$

Where P_p is the PER, P_e is the BER and N is the number of bits in each packet.

The regular IP packet length supported in the ensuing simulations are 128, 256, 512, 1024 and 1500 bytes.

Transposing (8-1) for P_e we obtain:

$$P_e = 1 - \left(1 - P_p\right)^{\frac{1}{N}} \qquad (8\text{-}2)$$

Figure 8-2 shows BER v SNR responses for 4, 16, 64 and 256 QAM modulation techniques. For a 1500 byte packet, equation (8.2) gives a BER = 8.33×10^{-11} which when correlated from the graph in Figure 8-2 for 256 QAM used in IEEE802.11af, gives an SNR threshold of 35dB, from which the maximum distance between a SU transmitter and receiver can be determined.

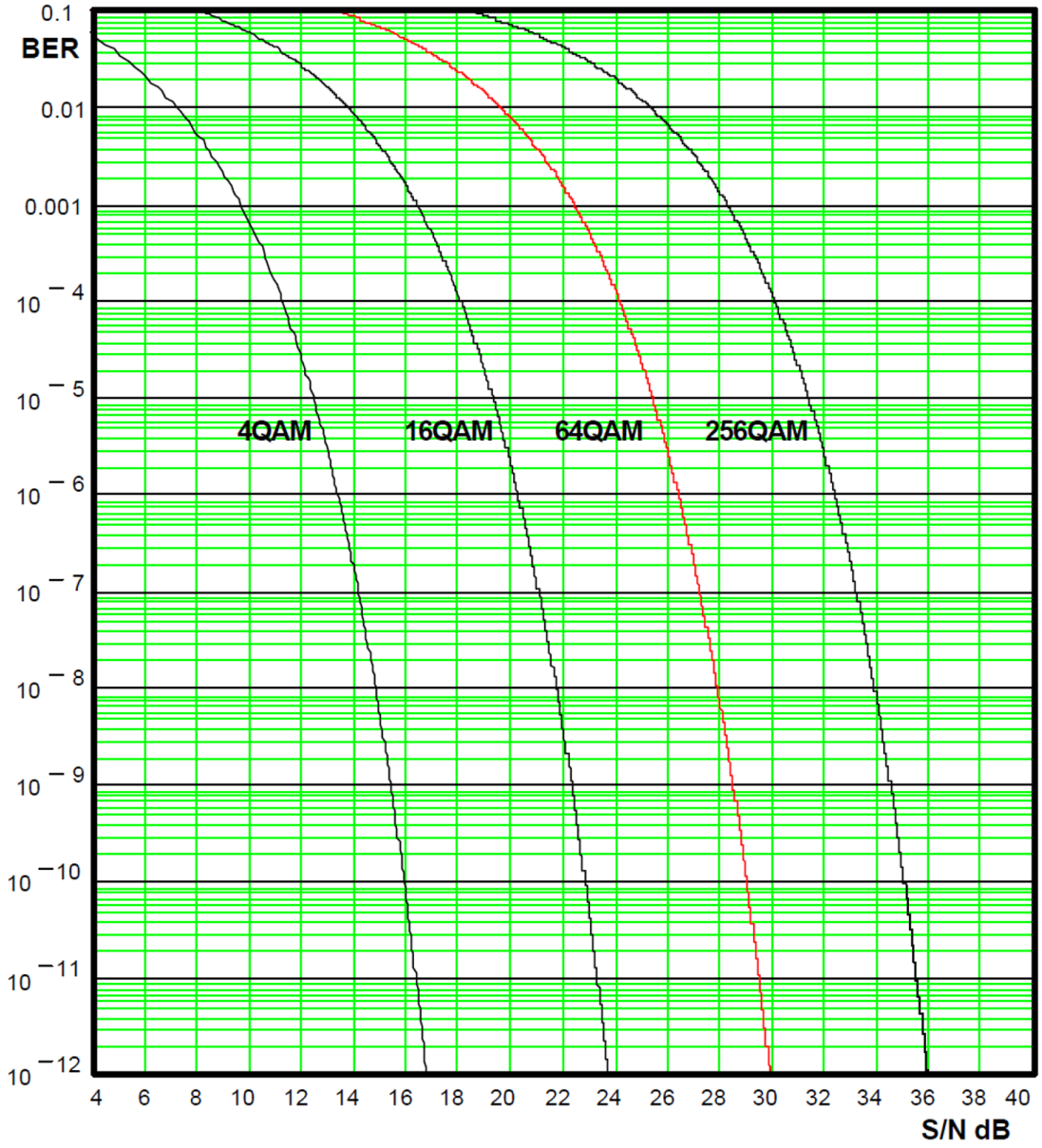

Figure 8-2: BER v SNR for QAM Modulation modes

Since the SU network uses much lower power compared to the PU, the predominant propagation system component will be the *free space loss* (FSL) defined in (8-3). This is in contrast to the PU, where it is a combination of FSL, reflection and diffraction which is the reason for selecting the Egli propagation model in the earlier PU critical analysis of Chapter 3. The FSL in dB for the SU is given by (Seybold JS, 2005):

$$Free\ Space\ Loss(FSL) = 20Log(D) + 20Log(Freq) + 20Log\left(\frac{4\pi}{c}\right) \qquad (8\text{-}3)$$

Where:

FSL= Free Space Loss in dB

D= Distance between SU transmitter and receiver in m

Freq= Frequency is Hz

c= Speed of light 3x 10^8 m/s

To determine the receiver signal at the demodulator, firstly the *receiver actual noise* (RAN) is calculated from:

$$RAN = 10Log(k \cdot T_o \cdot B) - NF \quad (8\text{-}4)$$

k= 1.38 x 10^{-23} (Boltzmann constant)

T_0= 290 ^{o}K (Ambient temperature 17^{o}C)

B= DTT bandwidth (8MHz in the UK and 6MHz in America)

NF= Receiver Noise Figure 7.5dB

Hence with the EIRP=17dBm and an *SNR*=35dB (see Figure 8-2), *D* can now be determined from (8-3) and (8-5):

$$SNR + RAN = EIRP - FSL + G_T + G_R \quad (8\text{-}5)$$

Where G_T and G_R are respectively the transmitter (0dB) and receiver antenna (2dB) gains.

So for the UK Mendip area case study, using a TVWS frequency of 706MHz which is not used by the PU, and EIRP=17dBm, this translates to a SU coverage radius is ≈400m. For the corresponding US scenario, and a TVWS frequency of 629MHz which again is not used by the PU and the same EIRP, the coverage area radius is ≈517m.

The next section will show how the QCI service structure can be implemented using physical, transport and IP layer measurements to provide the appropriate QoS service for SU mobile nodes.

8.3 Mobile Node Service area

As previously stated, the BS forward link is purely a single-hop link with no routing protocols used because of the disparity in EIRP values between the BS and mobile node. Section 8.2 examined the BS forward link behaviour to achieve a PER=10^{-6}, which is the

minimum PER service error QoS. In this section, the reverse link behaviour from multiple SU nodes to the BS is considered using the AODV and DSR MANET routing protocols (Chen and Prasad, 2009), (Hossain et al, 2009), (Sheng et al, 2010), (Yuanzhou and Weihua, 2010).

The routing simulator, INET Framework on OMNeT++ platform, uses a file which applies the SNR to PER data so the Physical wireless behaviour can be defined. This file is re-designed so that the behaviour mimics that of a IEEE802.11af mobile. This was done by using the 256QAM BER v SNR in Figure 8-2 and equation 8-1. Also, the mobile node EIRP of 4dBm is used as per the OFCOM standards (Nekovee, 2012).

8.3.1 AODV v DSR Routing

These are two routing protocols designed for wireless mesh/ad hoc networks which employ different mechanisms, resulting in varied performance levels. DSR and AODV can be critically evaluated based upon the packet delivery ratio and the average end-to-end delay by altering the number of source packets, the packet rate and mobile node speed.

The DSR protocol maintains all routing information at the mobile nodes. Source routing is a technique in which the packet sender identifies the entire node sequence the packet must pass through before sending a packet. The packet sender lists the route in the packet's header so that the next node knows where the packet must be transmitted to the destination host. The DSR scenario is shown in Figure 8-3.

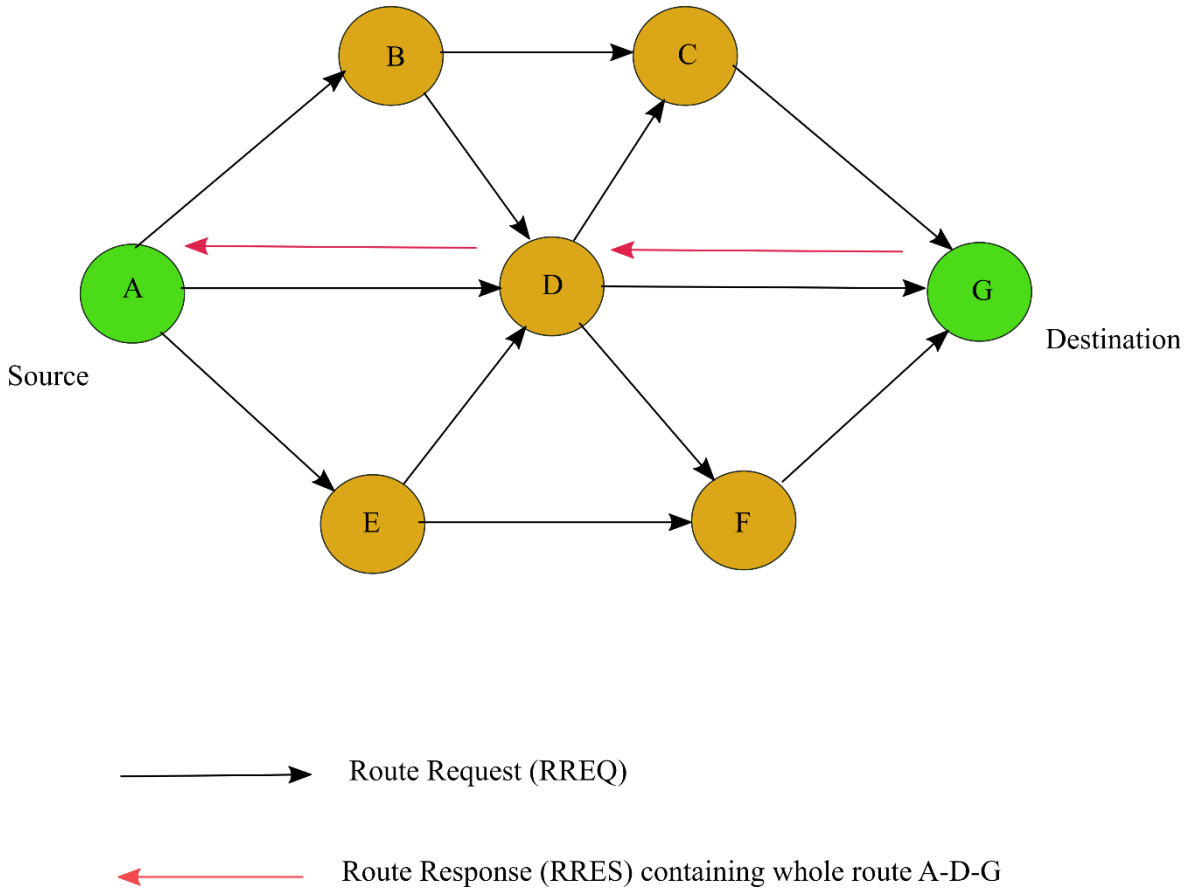

Figure 8-3: DSR routing scenario

Conversely, in AODV each node has a single hop to every destination in its routing table which is updated regularly by exchanging information between its neighbours. This means a route is set up one hop at a time as shown in Figure 8.4. By only traversing the network one hop at a time, packets can adapt to variations in network topology caused by nodes moving and can converge quickly on a successful route, though this benefit is counterbalanced by greater network overheads in controlling traffic flow.

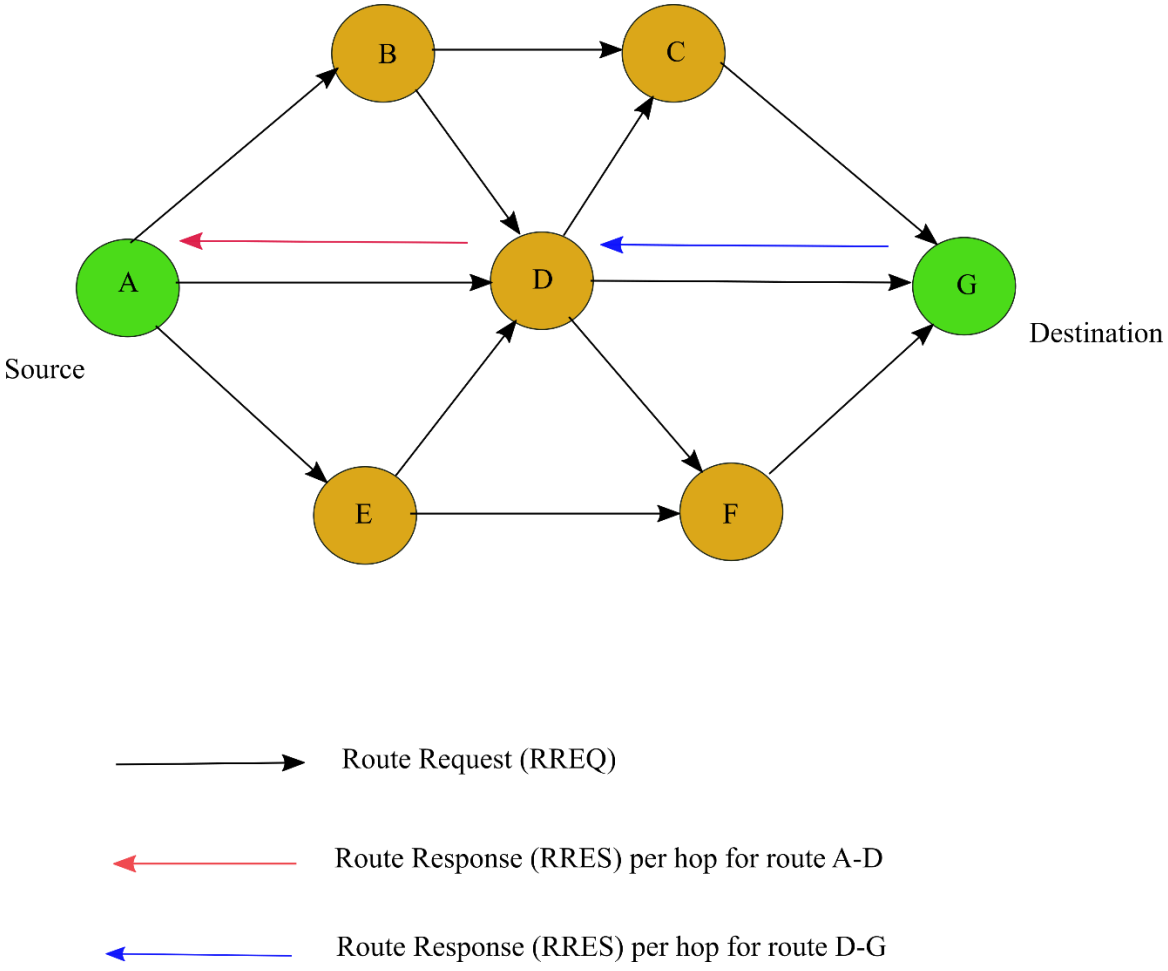

Figure 8-4: AODV routing scenario

To examine the comparative difference between the AODV and DSR routing protocols, the BS coverage radius determined in section 8.2 between 400m and 160m was used. The routing simulator applies a square routing boundary which is an equivalent routing area for the BS whose coverage radius is half of a side of the square boundary. A continuous variable packet rate between 0.25s and 0.5s was randomly chosen for each of the four simultaneous data sessions using 128bytes per UDP packet. This equates to a packet rate of 2 to 4 packets/s which will supply a UDP transport layer data speed in the range 2048bps to 4096bps per a mobile user session. To ensure the maximum hop count is achieved for accurate results, the *time to live* (TTL) in the IP header is set to 40 which is much greater than needed. The corresponding wireless parameters for the UK Mendip area used in this comparison are given in Table 8.2.

Table 8.2: UK wireless parameters settings

Parameter	Value
Frequency	706MHz
EIRP	4dBm
Modulation	IEEE802.11af 256QAM
WLAN Data Rate	54Mbit/s
Mobile Node Mobility	Random (1 to 20 m/s)
Bandwidth	8MHz

A decisive factor affecting the performance of a routing protocol is the number of intermediate routing nodes in the routing area. The assumption is to use accepted metrics (The World Bank, 2016) by considering the number of mobile routing devices in an area using a country's population per square Km and the number of mobile subscriptions per 100 people. If it is assumed there are 4 major operators managing TVWS devices and the mobile subscriber population P_{Pop} within a coverage area is uniformly distributed, then:

$$P_{Pop} = A_{network\ area} \cdot \left(\frac{M_{Km}}{4}\right) \cdot \left(\frac{S_{100}}{100}\right) \quad (8\text{-}6)$$

Where: M_{Km}= Country Population per Km^2

S_{100} = Mobile subscriptions per 100 people

P_{Pop} is calculated for each coverage radius and represents the total number of mobile nodes. Table 8.3 shows the P_{Pop} and corresponding coverage radius values for the UK Mendip area.

Table 8.3: Mobile population per coverage radius per operator

Mobile subscriber population (P_{Pop})	Coverage Radius (m)
42	400
36	370
32	350
27	320
24	300
19	270
16	250
13	220
11	200
9	180
7	160

The results in Table 8.3 are fed back into simulation parameters for the number of mobiles in a specific coverage radius for the AODV and DSR results shown Figure 8-3 and 8-4. The comparison between AODV and DSR used PER and packet delay has the key criteria highlight their differences.

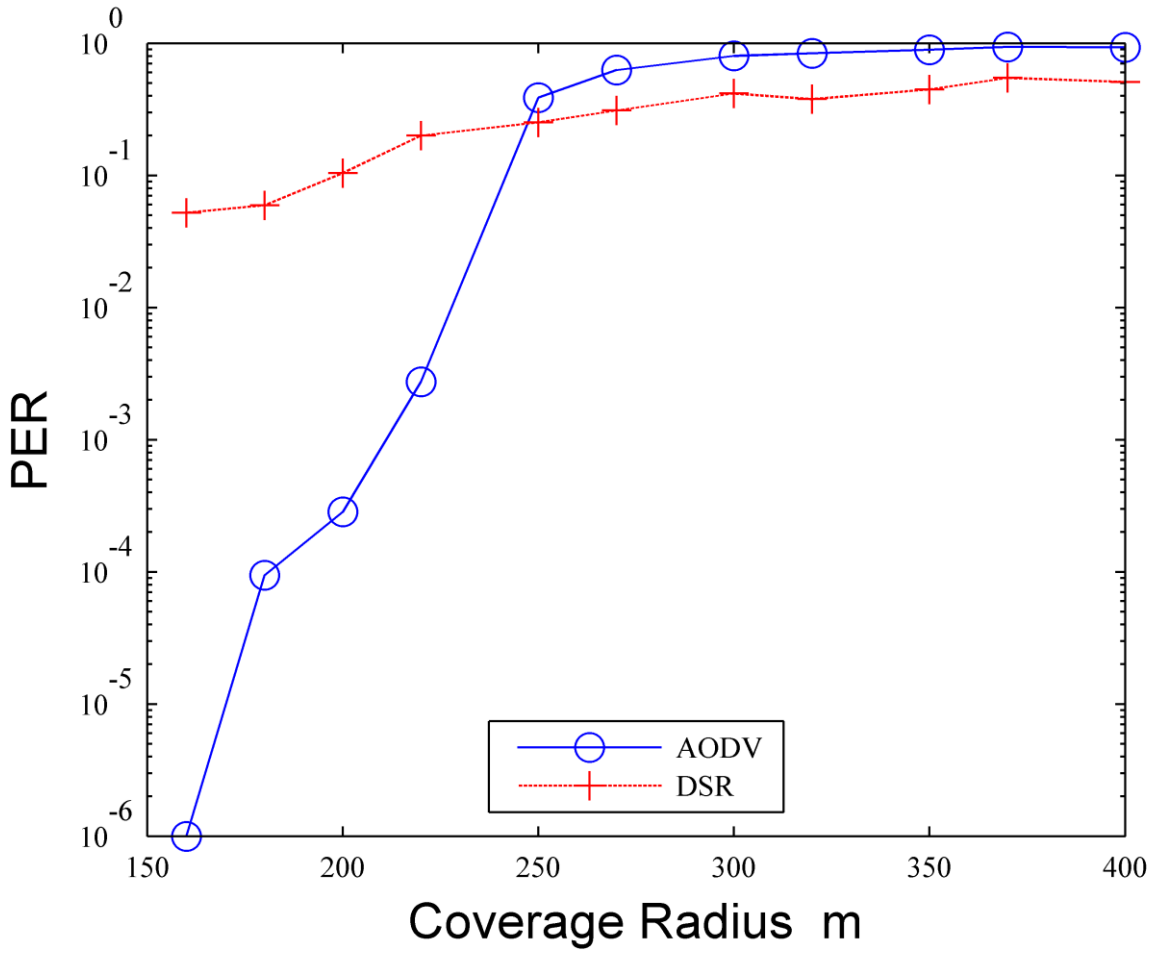

Figure 8-5: PER against Coverage Radius

Figure 8-5 evidently shows significant PER improvements for AODV with DSR failing to meet any of the PER requirements in the QCI standards specified in Table 8.1. The DSR poor performance results stems from the mobile nodes moving in an irregular manner so when a DSR route is established, the end-to-end route has changed. This has the effect of reducing the SNR on certain links in the DSR route which have changed due to node movement to the point where the route is not workable and the PER is very high. In the AODV case the packet is sent to the nearest routable mobile then that in turn sends the packet to the nearest routable mobile and so on until it reaches the BS so is more resilient to route changes. The PER in the AODV scenario increases with coverage radii which due to the hop distance increasing and so SNR increases even when the mobile population increases. This can be explained by when the coverage radius is doubled, the coverage area is increased by more than double so the distance between mobiles are likely to increase and so SNR.

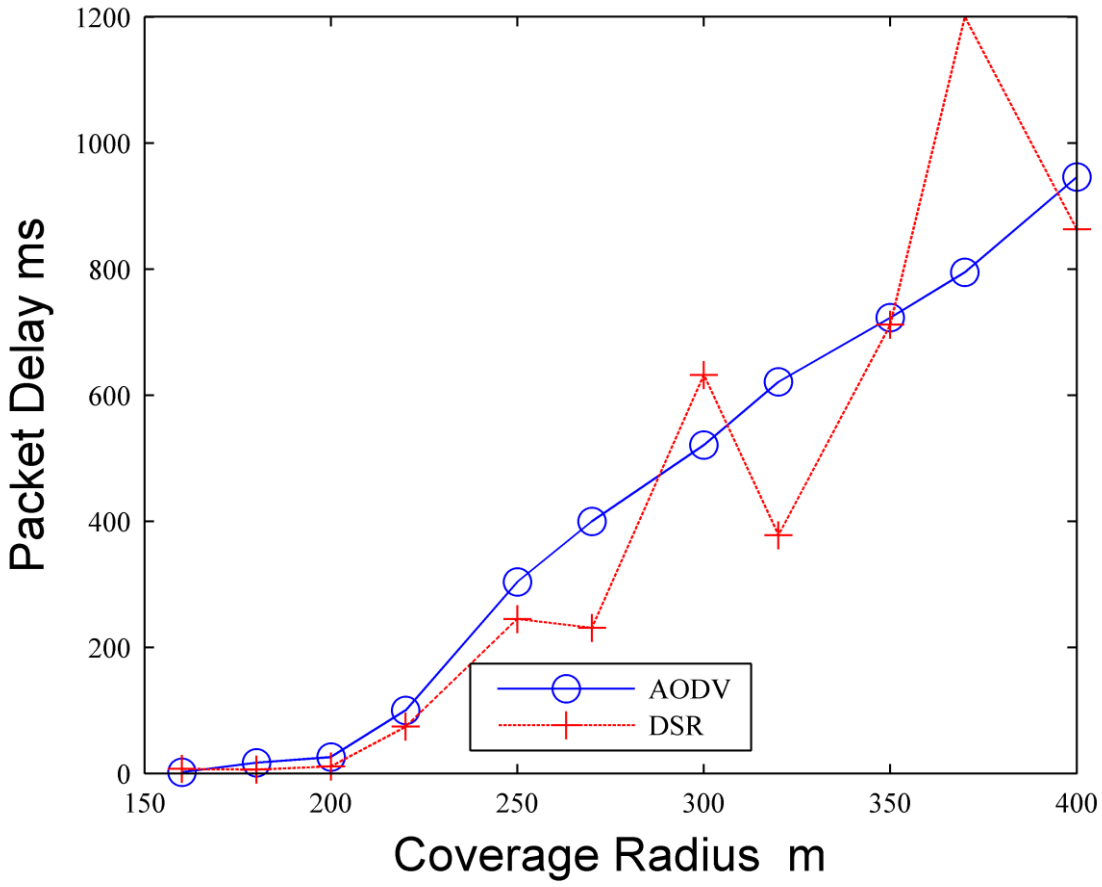

Figure 8-6: Packet delay against Coverage Radius

In evaluating the corresponding packet delay results for AODV and DSR in Figure 8-6, there is no significant difference between the protocols up to a coverage radius of 250m, however the DSR behaviour then becomes very erratic. The reason for this is that DSR uses source routing, so a packet is only transmitted when a route has been found to the destination, while in the interim, intermediate nodes can move and the final route be compromised. In contrast, AODV transmits the packet on a hop-by-hop basis with the routing tables in the intermediate nodes being updated as a packet progresses towards the destination.

In evaluating the respective PER and packet delay results, a general conclusion is that AODV delivers a much lower PER for a similar packet delay compared to DSR, thus justifying its choice as the routing protocol used to uphold the QCI QoS requirements (see Table 8.1). The next several sections will investigate the criteria which can be applied to optimise the AODV protocol for different QCI settings.

8.3.2 UK Case Study

The aim here is to optimise the coverage radius for the various QCI levels in Table 8.1 for the UK Mendip area case study. The wireless parameter values given in Table 8.2 are again used, while the assorted UDP and IP parameter values are shown in Table 8.4.

Table 8.4: UDP Parameters

Number of concurrent data sessions	UDP Maximum Transmission Unit (MTU) (bytes)	Application Data Rate per Data Session (kbit/s)	UDP Packet Rate (packets/s)	TTL
4	128	32	31.25	40
4	256	32	15.625	40
4	512	32	7.8125	40
4	1024	32	3.90625	40
4	1500	32	2.6667	40

The UDP parameters will be used in the coverage radii simulation model shown later but first the mobile population needs to also be known for these simulations. Using (8-6), the corresponding mobile subscriber population can be calculated for different coverage radii from the BS as displayed in Table 8.5.

Table 8.5: UK Mobile Subscriber Population per Mobile Operator

Coverage Radius (m)	Mobile Subscriber population
225	13
200	11
180	9
160	7
140	5
120	4
100	3

To assess the network QoS constraints, 4 concurrent data sessions were established, 1 per mobile node using the mobile population in Table 8.5. Each data session was driven by a 32kbit/s application (Nokia, 2015) that supported the *session initiation protocol* (SIP), *voice over LTE* (VoLTE) and *over the top* (OTT) *voice over* IP (VoIP) client applications, together with either an internet browsing or email application running in parallel. This particular set-up of 4 mobile nodes, was chosen to ensure the network was extended to rigorously demonstrate its behaviour against the QCI specification in Table 8.1. To optimise performance, various UDP MTU packet lengths were used to reflect differing effects like packet loss and delay and also to avoid packet fragmentation. The normal Ethernet MTU packet length is 1500bytes and if the network endpoints are using Ethernet MTU sizes, 1500bytes is the best MTU size as otherwise wireless propagation effects may be affected by increased packet error or delay, leading to a detrimental impact on the end user. There is an optimisation point where the MTU size is optimised for wireless performance so it is a balance of smaller packets to achieve lower packet error rate and larger packets to avoid fragmentation. The graphs in Figures 8-5 and 8-6 show the PER and packet delay parameters respectively reveal how the network can maximise the BS coverage radius in comparison to QCI standards (see Table 8.1).

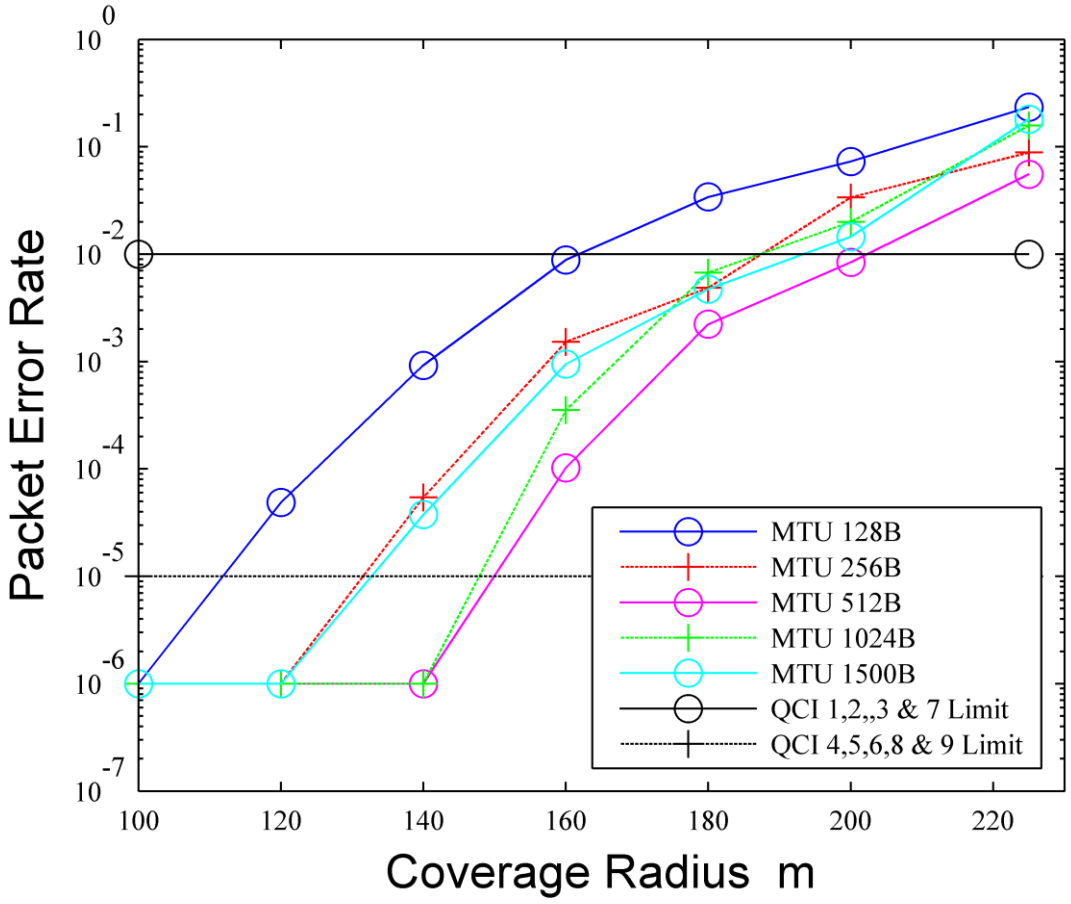

Figure 8-7: UK Packet Error Rate Results

Figure 8-7 shows the PER and various QCI categories for different MTU sizes, with the two horizontal lines being the 10^{-2} and 10^{-5} PER thresholds. It can be seen that the best performing MTU packet size is 512bytes, which is able to support QCI 1, 2, 3 and 7 up to 200m away from the BS and QCI 4, 5, 6, 8 and 9 up to 150m away from the BS. For the 128byte MTU size, more packets have to be transmitted to achieve the overall data rate which means an increased probability of a packet being transmitted with a low SNR thereby increasing the PER as shown in Figure 8-7. In contrast, the 1500byte MTU, incurs fragmentation due to fast changing node positions in the area during the time-frame of one packet, leading to errors mid-packet and increased PER. The MTU size of 512bytes represents a pragmatic solution in terms of packet size, so the probability of errors is reduced by minimising the number of packets sent, while the packet duration is small enough compared to node movement to ensure a minimal PER due to route changes in mid-packet. PER alone however, is insufficient to assess the quality of a routing system, since packet

delay is also considered in the QCI standards. The corresponding set of packet delay verses coverage responses are shown in Figure 8-8 for the same set of MTU sizes and QCI categories. Again, the horizontal plots are the various delay thresholds for specific QCI categories.

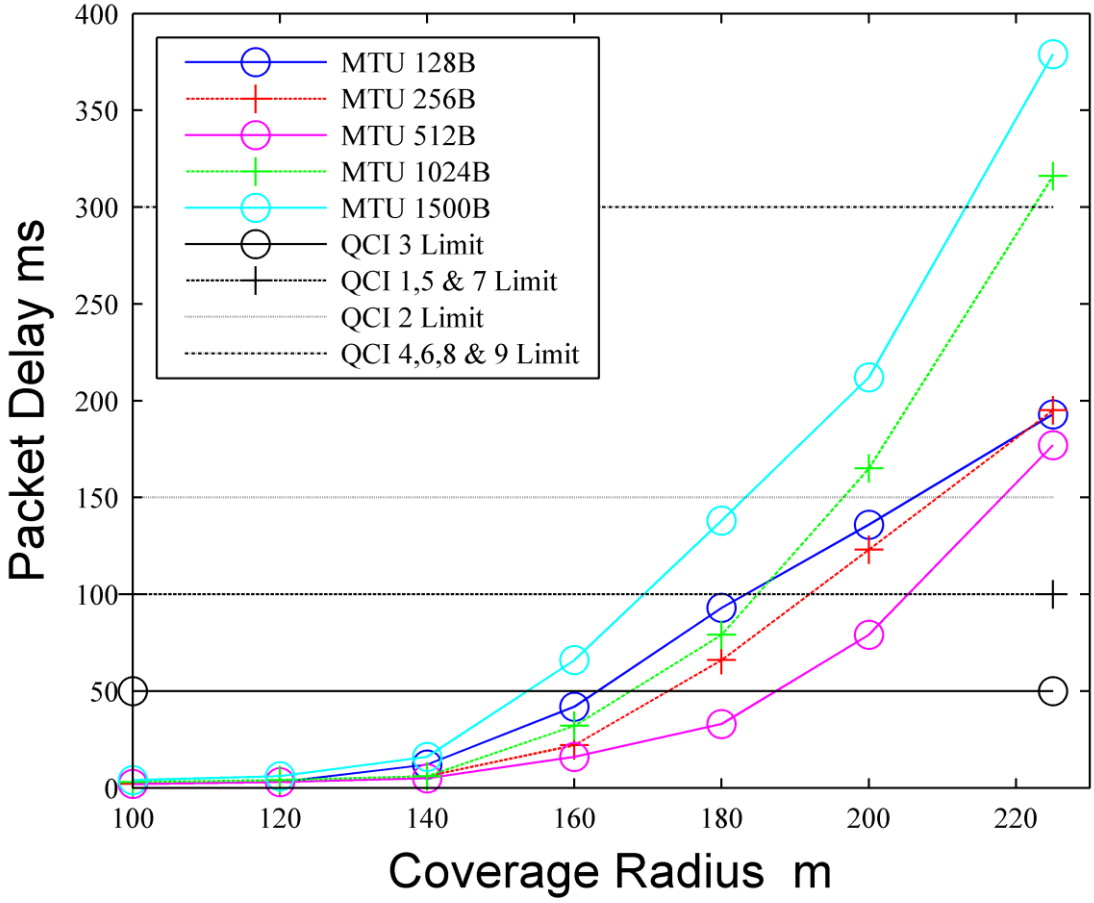

Figure 8-8: UK Packet Delay Results

The results again confirm an MTU size of 512 bytes outperforms all other MTU sizes so this is the best choice for any IEEE 802.11af based wireless network. For a MTU size of 128byte due to a smaller packet size then the packet processing time shall increase and so shall packet delay. In the 1500byte case due to the packet rate being lower compared to the node movement then a route integrity is impacted causing large PER. Table 8.6 correlates the QCI category against the shortest distance from the BS for this MTU size considering PER and packet delay.

Table 8.6: UK QCI against supported distance from BS for a MTU of 512bytes

QCI Category	Distance from BS in m
1	200
2	200
3	190
4	150
5	150
6	150
7	200
8	150
9	150

To help interpret these results, a further experiment was carried out to determine the maximum hop count for QCI 1, 2 and 7 that can support services at the maximum distance of 200m from the BS using the above experimental set-up with an MTU size of 512bytes and coverage radius of 200m. The simulation is repeated with TTL decremented by 1 during each simulation run until the PER increases from that for 200m and MTU size 512bytes in Figure 8-6. When this happens the minimum hop count is the TTL+1 which was found to be 23 which indicates this is the number of hops at which any increase will not result in any decrease in PER.

The next section performs the same analysis for the US scenario.

8.3.3 US Case Study

The major difference between the UK and US case studies is the wireless specification defined by FCC (Nekovee, 2012), with the mobile transmit power being 16dBm and DTT

bandwidth of 6MHz. The wireless parameters for the US based scenario are specified Table 8.7.

Table 8.7: US wireless parameter settings

Parameter	Value
Frequency	629MHz
EIRP	16dBm
Modulation	IEEE802.11af 256QAM
WLAN Data Rate	54Mbit/s
Mobile Node Mobility	Random (1 to 20 m/s)
Bandwidth	6MHz

The same UDP setup is used as in the UK case study (Table 8.3) with the US mobile subscriber population per coverage radius per operator from (8-6) given in Table 8.8

Table 8.8: US Mobile Subscriber Population per Mobile Operator

Coverage Radius (m)	Mobile Subscriber population
517	8
470	7
450	6
400	5
370	4
350	4
300	3

Using this configuration, the corresponding packet error rate and packet delay curves were constructed for the US case study as shown in Figures 8-9 and 8-10 respectively.

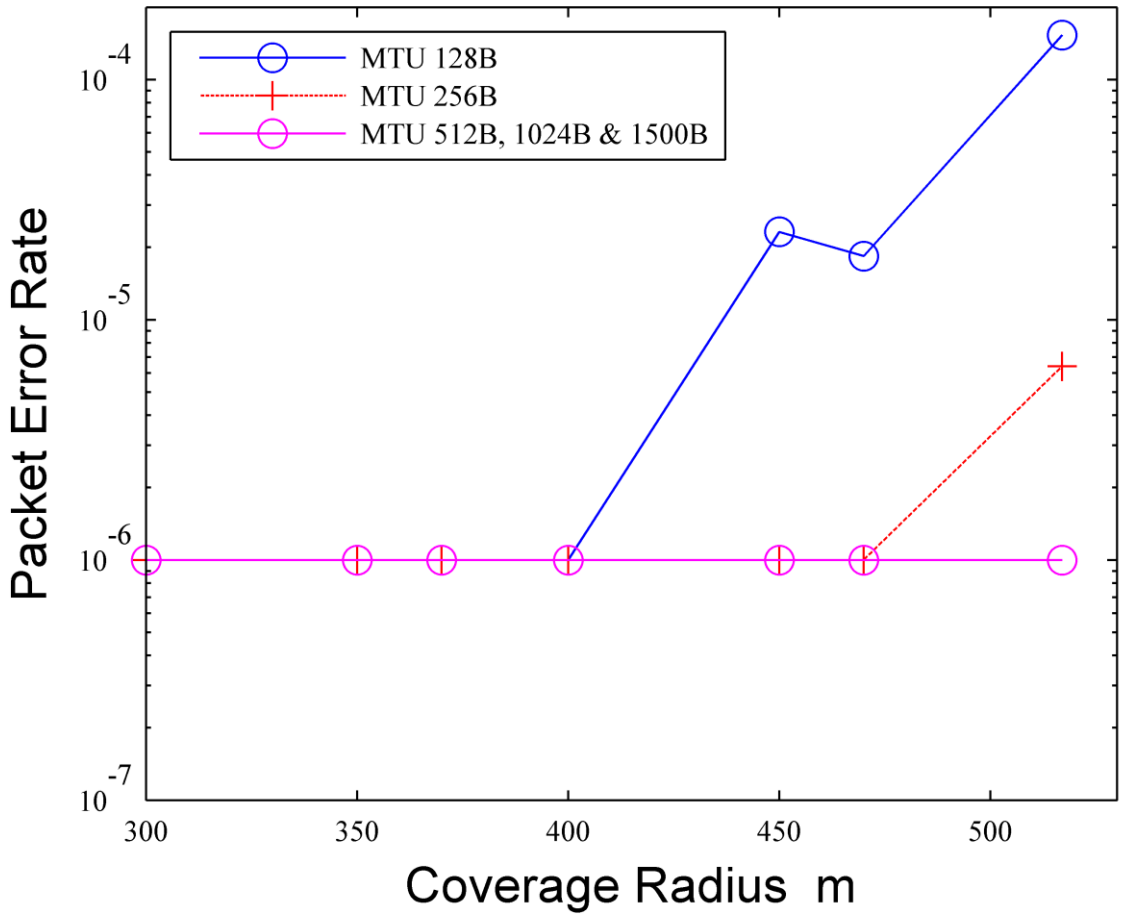

Figure 8-9: US PER versus coverage radius results

Figure 8-9 reveals that MTU sizes of 512, 1024 and 1500 bytes all achieve a PER of $1x10^{-6}$ across the full range of distances considered, while 256 and 128 bytes only achieve this PER value at coverage distance up to 400m and 470m respectively. Again, as in the UK scenario the MTU 128byte size increases the probability of error when more packets are sent. However, in contrast to the UK, the difference with the US scenario is that for larger MTU sizes, the effect of packet fragmentation is mitigated because higher SU RF transmit power is used which compensates for any node movement.

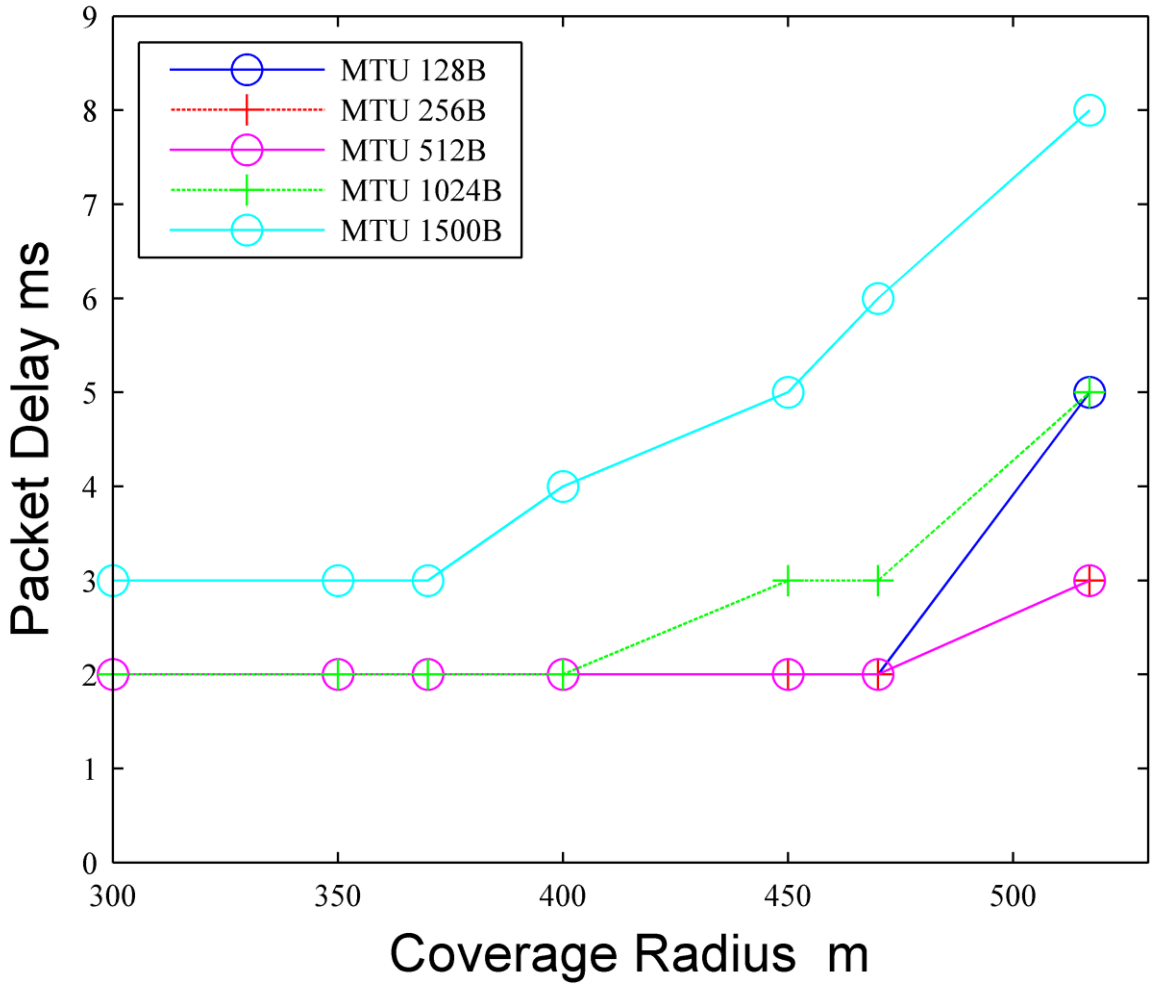

Figure 8-10: US packet delay versus coverage radius results

The corresponding packet delay results in Figure 8-10 show that all delays follow the same pattern as the UK scenario except 256byte and 512bytes achieve the same results and are well within the QCI limits for all categories due to the increased SU RF power, so this is not the deciding factor as to whether a specific category can be supported. Since from a PER perspective, MTU sizes of 512, 1024 and 1500 bytes are all able to support QCI categories up to 517m, which is the full coverage range of the BS, and given an MTU of 512bytes consistently achieved both the lowest PER and packet delay, this value was chosen for determining the maximum hop count for the US case study. Using the same process as for UK to determine the maximum hop count which was found to be 7.

8.3.4 Results Discussion

One of the key observations between the UK and US case study results, is that the PER and packet delay are much more critical in influencing performance for the UK scenario. This can be attributed in the US scenario by the FCC setting a mobile EIRP value ≈16 times greater than that of the UK. The corollary of this is that a mobile node is able to reach a BS in far fewer hops, just 7, compared with 23 hops for the UK scenario i.e., a saving of more than 66%.

8.4 QCI QoS maximisation using AODV

Evidently the QCI QoS limits will vary depending on the set EIRP values and the specific QCI service being utilised. One strategy would be to simply allow a mobile to use any QCI service within the BS coverage range and see whether it succeeds or fails. Such an approach would obviously work in the US case study, but not for the UK, where the furthest QCI service has a range of only half that of the BS capture range, so any mobile further away than 200m (Table 8.5) would receive no QoS at all. The situation can become even worse if we consider for example, QCI 4 and QCI 7, whose maximum distances from the BS are 150m and 200m respectively. If the QCI 4 mobile tries to initiate a data session from a distance of 170m, then the network shall attempt to route packets until it reaches the TTL limit, whereupon it will fail. If at the same time the QCI 7 mobile also initiates a data session, then because QCI 4 has higher priority (Table 8.1), its packets will be higher in the routing queue than QCI 7 packets, so diverting vital routing resources away from QCI 7. This means a QCI 4 packet which fails will directly impact the QoS of a QCI 7 packet which would normally be successfully transmitted.

The proposed innovative strategy is to only to allow access if a mobile node lies within the maximum distance from the BS for the specific QCI category of the intended data traffic. Furthermore, to eliminate rogue packets within the network, the TTL value is set to the

maximum hop count for the furthest QCI service in the particular country under consideration.

8.4.1 Accessing heterogeneous networks

Heterogeneous access networks allow mobile operators to move traffic from the macro-cellular network, where the capacity constraints are most acute, to shorter-range WLAN and micro-cells i.e., femto/picocell networks connected over a variety of backhaul connections. This will alleviate the issue in the UK case study where TVWS services using IEEE802.11af only use a portion of the BS coverage area. However, this increases the complexity of mobile connectivity due to the mix of technologies in both the air interface, backhaul and core, which is further compounded by complicated inter-operator roaming agreements. As all the mobile population calculations are based upon individual mobile operators, the issue of inter-operator roaming is beyond the scope of this chapter.

The overall heterogeneous network is shown in Figure 8-9 from (Alcatel-Lucent and BT, 2013) with IEEE 802.11 included has a technology that is supported so the extension of network to include IEEE 802.11af is a simple integration process.

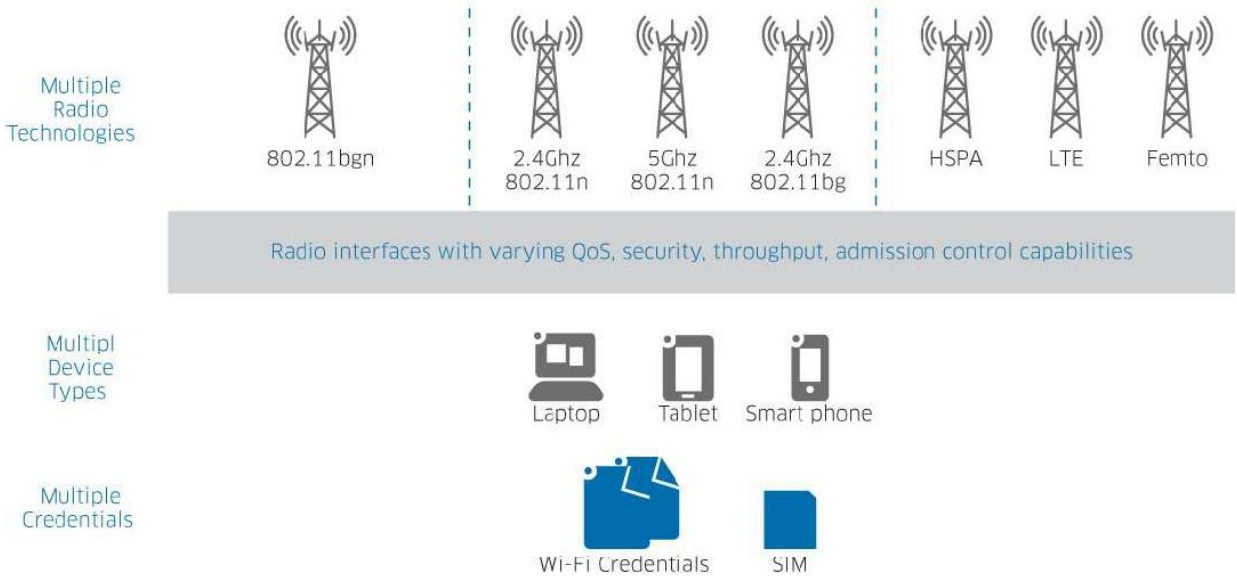

Figure 8-11: An example of a heterogeneous network (Alcatel-Lucent and BT, 2013)

Figure 8-11 shows an infrastructure which is being adopted by many mobile operators in how they can lever improved customer experience by adopting a flexible technology access tailored to the network condition and the subscriber requirements.

The network now has to make an informed choice concerning the type of access technology to be used. A new function introduced by the 3GPP standards (3GPP, 2016) is the *Access Network Discovery and Selection Function* (ANDSF) along LTE interface function such as S2a and S14. When a session request is received from an UE through either an UMTS or LTE network, ANDSF decides the most efficient access technology to allocate to the UE.

The heterogeneous network allows a call request from one technology and a decision from the ANDSF to which the technology the call shall be established on. Figure 8-10 shows the information and traffic flow for a heterogeneous network with an initial UE request via LTE over an S14 interface, which is normally the default technology as it has a greater range than WLAN. The request from the UE should detail the QCI category required from the UE application and GPS location data, which is sent to the ANDSF where the access rules are executed. These rules determine which access technology to use and allocate the nearest resource ID for the UE to access. In the particular WLAN example in Figure 8-12, this would be the *service set identifier* (SSID) with which the UE sets up a traffic connection using the IEEE802.11af parameters for the Evolved Packet Core (ePC), which is the LTE backhaul using interface S2a.

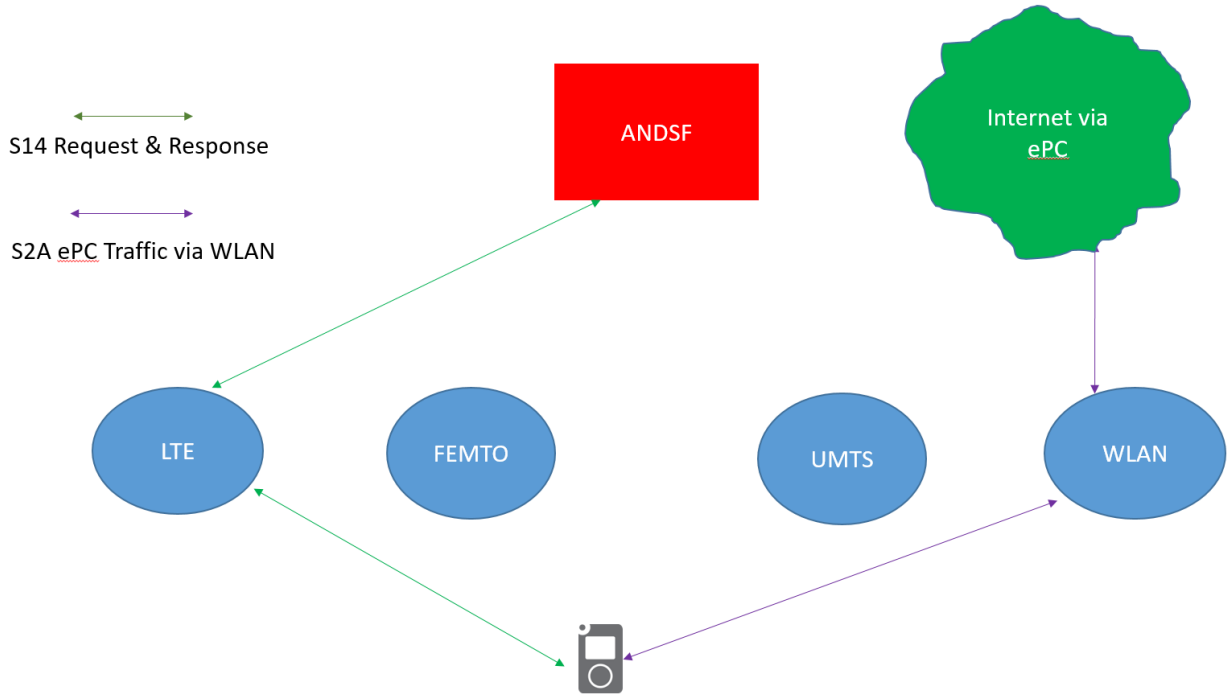

Figure 8-12: Heterogeneous Network using ANDSF access discovery (3GPP TS, 2016)

The ANDSF policy algorithm to support IEEE802.11af and also the QCI QoS categories discussed in Section 8.3.2 and 8.3.3 will now be explained. It is assumed that the ANDSF function being standardised in (3GPP, 2016) will be the heterogeneous mechanism used for technology selection.

The policy algorithm in the ANDSF to support the routing results given earlier in this chapter to support the QoS QCI categories is shown in next section.

8.4.2 IEEE802.11af ANDSF policy algorithm

The ANDSF policy algorithm has been validated upon both the UK and US case studies in sections 8.3.2 and 8.3.3 to implement an IEEE802.11af network using AODV as the routing protocol. The assorted control parameters are defined in Table 8.8, while the complete pseudo-code for the ANDSF IEEE802.11af access algorithm is presented in algorithm 8.1.

Table 8.9: ANDSF access control parameters

λ_1	Longitude of IEEE802.11af BS (radians)
Ψ_1	Latitude of IEEE802.11af BS (radians)
λ_2	Longitude of mobile UE in connection request from mobile UE (radians)
Ψ_2	Latitude of mobile UE in connection request from mobile UE (radians)
QCI	QCI category from mobile UE
D_{QCI}	Maximum distance from BS at which QCI category can be supported
N_{SSID}	SSID of BS identified by ANDSF (Algorithm 8.1)
N_{TTL}	Time-to-Live (TTL)
N_{MTU}	MTU Size (bytes)
R	Earths Radius in km (6371)

Algorithm 8.1: Pseudo-code representation for ANDSF IEEE802.11af access

1: **Inputs:** $\lambda_1, \Psi_1, \lambda_2, \Psi_2, QCI, D_{QCI}, R$
Outputs: $N_{SSID}, N_{TTL}, N_{MTU}$
2: $diff\lambda = \lambda_2 - \lambda_1$
3: $diff\varphi = \varphi_2 - \varphi_1$
4: $a = \left(\sin\left(\frac{diff\varphi}{2}\right)\right)^2 + \cos\varphi_1 \cdot \cos\varphi_2 \cdot \left(\sin\left(\frac{diff\lambda}{2}\right)\right)^2$
5: $c = 2 \cdot \tan^{-1}(2\,(\sqrt{a}\,, \sqrt{(1-a)}))$
6: $d = R \cdot c$
7: **IF** $d > D_{QCI}$ **THEN**
8: **No IEEE802.11af Access**
9: **ELSE**
10: **IEEE802.11af Access Allowed**
11: N_{SSID} **= SSID of BS Identified**
12: N_{TTL} **= TTL for country**
13: N_{MTU} **= MTU (512bytes)**
14: **END IF**

Steps 1-6 implement the Haversine formula (van Brummelen, 2013) which calculates distance between two GPS co-ordinates, while Steps 7-14 compare this distance with the maximum coverage distance from the BS for the specified QCI category, defined in sections 8.3.2 and 8.3.3. If it is greater than the maximum, access is denied over an IEEE802.11af network, otherwise access is allowed and the SSID along with the transport and IP layer parameters TTL and MTU size are sent to the mobile UE. By implementing these parameters, the results in sections 8.3.2 and 8.3.3 are adhered to, so produce the same results for the distance from the BS which is provided by the GPS co-ordinates given by the BS and

mobile. In achieving this the TVWS SU mobile shall not try to transmit a packet which will fail and hence absorb resource which will impact packets which should succeed.

8.5 Summary

This chapter has critically assessed the two MANET routing protocols AODV and DSR for use with the WLAN standard for TVWS, IEEE802.11af, and AODV found to be consistently superior from a PER performance perspective.

Using both UK and US scenarios, mobile population values were calculated, and PER and packet delay performance measures determined that generate the maximum distance from the BS which can be support by a specific QCI category.

Finally, a new ANDSF-based policy algorithm has been developed to implement a IEEE802.11af network using AODV routing in a heterogeneous network. The next section examines potential future research which can use the existing access framework presented in this thesis.

Chapter 9

9. FUTURE WORK

9.1 Introduction

The new cognitive TVWS access framework embraces a number of original contributions relating especially to exploiting the deployment of DTT frequency patterns, addressing the hidden node problem, effective PU interference management and the inherent SU RF power imbalance. It also affords a number of fertile openings for new research to be initiated. Some potential avenues which have been identified are discussed in the following sections.

9.2 Extending the TVWS Access Framework

One area for development in the new TVWS access framework, is to extend into other applications domains, such as radar, the unique way DTT channel patterns are exploited to enable spectrum to be innovatively re-used. The main difference between radar and TVWS is that radar SU spectrum-hole access opportunities occur on a temporal rather than purely a spectral basis. This could be implemented by using a *Multitaper Estimator method* (MTM) with the input radar signal being of sufficiently short frames that they can be considered as quasi-stationary but long enough to produce an accurate spectral estimate. This requires a rigorous investigation into enabling SU spectrum access with strict time-duration constraints, while still crucially upholding PU interference regulatory requirements.

The hidden node and interference management framework solutions are also sufficiently generic to be applicable to SU access of any licensed spectrum, so the underlying technology is transferable to other cognitive radio access applications, provided the diffraction parameters of the PU and SU access modulation schemes and respective RF powers are

known *a priori*. Similarly, the interference management framework is also globally applicable to any cognitive-based access system, in enabling lower overall interference within a locality. This in turn, will lead to improved SU access bandwidth availability and QoS provision.

9.3 TVWS SU Channel Bonding

If the standard IEEE 802.11af can incorporate non-contiguous channels (Gao et al, 2016) then greater bandwidth be levered so greater efficiency for TVWS access framework. This poses a great research opportunity which can deliver a large dividend. This research is transferrable to other spectrum opportunities not specifically TVWS. This could be implemented by using Non-Continuous OFDM (NC-OFDM) methods outlined in (Gao et al, 2016) but at the moment it has not been adopted for the IEEE 802.11af standard so needs research to raise the momentum in this area to be adopted.

9.4 Multi-Operator Heterogeneous Network Environments

Heterogeneous network environments were introduced in chapter 8, as a means of accessing different technologies to meet user requirements. One underlying assumption was that the available TVWS spectrum had to be shared between multiple mobile operators, with each setting up a separate WLAN. An interesting alternative strategy would be to critically investigate, an open WLAN arrangement, involving perhaps some commercial agreements between operators for resource sharing (Alcatel-Lucent and BT, 2013). Multi-operator heterogeneous networks have the advantage that any operator mobile could route packets so increasing the number of mobiles in a routing area because it is not restricted to one operator. This would have the effect of increasing the mobile routing population in an area, so reducing the PER and increasing the user area. A major research question for this environment however, would be how best to create a cross-operator heterogeneous framework that can

be easily implemented on existing platforms, including potentially, the new TVWS access framework.

9.5 *SF* Parameter

In the GEDA algorithm, the SF parameter is applied to decide if B_{Sec} is employed to determine whether a channel is occupied by a PU. SF is defined as the ratio of the RF energy of the highest DTT frequency to the lowest in the country of interest, which effectively means it defines a margin on the lowest detected PU channel equal to the energy difference across the DTT spectrum. However, in practice setting the reference to the lowest detected PU channel, potentially makes the energy threshold for triggering B_{Sec} very conservative and much lower than actually needs be, with the corresponding influence on increasing the likelihood of false detection because a larger number of channels have to be scanned than is actually necessary.

One possible option would be to examine relaxing the existing fixed threshold by introducing an adaptive trigger threshold derived in real-time from the sensor measurements. This would have the benefit of directly lowering the number of times B_{Sec} has to be applied in the sensing process.

9.6 Summary

From the future work presented all of them refer to the generic SU spectrum access except for the *SF* adaptation. The new work proposed on the SU access framework for other spectrum opportunities is a priority because it means that even more spectrum is released for SU access along with multivendor heterogeneous networks to allow sharing of the SU bandwidth. However, with the non-contiguous channel bonding, more efficient use of the acquired bandwidth in TVWS or other spectrum opportunities so could have a major impact.

10. CONCLUSION

With the unprecedented increase in mobile data traffic, the requirement for greater bandwidth to accommodate this increase is a major issue for mobile operators. *TV White Space* (TVWS) affords the prospect to enhance existing licensed spectrum by exploiting unused resources, due to their inherent static properties, as *primary user* (PU) channels do not change in a particular location. While this relaxes the requirement for rapid PU update as channels change only on a spatial rather than temporal basis, there are still a number of important obstacles to TVWS adoption. Among the challenges are accurate and reliable PU detection, the omnipresent hidden node problem and *secondary user* (SU) interference management to ensure *Quality of Service* (*QoS*) provision is always maintained for the PU.

The solution currently adopted by the regulatory authorities for *dynamic spectrum access* (DSA) decisions, is to use a static database. While this is a simple DSA implementation, it involves manual updating and the lack of real-time information means accuracy can become compromised. Another limitation is the inefficient usage of TVWS spectrum, which though somewhat addressed by the new WLAN standard, IEEE802.11af, which integrates TVWS into the IEEE802.11 standards, still leaves many challenges unresolved such as, the asymmetric RF power allocations between a SU base station and mobile device, which significantly limits SU mobile coverage. This was the motivation for this research.

This thesis has presented a new cognitive TVWS access framework which exploits the unique way *digital terrestrial TV* (DTT) channels are deployed in different geographical areas to accurately detect the presence of a PU. A new DSA model transforms an energy detector into a feature sensor to achieve significant sensing improvements compared to

existing DTT PU detection techniques. By incorporating a robust interference management scheme, the hidden node scenario is resolved and a practical sensing solution for SU networks formulated. Critical result analysis confirms the superior performance of the new framework in releasing extra valuable resources for SU accessing TVWS to secure notable *QoS* improvements for SU, as demonstrated in two different DTT case studies.

The new cognitive TVWS access framework offers a series of innovative features and benefits in terms of PU channel detection, interference management and efficient access mechanisms for SU to leverage TVWS resources for enhanced QoS provision. In comparison to current TVWS solutions, the new access framework represents a generic, flexible and practical platform for efficiently initiating TVWS SU networks, while crucially upholding compliance with current regulatory requirements in the country of interest.

By implementing these innovative features, a self-managing framework has been presented which meets the research goals outlined in chapter 1 of this thesis and importantly, the new cognitive TVWS access framework is transferable to alternative DTT deployments in other countries. Although simulation was used to verify the framework, the simulation models themselves were verified against real world data so confidence is high that the framework would work in a practical physical network.

The new TVWS framework makes four original contributions to the unlicensed DSA domain:

i) PU detection is accomplished by introducing a new *generalised enhanced detection algorithm* (GEDA) which exploits the unique deployment properties of DTT frequencies in different countries. GEDA uses an *enhanced detection algorithm* (EDA) based around a fuzzy logic inference model to convert a basic energy detector into a feature detector to accurately resolve the uncertain nature

of DTT signals. This is achieved by sequentially scanning a number of adjacent frequencies either side of the DTT channel of interest, with the scanning range adaptively determined to uphold PU detection requirements of both OFCOM and FCC. The performance of GEDA has been critically evaluated in both UK and USA scenarios to corroborate its agility to dynamically adapt to different DTT deployment rules.

ii) A novel *keep out contour* is established as part of an original PU interference management scheme to enhance the robustness of GEDA. This contour reflects the DTT diffraction conditions and introduces a margin on the service coverage area to deliver a solution to the hidden node problem. Results show when the peak PU transmit powers are used in sensing, the *keep out contour* gives superior PU detection performance and eliminates PU interference in the presence of a hidden node.

iii) A new SU resource strategy has been developed that uses the *keep out contour* together with a *sterilisation index* (SI) to maximise the available TVWS resources for SU access at any location. The SI maps sterilised DTT channels from being used in a locality, with analysis revealing the new framework releases a significant amount of bandwidth for SU networks in a single location, equivalent to a factor of five improvement in the UK, and up to seven in the US scenario, for a single 20MHz LTE system. This is manifest as enhanced *QoS* provision for SU accessing TVWS. These findings are congruent with alternative TVWS access studies that use physical RF surveys, though these incur much more resources in determining the available SU bandwidth.

iv) The final contribution addresses how an IEEE 802.11af compliant network can be implemented using MANET routing methods within heterogeneous network environments. Since regulators allocate lower SU mobile powers to achieve an equidistant coverage in the reverse link compared to the forward link, some form

of innovative routing is required in the reverse link. The new access framework accommodates this by applying a routing mechanism in the heterogeneous network in the form of an algorithm. A new cross-layer routing algorithm has been developed to enable TVWS access decisions to be made within a heterogeneous network based on user QoS requirements and the distance of an SU mobile from the base station. It crucially overcomes the inherent imbalance of SU transmit RF powers in the new TVWS IEEE 802.22, OFCOM and FCC standards, by enabling lower SU mobile powers and thereby reduced PU interference, while concomitantly maintaining the coverage radius, by incorporating a multi-hop MANET routing technique in the reverse network link.

The new access framework offers a set of innovative features from PU channel detection, interference management to efficient access to TVWS resources, which in comparison to existing solutions, is a flexible and practical platform for efficiently initiating TVWS SU networks. It crucially maintains compliance with regulatory requirements and is transferable to alternative DTT deployments in other countries, with results being verified for real world data to validate its significance as a viable DSA solution for TVWS. The major obstacle to sensing solutions is the hidden node issue which there is a proposed solution from this thesis but it needs extensive testing in live networks to enable regulators to agree its use.

APPENDIX

Appendix A: Detection Probability Algorithm

```
%--------------------------------------------------------------------------
'M-File of Detection Probability by John Martin';
%--------------------------------------------------------------------------
'Setting up of basic parameters';
%--------------------------------------------------------------------------
paramNameValStruct.SimulationMode ='rapid';
paramNameValStruct.AbsTol = '1e-5';
paramNameValStruct.SaveState = 'on';
paramNameValStruct.StateSaveName ='xoutNew';%enabling state output
paramNameValStruct.SaveOutput = 'on';
paramNameValStruct.OutputSaveName ='youtNew';%enabling output to workspace
paramNameValStruct.SaveOutput = 'on';
paramNameValStruct.OutputSaveName ='tout';%enabling output to workspace
load RegionCh.txt
%--------------------------------------------------------------------------
y=8;% Spectrum Spread
Bx=[-4 -3 -2 -1 1 2 3 4];% Setting the values of Spectrum Spread +/- 1 to 8
D=RegionCh;% Ch allocation for all 22 regions
R=[0 0 0 0 0 0 0 0 0 0;0 0 0 0 0 0 0 0 0 0;0 0 0 0 0 0 0 0 0 0;0 0 0 0 0 0 0 0 0 0;0 0 0 0 0 0 0 0 0 0;0 0 0 0 0 0 0 0 0 0;
0 0 0 0 0 0 0 0 0 0;0 0 0 0 0 0 0 0 0 0;0 0 0 0 0 0 0 0 0 0;0 0 0 0 0 0 0 0 0 0;0 0 0 0 0 0 0 0 0 0;0 0 0 0 0 0 0 0 0 0;
0 0 0 0 0 0 0 0 0 0;0 0 0 0 0 0 0 0 0 0;0 0 0 0 0 0 0 0 0 0;0 0 0 0 0 0 0 0 0 0;0 0 0 0 0 0 0 0 0 0;0 0 0 0 0 0 0 0 0 0;
0 0 0 0 0 0 0 0 0 0;0 0 0 0 0 0 0 0 0 0;0 0 0 0 0 0 0 0 0 0;0 0 0 0 0 0 0 0 0 0;0 0 0 0 0 0 0 0 0 0;0 0 0 0 0 0 0 0 0 0];% Results
k=1;
j=1;
e=1;
%--------------------------------------------------------------------------
'Calculating Number of Channels in each location ';
%--------------------------------------------------------------------------
w=0;
for m=1:22
   w=0;
for k=1:10;% iteration of next Ch next Bx
   if D(m,k)>0;
   w=w+1;
   end
N(m)=w;
end
end
%--------------------------------------------------------------------------
'Testing for Channel proximity';
%--------------------------------------------------------------------------
```

```
for m=1:22
for k=1:10;% iteration of next Ch next Bx

for e=1:y;% Iterations of Spectrum spread Bx
for j=1:10 ;% Iterations of next Ch for same Bx
   g=D(m,k)+Bx(e);
   f=D(m,j);
   if f==g;
   R(m,k)=R(m,k)+1;
   end
end
end
end
end

%--------------------------------------------------------------------------
z=1;%EDA detection for all Ch except 58 through the Adjacent Ch Interference
yy=1;%EDA detection for Ch 58 through the Adjacent Ch Interference
l=0;%EDA detection for all Ch through the Adjacent Ch Interference with no Ch in
proximityz=1;%EDA detection for all Ch except 58 through the Adjacent Ch Interferences
k=1;
m=1;
e=1;
%--------------------------------------------------------------------------
'Probability Calculation';
%--------------------------------------------------------------------------
for m=1:22
for k=1:10;% iteration of next Ch next Bx
   if R(m,k)>0
   R(m,k)=1;
   end
end
end
C=z;% Probability of a site Ch being detected by RF ED for a range of Adjacent Ch Noise
G=R*C;%Muliply Site matrix by RF ED detection Probability
for n=1:22
if G(n,3)>0
G(n,3)=yy;
end
end
m=1;
k=1;
for m=1:22
for k=1:10;% iteration of next Ch next Bx
   if G(m,k)==0
   G(m,k)=l;
   end
end
end
for m=1:22

F(m,1)=(G(m,1)+G(m,2)+G(m,3)+G(m,4)+G(m,5)+G(m,6)+G(m,7)+G(m,8)+G(m,9)+G(
m,10))/N(m);
```

```
end
E=sum(F,1);%Sum of aggregated Det of all sites
H=E/22% Averaged FD prbability
save ('result.txt','H','-ASCII')
save ('result-1.txt','G','-ASCII')
save ('result-2.txt','F','-ASCII')
```

Appendix B: False Detection Probability Algorithm

```
%-------------------------------------------------------------------------
--
'M-File of False Detection Probability by John Martin';
%-------------------------------------------------------------------------
--
'Setting up of basic parameters';
%-------------------------------------------------------------------------
--
paramNameValStruct.SimulationMode ='rapid';
paramNameValStruct.AbsTol = '1e-5';
paramNameValStruct.SaveState = 'on';
paramNameValStruct.StateSaveName ='xoutNew';%enabling state output
paramNameValStruct.SaveOutput = 'on';
paramNameValStruct.OutputSaveName ='youtNew';%enabling output to workspace
paramNameValStruct.SaveOutput = 'on';
paramNameValStruct.OutputSaveName ='tout';%enabling output to workspace
load RegionCh.txt
load BxSecRegions.txt
%-------------------------------------------------------------------------
--
%'Calculating Number of Channels in each location ';
%-------------------------------------------------------------------------
--
D=RegionCh;% Ch allocation for all 22 regions
w=0;
for m=1:22
    w=0;
for k=1:10;% iteration of next Ch next Bx
    if D(m,k)>0;
    w=w+1;
    end
N(m)=w;
end
end
%-------------------------------------------------------------------------
--
% Calculating the number of Ch used in 22 locations
%-------------------------------------------------------------------------
--
S=[0 0 0 0 0 0 0 0 0 0 0 0 0 0 0 0 0 0 0 0 0 0 0 0 0 0 0 0 0 0 0 0];
b=1;
x=0;
for m=1:22
    for k=1:10
        for h=1:32
            if D(m,k)==S(1,h)
             x=1;
            end
            if D(m,k)==0
                x=1;
            end
        end
        if x~=1
            S(1,b)=D(m,k);
            b=b+1;
        end
        x=0;
   end
    x=0;
end
```

```
ww=0;
for k=1:32;% iteration of next Ch next Bx
    if S(1,k)>0;
    ww=ww+1;
    end
NN(k)=ww;
end

%-------------------------------------------------------------------------
--
%   Calculating the sites which require Bx Hi
%-------------------------------------------------------------------------
--
P=BxSecRegions;% F matrix from det
u=0
for m=1:22
    u=0;
    if P(m,1)<1;
    u=u+1;
    v(u,1)=m;
    end
Z(m)=u;
end

%-------------------------------------------------------------------------
--
y=8;%Spectrum Spread for Bx=3
Bx=[-4 -3 -2 -1 1 2 3 4];% Setting the values of Spectrum Spread +/- 1 to
+/- Bx=3
yx=8;%Bx=7
Bxx=[-4 -3 -2 -1 1 2 3 4]; %Bx=7
bb=1;% Ch Index
%-------------------------------------------------------------------------
--
% SU Ch 1
%-------------------------------------------------------------------------
--
for Di=[21:69];%Secondary access channel
D=RegionCh;% Ch allocation for all 22 regions
R1a=[0 0 0 0 0 0 0 0 0 0;0 0 0 0 0 0 0 0 0 0;0 0 0 0 0 0 0 0 0 0;0 0 0 0
0 0 0 0 0 0;0 0 0 0 0 0 0 0 0 0;
0 0 0 0 0 0 0 0 0 0;0 0 0 0 0 0 0 0 0 0;0 0 0 0 0 0 0 0 0 0;0 0 0 0 0 0 0
0 0 0;0 0 0 0 0 0 0 0 0 0;0 0 0 0 0 0 0 0 0 0;
0 0 0 0 0 0 0 0 0 0;0 0 0 0 0 0 0 0 0 0;0 0 0 0 0 0 0 0 0 0;0 0 0 0 0 0 0
0 0 0;0 0 0 0 0 0 0 0 0 0;0 0 0 0 0 0 0 0 0 0
;0 0 0 0 0 0 0 0 0 0;0 0 0 0 0 0 0 0 0 0;0 0 0 0 0 0 0 0 0 0;0 0 0 0 0 0
0 0 0 0;0 0 0 0 0 0 0 0 0 0];% Results
k=1;
j=1;
e=1;
%-------------------------------------------------------------------------
--
%'SU Ch';
%-------------------------------------------------------------------------
--
for m=1:22
    d=0;
for k=1:10;% iteration of next Ch next Bx

for e=1:y;% Iterations of Spectrum spread Bx
    g=Di(1)+Bx(e);
    f=D(m,k);
    if f==g;
    R1a(m,k)=R1a(m,k)+1;
```

```
    end
    if f==Di
    d=1;
    end
end
end
if d==1;
R1a(m,:)=[0 0 0 0 0 0 0 0 0 0] ;
end
d=0;
end
d=0;
%-------------------------------------------------------------------------
--
% Modifying R for the 4 locations where Bx=7 are used
%-------------------------------------------------------------------------
--

for m1=1:Z(m);
  n=v(m1,1);
for k=1:10;% iteration of next Ch
    R1a(n,k)=0;
end;
e=1;
m=n;
d=0;
for k=1:10;% iteration of next Ch next Bx

for e=1:yx;% Iterations of Spectrum spread Bx
    g=Di(1)+Bxx(e);
    f=D(m,k);
    if f==g;
    R1a(m,k)=R1a(m,k)+1;
    end
    if f==Di(1)
    d=1;
    end
end
end
if d==1
R1a(m,:)=[0 0 0 0 0 0 0 0 0 0];
end
d=0
end
%-------------------------------------------------------------------------
--
z=1;%EDA detection for all Ch except 58 through the Adjacent Ch
Interferences
yy=1;%EDA detection for Ch 58 through the Adjacent Ch Interferences
c=0;%EDA detection for all Ch through the Adjacent Ch Interference with no
Ch in proximity
e=1;
Gx=[1];
for e=1:1;
if Gx(e)==1;%15 Site matrix for False Detection calculated by the Spectrum
False Coherence program for a particular Bristol Ch
R1=R1a;
end

C=z; % Probability of a site Ch being detected by RF ED for a range of
Adjacent Ch Noise except Ch 58
D1=R1*C;%Muliply Site matrix by RF ED detection Probability
end
m=1;
```

```
k=1;
for m=1:22
for k=1:10;% iteration of next Ch next Bx
    if D1(m,k)==0
    D1(m,k)=c;
    end
end
end
for m=1:22
    F1(m,1)=(sum(D1(m,:)))/N(m);% Summing all row entries & dividing by
total valid Ch in row
end
G1=sum(F1,1);%Sum of aggregated FD of all sites-Sum Columns
H1=G1/NN(32);% Averaged FD prbability per usable TVWS Ch
Result1(bb,1)=H1;% probability result
bb=bb+1;

end



%-------------------------------------------------------------------------
--
ResultT1=sum(Result1);
ResultT=(ResultT1)/49% per total number channels
save ('Probability.txt','ResultT','-ASCII')
```

Appendix C: EDA Results with FFT^2 and Covariance detectors

Table C.1: EDA Results with FFT2 and Covariance detectors

Signal Strength (dBm)	Interference Noise (dBm)	FFT2 Sensor O/P	Covariance Sensor O/P	FFT2 Aggregated Detection Probability PX	Covariance Aggregated Detection Probability PX
-125	-400	59.72	1.14	0	0
	-80	59.72	1.14		
	-70	59.72	1.14		
	-60	59.74	1.14		
	-50	59.79	1.14		
	-40	59.94	1.14		
	-28	60.60	1.14		
-122	-400	66.99	1.38	0	0
	-80	66.99	1.38		
	-70	67.00	1.38		
	-60	67.01	1.38		
	-50	67.04	1.38		
	-40	67.14	1.38		
	-28	67.60	1.38		
-120	-400	79.83	1.62	1	1
	-80	79.83	1.62		
	-70	79.84	1.62		
	-60	79.85	1.62		
	-50	79.89	1.62		
	-40	80.00	1.62		
	-28	80.50	1.63		
-117	-400	108.99	2.24	1	1
	-80	108.99	2.24		
	-70	108.99	2.24		
	-60	109.01	2.24		
	-50	109.05	2.24		
	-40	109.18	2.24		
	-28	109.77	2.24		
-115	-400	138.63	2.90	1	1

	-80	138.64	2.90		
	-70	138.64	2.90		
	-60	138.66	2.90		
	-50	138.70	2.91		
	-40	138.86	2.91		
	-28	139.52	2.91		
-112	-400	232.25	4.61	1	1
	-80	232.25	4.61		
	-70	232.25	4.61		
	-60	232.25	4.61		
	-50	232.25	4.61		
	-40	232.26	4.61		
	-28	232.27	4.61		
-110	-400	361.49	6.52	1	1
	-80	361.49	6.52		
	-70	361.49	6.52		
	-60	361.49	6.52		
	-50	361.49	6.52		
	-40	361.49	6.52		
	-28	361.51	6.52		
-95	-400	11185.75	168.25	1	1
	-80	11185.74	168.25		
	-70	11185.71	168.25		
	-60	11185.63	168.25		
	-50	11185.36	168.25		
	-40	11184.52	168.25		
	-28	11180.86	168.22		
-90	-400	36123.93	533.90	1	1
	-80	36123.91	533.90		
	-70	36123.86	533.90		
	-60	36123.71	533.90		
	-50	36123.23	533.90		
	-40	36121.72	533.89		
	-28	36115.14	533.84		
-85	-400	115581.27	1692.51	1	1
	-80	115581.23	1692.51		
	-70	115581.14	1692.51		
	-60	115580.87	1692.51		
	-50	115580.02	1692.50		

	-40	115577.32	1692.48		
	-28	115565.54	1692.40		
-80	-400	367907.06	5360.48	1	1
	-80	367906.99	5360.48		
	-70	367906.84	5360.48		
	-60	367906.36	5360.48		
	-50	367904.84	5360.47		
	-40	367900.02	5360.43		
	-28	367879.01	5360.29		
-75	-400	1167715.60	16967.00	1	1
	-80	1167715.50	16967.00		
	-70	1167715.20	16966.99		
	-60	1167714.40	16966.99		
	-50	1167711.70	16966.97		
	-40	1167703.10	16966.91		
	-28	1167665.60	16966.65		

REFERENCES

3GPP (2016) TS 23.402: Technical Specification Group Services and System Aspects; Architecture enhancements for non-3GPP accesses (Release 14) V14.0.0, France, 3rd Generation Partnership Project.

ACP (2014). BER estimation through Packet Error Rate Measurement [Online]. Available at www.icao.int/safety/.../ACP-WG-S_WP04-ErrorMeasurment_r11%20%20(2).doc (Accessed January 2016).

Ægis Systems and i2 Media (2009). Domestic TV aerial performance research for OFCOM [Online]. Available at https: //www.ofcom.org.uk/__data/ assets/pdf_file/0017/32057/ aerials_research.pdf? lang=en, (Accessed March 2016).

Akyildiz, I F., Lee, W-Y., Vuran M C., Mohanty, S. (2006) 'NeXt generation/dynamic spectrum access/cognitive radio wireless networks: A survey', Computer Networks vol. 50 pp. 2127–2159.

Akyildiz, I F., Lee, W-Y., Chowdhury, K R. (2009) 'CRAHNs: Cognitive radio ad hoc networks', Network IEEE vol.23 no. 4, pp 6—12.

Alcatel-Lucent and BT (2013) *WI-FI ROAMING – BUILDING ON ANDSF AND HOTSPOT2.0* [Online]. Available at http://www.tmcnet.com/tmc/whitepapers /documents/whitepapers/2013/6686-wi-fi-roaming-building-andsfand-hotspot20.pdf, (Accessed July 2015).

Analysys Mason (2013) Bandwidth allocation for the UK per an operator [Online], Available at http://www.analysysmason.com/ (Accessed 2013).

Angueira, P., Fadda, M., Morgade, J., M. Murroni, M., Popescu, V. (2016) 'Field measurements for practical unlicensed communication in the UHF band', *Telecommunication Systems*, vol. 61, no.3, pp. 443-449.

ATSC (2008) ATSC Recommended Practice: Transmission Measurement and Compliance for Digital Television, Washington DC, Document A/64B.

Australian Government Digital Switch Over Taskforce (2009), Digital TV Antenna systems for homes 1st Edition, Australia, Australian Government, 1st Edition.

Baldo, N. and Zorzi, M. (2008) 'Fuzzy Logic for Cross-layer Optimization in Cognitive Radio Networks', *IEEE Communications Magazine*, vol. 46, no. 4, pp. 64—71.

Bhalani, J., Kosta, Y P., Trivedi, A I. (2009), 'Performance comparison of non-linear and adaptive equalization algorithms for wireless digital communication', *AH-ICI 2009*, Kathmandu Nepal, 3-5 Nov 2009. IEEE [Online]. Available at http://ieeexplore.ieee.org.libezproxy.open.ac.uk/document/5340332/ (Accessed Jan 2016).

Cambridge White Spaces Consortium (2012), *Cambridge TV White Spaces Trial, A Summary of the Technical Findings* [online]. Available at http://www. cambridgewireless.co.uk/docs/Cambridge (Accessed 20th April 2013).

Carlsson, P., Constantinescu, D., Popescu, A., Fiedler, M., Nilsson, A. (2011), *Delay Performance in IP Routers* [Online]. Available at https://www.diva-portal.org/smash/get/diva2:837930/FULLTEXT01.pdf (Accessed May 2011).

Chen, K-C. and Prasad, R. (2009), *Cognitive Radio Networks*, Chichester UK, Wiley.

Chen, H-S. and Gao, W. (2011),'Spectrum Sensing for TV White Space in North America', *IEEE Journal on selected areas in communications*, vol. 29, no. 2, pp 1—11.

Cisco (2016) *Cisco Visual Networking Index: Global Mobile Data Traffic Forecast Update, 2015 – 2020* [Online], Available at http://www.cisco.com/c/dam/m/en_in/innovation/enterprise/assets/mobile-white-paper-c11-520862.pdf (Accessed February 2016).

COGEU (2009), *Cognitive radio systems for efficient sharing of TV white spaces in European context* [Online]. Available at http://www.ict-cogeu.eu/pdf/COGEU_D2_1%20(ICT_248560).pdf (Accessed 20th April 2015).

Cristian, A C. and Walden, A T. (2002), Multitaper Power Spectrum Estimation and Thresholding: Wavelet Packets Versus Wavelets, *IEEE Transactions on Signal Processing*, vol.50, no. 12, pp. 2976—2986.

Davies, L., Rix, A., Mezzarobba, E. (2013), Study on DTT Receiver Performance, UK, TTP, 75014-1.

DVB (2011), *Study on specification and use of in-line filters to reduce interference in broadcast bands from mobile base stations (SB2122)* [Online]. Available at https://www.dvb.org/resources/public/whitepapers/DVB-Interference-Filter-Study.pdf (Accessed Feb 2016).

EPRS (2016), *5G network technology- Putting Europe at the leading edge*, Brussels, European Parliament, PE 573.892.

ETSI (2004) ETSI EN 300 744 V1.5.1, *Digital Video Broadcasting (DVB); Framing structure, channel coding and modulation for digital terrestrial television*, France, ETSI.

Fadda, M., Murroni, M., Popescu, V., Angueira, P., Morgade, J., & Sanchez, M. (2012). Hidden node margin and man-made noise measurements in the UHF broadcasting bands. *IEEE International Symposium on Broadband Multimedia Systems and Broadcasting (BMSB)*, Seoul Korea, 27-29 June 2012, IEEE, pp. 1–5.

FCC (2007), *Interference Rejection Thresholds of Consumer Digital Television Receivers Available in 2005 and 2006* [Online], Available at https://transition.fcc.gov/oet/info/documents/reports/DTV_Interference_Rejection_Thresholds-03-30-07.pdf (Accessed November 2015).

FCC (2012), *Third Memorandum Opinion and Order* [Online], Available at https://apps.fcc.gov/edocs_public/attachmatch/FCC-12-36A1_Rcd.pdf (Accessed December 2015).

FCC (2015), *Engineering DTV Maps* [Online], Available at https://www.fcc.gov/media/engineering/dtvmaps (Accessed January 2015).

Fitch, M., Nekovee, M., Kawade, S., Briggs, K., MacKenzie, R. (2011) 'Wireless service provision in TV white space with cognitive radio technology: A telecom operator's perspective and experience', *IEEE Communications Magazine*, vol. 49, no. 3, pp. 64-73.

Forouzan, B A. and Fegan, S. (2003), Data Communications and Networking 3rd Edition, New York USA, McGraw-Hill.

Ghanekar, P., Dhole, P., Patil, N. (2014) 'Interference based Detection Spectrum Sensing in Cognitive Radio - A Survey', *ISSN*, vol.3, no.3, pp. 31-36.

Ghosh, C. and Agrawal, D P. (2007) 'ROPAS: Cross-layer Cognitive Architecture for Wireless Mobile Adhoc Networks', *IEEE International Conference on Mobile Adhoc and Sensor Systems*, Pisa Italy, pp 1—7.

GSA (2016), Evolution to LTE Report [Online]. Available at: https://gsacom.com/content/uploads/2015/10/151013-Evolution_to_LTE_report.pdf (Accessed April 2016).

GSMA (2014), *Understanding 5G: Perspectives on future technological advancements in mobile* [Online]. Available at https://www.gsmaintelligence.com/research/?file=141208-5g.pdf&download (Accessed February 2016).

Haykin, S. (2005) 'Cognitive radio: Brain empowered wireless communication', *IEEE JSAC*, vol. 23, no. 2, pp. 201-220.

He, A., Bae, K K., Newman, T R., Gaeddert, J., Kim, K., Menon, R., Morales-Tirado, L., Neel, J., Zhao, Y., Reed, J H., Tranter, W H. (2010) 'A Survey of Artificial Intelligence for

Cognitive Radios', IEEE Transactions on Vehicular Technology, vol. 59 no. 4, pp. 1578—1592.

Hossain, E. and Niyato, D., Han, Z. (2009) *Dynamic Spectrum Access and Management in Cognitive Radio Networks*, Cambridge UK, Cambridge University Press.

Hosseini, H., Izzati, A., Zamani, A., Kamilah, S., Yusof, S., Fisal, N. (2009) 'CSI Feedback Model in the Context of Adaptive Cognitive Radio Systems', T*hird Asia International Conference on Modelling & Simulation*. Bali, 25-29 May 2009, USA, IEEE, pp. 681-686.

IEEE (2013) 802.11af™-2013: *IEEE Standards- Amendment 5: Television White Spaces (TVWS) Operation*, USA, IEEE Computer Society.

INET (2012), INET Framework for OMNeT++ Manual [Online]. Available at https://omnetpp.org/doc/inet/api-current/inet-manual-draft.pdf (Accessed May 2014).

ITU-R (1997) RECOMMENDATION ITU-R P.526-5 PROPAGATION BY DIFFRACTION [Online]. Available at https://www.itu.int/rec/R-REC-P.526/en (Accessed April 2012).

ITU-R (2009) Guidelines for evaluation of radio interface technologies for IMT-Advanced, [Online]. Available at http://www.itu.int/dms_pub/itu-r/opb/rep/R-REP-M.2135-1-2009-PDF-E.pdf (Accessed June 2014)

Kang, K-M., Park, J C., Cho, S-I., Jeong, B J., Kim, Y-J., Lim, H-J., Im, G-H. (2012) 'Deployment and Coverage of Cognitive Radio Networks in TV White Space', *IEEE Communications Magazine*, vol. 50, no.12, pp. 88-94.

Kasch, W T., Ward, J R., Andrusenko, J. (2009) ‘Wireless Network Modeling and Simulation Tools for Designers and Developers’, *IEEE Communications*, vol. 47, no. 3, pp 120—127.

Kokar, M M. and Lechowicz, L. (2009) ‘Language Issues for Cognitive Radio’, *Proc. of IEEE*, vol. 97, no. 4, pp. 689—707.

Kuhn, M G. (2013) ‘Compromising Emanations of LCD TV Sets’, *IEEE Transactions on Electromagnetic Compatibility*, vol. 55, no. 3, pp. 564-570.

Lei Qiu Jing, C., Viessmann, A., Kocks, C., Bruck, G H., Jung, P., Qingyang Hu, R. (2011) ’A Spectrum Sensing Prototype for TV White Space in China’, *GLOBECOM 2011*, Kathmandu Nepal, 5-9 Dec. 2011, USA, IEEE, pp. 1—6.

Loeffler, W H T. and Wegener, J. (2012),’ Quality Model based on ISO/lEe 9126 for Internal Quality of MATLAB/Simulink iStateflow Models’, *ICIT 2012*, Athens Greece, 19-21 March 2012, USA, IEEE, pp. 325—330.

Martin, J H., Dooley, L S., Wong, K C P. (2011) ‘A New Cross-Layer Design Strategy for TV White Space Cognitive Radio Applications’, *IWCLD 2011*. Rennes France, 30 Nov.-1 Dec. 2011, USA, IEEE, pp. 1—5.

Martin, J H., Dooley, L S., Wong, K C P. (2013) ‘A New Cross-Layer Dynamic Spectrum Access Architecture for TV White Space Cognitive Radio Applications’, ISP 2013. London UK, 2-3 Dec. 2013, UK, IET, pp. 1—6.

Martin, J H., Dooley, L S., Wong, K C P. (2016) 'A New Dynamic Spectrum Access Algorithm for TV White Space Cognitive Radio Networks', *IET Communications Journal*, vol. 10, no.18, pp. 2591 – 2597.

Matlab (2010), *Matlab and Simulink user guides* [Online]. Available at http://www.mathworks.com/help/releases/R2010a/techdoc/ (Jan 2010) (Accessed Feb 2010).

Mitola, J. and Maguire, G Q. (1999) 'Cognitive Radio : Making Software Radios More Personal', *IEEE Personal Communications*, vol. 6, no. 4, pp. 13—18.

Nekovee, M. (2010) 'Cognitive Radio Access to TV White Spaces: Spectrum Opportunities, Commercial Applications and Remaining Technology Challenges', *IEEE DySPAN*, Singapore, 6-9 April 2010, USA, IEEE, pp. 1-10.

Nekovee, M. (2011) 'Current Trends in Regulation of Secondary Access to TV White Spaces Using Cognitive Radio', *IEEE Globecom 2011*, Kathmandu Nepal, 5-9 Dec 2011, USA, IEEE, pp. 1—6.

Nekovee, M. (2012), *TV White Space Services in the UK: Current Status and Future Directions*, BT, HSN 2012 Conference presentation 12/1/2012 Jeju Island, South Korea.

Newnes (2003) *Newnes Guide to Digital TV*, Oxford UK, Elsevier Science.

NGMN (2015), *NGMN 5G White Paper*, Frankfurt Germany, NGMN, Version 1.0.

OFCOM (2015), *Implementing TV White Spaces*, London UK, OFCOM, 12 February 2015.

OFCOM (2016) *Digital Switchover Transmitter Details* [Online]. Available at https://www.ofcom.org.uk/spectrum/information/transmitter-frequency (Accessed 14th Mar 2017).

OMNeT++ (2011) OMNeT++ User Manual Version 4.3 [Online]. https://omnetpp.org/doc/omnetpp/manual (Accessed May 2014).

Ramjee, R., Roy, S., Chintalapudi, K. (2016) 'A critique of FCC's TV white space regulations', GetMobile, vol. 20, no. 1, pp. 20-25.

Randhawa, B S., Wang, Z., Parker, I. (2008), *Conducted and Radiated Measurements to Quantify DVB-T, UMTS and WiMAX Interference into DTT*, Leatherhead UK, ERA, 2008-0296.

Rhode and Schwarz (2015), *Application Note- Bit Error Ratio BER in DVB as a Function of S/N* [online]. Available at https://cdn.rohde-schwarz.com/pws/dl_downloads/dl_application/application_notes/7bm03/7BM03_4E.pdf (Accessed Oct 2015).

Seybold JS (2005), *Introduction to RF Propagation*, Chichester UK, Wiley.

Sheng, L., Shao, J., Ding, J. (2010) 'A Novel Energy-Efficient Approach to DSR Based Routing Protocol for Ad Hoc Network', *ICECE 2010*. Wuhan China, 25-27 June 2010, USA, IEEE, pp. 2618 – 2620.

Spectrum Bridge (2010), *United States TV White Spaces: Usage & Availability Analysis, White Spaces Report 2Q 2010*, USA, Spectrum Bridge.

The World Bank (2016), *Population density (people per sq. km of land area) & Mobile cellular subscriptions (per 100 people)* [Online]. Available at http://data.worldbank.org/indicator/ (April 2016).

The Royal Borough of Kensington and Chelsea Council (2010) *Building Height in the Royal Borough– A Supplementary Planning Document*, UK, The Royal Borough of Kensington and Chelsea Council.

Tranter, W. H., Shanmugan, K. S., Rappaport, Th. S. and Kosbar, K. L. (2003) *Principles of communication systems simulation with wireless applications*, New Jersey USA, Prentice Hall.

UK Free TV (2013), *Freeview: Full service Freeview transmitters* [Online]. Available at http://www.ukfree.tv/txlist.php, (Accessed 23rd Feb 2013).

Van Brummelen, G. (2013), *Heavenly Mathematics: The Forgotten Art of Spherical Trigonometry*, New Jersey USA, Princeton University Press.

Wolfram (2015), *Circle Intersection* [Online], Available at http://mathworld.wolfram.com/Circle-CircleIntersection.html (Accessed June 2015).

Yagci, A. (2011), *Master Thesis - Comparison and Evaluation of Routing Mechanisms for Wi-Fi Mesh Networks* [Online]. Available at https://www.diva-portal.org/smash/get/diva2:829482/FULLTEXT01.pdf (Accessed Jan 2016).

Yuanzhou, L. and Weihua, H. (2010) 'Optimization Strategy for Mobile Ad Hoc Network Based on AODV Routing Protocol', *WiCOM 2010*, Chengdu China, 23-25 Sept. 2010, USA, IEEE, pp. 1-4.

Zhang, Y., Zhang, R J X., Yang, D. (2011) 'Study on link-level simulation in multi-cell LTE downlink system', *IC-BNMT 2011*, Shenzhen China, 28-30 Oct. 2011, pp168-172.

Zhu, X., Champagne, B., Zhu, W-P. (2013) 'Cooperative Spectrum Sensing Based on the Rao Test in Non-Gaussian Noise Environments', *WCSP 2013*, Hangzhou China, 24-26 Oct. 2013, USA, IEEE, pp. 1-6.